Biodegradation of Anaerobic, Alkaline Cellulose Degradation Products

Simon Peter Rout, BSc (Hons)

A thesis submitted to the University of Huddersfield in the partial fulfilment of the requirements for the degree of Doctor of Philosophy

Department of Biological Sciences
September 2015

Copyright Statement

i. The author of this thesis (including any appendices and/or schedules to this thesis) owns any copyright in it (the "Copyright") and s/he has given The University of Huddersfield the right to use such Copyright for any administrative, promotional, educational and/or teaching purposes.
ii. Copies of this thesis, either in full or in extracts, may be made only in accordance with the regulations of the University Library. Details of these regulations may be obtained from the Librarian. This page must form part of any such copies made.
iii. The ownership of any patents, designs, trade marks and any and all other intellectual property rights except for the Copyright (the "Intellectual Property Rights") and any reproductions of copyright works, for example graphs and tables ("Reproductions"), which may be described in this thesis, may not be owned by the author and may be owned by third parties. Such Intellectual Property Rights and Reproductions cannot and must not be made available for use without the prior written permission of the owner(s) of the relevant Intellectual Property Rights and/or Reproductions

I would like to dedicate this work to my father, Peter George Rout, who with great sadness, could not be here to see its completion.

Acknowledgements

I sincerely thank my supervisor Dr Paul Humphreys for the opportunity to undertake this research degree. Without the guidance, support and encouragement received not only throughout the studentship, but also the opportunities and advice provided as early as 2008 I suspect I would not be in the position I am now. I would also like to thank my co-supervisor Prof. Andrew Laws for helpful discussions with regards to the organic and analytical chemistry aspects of the work. I would also like to take the opportunity to thank Prof. Alan McCarthy and his team within the Institute of Integrative Biology at the University of Liverpool for their assistance and advice with the molecular biology and bioinformatical approaches to the project. I also acknowledge the financial support to the studentship provided by the University of Huddersfield.

I would also like to thank my colleagues both within the research group and department. Of particular note, thanks go to Chris Charles for his aid; not just in the laboratory, but also for the help and companionship over various field trips and conferences; and to Kimberley Bexon for her support when it really mattered. Within the department I would also like to thank the various characters who I have shared working space with who have provided me with occasional advice, the odd laugh, and the constant reminder it wasn't just me who was suffering! Away from work I would like to thank (Captain) Daniel Lucas for providing beer, anecdotes about commercial airliners and stints as manager of various league 2 football clubs.

At the risk of this section becoming an Oscar award speech, I would finally like to thank my family, who put up with the late nights, stressed looks and absenteeism. Without their unconditional support over the last 27 (and a bit) years, I simply wouldn't be the person I am today.

Abstract

The proposed strategy for the disposal of the United Kingdom's nuclear waste inventory is placement within a deep geological disposal facility (GDF). The prevailing conditions of a GDF are expected to be anaerobic, with alkaline conditions (10.5<pH>13) over a long timescale. In these anaerobic, alkaline conditions the cellulosic components of intermediate level wastes are expected to degrade, with the major products being the α- and β-forms of isosaccharinic acid (ISA). ISAs have received particular attention because of their ability to form complexes with radionuclides, potentially influencing their migration through the GDF.

The potential for microbial colonisation of a GDF means that ISAs present a source of organic carbon for utilisation. The ability of micro-organisms to utilise cellulose degradation products including ISA is poorly understood. The work presented in this thesis has shown that near surface microbial consortia are capable of the degradation of ISA under iron reducing, sulphate reducing and methanogenic conditions at circum-neutral pH values expected within geochemical niches of the near field and far field of a facility, with PCR analysis suggesting groups responsible for these metabolic processes were present in each instance.

The same near surface consortium studied was capable of ISA degradation up to a pH of 10 within 8 weeks. Degradation rates were retarded by the increase in pH, in particular that of the β- stereoisomer. Clostridia were the likely bacterial Class responsible for fermentation of ISA to acetic acid, carbon dioxide and hydrogen. These secondary metabolites were then used in the generation of methane by methanogenic Archaea, however the acetoclastic methanogen component of the consortium was absent at elevated pH; evidenced by the persistence of acetic acid within the microcosm chemistry.

The mesophilic consortium used in these initial investigations was not capable of ISA degradation above pH 10 within the short timescales imposed within the project. As a result, a soil consortium was obtained from a hyper alkaline contaminated site, where waste products from lime burning had occurred between 1883 and 1944. Initial surveying of the site showed that ISA was present and generated through interactions between the hyperalkaline leachate and organic soil matter. Following sub-culture of the soil consortia at pH 11, complete ISA degradation was observed within 14 days where again, fermentation processes followed by methanogenesis occurred. Clone libraries showed that again Clostridia was the dominant phylogenetic Class, represented by species from the genus *Alkaliphilus*. As observed with the mesophilic microcosms at pH 10, hydrogenotrophic methanogens dominated the Archaeal components of the consortia.

The results presented in the following body of work suggest that the microbial colonisation of a GDF is likely within the construction and operational phases of the facility. Carbon dioxide is likely to be the predominant terminal electron acceptor within the facility and here methanogenesis has been observed up to a pH of 11.0. In each case, fermentation is likely to be as a result of alkaliphilic Clostridia, where methanogenesis appears to be limited to the hydrogenotrophic pathway at elevated pH. These findings are likely to inform safety assessments through both the application of rate data and gas generation predictions.

Contents

1. Nuclear waste disposal concept and the generation of cellulose degradation products ... 18
1.1. Overview ... 19
1.2. Nuclear waste legacy ... 19
1.2.1. High-level wastes ... 19
1.2.2. Low-level wastes ... 20
1.2.3. Intermediate-level wastes ... 20
1.3. Geological disposal of nuclear wastes ... 20
1.4. Cellulose Degradation with respect to a GDF ... 24
1.4.1. Cellulosic materials ... 24
1.4.2. Anaerobic, alkaline degradation of cellulose ... 24
1.4.3. Significance of ISAs with respect to geological disposal ... 26
1.4.4. Other instances of ISA generation ... 27
1.5. Summary of Chapter 1 ... 27
2. Methods for the characterisation of microbiology within natural and model systems ... 29
2.1. Overview ... 30
2.2. Direct culturing techniques ... 30
2.3. Microcosm studies ... 31
2.4. Direct visualisation methods ... 31
2.5. Detection of viable micro-organisms ... 32
2.6. Nucleic acid based methods ... 32
2.6.1. Nucleic acid extraction ... 32
2.6.2. Polymerase chain reaction (PCR) ... 33
2.6.3. PCR-gradient electrophoresis techniques ... 34
2.6.4. Cloning of PCR products ... 34
2.6.5. Analysis of sequence data ... 35
2.6.6. Emerging techniques ... 35
2.7. Summary of Chapter 2 ... 37

3. Microbial processes relevant to geological disposal 38
3.1 Overview 39
3.2 Microbial degradation of ISA 39
3.3 Survival of micro-organisms under the conditions of a GDF 42
3.4 Natural and anthropogenic analogues to a GDF 43
3.4.1 Natural analogues 43
3.4.2 Anthropogenic analogues 44
3.5 Fermentation processes 45
3.6 Iron reduction 45
3.7 Sulphate reduction 47
3.8 The Archaea 50
3.9 Methanogenesis 50
3.10 Summary of Chapter 3 52
4. Aims and Objectives 53
5. Experimental methods 55
5.1. General reagents 56
5.2. Media 56
5.2.1. Mineral media 56
5.2.2. Production of Cellulose Degradation Products (CDP) 57
5.2.3. Sample preparation 57
5.3 Analytical Methods 58
5.3.1 Detection and quantification of α and β isosaccharinic acids using high performance anion exchange chromatography with pulsed amperometric detection (HPAEC-PAD) 58
5.3.2 Detection and quantification of volatile free acids using gas chromatography with flame ionisation detection (GC-FID) 58
5.3.3 Measurement of total carbon, total inorganic carbon and total organic carbon using TOC5000A 59
5.3.4 Determination of iron (II) and (III) content 59

5.3.5 Detection and quantification of sulphate and nitrate concentration using ion chromatography with pulsed amperometric detection 59

5.3.6 Detection and quantification of aqueous sulphide concentration 60

5.3.7 Detection and quantification of total sulphide concentration using gas chromatography with thermal conductivity detection (GC-TCD) 60

5.3.8 Measurement of total protein concentration 60

5.3.9 Measurement of total carbohydrate concentration 61

5.3.10 X-ray diffraction (XRD) analysis of iron samples 61

5.3.11 Brunauer–Emmett–Teller (BET) analysis 61

5.3.12 Scanning electron microscopy and elemental analysis 61

5.3.13 Measurement of pH and redox potential 61

5.3.14 Gas Volume 62

5.3.15 Gas Identity 62

5.4 Microbial Ecology studies 62

5.4.1 DNA extraction and purification 62

5.4.1.1 MO-BIO PowerSoil® DNA extraction kit 62

5.4.1.2 Co-extraction method 63

5.4.2 Polymerase chain reaction (PCR) for the amplification of ribosomal RNA and detection of bacterial and archaeal groups within samples 64

5.4.2.1 Detection of groups of organisms through direct PCR 64

5.4.2.2 Detection of groups of organisms through nested PCR 64

5.4.2.3 Control template DNA 64

5.4.2.4 Oligonucleotide primers and probe synthesis 65

5.4.2.5 Visualisation of DNA/RNA by gel electrophoresis 67

5.4.3 PCR product purification 67

5.4.3.1 PCR product purification using Qiaquick PCR purification kit 67

5.4.3.2 PCR product purification by gel extraction method 67

5.4.4 Vector Cloning 68

5.4.4.1 Preparation of SOC medium 69

5.4.4.2 Preparation of LB ampicillin/IPTG/X-Gal plates 69
5.4.4.3 Plasmid extraction to verify insertion 69
5.4.5 Sequencing 70
5.4.6 Sequence analysis 70
5.4.7 Inference of phylogeny 71
5.4.8 Nucleotide accession numbers 71
5.5 Microcosm studies 71
5.5.1 Batch feed cycles 71
5.5.2 Inoculum 72
5.5.2.1 Canal sediments 72
5.5.2.2 Reed bed sediments 72
5.5.2.3 Hyperalkaline sediment 72
5.5.3 Neutral pH Study 72
5.5.4 Methanogenic microcosms operating up to pH 11.0 73
5.5.5 Methanogenic microcosms operating at pH 11.0 using hyperalkaline soil 73
5.5.6 Control microcosms 74
5.6 Site study 74
5.7 *Ex-situ* ISA generation experiments 74
5.8 Isolation of alkaliphilic micro-organisms 74
5.9 Pure culture ISA degradation studies 75
5.10 Data Processing and statistical analysis 75
6. Biodegradation of ISAs from CDP at neutral pH 77
6.1 Rationale 78
6.2 Results and discussion 78
6.1.1. Characterisation of cellulose degradation products 78
6.1.2. Microcosm experiments 79
6.3 Conclusion 91
6.4 Key Findings 92

7. Fermentation studies at elevated pH 93
7.1 Rationale 94
7.2 Results and Discussion 94
7.3 Conclusion 109
7.4 Key Findings 110
8. Isolation of ISA degrading micro-organisms 111
8.1 Background 112
8.2 Results and discussion 115
8.2.1 Colony morphology 115
8.2.2 ISA degradation potential of *Exiguobacterium* sp strain HUD 115
8.2.3 16S rDNA sequencing 117
8.2.4 Whole genome sequencing and annotation 121
8.3 Conclusion 123
8.4 Key Findings 123
9. Hyper-alkaline contaminated site field study 125
9.1 Rationale 126
9.2 Results and Discussion 126
9.3 Conclusion 136
9.4 Key Findings 136
10. Concluding remarks 138
11. References 151
Data 169
Statistical Analyses 188

Word count excluding appendices- 47,884

List of Figures

Figure 1.1 Conceptual illustration of a deep geological disposal facility, taken from the 2010 NDA status report (N.D.A., 2010). Here vaults for the containment of various wasteforms can be seen at depth, where access to the vaults pre –closure is facilitated by access shafts from a central surface facility. 21

Figure 1.2 Illustration of multi barrier concept for waste encapsulation. Physical containment is provided by immobilising waste-forms within an appropriate container prior (A) geological isolation within the vaults of a deep GDF (B and D). The GDF is then backfilled with cementitious materials to provide the chemical conditions for optimum containment (C)..... 22

Figure 1.3 ILW 500 litre steel drum cutaway (taken from NDA, 2010). Example waste can be seen packaged and backfilled within the drum. 22

Figure 1.4 Expected pH evolution in the cementitious GDF concept (taken from NDA, 2010). pH is mediated by the dissolution of cementitious materials into ingressing groundwater from an initial value of >12.5 (stage I), down to a pH value ~10.0. 23

Figure 1.5 Chemical structure of cellulose, taken from [23]. Anhydroglucose units are linked via β (1-4) glycosidic bonds, during the peeling reaction units are stripped from the reducing end. 25

Figure 1.6 The α (left) and β (right) stereoisomers of isosaccharinic acid..... 26

Figure 3.1 Strategies employed by iron reducing micro-organisms for electron transfer (reproduced from [146]) e-=electrons L=ligand. In some cases (A) the micro-organism may be capable of the direct contact with an Fe(III) source through nanowires. The use of enogenous/ exogenous electron shuttles (B) or ligands (C) provide an abiotic method being oxidised to reduce Fe(III) sources which can in turn be reduced my the micro-organism. 46

Figure 3.2 Pictorial representation of the dissimilatory sulphate reducing pathway. (Reproduced from [165]). Sulphate is converted to thiosulphate through the action of ATP sulphurylase and APS reductase enzymes. Production of hydrogen sulphide is mediated through the dissimilatory sulphite reductase enzyme..... 48

Figure 3.3 Composite of CO2-reduction and aceticlastic methane generating pathways. Reactions (1-4) are unique to the aceticlastic pathway, reactions (5-9) are unique to the CO2 reducing pathway. Pathways diverge and reactions (10-12) are present in both pathways (Taken from [186]). 51

Figure 5.1 Nomenclature of Fasta files containing collated sequence data..... 70

Figure 6.1 Chemical evolution of iron reducing reactors (n=6). Both stereoisomers of isosaccharinic acid were removed (α, closed circles. B, closed triangles) coinciding with the generation of gas (crosses) and generation and subsequent removal of acetic acid (open circles). 80

Figure 6.2 Chemical evolution of sulphate reducing reactors (n=6). Both stereoisomers of isosaccharinic acid were removed (α, closed circles. B, closed triangles) coinciding with the generation of gas (crosses) and generation and subsequent removal of acetic acid (open circles). 80

Figure 6.3 Chemical evolution of methanogenic reactors (n=6). Both stereoisomers of isosaccharinic acid were removed (α, closed circles. B, closed triangles) coinciding with the generation of gas (crosses) and generation and subsequent removal of acetic acid (open circles). 81

Figure 6.4 Mean first order degradation rates of individual stereoisomers of ISA under each microcosm condition. Values presented are the mean value ± SE (n=6). 82

Figure 6.5 Non-acetic volatile fatty acid profiles within the iron reducing (A), sulphate reducing (B) and methanogenic (C) microcosms (n=6). 83

Figure 6.6 Iron (II) (aq) generation in biotic reactors (closed diamonds) amended with ferric iron. 84

Figure 6.7 XRD patterns for the iron oxide used in microcosms (Sample 1), identified as haematite through comparison with diffraction database (peaks at 24, 33, 36, 41, 49 54, 62 and 64 2 Theta) and pattern at the end of the sampling period (Sample 2), where haematite contained an impurity, determined as magnetite through comparison with diffraction database (peaks at 30, 58 and 74 2 Theta, circled)..... 85

Figure 6.8 EDS output from analysis of calcite deposit in Figure 3, D. Carbon, calcium, oxygen and iron were the predominant elements detected, suggesting the potential presence of calcium carbonate amongst the bulk iron oxide. 87

Figure 6.9 Composition of microcosm headspace gases (n=6). Methane and carbon dioxide were detected in both iron reducing and methanogenic microcosms, whereas carbon dioxide as detected exclusively within sulphate reducing microcoms 89

Figure 6.10 Generation of dissolved sulphides and removal of sulphates within the sulphate reducing microcosm. 89

Figure 6.11 Removal of ISA is biotically mediated, where ISA remains in solution when microcosm is treated with chloramphenicol. Removal of ISA was seen with both biotic canal

(closed triangles) and NCM sediments (crosses), with no distinct removal observed within chlormaphenicol treated canal (closed diamonds) and NCM (closed squares) sediments..... 90

Figure 6.12 Removal and recalcitrance of other organic carbon components within the chemistry of iron reducing (closed diamonds), sulphate reducing (closed squares) and methanogenic (closed triangles) microcosms..... 91

Figure 7.1 Removal of organic carbon from microcosms over 7 day sample period (A). pH 7.5 microcosm chemical evolution(B), pH 9.5 chemical evolution (C) and pH 10.0 chemical evolution (D). Mean values (n=3) are presented ± SE. 96

Figure 7.2 Rate of α and β ISA degradation at each pH system sampled. Mean values (n=3) are presented ± SE..... 97

Figure 7.3 Non- acetic volatile fatty acid production at pH 7.5 (A), pH9.5 (B) and pH10.0 (C). 98

Figure 7.4 Liquid phase carbon mass balance profiles for pH7.5 (A), 9.5 (B) and 10.0 (C) microcosms. Mean values (n=3) are presented ± SE. 100

Figure 7.5 Bradford assayed protein levels across all pH7.5 (open triangles), pH9.5 (open squares) and pH 10.0 (closed diamonds) microcosms. 101

Figure 7.6 Total carbohydrate assay across pH7.5 (open triangles), pH9.5 (open squares) and pH 10.0 (closed diamonds) microcosms. 101

Figure 7.7 Methane gas evolution across pH7.5 (open triangles), pH9.5 (open squares) and pH 10.0 (closed diamonds) microcosms. 102

Figure 7.8 Total ISA is not degraded or subjected to sorption events when amended with chloramphenicol. 103

Figure 7.9 Eubacterial 16S rRNA gene clone libraries of CDP driven microcosms at pH7.5 (n=47), 9.5 (n=43) and 10.0 (n=39). Clones were assigned to a family based on the closest sequence match obtained through MegaBLAST database search. Families associated to the group Clostridia are indicated by the black parentheses. 104

Figure 7.10 Archaeal 16S rRNA gene clone libraries of CDP driven microcosms at pH7.5 (column A n=45), 9.5 (column B n=48) and 10.0 (column C n=45). Clones were assigned to a family based on the closest sequence match obtained through MegaBLAST database search strategy. 106

Figure 7.11 Typical HPAEC-PAD trace of CDP liquor system peak (1). α-ISA (2), X-ISA (3), β-ISA (4), α and β MSA (5), unknown (6) , octanedioic acid derivative (7) and D- ribonic acid(8), used as an internal standard for quantification..... 107

Figure 8.1 Phylogenetic representation of the order Bacillales, where members of the genus *Exiguobacterium* fall within the family Bacillales Insertae Sedis XII. 113

Figure 8.2 Gram stain of *Exiguobacterium* sp strain HUD. The strain exhibited morphology of short Gram positive rods. 115

Figure 8.3 Degradation of ISA (closed diamonds) and pH evolution (open triangles) by Exiguobacterium sp strain HUD. 116

Figure 8.4 ISA degradation (closed diamonds) and pH evolution (open triangles) within uninoculated control reactions. 117

Figure 8.5 Bootstrap consensus tree inferred from 1000 replicates using neighbour joining method. Branches reproduced in >50% of the replicates are collapsed. 120

Figure 8.6 RAST subsystem output following annotation. The subsystem covered 48% of the genome where 1361 non-hypothetic proteins were coded alongside 81 hypothetical proteins. 122

Figure 9.1 Overview of Brookbottom, Harpur Hill, Derbyshire. Sampling points are numbered and indicated by black stars. (Image reproduced from Google Maps.)..... 126

Figure 9.2 Generation of ISA's in abiotic (closed diamonds) and biotic (open squares) uncontaminated soils mixed with hyperalkaline leachate at 4ºC (A), 10ºC (B) and 20ºC (C).130

Figure 9.3 Arrhenius plot of rates of ISA generation. 131

Figure 9.4 pH 11.0 microcosm chemistry. Both stereoisomers of ISA (open diamonds, open squares) were removed over the course of sampling. Acetic acid (closed triangles) was generated and subsequently removed alongside the generaton of methane (crosses) and hydrogen (closed diamonds). 132

Figure 9.5 Fate of acetic acid in biotic (open triangles) and abiotic (open squares) reactions.133

Figure 9.6 Fate of total ISA in biotic (open triangles) and abiotic (open squares) reactions. The bacterial library was dominated by members of Clostridiaceae 2 where methanobacteriaceae dominated the archaeal library. 133

Figure 9.7 Taxonomic composition of Eubacterial (A) and Archaeal (B) clone libraries. 135

Figure 10.1 Two stage pathway of complete ISA biodegradation at neutral pH values. Initial fermentation to volatile fatty acids, hydrogen and carbon dioxide is followed by iron reduction, sulphate reduction and methanogenesis dependent on the presence/absence of required terminal electron acceptors. 141

Figure 10.2 Theoretical curve of total ISA concentration in an abiotic system employing the batch waste feed cycle. Continued batch feeding of the abiotic system results in ISA

concentration approaching the concentration of the feedstock before microcosm inoculum is completely replaced by feedstock where the concentration plateaus. 145

Figure 10.3 Rates of total ISA degradation across all microcosm studies using both canal (open diamonds) and hyperalkaline sediments (open squares). 146

Figure 10.4 pH evolution of the near-field post closure of an ILW-GDF. 148

List of Tables

Table 5.1 Components of mineral media per litre of oxygen free water. 56

Table 5.2 Components of trace elements solution per litre of oxygen free water. 57

Table 5.3 Primers used within the study. 66

Table 5.4 Ligation reaction mixtures. 68

Table 6.1Composition of CDP feedstock. Individual components are expressed as a percetange of the total organic carbon. 79

Table 6.2 DNA analysis by direct and nested PCR techniques. 88

Table 7.1 Gas generation volumes at each microcosm pH. Mean values are presented ± SEM (n=3). 102

Table 8.1 Pairwise distance matrix to estimate the evolutionary distance between sequences. The numbers of base substitutions per site are shown (highlighted red). The standard error estimates can be seen above the diagonal (highlighted blue). 119

Table 9.1 Pore water and soil analysis from twelve sample sites around the Brookfoot site, Harpur Hill, Buxton, UK 128

List of Abbreviations

APS- adenosine phosphosulphate

ATP- adenosine triphosphate

BET- Brunauer–Emmett–Teller

BLAST- Basic Local Alignment Search Tool

cDNA- complementary deoxyribonucleic acid

CDP- cellulose degradation products

DGGE- denaturing gradient gel electrophoresis

DNA- deoxyribonucleic acid

DNase- deoxyribonuclease

EDS- electron dispersive X-ray spectroscopy

GC-FID- gas chromatography with flame ionisation detection

GC-TCD- gas chromatography with thermal conductivity detection

GDF- geological disposal facility

HLW- high level waste

HPAEC-PAD- high performance anion exchange chromatography with pulsed amperometric detection

IC- ion chromatography

ILW- intermediate level waste

IRB- iron reducing bacteria

ISA- isosaccharinic acid

LLW- low level waste

LLWR- low level waste repository

MPN- most probable number

mRNA- messenger ribonucleic acid

MSA- metasaccharinic acid

NCBI- National Center for Biotechnology Information

NDA-Nuclear Decommissioning Authority

NRVB- Nirex reference vault backfill

PCR- polymerase chain reaction

PFLA- phospholipid fatty acid

qPCR- quantitative polymerase chain reaction

RFLP- restriction fragment length polymorphism

RNA-ribonucleic acid

RNase- ribonuclease

rRNA/rDNA- ribosomal ribonucleic acid/deoxyribonucleic acid

SEM- scanning electron microscopy

SIP- stable isotope probing

SRB- sulphate reducing bacteria

TC- total carbon

TIC- total inorganic carbon

TOC- total organic carbon

TTGE- temporal thermal gradient electrophoresis

U.S.- United States (of America)

UK- United Kingdom

VFA- volatile fatty acid

X-ISA- xyloisosaccharinic acid

XRD- X-ray diffraction

XRF- X-ray fluorescence

1.Nuclear waste disposal concept and the generation of cellulose degradation products

1.1. Overview

The current accepted method for the long term disposal of nuclear wastes is that of a deep, underground facility for the disposal of intermediate and high level wastes alongside spent nuclear fuel. This introductory chapter will describe the geological disposal facility (GDF) concept with regards to the United Kingdom's nuclear waste inventory. Although a range of wastes forms are expected to be emplaced within a GDF, materials made from cellulose are primarily found within intermediate level wastes. Cellulose forms a main constituent of the intermediate level waste inventory and the products of its anaerobic alkaline degradation are of particular interest. The main products of this degradation are isosachharinic acids, which are capable of influencing the long-term retention of radionuclides and therefore the performance of a GDF.

1.2. Nuclear waste legacy

Radioactive waste production in the UK began in the 1940s, with sources including: nuclear power plants and reprocessing, defence, medical and industrial processes. In 2010 it was estimated that the future arisings of radioactive waste from all sources would stand at just over 4.5 million cubic metres, in addition to the 4.7 million cubic metres already part of the inventory; of which a significant proportion would be generated through the nuclear industry [1]. The first nuclear power station to operate within the UK was Calder Hall which was opened in 1952 by Queen Elizabeth II, which was soon followed by nine full-scale Magnox power stations throughout the 60's and seven advanced gas-cooled reactors operating from in 1976. The wastes that were generated throughout operation of these reactors are broadly categorised based on their thermal and radioactive outputs following decommission of facilities or reprocessing. Within the current 4.7 million cubic metres of current waste, the volume is represented by high level waste (0.1%), intermediate level waste (6.1%) and low level waste (93.9%) [1]. The wastes are discussed briefly below.

1.2.1. High-level wastes

Although high level waste and spent nuclear fuel are expected to account for over 95% of the total radioactivity held in the UK inventory by 1 April 2040, it is only expected to account for 0.3% of the packaged volume [2]. The waste itself is produced as a nitric acid solution containing fission products from the primary stage of reprocessing of spent nuclear fuels; this waste is vitrified prior to storage [3]. These wastes are classified as High Level Wastes (HLW) due to their high radioactive and thermal outputs following removal from a reactor and the long time frames required for the heat and radiation to decay to background levels [4]. Cellulose is not present in these wastes and as such only low and intermediate level wastes will be further discussed.

1.2.2. Low-level wastes

Organic materials represent 4% of the total low level waste inventory, with 100,000 tonnes being cellulosic in nature [3]. The bulk of this waste has radioactive emissions which fall substantially below the upper limits for consideration for disposal within the GDF and as such emplacement began in 1959 at the low-level waste repository (LLWR) in Drigg, Cumbria, four miles south of the Sellafield reprocessing plant [4]. Waste forms here were historically loosely tipped into to trenches, prior to the introduction of grouted containers and cement based vaults. Since storage in this case is not dependent upon saturated alkaline conditions, anaerobic cellulose degradation is microbially mediated and has previously been described [5]. The remaining quantities of LLW that emit radiation above acceptable levels for the LLWR are treated in a similar manner to intermediate level wastes.

1.2.3. Intermediate-level wastes

Where the heat produced by a waste form is below that for HLW classification, these wastes are described as intermediate level wastes (ILW) [2]. As of 2010, the total activity of the ILW stood at 3.9×10^6 TBq, representing 5% of the total activity of the entire waste inventory, although this is expected to fall to 5.5×10^5 TBq by 2150 [1]. Cellulosic materials represent 2,000 tonnes of intermediate level wastes (ILW), where materials such as paper, wood and cotton have been disposed of during the operational period and decommissioning of reactors [2]. Other organics such as plastics and rubbers are also present in the bulk ILW, with the remainder of the mass being composed of metals and other inorganics resulting from the decommissioning [1].

1.3. Geological disposal of nuclear wastes

The UK Government policy for the management of these wastes is that of a deep geological disposal facility (GDF), 200-1,000m below the surface with no intention to retrieve the wastes post closure (Figure 1.1) [3]. The site of such a facility is, at the time of writing undecided, where any such siting would require voluntarism and partnership with the local community.

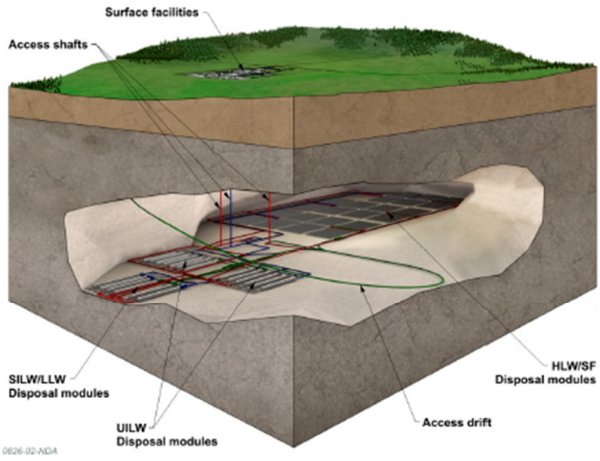

Figure 1.1 Conceptual illustration of a deep geological disposal facility, taken from the 2010 NDA status report (N.D.A., 2010). Here vaults for the containment of various wasteforms can be seen at depth, where access to the vaults pre –closure is facilitated by access shafts from a central surface facility.

The GDF concept centres on a multi-barrier approach for the containment of wastes and long-term isolation from the biosphere (Figure 1.2), where each individual component is intended to contribute to the containment. The outer most barrier is provided by the host rock at the depth the GDF is built. Since heat and gas are likely to be produced during the disposal process, the host rock must be capable of the conduction of heat to prevent temperature rises, whilst also have sufficient gas dispersal properties such that the mechanical strength of the barrier system is not compromised by increases in pressure [6]. The host rock itself will have a range of geochemical and mechanical properties, and as such for effective utilisation for a GDF, these properties must show little fluctuation over the long timescale of storage.

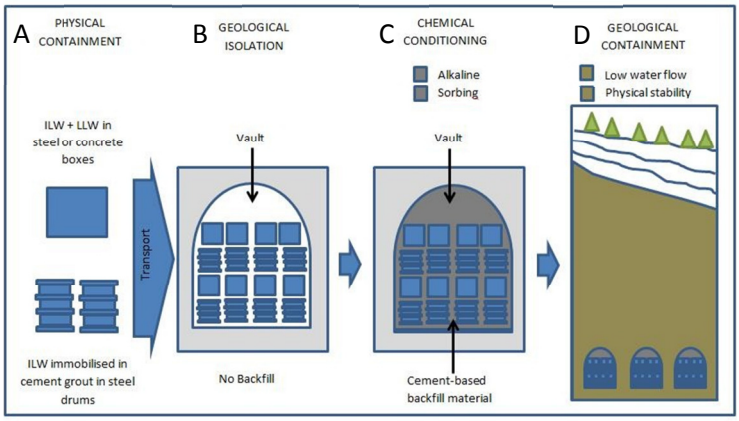

Figure 1.2 Illustration of multi barrier concept for waste encapsulation. Physical containment is provided by immobilising waste-forms within an appropriate container prior (A) geological isolation within the vaults of a deep GDF (B and D). The GDF is then backfilled with cementitious materials to provide the chemical conditions for optimum containment (C).

Intermediate level wastes (ILW) are generally heterogeneous, however the wastes are classified into three main categories: homogeneous sludges, liquids and slurries immobilised in a solid matrix; intimately grouted wastes and annular grouted wastes [2,7]. The generic container for the ILW is the 500 litre drum composed of stainless steel (Figure 1.3), vents in the lids of these drums allow for the release of gases formed by corrosion as well as allowing the transport of groundwater and radionuclides throughout the system post backfilling [2,7,8].

Figure 1.3 ILW 500 litre steel drum cutaway (taken from NDA, 2010). Example waste can be seen packaged and backfilled within the drum.

The cementitious backfill, a composite of Ordinary Portland Cement, lime and limestone flour contains the waste in both containers and in the complete closure of a disposal facility. This aids radionuclide retention through adsorption and maintenance of high pH with the expectation that radionuclides will be sorbed to the surface of the backfill or form insoluble carbonates [2,7,9].

Upon closure, re-saturation of the facility with deep ground waters will lead to the generation of high pH through the formation of alkali metal hydroxides (such as KOH, NaOH and $Ca(OH)_2$) and high temperature (up to 80ºC [2]) from higher level wastes and through cement curing processes. The facility would then be expected to develop into an anaerobic system through the removal of oxygen associated with corrosion events involving the steels present within the structural components of the facility and waste form canisters and containers [2,7,10]. As time progresses, the temperature and pH of the facility are expected to fall. Immediately post-closure (Figure 1.4, stage I) the bulk pH of a GDF is expected to be >12.5 following the dissolution of sodium and potassium oxides [2]. Interactions of inflowing groundwater with the cementitious backfill mean that the initial pH of a GDF is likely to be ~12.5 following dissolution of Portlandite and generation of hydroxyl ions (Figure 1.4, stage II). Within time, further cement hydration products including calcium silicate hydrates are expected to buffer the bulk pH of the GDF to ~10.0-12.5 depending on composition and prevailing conditions (Figure 1.4, stage III). Beyond stage III, the pH buffering will be mediated by the remaining phases such as calcite and is expected to be ~pH 10 (Figure 1.4, stage IV).

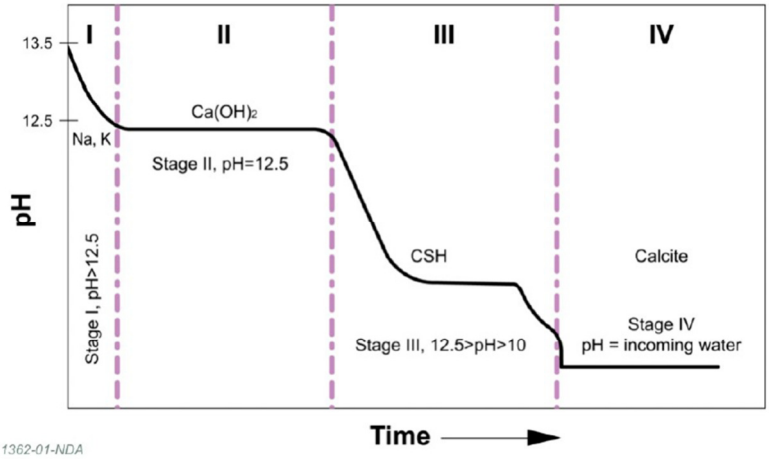

Figure 1.4 Expected pH evolution in the cementitious GDF concept (taken from NDA, 2010). pH is mediated by the dissolution of cementitious materials into ingressing groundwater from an initial value of >12.5 (stage I), down to a pH value ~10.0.

The cementitious material present within a GDF are likely to interact with the wastes themselves throughout the duration of disposal. Interactions with organic materials are the predominant concern with regards geological disposal of ILW and will be discussed further in 1.4.

1.4. Cellulose Degradation with respect to a GDF

1.4.1. Cellulosic materials

As mentioned previously, cellulosic materials found in the ILW include wood, paper and cloth from contaminated furniture, disposables and laboratory wear [2,11,12]. Cottons within the waste are composed primarily of cellulose, but much of the material present will be composed of varying amounts of cellulose, hemicelluloses and lignin in the case of wood. Within wood and other plant matter, these cellulose and hemicellulose fibres are aggregated together by lignin, a complex biopolymer [13], lignin provides mechanical strength and a degree of resistance to microbial degradation [14]. The structure of cellulose is made up of repeating units of cellobiose, a disaccharide formed through (1,4)-β-D-glucose unit linkage where each glucose unit is rotated 180° with respect to its neighbouring unit [11,15]. Hemicelluloses make up the non cellulose polysaccharides present in the cell walls of many plants and are generally varied in structure but include: xylans, galactoglucomannans, glucomannans and arabinogalactans [11,16]. It is thought that celluloses are biosynthesised in such a manner that chain elongation occurs from the non-reducing end of the chain. The crystallisation that occurs as the cellulose chain elongates results in the generation of both crystalline and amorphous regions, it is these amorphous regions that are susceptible to degradation reactions [11].

1.4.2. Anaerobic, alkaline degradation of cellulose

Following maturation of cementitious materials; the facility will experience a pH of 12.5, temperatures of 60°C and largely anaerobic conditions within the first four months post closure [12]. A chemically reducing environment is formed in which cellulose may be degraded [12,17-20]. Under these conditions cellulose is degraded via a three stage process. The initial stage of degradation is expected to have the highest rate of reaction involving ‘peeling’ reaction in which glucose like units are progressively stripped from the reducing ends of the D-anhydroglucopyranose units (Figure 1.5) [11,12].

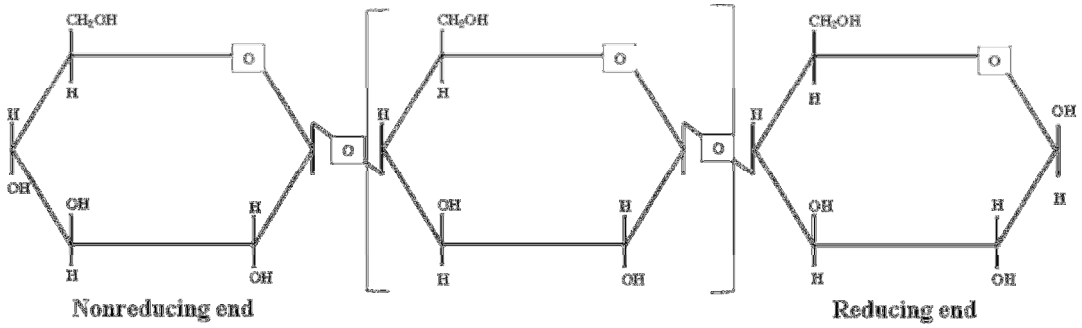

Figure 1.5 Chemical structure of cellulose, taken from [23]. Anhydroglucose units are linked via β (1-4) glycosidic bonds, during the peeling reaction units are stripped from the reducing end.

This results in formation of a range of cellulose degradation products. The main degradation products are the α and β forms of ISA discussed in 1.4.3, however other potentially degradable sources of carbon are also generated during this reaction. Knill and Kennedy [12] provide an extensive review of the other commonly identified products where a range of cellulose sources have been reacted under a range of conditions related to varying temperatures and alkali sources. In addition to ISAs, in some cases the formation of formic, acetic and lactic acids have been observed [12], which themselves are likely to as a substrate for microbial degradation (see Chapter 3). As previously discussed, the cellulosic materials present within ILW are likely to include hemicelluloses, which, due to their soluble nature are likely to be completely hydrolysed under the conditions of a GDF. The gluco- and galactoglucomannan components are degraded in the same fashion as cellulose, resulting in the production of ISAs and other small organic acids, whereas the xylan component results in the formation of xylosaccharinic acid (3-deoxy-2-C-(hydroxymethyl)-tetronic acid, X-ISA) [11,21]. Recent work by Randall *et al* [22], suggests that X-ISA can exhibit similar complexation behaviour as ISAs, discussed further in 1.4.3, however, it was reported that the concentrations of X-ISA are likely to be insufficient to have a measurable impact on radionuclide migration within a GDF.

Propagation of peeling along the reducing end of a cellulose chain is stopped when end groups that are stable to alkaline attack are formed and through competing reactions at the reducing end. Should the cellulose molecule be peeled back to a crystalline region, a physical stopping reaction takes place due to a reduced accessibility of the reagents to the end groups [9,12]. The α and β forms of gluco-metasaccharinic acid are formed in the termination reaction, these compounds may also present a source of organic carbon for microbial metabolism, however current literature fails to clarify whether these products are capable of the same complexation events discussed in 1.4.3. It should be noted however; that ISAs are likely to compose ~80% of the CDPs observed suggesting MSA's may not have as significant an impact as the ISA with respect to GDF performance [17]. Reactions can continue if an end group becomes soluble or

if mid-chain scission takes place, the latter of which has been seen through radiolytic processes and temperatures >170°C [11,12,20]. With regards to the disposal facility, it is expected that the chemical degradation of cellulose will constitute the majority of degradation in comparison to radiolytic degradation caused by the waste form [9,17].

1.4.3.Significance of ISAs with respect to geological disposal

As discussed in 1.4.2, the major products from the alkaline degradation of cellulose comprise the alpha (α) and beta (β) diastereomers of 2-C-(hydroxymethyl)-3-deoxy-D-pentonic (isosaccharinic) acid (ISA, Figure 1.5), alongside other small chain organic acids [11,17,23,24].

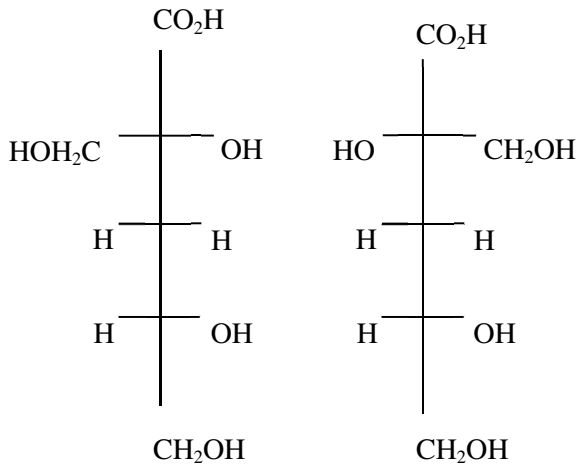

Figure 1.6 The α (left) and β (right) stereoisomers of isosaccharinic acid.

The diastereomers of isosaccharinic acid have received particular attention in the literature due to its ability to complex a range of radionuclides, potentially affecting the migration of the radionuclides. Work by Greenfield *et al*, found that ISA and constituents formed in a cellulose degradation leachate were capable of forming soluble complexes with thorium, uranium (IV) and plutonium [25]. In the case of plutonium, ISA concentrations above 10^{-5} M were capable of increasing solubility above pH 12.0, where concentrations of 1-5 x 10^{-3} M were found to increase the solubility by an order of magnitude from 10^{-5} to 10^{-4} M. The work of Allard *et al* [26] found that a concentration of ISA of 2 x 10^{-3} M could increase plutonium solubility by a factor of 2 x 10^{5}. In addition a range of studies on the complexation properties of α-isosaccharinic acid in alkaline solutions with various metals, including nickel, thorium, americium and europium have been conducted [27-31].

The work of Vercammen *et al* [27] showed that although Ca(α-ISA)$_2$ is sparingly soluble [32], both europium and thorium were capable of forming soluble complexes with ISA between pH 10.7 and 13.3, where a mixed metal complex was observed in the presence of thorium.

Wieland also observed that α-ISA prevented the uptake of thorium by hardened cement pastes [30]. The works of Warwick *et al* have also shown that ISA is capable of influencing the solubility both uranium and nickel through complexation [28,29]. Tits *et al* [31] observed that in the absence of ISA, europium, americium and thorium will sorb to the calcite present within an ILW GDF. Should ISA concentrations within the facility exceed 10^{-5} mol L^{-1} ($2x10^{-5}$ mol L^{-1} in the case of Th(IV)), it was reported that the sorption onto the calcite would be significantly affected such that the radionuclides studied would no longer be sorbed to the cement and instead be complexed with the ISA.

Most recently, work was carried out in order to determine the effect of cellulose degradation products on radionuclide solubility and sorption [22]. Cellulose degradation product leachates were first produced by contacting cellulose sources (wood, rad wipes or cotton wool) with calcium hydroxide (pH 12.7) under anaerobic conditions. Analysis of the leachates across 103 days suggested that the primary product of the degradation was ISA, although a range of other organic compounds were formed and varied across cellulose source. In these experiments both ISA and X-ISA were able to increase the solubility of europium at pH 12, where in experiments with thorium ISA had a more profound effect on thorium solubility than that of X-ISA, where little effect was observed. As well as acting as a complexant, ISA (but also CDP's and un-hydrolysed cellulose) are likely to act as a source of organic carbon for microbial utilisation. The likely mechanisms of which are discussed further in Chapter 3..

1.4.4. Other instances of ISA generation

The Kraft process also generates a range of CDP's including ISA and is a common method of treating wood to form a bleached pulp, and was described by Rydholm in 1965 [33]. Wood is put through a chipper to increase surface area before being heated with white liquor containing sulphides and sodium hydroxide to 160-180°C. The alkaline conditions cleave bonds holding the lignin layer surrounding the polysaccharide layer, followed by solubilisation and degradation of the lignin [34]. Equally at this point, celluloses and hemicelluloses are also dissolved into the alkaline solution and are partially degraded via the peeling reaction [12,34]. A black liquor forms containing the dissolved: lignin, cellulose, hemicellulose and the alkaline degradation products of these which are removed at this stage of the process. Although no radionuclides are present within this process, the black liquor produced has been used as an ISA source for microbial research, discussed further in Chapter 3.

1.5. Summary of Chapter 1

The United Kingdom has a considerable volume of radionuclide contaminated wastes, broadly categorised into high-, intermediate- and low- level wastes. A geological disposal facility concept is currently the preferred method for disposal of these wastes, where a multi-barrier

concept is proposed. In this concept, a combination of the host rock, cementitious backfill and physical containment of the wastes aids radionuclide retention within the facility. An anoxic, high pH system is expected post-closure of a facility. Cellulosic materials comprise a significant proportion of intermediate level waste inventory and are degraded under the expected geochemical conditions of a GDF to a range of cellulose degradation products. Of these degradation products, the α and β forms of isosaccharinic acid are produced which are capable of forming soluble complexes with certain radionuclides present within the inventory. The generation of soluble ISA-radionuclide complexes may have an influence upon their retention within the GDF by enhancing their migration.

2. Methods for the characterisation of microbiology within natural and model systems

2.1. Overview

Effective characterisation of a particular system, be it a natural or model environment, can provide important insights into the potential impact of the microbiology that is occurring, or can occur within that system. From a radioactive waste disposal perspective, this characterisation is usually divided into two areas. The first is that of the characterisation of a relevant site, where direct isolation and enumeration is likely to occur. In the second strategy, samples from a relevant site can be taken and sub-cultured under specific geochemical conditions with the wider context of predicting the effect of certain parameters on GDF performance. Current methodologies for the determination of microbiology can be culture based, which can be used for process identification and molecular based methods which are used for community identification. The following Chapter provides a brief description of the current methods for characterisation of these systems, with respect to radioactive waste disposal where possible. The primary focus of this body of work is the microbiological impact on ISA's within a GDF, and as such, previous works involving these techniques will be discussed in Chapter 3.

2.2. Direct culturing techniques

Enumeration of micro-organisms from environments associated with radioactive waste disposal using direct culturing methods involves the growth of these micro-organisms on solid or liquid medium. The specific composition of each medium is often the greatest influence on the group of organisms that is isolated. The work of Vreeland *et al* [35] showed that halophilic micro-organisms could be isolated from a salt mine intended for the disposal of transuranic wastes in the U.S. In a similar fashion, the numbers of micro-organisms, be it total, or of a specific group can also be estimated. Approaches such as the Most Probable Number (MPN) technique, where serial dilutions of a sample are prepared in either solid or liquid medium to observe growth are most commonly used [36]. Using these techniques the number of organisms likely to be present in within the disposal sites of Japanese [37], the U.S. [38] and Scandinavian programmes [39] have been estimated. The advantages of these methods are their relatively low-cost approach alongside well established yet undemanding technical aspects. Unfortunately, only a small number of environmental micro-organisms are believed to be culturable using liquid and solid media, where solid media in particular results in low recoveries [39,40]. Some groups of micro-organisms have been shown to be unculturable using these techniques and as a result the organisms that are cultured from a system may not represent the key groups acting within it [41]. Matching the specific geochemical needs such as nutrient concentration and incubation time/growth rate can also prove difficult. MPN methods appear to improve the recovery of micro-organisms, but the fine tuning required for culture conditions can prove time consuming [39]. The disadvantages of these methods mean that

direct culturing may not provide a great degree of value when describing an environmental site or system. The ability to culture single isolates however can prove useful where a determination of rates or other physiological processes are required. Within radioactive waste disposal investigations, Fields *et al* [42] isolated a range of micro-organisms from groundwaters contaminated with uranium waste. Nedelkova *et al* [43] were capable of describing a range of *Microbacterium* ssp that were capable of the bioaccumulation of uranium between pH 2.0-4.5 and an *Acetobactrium* sp was isolated from the Swiss Grimsel testing site that was capable of uranium biosorption [44].

2.3. Microcosm studies

An effective way of simulating the conditions of interest within a system is through the development of microcosms, which can be developed using single isolates or mixed cultures, either defined or undefined. Again, the operation of these microcosms is open to a large degree of flexibility, since they can be run as a batch process where the system is sealed and geochemistry allowed to develop; or run as a continuous flow system where nutrients are continuously fed through the system. The use of single isolates to conduct microcosm experiments has been carried out to investigate the interactions micro-organisms may have with radionuclides [43,45]. Continuous flow reactions allow for the monitoring of dissolved chemicals within a reaction and have been used to investigate the microbial impact on rock samples and radionuclide release using column flow reactions [46,47]. The use of batch microcosms have been used extensively to evaluate gas production within simulated conditions of low level wastes where microbial degradation of cellulose is likely to occur. The work of Beadle *et al* [5] used large scale (215 L) simulations to estimate gas production related to safety assessments. Since ISA's are not normally found in the natural environment, the batch microcosms employed within this body of work would require enrichment with ISA. Previous authors have used enriched microcosms to demonstrate the effect of terminal electron acceptors within sites and also on uranium redox behaviour [5,48]. Enrichment of cultures obviously provides a selection bias towards particular groups of organisms, and as such this methodology is best for predicting the microbial populations that may dominate a contaminated system rather than the actual population as microcosm operating under *in-situ* conditions would.

2.4. Direct visualisation methods

The presence of micro-organisms within a sample can often be confirmed using simple staining in conjunction with microscopy as a detection method. Total microbial counts within ground water and leachate samples from sites associated with European, US and Swiss disposal concepts have been achieved previously. In each case a DNA specific stain (DAPI or acridine orange) was used and the fluorescence observed using epifluorescence microscopy

[44,49,50]. The use of filtration techniques can improve the detection of micro-organisms when they are expected to be low in number or when large volumes of sample are present, this method was employed by Hallback and Pederson to achieve total cell counts in groundwaters relevant to the Scandinavian concept [39]. Chicote *et al* [51] used SYTO 9 and propidium iodide stains from a commercial kit to differentiate between viable and dead cells present within spent fuel ponds, where propidium iodide stains cells with compromised membranes. Alongside the development of nucleic acid based methods, fluorescent probes can also be used, where the probe itself is complementary to DNA or RNA within a sample. Fluorescent in situ hybridisation has been used by a number of authors where specificity of the probes have been exploited to differentiate organisms with different groups or those containing particular genes, allowing for the quantification of organisms of a particular type alongside total counts [52,53]. The ability to determine the number of viable cells or presence of particular groups within a disposal concept is of interest with respect to predictions associated with facility colonisation. These methods however are limited in the amount of information that can be obtained when the number of micro-organisms present is below detection limits, or indeed when the number of groups present within the sample is such that a large number of probes is required.

2.5. Detection of viable micro-organisms

A number of biochemical markers are available for the detection of viable organisms *in-situ*. Adenosine tri-phosphate (ATP) is the cornerstone of energy transfer within cells and as such is an indicator of microbial activity within a system [54]. ATP levels within groundwaters relating to the Scandinavian concept demonstrated that the technique was a useful method for the detection viable cells with a limit of 2×10^3 cells mL^{-1} [55]. Another method for the detection of the presence of micro-organisms is phospholipid fatty acid (PLFA) analysis, in which microbial membrane components are extracted from using an organic solvent [56]. PFLA analysis not only provides an estimate for the total number of micro-organisms within a sample, but can also give a representation of which groups are present since specific groups are represented by certain biomarkers. This method has been used to estimate the total numbers and populations present within both the U.S, Swiss and Canadian concepts in clays, buffers and in corrosion experiments [38,57,58].

2.6. Nucleic acid based methods

2.6.1. Nucleic acid extraction

In order to determine the species present or contributing to a biological system the use of molecular biology techniques has come to the fore by exploiting the unique characteristics of the genome. The initial stages of these analyses involve isolation of nucleic acids from the sample, where extraction from environmental samples can prove to be difficult due to number

of factors such as pH and the presence of high organic loads [58]. Various techniques have previously been described using chemical and physical methods in synergy to lyse the cells, followed by further chemical treatment to remove cell debris and other constituents that would otherwise contaminate the nucleic acid sample [59,60]. Equally a range of commercial kits have been made available to rapidly and reproducibly extract nucleic acids from environmental samples which drastically speed up the process of extraction of large sample numbers. The extraction of both DNA and RNA can be utilised for downstream applications, where a cDNA synthesis step is required of RNA prior to use.

2.6.2. Polymerase chain reaction (PCR)

PCR is used to then amplify specific regions of DNA, which in themselves may be group or species specific. The reaction itself takes advantage of a DNA polymerase that operates under thermophilic conditions, originally isolated from *Thermus aquaticus* [61]. Primers, small (18-25bp) oligonucleotides that are complementary to the 3' and 5' regions of the sense and antisense strands of DNA around or within the amplicon of interest are also required. This technique is a cost effective method of sampling a range of specific sites within a sample, where nested PCR can find a secondary region within an initial amplicon to further differentiate between groups. This technique has been used by previous authors to determine the presence of anaerobic gut fungi within cellulose wastes and determining the presence/absence of known cellulose degrading bacteria from samples [62,63].

Although this technique can show a degree of specificity, this technique is unable to strongly differentiate between species when a large sample mixture is present. PCR can also suffer from bias, where the nature of primers means that they may bind the DNA of certain species more strongly than others, which can lead to issues if further downstream techniques are to be applied [64-66]. Another potential criticism is the manner in which PCR is a presence/absence approach, however recent technological developments have allowed for the quantification of groups within a total sample by either relative abundance or by number of gene copies using a quantitative PCR (qPCR) approach. qPCR takes advantage of fluorescent markers within a PCR mix that fluoresce on formation of a PCR product, the relative fluorescence can then be compared against a standard curve in order to quantify the initial concentrations of gene copies. Green *et al* [67] used qPCR techniques to establish the abundance of nitrate reductase genes and the presence of *Rhodanobacter* sp within nitrate and uranium contaminated sediments and ground waters at Oakridge. Similarly, Lear *et al* [68] were able to track the abundance of micro-organisms from the Family *Geobateriaceae* in flow through columns investigating the effect of iron reducing micro-organisms on the solubility of technetium.

2.6.3. PCR-gradient electrophoresis techniques

One of the most commonly used primer targets is the gene encoding a micro-organisms 16S ribosomal RNA. The 16S rRNA gene is present in all bacterial species, and although different from the bacterial 16S, a similar gene is also present in Archaeal taxa. Despite having ubiquity between species, the gene itself contains regions of variability between species and as such these variations can be exploited through advances in sequencing to determine identity of individual organisms. Following initial PCR reactions to amplify the 16S rDNA, studies on microbial populations have been carried out using temporal thermal gradient electrophoresis (TTGE) and denaturing gradient gel electrophoresis (DGGE). Both of these techniques exploit the variation in G-C content within the amplified PCR product, such that as the temperature/denaturant concentration increases, products with lower G-C content have hindered mobility through the gel [69-71]. Most recently, Islam *et al* [72] used DGGE to describe the microbial populations present within uranium deposits in two Indian regions, detecting a range of microbial groups. The use of these techniques in environmental samples suffers from issues surrounding band resolution, due to the potential for a large numbers of bands to be present, where in some instances organisms can generate more than one band. Despite this, the use of these methods can prove a potentially useful tool in enriched microcosms to determine the point at which the microbial population within the sample has stabilised, as the gels produced during the sample period should converge to a common profile.

2.6.4. Cloning of PCR products

As with DNA extraction, the availability of kits, and in particular plasmids and improved competency of *Escherichia coli* sp has allowed cloning techniques to be implemented on a greater scale. In this case the PCR products are ligated into a plasmid, which are then transformed into competent *E.coli*. As each *E.coli* is generally only capable of the uptake of one plasmid, each resultant colony should contain multiple copies of one PCR product which can then be extracted and sequenced [71,73]. This approach was used by Wilkins *et al* [74], where alterations in community structure were described with the introduction of ferric iron into far field sediments obtained from LLWR to investigate the behaviour of uranium and technetium. In a similar fashion Fox *et al* [48] were able to describe the changes in community structure under conditions favouring microbial uranium reduction. In terms of the use of this technique in order to describe the micro-organisms present within a radioactive waste disposal site, Pedersen *et al* [75] were capable of describing 155 unique sequences from 50 sample sites, where a number of other genera were also identified.

The use of sequencing techniques can be used downstream of both the TT/DGGE and vector cloning techniques to determine the nucleotide sequence of the 16S rDNA isolated. The use of databases to compare nucleotide sequence data will be discussed further in the next section

(2.6.5), however the clearest advantage of these techniques is that the nucleotide sequence can be compared to get a closest match at a species level to describe an isolate or entire community without direct isolation. These techniques are influenced by the PCR bias previous described, as the use of degenerate primers to amplify the 16S rRNA gene means that primers may bind the DNA of some organisms more than others [64]. The exponential nature of the PCR reaction means that as a result, where primers bind with less efficiency, these organisms will be less well represented following gradient electrophoresis and clone library generation. The cost of sequencing can also be prohibitive, where organisms that are present in smaller proportions are likely to be missed. One method that may be employed to reduce sequencing costs is the use of restriction fragment length polymorphism (RFLP). This method is often employed in conjunction with a clone library, such that the vector inserts are isolated and amplified prior to incubation with a number of restriction enzymes. The enzyme treated amplicons are then electrophoresed, subsequent clones with the same RFLP profile are then assumed to be similar enough such that only one insert requires further sequencing. This method was used to differentiate phylotypes within arid soils in conjunction with clone libraries by Dunbar *et al* [76]. Terminal restriction length fragment polymorphism (T-RFLP) has also been employed as a standalone method, wherein the primers used are fluorescently labelled prior to enzymatic treatment. Lukow *et al* [77] successfully used this method to detect the changes in soil profiles by detecting the changes in fragment sizes when the enzyme treated reactions were separated.

2.6.5. Analysis of sequence data

The generation of a large number of sequences from the techniques previously mentioned would be useless without a means of comparison with genomic data from isolated species. An integrated database of genomic information is available from Genbank [78], where sequence data generated across the globe is stored for comparison. In addition a number of search strategies are available to allow for comparison of obtained sequences with those in the database, these are part of the National Center for Biotechnology Information's suite of resources [79]. The use of these search strategies allows for comparison and data retrieval in order to describe microbial communities as well as provide sequence data for phylogenetic analyses and descriptions.

2.6.6. Emerging techniques

There are a number of emerging techniques that seek to overcome the issues outlined above, these techniques can often be used in conjunction with each other and commonly use high throughput sequencing, where millions of sequences are generated. In addition, the functional side of the system can be investigated by sequencing the mRNA present within the cells to generate a transcriptome (single isolate) or metatranscriptome (mixed community). Stable isotope approaches; where degraded, labelled substrates are incorporated into the genome of

the micro-organisms prior to the use of sequencing techniques are also employed. The field of metagenomics involves a high throughput sequencing approach, where gDNA is fragmented using a 'shotgun' approach before being sequenced, giving both a greater sequence length but also a broader range of loci, where the use of high throughput sequencing over basic Sanger approaches gives read numbers of >millions. This approach has been utilised in a range of soils to identify the organisms present as well as a tool for searching for particular genes within a sample (bioprospecting) [80,81]. A combination of these methods was used by Edwards *et al* [82], who constructed a metagenome to determine the phylogenetic groups involved in the degradation of cellulose emplaced *in-situ* in the Irish Sea. The subsequent reads were used to also determine the presence and number of genes involved with cellulose degradation. A caveat to the construction of metagenomics libraries is that they are more suited to 'simple' populations where diversity is low. Equally, the indirect sequencing of genomic information means that much of the analysis is difficult due to the lack of complete reference sequences. Where a sample of interest is likely to display heterogeneity, the targeting of the 16S rDNA again provides a platform for the determination of phylogeny within that sample, where a significantly large database exists for comparison. This approach has also been used to describe the biomes of soils, gut and ocean [83-85], it should be noted however, that some authors have reported that these two approaches using the same sample can give variation in result [86]. Isolation of the 16S rRNA directly from a sample prior to the generation of a cDNA library through reverse transcription can show which organisms are active within a system. An example of this can be found in [67], where the authors obtained 1,550 sequences from ground waters at the Oak Ridge facility.

Where a metagenomic library gives the phylogeny present within a sample, sequencing of the RNA present within a sample can give a functional analysis to a system, by describing the genes being expressed within a sample. Metatranscriptomic approaches involve the sequencing of reverse transcribed mRNA. As previously described, the main benefit of this strategy is that the community described is the one which is metabolically active within the system. Again, a strong dependency on a large database for comparison against reference sequences or the generation of a metagenome is required. Zakrzewski *et al* [87] used the latter approach to describe the expression occurring within a biogas producing reactor. Using this approach the authors found that over 90% of the expressed RNA was 16S rRNA, stressing the importance of enriching mRNA prior to sequencing where little over 2% of total reads were mRNA in origin. Subsequent authors have removed rRNA using commercial kits prior to sequencing in the description of the expression occurring in a deep sea hydrothermal vent, which exhibited strong expression of ammonium, methane and sulphur oxidising genes [88].

Another synergistic approach that can be used alongside these sequencing techniques is that of stable isotope probing, to further differentiate the specific taxa functioning within a system.

Stable isotope probing (SIP) involves enriching a system with a substrate which has a stable/radioactive isotope (e.g. ^{13}C, ^{14}N, ^{34}S, ^{18}O, ^{14}C). Following microbial action, the metabolites of the SIP substrate can be determined using mass spectroscopy where the mass peaks can be compared to a non-SIP system [89]. In addition, isotopes are also incorporated into the DNA and RNA of the micro-organisms using the substrate. Following separation of the heavier fraction of SIP-DNA or SIP-RNA, a sequencing strategy can then be carried out. In examples of SIP, Eichorst and Kuske were capable of determining the organisms present within grassland soils that were responsible for cellulose degradation through enriching microcosms with ^{13}C- cellulose [90]. Dumont *et al* carried out SIP on methanotrophs from aerobic sediments and analysed DNA, rRNA and mRNA to determine the species and genes involved in the degradation of ^{13}C labelled methane [91]. SIP methods are useful for the differentiation of organisms present within a sample and those contributing to the cycling of substrates of interest, however the timing of sample extraction appears to play an important role in the yield of labelled nucleic acids [91]. In addition, the methods for the separation of labelled nucleic acids require centrifuges capable of large G-forces and can often require lots of time with regards to method development [92].

2.7. Summary of Chapter 2

The detection and identification of micro-organisms within any system is clearly a challenge, where methods are split between 'traditional' culturing methods and more 'modern' molecular approaches. Traditional approaches are useful tools in the isolation of individual isolates, which in turn may indicate the biochemical pathways involved in ISA metabolism. As no disposal facility is in an operational phase, the use of microcosm studies provides a platform for the simulation of the prevailing geochemical conditions likely to be influencing microbial activity. The use of more modern, molecular sequencing techniques will provide a useful adjunct in predicting the taxonomic structure of the microcosms, as well as potentially the genes expressed.

3. Microbial processes relevant to geological disposal

3.1 Overview

It is entirely possible that micro-organisms may colonise the GDF in the construction and post closure phases of its operation. These microbial consortia may have a significant impact on the fate of both CDP and associated ISA's and furthermore, any radionuclides that may be associated with these substrates. Microbial processes that may occur within the GDF are considered in the following section, where individual processes will be governed by the prevailing geochemical conditions of the niches that are likely to form within the facility [93].

Classically, microbially mediated reduction processes are governed by a chemical redox cascade where oxygen, nitrate reduction, iron (III) reduction, sulphate reduction and finally methanogenesis are sequentially carried out based upon the local geochemistry [94]. Where larger organic substrates are concerned, such as glucose, fermentation processes are likely to occur in the absence of oxygen, where the substrate is simultaneously oxidised and reduced through disproportionation of the molecule [95].

With respect to a GDF, oxygen is likely to be consumed during the early post closure phase of the facility through corrosion of the steel canisters containing the waste form [2]. Ferric iron is therefore likely to be present as a result of the corrosion processes mentioned above, however, the solubility of these ferric iron phases at high pH may limit iron reducing processes to the corroded surfaces or be absent altogether due to thermodynamic challenges [96]. Similarly, although present within in the waste forms, nitrate is unlikely to influence the bulk geochemistry of a GDF. Analyses suggest that the deep ground-waters throughout the United Kingdom contain significant amounts of sulphate, which, as ground-water permeates a GDF during re-saturation potentially provides a source of sulphate for microbial reduction processes [97]. The presence of carbon dioxide in a GDF is likely to be as a result of fermentation processes occurring, where carbon dioxide is one of the products of this process. The availability of carbon dioxide prior to fermentation processes may be limited due to the presence of cementitious materials used as a backfill, where carbon dioxide is likely to found as carbonates following carbonation processes [2].

The following section will discuss previous research conducted on microbial metabolism of ISA. In addition, further discussion is provided as to the relevant processes described above: fermentation, iron reduction, sulphate reduction and methanogenesis, with particular attention to the processes occurring at high pH.

3.2 Microbial degradation of ISA

The first reported work on the use of ISA as a substrate for microbial growth was produced by Williams and Morrison in 1982 [98]. Unlike subsequent work, which would involve the remediation of the wastes associated with the Kraft process or influence of microbes on the

fate of ISA in a GDF concept; this initial work sought to use ISA as feed stock for rumen micro-organisms. In these experiments, low quality forage material was pre- treated with sodium hydroxide, generating saccharinic acids, including meta and isosaccharinic acids. This was then used as a carbon source for bacteria and protozoa isolated from sheep rumen, with the principle findings being that under anaerobic conditions, the pre- treatment of forage material generated ISA and MSA which were degradable by rumen micro-organisms, although they were both poorly utilised in comparison with glucose.

The work of Horiko *et al* [99], filed as a patent in 1982 described a method for the cultivation of micro-organisms present within natural soils that were capable of growth within media containing the components of black liquor including both ISA and MSA in liquid and solid media. The patent also describes a catalogue of organisms through a range of biochemical methods. A potential criticism of this work, which the authors acknowledge, is that no attempt was made to determine the carbon source being utilized and as such the organisms cultivated may or may not be utilising the ISA or MSA present within the source media. The work also reported that these organisms were capable of survival and growth at optimum pH values of 10.0.

Strand *et al* [100] attempted to determine whether ISA could be degraded under aerobic conditions, where α-ISA was chosen as a substrate due to its (relative) ease of production over the β-ISA counterpart. A range of samples were taken from areas in and around a Kraft paper mill and a mixture of enrichments and streak plates produced on a base media containing peptone and yeast extract, with glucose or α-ISA included as a carbon source. In addition, these media were used with a range of laboratory strains isolated from forest soils. The authors found that none of their laboratory strains were capable of growth on the media containing ISA, however, isolates from the Kraft mill inoculum were found to degrade ISA at pH values 7.2 and 9.5. As a result, the authors came to the conclusion, like Horiko, that common forest soil bacteria were incapable of utilising ISA as a substrate. They predicted that the catabolism of ISA required "some unusual or modified enzyme(s) compared with breakdown of other carbohydrates" that was only present in the micro-organisms colonising a paper mill site.

The work produced by Strand described a contaminated pond isolate *Ancylobacter aquaticus* strain through microscopic techniques that was capable of ISA degradation. In a similar fashion, works by Bailey [101] and Pekarovičová [102] have also described aerobic ISA degrading isolates, both from contaminated land surrounding a paper pulping mill. Bailey described two isolates that were capable of growth in a medium containing ISA, but both were unable to degrade glucose, both grew at relatively acidic to neutral pH values (5.1-7.2) and seemed to grow without the need for organic nitrogen. Pekarovičová described an ISA degrading isolate of *Micrococcus lylae* that was active at pH 5.0-9.0.

Wang and colleagues [103], were the first to investigate anaerobic biodegradation of α- ISA and ISAs present within Kraft black liquor for industrial processing. Initial experiments investigated the ability of micro-organisms taken from a bioreactor used to treat Kraft waste waters to degrade glucose or ISA in the presence/absence of chlorinated phenols. In these experiments; the inoculum was capable of degrading both carbon sources in the presence or absence of the halogenated compounds, with the result being the generation of methane. Equally, the investigators reported that the production of methane appeared to be a two stage process, where production followed an initial lag. Interestingly, the authors also speculated that the carbon source may have resulted in two different (glucose or ISA based) anaerobic consortia developing, leading to a variation in methane production rates. In Kraft black liquor experiments, where the Kraft black liquor contained lignin alongside a range of small acids including the α and β stereoisomers of ISA, the initial liquor was treated in a range of ways prior to inoculation (acidification, filtration and dilution) to remove a portion of the lignin content. In these experiments, the pre-treatments (acidification/filtration) used increased the concentration of aliphatic acid added to reactors. As a result, increased methane production was observed with the caveat that methane production was not stoichiometric, suggesting that the other organics (including ISA) present in the liquor were contributing to the production of methane.

The most recent work studying microbial interactions with ISAs, and one of the first with regards its effect on radionuclide solubility, came as part of a report for the United Kingdom Nirex Ltd by Grant and colleagues [93], A range of consortia were isolated from both natural and contaminated alkaline sites, where growth at pH 10.5 in the presence of ISA was limited with consortia from 'common' uncontaminated soils. These consortia were taken and provided with a source of ^{14}C ISA and a nitrogen source in the form of nitrate, resulting in the oxidation of ISA through the reduction of nitrate to nitrite followed by a second reduction to nitrogen coupled with the formation of $^{14}CO_2$. Using continuous flow, chemostatic reactors, a large variation in rates was seen from the planktonic cells, with a maximum between 5.6 and 0.2 mol ISA yr^{-1} g^{-1} observed. In addition to planktonic cell experiments, a range of biofilms were grown on the surface of NRVB blocks, in these experiments the rate of degradation was again varied, with rates between 40.6 and 350 mol yr^{-1} m^{-2} NRVB observed. In these cases the differences in rates between biofilms was attributed to the variations in film thickness and species present within the film, more importantly, these biofilms demonstrated the ability to degrade ISA up to pH values of 12.5.

Francis and Dodge [104] also described an aerobic bacteria capable of degrading ISA. In the same year, whilst investigating the effect of ISA, EDTA and NTA on the solubility of technetium and rhenium, found that soil consortia present within grassland soils appeared to be

capable of the degradation of ISA at pH 6.25 within 42 days under nitrate and iron reducing conditions [105].

In 2014, Bassil *et al* [106] produced a range of cultures using calcium ISA as a sole carbon source. In this case, micro-organisms from hyper-alkaline sediment (discussed further in 3.3.2) were used and ISA consumption profiles generated under aerobic, nitrate reducing conditions at pH 10.0. Since Horikos' work did not determine the carbon source utilised, this study represents the highest recorded pH for the degradation of α-ISA under aerobic conditions. Subsequent analysis of the consortia ecology suggested the aerobic system was dominated by Proteobacteria, however at a genus level, a number of species were present from this phylum. In a similar fashion to the study by Grant *et al*, nitrate reduction was observed linked to both the oxidation of α-ISA, and acetic acid resulting from the fermentation of α- ISA. Analysis of 16S rRNA sequences showed that this culture was dominated by Proteobacteria, with Firmicutes and Bacteroidetes also present. At a genus level, these groups were exclusively represented by *Azoarcus* sp, *Anaerobacillus* sp and *Pauludibacter* sp. Iron and sulphate reducing cultures were also prepared in this study, however they will be discussed further in sections 1.5.2 and 1.5.3 respectively.

3.3 Survival of micro-organisms under the conditions of a GDF

The survival of a micro-organism rests with its ability to carry out enzymatic reactions within its cytoplasm in order to generate energy and maintain essential chemical processes [93]. To micro-organisms from near surface environments, the optimum conditions required to maintain these processes are that of circa-neutral pH and soil temperatures of 10-20ºC In optimum conditions, a micro-organism is at its most metabolically active and as a result, will grow and proliferate [93]. Shifts to extremes of pH, which with respect to a GDF concept deal solely with that of alkaline conditions, require a response from the micro-organisms in order to return the cytoplasm to optimal pH [107]. Failure to respond to the changes in pH will ultimately result in the death of the organism, as is found with *Caloramator fervidus* [108]. Other organisms are merely capable of surviving in the extremes of pH, in which they are still viable, but unable to grow and proliferate. It is thought that this pH gradient is maintained by the use of Na^+/H^+ antiporters which allow the acidification of the cytoplasm through pumping H^+ into the cell [107,109]. Micro-organisms that are capable of growth and proliferation in optimal pH values between 8.5-11.0 are referred to as alkaliphiles [110]. These organisms often have a cytoplasmic pH greater than 7.6, and as such their internal enzymes, such as those required for protein synthesis, operate at a higher pH than that of neutraphiles [110]. Other mechanisms include the incorporation of more acidic polymers and amino acids into the cell walls than is found in neutraphilic species [110,111]. Evidently, micro-organisms exhibiting facultative or obligate alkaliphilic characteristics are the most likely to colonise a GDF, predictions can be

made as to the taxa likely to colonise a GDF by observing the taxa present within soils where the *in-situ* pH is alkaline.

3.4 Natural and anthropogenic analogues to a GDF

3.4.1 Natural analogues

Natural and anthropogenic analogues for the conditions experienced in the facility give an interesting insight into conditions and behaviour of stored waste, in addition to being a potential reservoir of organisms that are capable of surviving in extremes of pH and radiation, relevant to the disposal concept [112-114]. The presence of alkaline waters and sediments have been reported in a number of countries across the globe in North America [115], Africa [116] and Asia [117]. These environments are usually formed through the interaction with salts present within the local rock formations, with subsequent evaporation processes leading to high alkalinity and salinity [116]. Studies into the diversity of the micro-organisms and metabolisms occurring at these sites are numerous, and have led to the description of a number of novel species. In North America, Mono Lake (pH~10.0) in California has been described as meromictic (having layers that do not intermix) by Humayoun and colleagues [115]. Each sub region within the lake was seen to have varying physiochemical propertied at varying depth, which in turn led to a varying degree of bacterial subtypes including α, β and γ Proteobacteria, alongside a range of low and high G+C content organisms by 16S sequencing techniques [115]. To this effect, Mono Lake has been the source of a range of novel haloalkaliphilic isolates. Blum *et al,* isolated two *Bacillus* species that were capable of reducing both selenium and arsenic under anaerobic conditions where both elements were present at source [118]. Other work in this area has shown that fermentative [119,120], sulphate reducing [121,122] and sulphur oxidising species [123] are present within the area. Kenyan soda lakes in the Kenyan-Tanzanian Rift Valley have also been investigated, with again a range of α, β and γ Proteobacteria, alongside a range of low and high G+C content organisms akin to Mono Lake observed [116,124].

Away from soda lakes, another natural analogue is present in Cyprus, in the Troodos mountains, where hyperalkaline springs are a result of serpentinisation of ophiolites and the interactions these complex rocks have with local waters [125]. Recent studies into the micro-organisms present within these alkaline waters have shown that the sediments were phylogenetically diverse. A range of iron reducing isolates were obtained from the water samples, which through batch experiments were shown to reduce ferric citrate up to a pH of 9.5 [126]. Another ophiolite based natural analogue can be found in Oman, and the presence of microbial activity here has also been studied [127], although low numbers of viable micro-organisms (10^1-10^3 mL^{-1}) were observed, again a diverse community was isolated from the samples obtained. A site at Maqarin, Jordan also exists where hyperalkaline waters are present

due to interactions with groundwater and naturally occurring cement like materials at the site [117]. Subsequent studies on the microbial ecology of the site has shown that total numbers of organisms were higher than those observed with the Oman site (10^3-10^5 mL^{-1}) and 16S rRNA showed that Proteobacteria were the most common phylum present [128].

3.4.2 Anthropogenic analogues

Anthropogenic sites often arise due to land contamination through industrial processes, which can lead to the formation of extreme geochemical environments. The contamination itself may result in the increased concentration of potentially bactericidal heavy metals (such as arsenic, zinc, copper and chromium [129-131]) or other chemical compounds [132-134]. In addition, the contamination may present a change within the basic conditions within a site by influencing parameters such as temperature, radioactivity and pH. In the short term, these changes are likely to detrimentally impact on the microbial consortia present within these environments by reducing population size. Following both time and re-colonisation, it would appear that the micro-organisms can be detected within these sites regardless of the stresses placed upon them by the change in local environment.

With relevance to geological disposal, a site in Buxton, Derbyshire was investigated previously. The *in-situ* pH at the site is elevated as a result of the disposal of lime kiln wastes which were tipped into over the sides of the adjacent valley, known as Brook Bottom. Large volumes of waste made up of partially calcined limestone, lime, part burnt coal, coal ash and coal clinker were disposed of [135]. Percolation of groundwater leads to the formation of a calcium hydroxide leachate, which generates a calcium carbonate tufa following the dissolution of atmospheric carbon dioxide. Beneath the carbonate precipitate, Burke *et al* [114] found that the soil consortia was capable of nitrate and iron reduction at pH~12.0, where the electron donor was unknown. Subsequent 16S rRNA gene profiles suggested that β-proteobacteria were the dominant phylogenetic class present, although organisms from the Families: Bacteroidetes, Thermotogae and Firmicutes were also detectable. The same sediments were used as an inoculum for single batch reactors investigating the potential for the micro-organisms present to carry out nitrate, iron and sulphate reductions up to a pH of 12.0 [96]. In this study, microbial activity above pH 11.0 could not be achieved in the presence of any of the terminal electron acceptors using a lactate/acetate mix as an electron donor. The sediment from this area was also used as an inoculum for the ISA degradation of Bassil *et al* discussed previously [106]. The disposal of chromium residues also leads to the formation of hyperalkaline conditions where the extraction of chromium from its ore is carried out in the presence of alkali hydroxides, which is disposed alongside the chromium residues [136]. Subsequent studies into a site in the north of England have shown that the consortia present in the sediments at the site were capable of chromate, nitrate and iron reduction in a pH range of

8.9-11.7. *Deinococcus* sp dominated the background sediment, however the samples were later dominated by Firmicutes and β-proteobacteria depending on the geochemical conditions experienced [137].

3.5 Fermentation processes

Within fermentation reactions, the organic carbon source acts as both the electron donor and acceptor [94]. The most common end products of fermentation are volatile fatty acids (VFA) and gas, although alcohols may also be formed, where this process is commonly utilised in wine, beer and cheese making. These examples often involve the use of a single species of micro-organism, where a specific outcome in terms of end products is desired within a commercial product. Within mixed, undefined cultures, the products of the fermentation are more likely to be a mixture of VFA, gases and alcohol [94]. A number of authors have investigated fermentation processes under alkaline pH. Increasing the pH of a fermentative system up to pH values of 10.0 and 11.0 reduced the rates of both protein and carbohydrate fermentation in studies by Yuan *et al* [138]. Liu *et al* [139] found that increasing the alkalinity of a batch reactor using a near surface leachate as a seed source through the addition of carbonate increased the yields of both hydrogen and acetic acid production at a pH range of 8.0-11.0.

3.6 Iron reduction

Under anoxic conditions, certain micro-organisms are capable of oxidising organic matter via the reduction of Fe (III) to Fe (II) in the presence on H_2. Such organisms that are capable of utilising Fe (III) are present in a range of near surface environments [140]. The crystalline nature of iron (III) oxides at pH >4.0 provides a challenge for these iron reducing micro-organisms and three strategies have been described to overcome this. Reguera *et al* [141] observed a process of electron transfer involving direct contact with the oxide through the use of extracellular nanowires (Figure 3.1A). Other species, including *Shewanella* sp have employed the oxidation of endogenous or exogenous electron shuttles, such as flavins [142] or anthraquinone disulfonate (AQDS) [143,144], to carry out the initial reduction of iron (III) before reducing the humic matter as a two stage process involving abiotic and biotic mechanisms (Figure 3.1 B) [144]. Finally certain species are capable of generating organic ligands that are capable of acting as a chelating agents which alter the chemical composition of Fe(III) and increase its availability for reduction (Figure 3.1 C)[145].

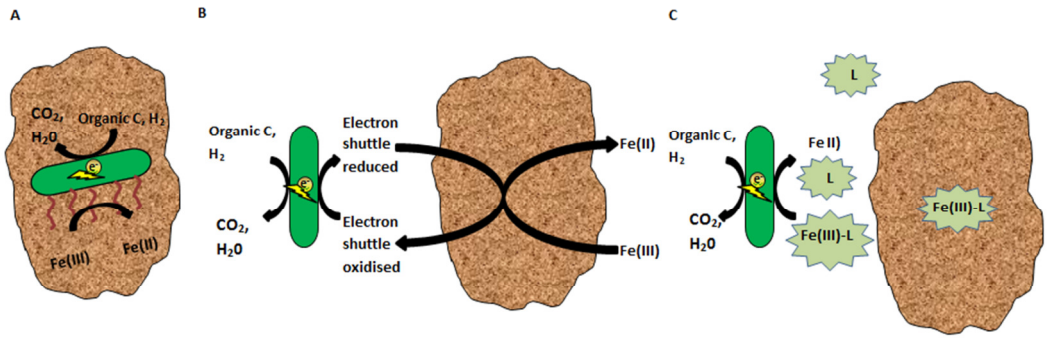

Figure 3.1 Strategies employed by iron reducing micro-organisms for electron transfer (reproduced from [146]) e-=electrons L=ligand. In some cases (A) the micro-organism may be capable of the direct contact with an Fe(III) source through nanowires. The use of enogenous/ exogenous electron shuttles (B) or ligands (C) provide an abiotic method being oxidised to reduce Fe(III) sources which can in turn be reduced my the micro-organism.

Within a GDF concept sources of iron (III) are likely to arise from corrosion of waste canisters where C-steel is included [147] and potentially from the host rock of the chosen site. Much of the research conducted has sought to determine the ability of near surface organisms to reduce iron present in both amorphous and crystalline forms. Lovley *et al* showed that amorphous iron was more readily reducible than more crystalline forms by iron reducing *Geobacter metallireducens* [148]. Work by the same authors showed that iron reduction could occur alongside methanogenesis when enrichments from the Potomac river were supplemented with hematite or amorphous iron (III) oxyhydroxide [149], having previously shown a portion of Fe(III) present at the site was microbially reducible [150].

Previous authors have noted the ability of these consortia to reduce and cycle other elements following reduced availability or absence of iron, including uranium, arsenic and chromate alongside a range of other metals [151-154]. Equally consortia have been noted as contaminants and bioremediation aids in the petrochemical industry [155-157]. With regards to the alkaline conditions observed within a GDF concept, a few species have been described with the ability to utilise iron at high pH. Ye *et al* [158] appear to be one of the first authors to describe an isolate capable of metal reduction at alkaline pH. Sediments from leachate ponds at the Borax Company in California were the source of an *Alkaliphilus* sp that was capable of the reduction complexed iron (III) where yeast extract and lactate could serve as an electron donor. The isolate was reported to grow between pH 7.5 and 11.0 with an optimum of pH 9.5.

A species from the family Geobacteriaceae, *Geoalkalibacter ferrihydriticus* was isolated from a Russian alkaline soda lake (Lake Khadyn, Tuva, Russia). This isolate was capable of reducing amorphous iron hydroxide and EDTA-Fe (III) where acetate was the electron donor, but was also capable of using AQDS, Mn (IV) and S^0. This species was also found to be

halotolerant, demonstrating an facultatively allkaliphilic nature; it survived at a range of alkaline pH values from pH 7.8-10.0, with an optimum pH of 8.6 [159]. From the same sediment, Zhilina *et al* were capable isolating a novel *Natronincola ferrireducens,* where this species was an obligate alkaliphile that was not only capable of peptide fermentation processes, but also of the reduction fumerate, crotonate amorphous iron hydroxide and EDTA-Fe(III) as electron acceptors at an optimum pH of 8.4 [160]. The same authors also isolated a similar strain, *Natronincola peptidovorans,* from Lake Verkhnee Beloe, which had similar characteristics to *N. ferrireducens* with major differences being the ability to ferment pyruvate, only being able to use amorphous iron (III) hydroxide as an iron (III) based electron source and an optimum pH of 8.4-8.8 [160]. Soda lakes in the US have also provided new isolates of iron reducing bacteria; in this case a novel *Bacillus* sp was isolated from Soap Lake, WA. Due to its facultatively anaerobic nature; this isolate was capable of aerobic respiration as well as fermentation processes alongside reduction of iron complexes, at an optimum pH of 9.0, although growth was observed at pH 11.0 [161].

Thorpe *et al* [162] isolated a novel *Serratia* species isolated from an enrichment of sediments close to Sellafield, (Cumbria, UK) that was capable of reducing a range of iron (III) complexes across a range of pH values from 3.5 to 9.5. In these experiments iron reduction at high pH was achieved utilising glycerol as a substrate and iron (III) citrate as a source of reducible iron. Burke *et al* [114] observed the presence of iron (II) at depth at a hyper-alkaline contaminated site at Harpur Hill, Buxton, UK and following on from this both Rizoulis *et al* and Williamson *et al* showed that micro-organisms present at the site were capable of reducing ferrihydrite and/or ferric citrate at pH 10.0-12.0 coupled to lactate and yeast extract oxidation [96,163].

With respect to the utilisation of ISA under iron reducing conditions, an inoculum from the same site that Burke *et al* has been used to generate an iron reducing consortia capable of the degradation of α-ISA by Bassil *et al* [106]. Overlying water from the sediments were taken and mixed with a minimal media containing calcium α-ISA and insoluble ferrihydrite as a ferric iron source at pH 10.0. Following 90 days of incubation, ~36% of the α-ISA present was removed, with the generation of acetate and Fe (II) observed. Subsequent 16S rRNA suggested that the microbial consortia was completely dominated by organisms from the phylum Firmicutes, where at a genus level over 99% of the sequences were most closely related to *Anaerobacillus* sp.

3.7 Sulphate reduction

The sulphate reducing bacteria (SRB) play a key role in the sulphur cycle in anaerobic sediments and are capable of metabolising both carbonaceous substrates and hydrogen [164]. Anaerobic sulphate reduction often involves the dissimilatory pathway, in which elemental sulphur is excreted from the cell as hydrogen sulphide, rather than an assimilatory one in which

sulphur is taken up into the cell. Sulphate is initially converted to adenosine phosphosulphate (APS) via ATP sulphurylase, where the sulphate is transferred to the adenine monophosphate moiety of ATP to form APS and pyrophosphate (Figure 3.2) [165]. APS reductase enzymatically transforms the APS to sulphite, before being further reduced by the dissimilatory sulphite reductase complex *Dsr*AB-C to hydrogen sulphide [166]. In environmental sulphate reduction, the hydrogen sulphide produced in this process will often complex with iron to form a black siderite precipitate. The SRB are of particular interest due to their potential benefits associated with acid mine drainage, but also negative effects involving the corrosion of mild steels [167-169]. Other authors have also noted the potential for SRB to utilise iron and uranium as a terminal electron acceptor, suggesting that many of the taxa are capable of adapting their metabolisms to suit the local geochemical environment [170].

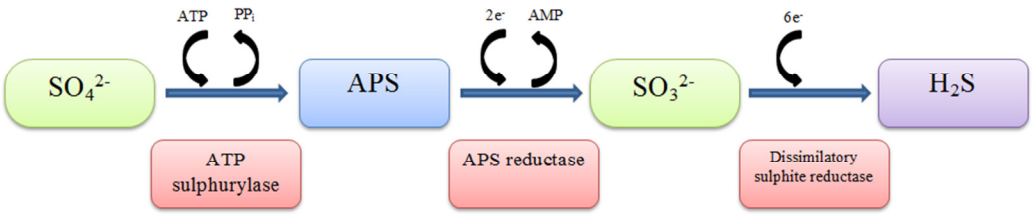

Figure 3.2 Pictorial representation of the dissimilatory sulphate reducing pathway. (Reproduced from [165]). Sulphate is converted to thiosulphate through the action of ATP sulphurylase and APS reductase enzymes. Production of hydrogen sulphide is mediated through the dissimilatory sulphite reductase enzyme.

Sulphate reduction at high pH has been extensively studied using soda lakes (discussed in 3.4.1) as a reservoir of alkaliphilic micro-organisms, where reduction is often traced through the use of $^{35}SO_4^{2-}$. Previous research indicates that micro-organisms present within alkaline lakes in Altai, Russia, were capable of the utilisation of sulphite and thiosulphate at pH10.0 [171], the same lakes were studied for the presence of sulphate specific sulphidogenic activity. Enrichment cultures of sediments from the Kulunda Steppe region showed that sulphate reducing organisms from the family *Desulfobacteriaceae* were present as well as high copy numbers of the *dsr* gene [172]. A longer, more extensive study of a range of lakes in the region was carried out over a five year period [173]. The lakes studied exhibited an *in-situ* pH value of >9.95 across the five years of study with a maximal rate of sulphate reduction of 59.4 nmol cm^{-3} h^{-1} observed at Lake Bitter at a pH of 10.2 in 2006. In addition, the sediments acquired from the lakes were enriched and isolated within the laboratory at pH 10.0 with exposure to varying salinity from 0.6 – 4.0 M Na^+. When cultured, the sediments were capable of both reducing both sulphate and thiosulphate through the oxidation of a range of electron donors. 16S rRNA gene analysis indicated that *Desulfonatronovibrio* and *Desulfonatronum* sp may play a significant role in sulphate reduction taking place *in situ.*

Across the Pacific another hyperalkaline lake, Lake Mono, California, USA has also been investigated. Although much of the work conducted at this site has focussed on the reduction of the arsenate that is present at elevated concentrations [118,174], research into the presence of sulphate reducing bacteria has also been carried out. Work by Oremland *et al* [121] found that sulphate reduction was occurring in the water columns of this meromictic lake at depth at rates of up to 3 µmol L^{-1} d^{-1} at depths of up to 28m within the water columns. Rate constants of 7.6 x 10^{-4} – 3.2 x 10^{-6} hr^{-1} were observed within sediments with an *in-situ* pH of 9.8 representing a sulphate reducing rates of 27.8 mmol m^{-2} day^{-1} [175]. Subsequent enrichment of the sediments has led to the description of a range of isolates capable of sulphate reduction at high pH, where Pikuta *et al* [176] described *Desulfonatronum thiodismutans* from Mono Lake sediments. This isolate was capable of growth at a pH range of 8.0-10.0 with and optimal of 9.5, where hydrogen/carbon dioxide and ethanol were utilised as electron acceptors.

Presence of microbial sulphate reduction occurring at Lake Wadi el Natrun in Egypt was recorded as early as 1963 [177], however subsequent work in isolating sulphate reducing organisms or description of rates *in-situ* is scarce. Lake Magadi, in the east African rift, Kenya, has also been subjected to studies with regards the presence of alkaliphilic sulphate reducing micro-organisms. Jones *et al* found that sediments from this lake were capable of sulphate reduction through positive culture enrichments, although none could be isolated [178]. Following on from this Duckworth *et al* [179] used sediments from lakes in the same region where pH ranged between 10.0 and 12.0, where again, using positive enrichments evidence of sulphate reduction was observed where lactate, acetate, butyrate, formate, fumerate, and ethanol were utilised as electron donors. In 1997, Zhilina *et al* isolated a novel strain from Lake Magadi, which was capable of utilising formate and hydrogen as electron donors, whilst growing at an optimum pH between 9.5 and 9.7 [180].

Away from soda lakes, Goeres *et al* [181] found that mesophilic sulphate reducing bacteria were capable of survival within alkaline waters. In this case, corrosion within a heating plant was occurring, where water was made both anaerobic and alkaline through sodium hydroxide treatment. A mesophilic sulphate reducing consortium was added to samples of the alkaline effluent and was found to be capable of surviving up to a pH of 10.5, with sulphate reduction/sulphide production occurring when the pH was lowered to 9.3. When the same consortium was allowed to generate a biofilm, sulphate reduction could occur at pH 10.2. Other authors have however found that organisms present within sediments from a hyperalkaline contaminated site in Derbyshire were incapable of sulphate reduction at pH 10.0,11.0, and 12.0 where lactate, acetate and yeast extract were present as potential electron donors [96]. Following on from this, Bassil *et al* found that microbial consortia present at this site were also incapable of sulphate reduction when calcium ISA was used at an electron donor at pH 10.0 and 11.0 [106]. These reports suggest that at higher pH values (approaching 10.0-

12.0) microbial sulphate reduction becomes energetically difficult, but not impossible, for micro-organisms. The long timescales involved with the disposal of waste in a GDF mirror the long timescales seen in hyperalkaline lakes across the globe, which suggest that SRB are capable of survival and adaptation to alkaline pH.

3.8 The Archaea

In the absence of terminal electron acceptors such as nitrate, iron and sulphate within a GDF, should ISAs be subjected to fermentation process, the generation of volatile fatty acids such as formate and acetate, alongside carbon dioxide and hydrogen gases are likely to be generated. Any C1-2 organics and hydrogen/carbon dioxide generated are likely to be utilised by methanogens. Methanogenic organisms all belong to the prokaryotic kingdom Archaea. Organisms in this kingdom differ biochemically from the Eubacteria, with variation seen in cell membrane and cell wall compositions in addition to DNA replication and protein synthesis apparatus [182,183]. In the case of methanogens, a range of unique enzymes are used in the generation of methane that are completely absent from Eubacteria and Eukarya [184,185].

3.9 Methanogenesis

The methanogens fall under 5 orders based of their 16S rDNA sequences: Methanopyrales, Methanococcales, Methanobacteriales, Methanomicrobiales, and Methanosarcinales [185]. The methanogens are generally sub divided into two classes; those capable of methane generation from carbon dioxide/hydrogen and formate, with the second class comprising organisms capable of generating methane from acetate. The unique pathways each contain separate coenzymes, tetrahydromethanopterin (H_4MPT) in the CO_2/formate reductive pathway; and tetrahydrosarcinapterin (H_4SPT) in the aceticlastic pathway (Figure 3.3)

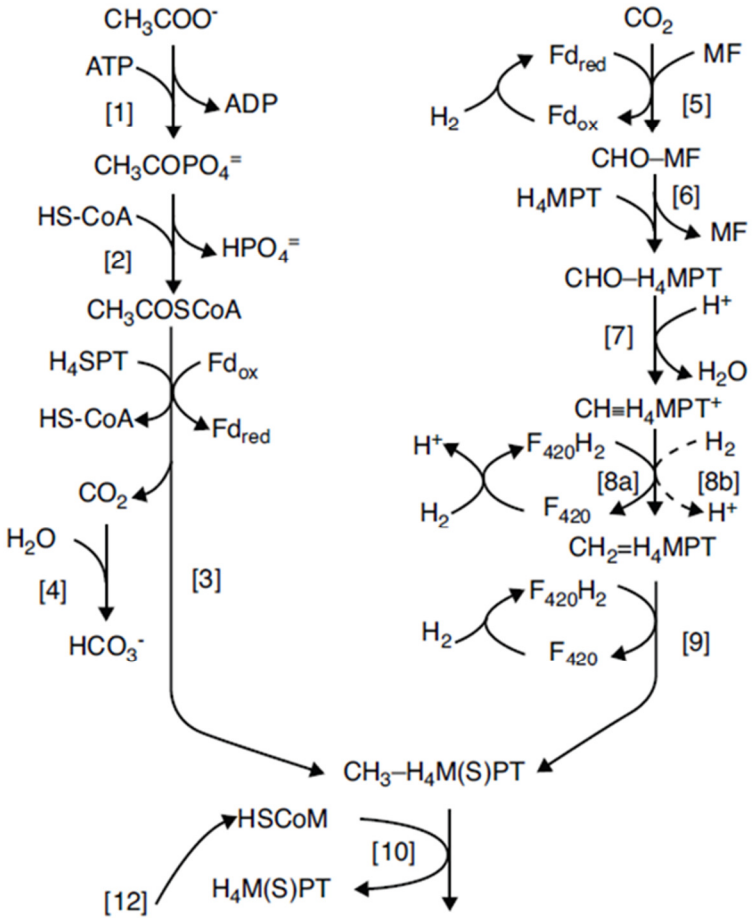

Figure 3.3 Composite of CO2-reduction and aceticlastic methane generating pathways. Reactions (1-4) are unique to the aceticlastic pathway, reactions (5-9) are unique to the CO2 reducing pathway. Pathways diverge and reactions (10-12) are present in both pathways (Taken from [186]).

In each arm, the unique coenzyme is methylated before the pathways diverge, with a methyl-transferase (*Mtr*) enzyme transferring the methyl group to coenzyme M allowing methyl coM-reductase (*Mcr*) to complete the conversion of the methyl group to methane [186]. Authors have also noted the ability of class II organisms being able to utilise methyl compounds such as acetic acid, methylamines and methanol [187,188].

The work of Wu *et al* [189] showed that a range of moderate alkaliphilic methanogens could be isolated from syntrophic methanogenic granules, where *Methanosarcina, Methanospirillium* and *Methanobacterium* ssp were isolated and growth observed up to a pH of 8.5. The same soda lakes that were reservoirs of sulphate reducing bacteria appear to also be capable of supporting methanogenic Archaea due to the varying chemical niches occurring within the sediments. Methanogenesis was observed from enriched sediments slurries at Big Lake, Nevada, US, utilising C1 compounds methanol and trimethylamine at an optimum pH of 9.7 [190]. *Methanohalophilus zhilinae,* was isolated from Bosa Lake in Egypt, which was also

capable of utilising these substrates at a pH of 9.7 [191]. Acetotrophic methanogenesis has been observed within sediment studies of the methanogens present at Soap Lake, Washington US [192]. Hydrogenotrophic methanogenesis appears to be the most common methanogenic process occurring within hyperalkaline lakes. Worakit *et al* [193] isolated four *Methanobacterium* sp from Lake Wadi el Natrun in Egypt, where one of the strains WeN4 was described as *Methanobacterium alcaliphilum.* This novel isolate was capable of oxidising hydrogen coupled to carbon dioxide reduction for the generation of methane, with and optimum growth pH of 8.4, with growth observed up to pH 9.9. A further four isolates were obtained from the same region by Boone *et al* [194], again, these were hydrogenotrophic and isolated from low-saline areas where pH was between 8.3 and 9.3.

3.10 Summary of Chapter 3

The prevailing alkaline conditions of a GDF concept present a challenge to any colonising microbial consortia. Current research suggests that the prevalent source of organic carbon within the GDF, ISA, is degradable up to pH of 10.5 under certain geochemical conditions, predominantly aerobic or nitrate reducing conditions. Studies of natural and anthropogenic analogues suggest that a microbial presence can develop despite the introduction of alkaline conditions given time. The prevailing geochemical conditions within a GDF are likely to result in a fermentative system, with methanogenesis also occurring depending on the availability of fermentation end products and survival of associated Archaea. The presence of ferric iron and sulphate may also be present within niches and current research suggests that alkaliphilic microbial activity along this redox cascade is possible.

4. Aims and Objectives

The long term fate of radionuclides emplaced within a GDF is of clear importance. A range of safety assessments are carried out on each individual component of the multi-barrier approach. The emplacement of cellulose wastes and subsequent generation of CDPs is of particular interest, being that the ISAs that are part of the CDPs are capable of complexation with certain radionuclides. The microbiology of anthropogenic and natural analogues suggests that organisms, as either consortia or isolates are capable of tolerating and growing at elevated pH in combination with a suitable electron donor and acceptor. Previous work has also shown that the α-ISA stereoisomers appears to be degradable by micro-organisms at a range of pH, although in many of these cases, conditions that are relevant to those observed in a potential GDF are absent from the literature.

The ability of micro-organisms to utilise β-ISA is completely absent from the literature, almost certainly due to the difficulties faced with generating sufficient quantities for analytical purposes. Given that ISAs are not observed in the natural environment, it is of interest to determine initially if mesophilic organisms are capable of the degradation of ISAs generated from CDP. Particular interest will be shown to iron reducing, sulphate reducing and methanogenic conditions. With the consideration that carbon dioxide is likely to be the most prominent electron acceptor within a GDF, the ability of generic mesophilic organisms to utilise ISAs at higher pH values and whether carbon flow continues through to methanogenesis will also be investigated. The isolation of any micro-organisms from alkaline pH microcosms could provide a platform for further exploration of ISA degradation rates, potentially providing a route for the bioprospecting of genes relevant to ISA degradation and alkaliphilic properties.

As previous research has suggested that hyperalkaline sediments in Buxton, Derbyshire have the ability to degrade α-ISA under aerobic, nitrate and iron reducing conditions, a site survey will be conducted to determine the presence of both stereoisomers *in situ*. Should they be present, it would suggest that the local microbial consortium has had ca. 140 years with which to select for alkaliphilic or alkalitolerent species capable of the degradation of ISAs. Again, microcosm experiments using these sediments may provide another platform for the determination of rates of ISA degradation by mixed consortia, as well as the micro-organisms involved.

5. Experimental methods

5.1. General reagents

The general reagents described throughout the experimental section were all purchased from either: Fisher Scientific UK (Loughborough, Leicestershire, UK), LabM Limited (Haywood, Lancashire, UK) or Sigma-Aldrich Co. Ltd (Gillingham, Dorset, UK) unless stated otherwise.

5.2. Media

5.2.1. Mineral media

Mineral media was prepared as described previously [195]. Briefly, the reagents listed in Table 5.1 were added to a volumetric flask and made up to volume with ultrapure water that had been flushed with nitrogen for a minimum of 20 minutes to exclude atmosphere. pH of the mineral media was then adjusted as required using 2M sodium hydroxide or 2M hydrochloric acid.

Reagent	Chemical Formula	Mass (g L^{-1})
Anhydrous potassium dihydrogen phosphate	KH_2PO_4	0.27
Disodium hydrogen phosphate dodecahydrate	$Na_2HPO_4.12H_2O$	1.12
Ammonium chloride	NH_4Cl	0.53
Calcium chloride dihydrate	$CaCl_2.2H_2O$	0.075
Magnesium chloride hexahydrate	$MgCl_2.6H_2O$	0.1
Iron(II) chloride tetrahydrate	$FeCl_2.4H_2O$	0.02
Resazurin (oxygen indicator)		0.001
Disodium sulphide	$Na_2S.9H_2O$	0.1
Stock solution of trace elements	See Table 5.2	10 mLs

Table 5.1 Components of mineral media per litre of oxygen free water.

Reagent	Chemical Formula	Mass (g L^{-1})
Manganese chloride tetrahydrate	$MnCl_2.4H_2O$	0.05
Boric acid	H_3BO_3	0.005
Zinc chloride	$ZnCl_2$	0.005
Copper chloride	$CuCl_2$	0.003
Disodium molybdate dihydrate	$Na_2MoO_4.2H_2O$	0.001
Cobalt chloride hexahydrate	$CoCl_2.6H_2O$	0.1
Nickel chloride hexahydrate	$NiCl_2.6H_2O$	0.01
Disodium selenite	Na_2SeO_3	0.005
Disodium tungstate	$Na_2WO_4.2H_2O$	0.002

Table 5.2 Components of trace elements solution per litre of oxygen free water.

5.2.2. Production of Cellulose Degradation Products (CDP)

Cellulose degradation products (CDP) were prepared using a previously described method [196]. Laboratory tissue (200g, Pristine Paper Hygiene, London, UK) was added to 1.8 L of 0.1 M sodium hydroxide and 10 g/L calcium hydroxide in nitrogen purged (ca. 30 minutes) ultrapure water in a pressure vessel. The vessel was then sealed and the headspace flushed for 30 minutes with nitrogen to remove oxygen. The vessel was then incubated at 80°C for 30 days. Following incubation the resultant liquor was filtered under nitrogen in a sealed glove box through a 0.22 µm filter unit (Millipore, Watford, UK) into 1 L vessels that had been flushed with nitrogen before being autoclaved at 121°C for 15 minutes prior to use. CDP was then stored in the dark under ambient conditions.

5.2.3. Sample preparation

Fluids removed from microcosms were transferred to sterile sample tubes (1.5 mL or 50 mL in volume), where tubes were not completely filled a nitrogen headspace was applied. Tubes were then centrifuged at 8000 x *g* to pellet any solids. Following centrifugation the supernatant was transferred to a sterile disposable syringe and filtered through a 0.45 µm filter into sterile sample tubes prior to analysis. In the following section, 'sample' refers to the centrifuged, sterile filtered supernatant obtained from the microcosm.

5.3 Analytical Methods

5.3.1 Detection and quantification of α and β isosaccharinic acids using high performance anion exchange chromatography with pulsed amperometric detection (HPAEC-PAD)

In order to determine concentrations of cellulose degradation products, and in particular the α and β forms of isosaccharinic acid, HPAEC-PAD was employed using a Dionex 3000 or 5000 ion chromatography system (Dionex, Camberley, UK). Software package 'Chromeleon 7.0' was used to integrate and process chromatograms. The system comprised auto-sampler (AS50), gradient pump (GS50) and electrochemical detector (ED50) with gold working electrode and Ag/AgCl reference electrode in amperometric detection mode employing a pre-programmed quadrupole wave form. Analytes were eluted using an isocratic mobile phase of NaOH (50 mM) at a flow rate of 0.5 mL min^{-1} and separation was performed on a Dionex CarboPac PA20 column (6 μm particle size, 250 mm length, 3 mm internal diameter and ≤10 Å pore size) and a CarboPac PA20 guard column (3 x 150 mm). Between analyses, the column was regenerated by eluting with 200 mM NaOH for 20 minutes. Samples amended with 40 ppm D-ribonic acid prior to analysis as an internal standard, 10 μL of sample was injected onto the column and a range of standards prepared using pure α and β ISA prepared using previously described methods [24].

5.3.2 Detection and quantification of volatile free acids using gas chromatography with flame ionisation detection (GC-FID)

Presence and concentration of volatile fatty acids were determined using gas chromatography on a HP GC6890 (Hewlett Packard, UK) using standard methods for environmental sampling [36]. Sample (900 μL) was transferred 1.5 mL tube containing 100 μL of 85% phosphoric acid. Typically 1 μL of sample was injected onto the column. Samples were passed through a HP-FFAP column (30 m x 0.535 m x 1.00 μm; Agilent Technologies, Agilent Technologies) using a helium carrier gas and volatile free acids detected by flame ionization detection with hydrogen/air detector gas under the following conditions: initial temperature of 95°C for 2 minutes, followed by an increase to 140°C at a ramp rate of 10°C min^{-1} with no hold, followed by a second ramp to 200°C at a ramp rate of 40°C min^{-1} with a hold of 10 minutes, falling to a post run temperature of 50°C. A range of standards was prepared from a stock solution of volatile free acids (Supelco analytical, Pennsylvania, US) at a range of concentrations in order to produce a calibration curve for each acid. In each case, the linear regression of each curve was >0.99.

5.3.3 Measurement of total carbon, total inorganic carbon and total organic carbon using TOC5000A

Total carbon (TC) and total inorganic carbon (TIC) were measured using a Shimadzu TOC5000A (Shimadzu, Japan, UK) with nitrogen carrier gas at 150 mL min^{-1} and total organic carbon (TOC) within a sample calculated as the difference between the two. TC was analysed by combustion in the presence of an oxidation catalyst at a temperature of 680°C, carbon dioxide formed as a result of combustion or decomposition was then detected by non-dispersive infrared gas analyser (NDIR). TIC was acidified within the TIC reaction vessel of the instrument, where TIC was decomposed to carbon dioxide and detected by NDIR. The internal processor of the instrument then converts the input signal into a peak area for processing. Standard solutions of TC were prepared by dilution of potassium hydrogen phthalate in ultrapure water at a carbon concentration of 1 g L^{-1}, and standard solutions of TIC component were prepared from a suspension of sodium hydrogen carbonate and sodium carbonate prepared to 1 g L^{-1} IC. Samples were diluted 25-fold in ultrapure water and where necessary, sample pH reduced to <7.0 through the addition of 2 M hydrochloric acid (100 µL per 2.5 mL sample).

5.3.4 Determination of iron (II) and (III) content

Presence and concentration of aqueous iron (II) and (III) concentrations within both samples retrieved from the hyperalkaline contaminated site and microcosm samples was achieved using the methods of Viollier *et al* [197]. Briefly, 1 mL of filtered sample was added to 100µL of 0.01 mol L^{-1} ferrozine reagent prepared in 0.1 mol L^{-1} ammonium acetate and absorbance measured at a wavelength of 562nm. The complete reduction of remaining iron (III) was achieved through the addition of 800 µL of sample to 150 µL of 1.4 mol L^{-1} hydroxylamine hydrochloride (prepared in 2 mol L^{-1} HCl), mixed through gentle pipetting and left for 10 minutes at room temperature. At the end of this time 50 µL of 10 mol L^{-1} ammonium acetate (adjusted to pH 9.5 with ammonium hydroxide) was added and a second absorbance measured. A range of standards of ferrous ethylene diammonium sulphate were prepared to generate a calibration curve.

5.3.5 Detection and quantification of sulphate and nitrate concentration using ion chromatography with pulsed amperometric detection

Presence and quantity of sulphate within the samples was determined using a Metrohm 850 Professional IC (Metrohm, Cheshire, UK) with pulsed amperometric detection, employing a Metrohm Metrosep A Supp 5 column (4 x 150mm, 5 µm particle size) and eluting with an isocratic mobile phase of sodium carbonate and sodium hydrogen carbonate (3.2 mmol L^{-1}, 1.0 mmol L^{-1} respectively). Samples were diluted 10-fold in ultrapure water and 40ppm phosphate

(in the form of potassium phosphate) used as an internal standard. A calibration curve was prepared by analysing a range of sulphate standards (0-1 g L^{-1}) in the form of potassium sulphate.

5.3.6 Detection and quantification of aqueous sulphide concentration

Dissolved sulphides in the samples were determined using a micro ion electrode (LIS-146AGSCM, Lazar research laboratories Inc, California, US). 1 mL of sample was added to 5 mL of sulphide anti-oxidant buffer (SAOB) and 4 mL of nitrogen purged ultrapure water in a nitrogen atmosphere. The electrode was then submerged following vortexing of the mixture and allowed to equilibrate for 2 minutes, after which a reading was taken in mV. SAOB was prepared by dissolving 80 g of sodium hydroxide and 67 g of sodium ethylenediaminetetraacetic acid (EDTA) in 1 L nitrogen purged ultrapure water, after which 35 g of ascorbic acid were added. A standard curve was prepared by the addition of known concentrations of sulphide from 1-1000 ppm, where 3.75 g sodium sulphide nonahydrate was added to 1 L nitrogen purged ultrapure water to generate a 1000 ppm stock solution.

5.3.7 Detection and quantification of total sulphide concentration using gas chromatography with thermal conductivity detection (GC-TCD)

Total sulphide content of solid/liquid mixtures was determined by the addition of 900 µL of phosphoric acid to 100 µL of sample. 25 µL of headspace gas was then removed and injected into an Agilent GC6850 equipped with HP-PLOT/Q column with particle traps (35 m x 0.32 mm x 20 µm, Agilent Technologies, Berkshire, UK). Samples were passed through the column with a helium carrier gas with an oven temperature of 60 °C, which was subsequently heated at 30 °C min^{-1} to a final temperature of 240 °C, where it was held for three minutes. Detection and quantification of sulphide gas was achieved through the injection of known quantities of sulphide gas, through the complete acidification of know quantities of sodium sulphide nonahydrate. Manipulations were carried out in a nitrogen glove box to prevent oxidation and inhalation of sulphide fumes.

5.3.8 Measurement of total protein concentration

Total protein content in microcosm fluid was determined using Bradford assay method [198]. Bradford reagent was prepared by adding 25 mg of Coomassie blue G250 to 15 mL 95% ethanol and 30 mL phosphoric acid, made up with ultrapure water to a total volume of 250 mL. 100 µL of sample was then added to 3 mL of reagent, which was then vortexed and left at room temperature for 20 minutes. Following the incubation period, the mixture was vortexed and 1 mL transferred to a cuvette, where absorbance was read at 595 nm. In addition, a range of standards were prepared using bovine serum albumin as a protein source, these standards were used to prepare a calibration curve for interpretation of results.

5.3.9 Measurement of total carbohydrate concentration

Total carbohydrate concentration present in microcosm samples was detected using the methods of Masuko *et al* [199]. Briefly 50 µL of sample was pipetted into a 96-well plate, followed by the addition of 150 µL of concentrated sulphuric acid. 30 µL of 5% phenol dissolved in ultrapure water was then immediately added to each well and the entire plate incubated at 90 °C in a static water bath by carefully floating the plate on the surface. After incubation for 5 minutes at 90 °C, the plate was removed and placed in a water bath at room temperature for 5 further minutes. The plate was then wiped dry and absorbance read at 490 nm using a microplate reader (Multiskan EX, Thermolab Systems, UK). A range of standard concentrations of carbohydrate were prepared using glucose and ultrapure water used as a baseline absorbance.

5.3.10 X-ray diffraction (XRD) analysis of iron samples

All XRD analysis was carried out within the Materials and Catalysis Research Centre within the University of Huddersfield. Analysis was carried out employing a Bruker D2 phaser; and diffraction patterns recorded using Cu-K_α radiation (λ=1.54184 Å) utilising a LYNXEYE detector. Spectra were analysed by comparison with Bragg peaks obtained from the Powder Diffraction File database.

5.3.11 Brunauer–Emmett–Teller (BET) analysis

Surface areas and pore sizes were calculated by nitrogen adsorption at 77K using an ASAP2020 (Micromeritics). All BET analysis was carried out within the Materials and Catalysis Research Centre within the University of Huddersfield.

5.3.12 Scanning electron microscopy and elemental analysis

Scanning electron microscopy was carried out using an FEI Quanta FEG 250 equipped with electron dispersive X-ray spectroscopy (EDS).

5.3.13 Measurement of pH and redox potential

Microcosm pH was measured using a portable pH meter and calibrated electrodes (Mettler Toledo, UK). For field site studies, pH was measured using a submersible pH electrodes ORP (Lazar labs, California, US) and collected samples determined using British standard ISO 10390:2005 (BSI, 2005). Redox potential was measured using an InLab Redox Micro probe (Mettler Toledo, UK) and in field studies using a submersible Eh electrode ORF (Lazar labs, California, US).

5.3.14 Gas Volume

Volume of gas produced was measured using quick scan 1.8c software and apparatus (Challenge Technology, Arkansas, US).

5.3.15 Gas Identity

5.3.15.1 Gas Chromatography equipped with Thermal Conductivity Detection (GC-TCD)

Nitrogen, carbon dioxide and methane content were determined using an Agilent 6850 gas chromatograph, with a TCD fitted with a GS-Q column (30m x 0.53mm ID, Agilent technologies, Berkshire, UK) with 4 mL min^{-1} helium carrier gas. 25µl of headspace gas was removed using a lockable gas syringe from microcosms and passed through the column at 30°C with a detector temperature of 200°C. The instrument was calibrated using known concentration of each gas.

5.3.15.2 BacVis detection system

Gas sensors for methane (BCP-CH4), carbon dioxide (BCP-CO2) and hydrogen (BCP-H2) connected to BACCom12 multiplexer utilising BACVis software (BlueSens gas sensor GmbH, Herten, Germany).

5.4 Microbial Ecology studies

5.4.1 DNA extraction and purification

5.4.1.1 MO-BIO PowerSoil® DNA extraction kit

For mesophilic microcosms and pure culture work, a MO-BIO PowerSoil® DNA extraction kit (MO-BIO, Carlsbad, CA, US) was used to the manufacturers' instructions. Microcosm effluent or pure isolate broth culture (50 mL) was centrifuged at 8000 x *g* for 15 minutes at room temperature, 4 mL of supernatant was retained and used to re-suspend the pellet. Briefly, 0.25 mL of wet sediment sample was added to a PowerBead tube along with 60 µL of cell disruption and lysing solution, C1, before being vortexed and homogenised by placing the bead tubes in the attachment vortex adapter (MO-BIO #13000-V1-12) at maximum speed for 10 minutes. Tubes were then centrifuged for 60 seconds at 10,000 rpm, with the supernatant being transferred to a clean 2mL collection tube (supplied). Debris, humics, non-DNA organic and inorganic materials were then removed from the sample by the addition of 250 µL of solution C2 prior to incubation at 4°C for 5 minutes. The sample was subjected to a further centrifugation step at 10,000 rpm for 60 seconds, before the supernatant (~600 µL) was transferred to a clean 2 mL collection tube. Any residual non-DNA materials were then removed through the addition of 200 µL of solution C3 and a further incubation for 5 minutes

at 4°C. The sample was centrifuged again for a further 60 seconds at 10,000 rpm, before the supernatant transferred to a clean collection tube. 1.2 mL of solution C4 was then added to the supernatant, the high salt concentration of solution C4 aids in the aggregation of DNA through binding with the phosphate backbone, the samples were then centrifuged at 10,000 rpm for 60 seconds through a silica membrane column. Solution C5, an ethanol based wash solution was then added to the filter to remove any remaining non-DNA wastes by centrifugation at 10,000 rpm for 60 seconds. Following discard of the flow through a second centrifugation step was performed to remove all remaining ethanol which would potentially interfere with downstream applications. Finally, 30 µL of solution C6 was added to the membrane, allowing DNA to be eluted by centrifugation at 10,000 rpm for 60 seconds.

5.4.1.2 Co-extraction method

For extraction of DNA from microcosms operating at pH > 9.0, a modified version of a previous method by Griffiths *et al* [59] was employed. Effluent was concentrated by centrifugation as per 5.4.1.1, before 0.5 g of sample was mixed with 0.5 mL of extraction buffer (cetyl-trimethylammonium bromide (CTAB) 5% wt/vol prepared in 0.35 M sodium chloride/240 mM phosphate buffer, pH 8.0) and 0.5 mL phenol-chloroform-isoamyl alcohol (25:24:1 ratio) in a bead tube containing 0.1mm diameter glass beads. Tubes were then bead beaten for 30 seconds at 5.5ms^{-1} (Hybaid RiboLyser, Hybaid, Teddington, UK) or by attachment vortex adapter (MO-BIO vortex adapter, MO-BIO, Carlsbad, CA, US) and beaten for 15 minutes with the vortex set to full speed. The resultant suspension was then centrifuged at 13,500 rpm for 5 minutes at 4°C and the top aqueous layer (~500 µL) was transferred to a sterile, DNase/RNase free 1.5 mL tube with 500 µL chloroform-isoamyl alcohol (24:1 ratio). The mixture was vortexed to form a suspension before being centrifuged at 13,500 rpm for a further 5 minutes. The aqueous top layer (~500 µL) was transferred to a fresh 1.5 mL tube, before 1 mL of poly(ethylene) glycol (PEG) solution was added (30% PEG-6000 (wt/vol) in 1.6M sodium chloride). Following mixing, samples were incubated overnight at 4°C. Following the overnight incubation step, sample tubes were centrifuged for 10 minutes at 14,000 rpm for 10 minutes and the supernatant removed leaving pelleted DNA and RNA. 200 µL of 70% ice cold ethanol was then added to each sample tube to wash the pellet, before the bulk ethanol was removed using a pipette. Any residual ethanol was then removed under vacuum at 39°C. Finally the pellet was re-suspended 30 µL in diethyl pyrocarbonate (DEPC) treated water.

5.4.1.3 Quantification of nucleic acids

Nucleic acid concentration was determined spectrophotometrically by exposure to UV light at 260nm. At this wavelength the extinction co-efficient of double stranded DNA is 0.020 (µg/mL)$^{-1}$ cm^{-1} and 0.025 (µg/mL)$^{-1}$ cm^{-1} for RNA. Therefore and optical density of 1

corresponds to a concentration of 50 ng μL^{-1} of DNA and 40 ng μL^{-1} of RNA. Equally, the purity of DNA and RNA was determined by the ratio of optical densities at 260:280nm, with a ratio between 1.8-2.0 for DNA and 2.0 for RNA considered to be containing minimal protein contamination.

5.4.2 Polymerase chain reaction (PCR) for the amplification of ribosomal RNA and detection of bacterial and archaeal groups within samples

5.4.2.1 Detection of groups of organisms through direct PCR

Direct PCR was carried out on extracted DNA samples using range of Eubacterial and Archaeal primers listed in 5.4.2.4. The *Taq* polymerase used in this study was BIOTAQ™ as part of Biomix™ Red (Bioline, London, UK). Biomix™ Red is a 2X concentrated mix containing reaction buffer, magnesium (5mM), dNTPs and polymerase. Each direct PCR reaction contained 25 µL of Biomix™ Red, 17 µL of DEPC water, 3 µL of a 50:50 mix of forward and reverse primers at a concentration of 10 pmol and 5 µL of DNA template at a concentration of 5-10 ng μL^{-1}. Sample tubes were then transferred to a thermocycler (Techne TC-312, Bibby Scientific Group, Staffordshire, UK) and the reaction carried out under the following conditions: initial denaturation at 94°C for 5 min, followed by 35 cycles of: denaturing (94°C, 1 minute), annealing (*Variable* °C, 1 minute), primer extension (72°C, 1minute 30s). This was followed by a final extension step of 72°C for 5 minutes. Samples were then cooled to 4 °C and stored at the same prior to visualisation and downstream applications. Annealing temperatures were selected based on the optimal binding temperature provided by the primer manufacturer and would fall between 50-62 °C.

5.4.2.2 Detection of groups of organisms through nested PCR

In the case of nested PCR, an initial primer set was used to amplify either the entire eubacterial 16S rRNA gene (1.5 kb approx.) or the archaeal 16S rRNA gene (660bp approx.). Following this initial amplification the PCR product was then purified (see 5.4.3) and diluted 100 fold in DEPC water. The resultant dilution used as template for a further round of PCR amplification using primers whose annealing points are within the initial PCR product, increasing the sensitivity and detection level than is seen with direct techniques.

5.4.2.3 Control template DNA

Organisms used as positive controls for direct and nested PCR can be seen in Table 5.3. The organisms were commercially cultured and their DNA cultivated by DSMZ. 25 µL of genomic DNA was provided per organism, upon arrival, 1:10 dilutions of the stock DNA were prepared in DEPC water and stored at -20 °C.

Organism	DSMZ Reference	Target group
Clostridium pasteurianum	525	Clostridium cluster I
Clostridium termitidis	5398	Clostridium cluster III
Clostridium sporosphaeroides	1294	Clostridium cluster IV
Clostridium celerecrescens	5628	Clostridium cluster XIVab
Geobacter metallireducens	7210	Geobacter sp.
Shewanella putrifaciens	6067	Shewanella sp.
Desulfobulbus propionicus	2032	SRB group 1
Desulfobacterium niacini	2650	SRB group 2
Desulfobacter postgatei	2034	SRB group 3
Desulfococcus multivorans	2059	SRB group 4
Desulfovibrio africanus	2603	SRB group 5
Desulfotomaculum nigrificans	574	SRB group 6
Methanococcus voltae	1537	Methanococcales
Methanobacterium bryantii	863	Methanobacteriales
Methanomicrobium mobile	1539	Methanomicrobiales
Methanosarcina acetivorans	2834	Methanosarcinales
Methanosaeta pelagica	24271	Methanosaeta

Table 5.3 Organisms used as positive control templates for PCR primers used in the study.

5.4.2.4 Oligonucleotide primers and probe synthesis

All oligonucleotides used in the study were commercially synthesised HPSF (High purity salt free), by MWG Biotech. Oligonucleotides were prepared using instructions provided on the synthesis report to make 100 pmol μL^{-1} stocks. All stock solutions were stored at -20 °C and a full lest of primers can be found in Table 5.3.

Target	Name	Sequence (5'-3')	Size	Reference
Eubacterial 16S rDNA	PA	AGAGTTTGATCCTGGCTAG	1534	[202]
	PH'	AAGGAGGTGATCCAGCCGCA		
Archeael 16S rDNA	Af	CCCTAYGGGGYGCASGAG	660	[203]
	Ar	GGGCATGCACYWCYTCTC		
Clostridium cluster I	Chis 150	TTATGCGGTATTAATCTYCCTTT	820	[207]
	Chot 983	CARGRGATGTCAAGYCYAGGT		
Clostridium cluster III	Cther 650	TCTTGAGTGYYGGAGAGGAAAGC	720	[207]
	Cther 1352	GRCAGTATDCTGACCTRCC		
Clostridium cluster IV	Clos 561	TTACTGGGTGTAAAGGG	580	[207]
	Clept 1129	TAGAGTGCTCTTGCGTA		
Clostridium cluster XIVab	Erec 482	GCTTCTTAGTCARGTACC	620	[207]
	Cooc 112	TGGCTACTRFRVAYARG		
Methanococcales	MCC495F	TAAGGGCTGGGCAAGT	340	[209]
	MCC832R	CACCTAGTYCGCARAGTTTA		
Methanobacteriales	MBT857F	CGWAGGGAAGCTGTTAAGT	345	[209]
	MBT1196R	TACCGTCGTCCACTCCTT		
Methanomicrobiales	MMB282f	ATCGR TACGGGTTGTGGG	506	[209]
	MMB832R	CACCTAACGCRCATHGTTAC		
Methanosarcinales	MSL812F	GTAAACGATRYTCGCTAGGT	350	[209]
	MSL1159R	GGTCCCCACAGWGTACC		
Methanosaeta	MS1585F	CCGGCCGGATAAGTCTCTTGA	270	[205]
	SAE835R	GACAACGGTCGCACCGTGGCC		
SRB group 1	DFM140	TAGMCYGGGATAACRSKYG	702	[201]
	DFM842	ATACCCSCWWCWCCTAGCAC		
SRB group 2	DBB121	CGCGTAGATAACCTGTCYTCATG	1120	[201]
	DBB1237	GTAGKACGTGTGTAGCCCTGGTC		
SRB group 3	DBM169	CTAATRCCGGATRAAGTCAG	840	[201]
	DBM1006	ATTCTCARGATGTCAAGTCTG		
SRB group 4	DSB127	GATAATCTGCCTTCAAGCCTGG	1150	[201]
	DSB1273	CYYYYYGCRRAGTCGSTGCCCT		
SRB group 5	DCC305	GATCAGCCACACTGGRACTGACA	860	[201]
	DCC1165	GGGGCAGTATCTTYAGAGTYC		
SRB group 6	DSV230	GRGYCYGCGTYYCATTAGC	610	[201]
	DSV838	SYCCGRCAYCTAGYRTYCATC		
Geobacter sp	GEOF	ATGGCGAGAACAGACGAG	300	[204]
	GEOR	CTTCTGCGCCGTCGGC		
Shewanella sp	She211f	CGCGATTGGATGAACCTAG	1040	[206]
	She1259r	GGCTTTGCAACCCTCTGTA		
M13 plasmid insert	M13F	GTTTTCCCAGTCACGAC	N/A	[208]
	M13R	CAGGAAACAGCTATGAC		

Ambiguities: R (G or A); Y (C or T); K (G or T); M (A or C); S (G or C); W (A or T).

Table 5.3 Primers used within the study.

5.4.2.5 Visualisation of DNA/RNA by gel electrophoresis

Extracted DNA/RNA and PCR products were visualised using gel electrophoresis on 1% agarose gels prepared in tris-acetate EDTA buffer (TAE). A 50X concentrated solution was prepared by dissolving 242 g tris base, 57.1 mL glacial acetic acid and 100 mL 0.5M EDTA per litre of ultrapure water (pH 8.0) and diluted when required. The 1% agarose solution was then completely melted by microwaving (2-3 minutes per 100 mL) before being allowed to cool to ~45°C, prior to the addition of 1 µL of SYBR® safe stain (Life Technologies, Paisley, UK). The gel was then cast and allowed to set. 5 µL of extracted sample was then mixed with 1 µL of 5X loading dye (Bioline, London, UK) and inserted into each well alongside a 1-10kb ladder (Hyperladder 1kb, Bioline, London, UK), the gel was then subjected to electrophoresis submerged in TAE buffer for 60 minutes at 100V. Following PCR reactions, 5 µL of each PCR product was loaded into each gel utilising the dye present in the original PCR master mix, alongside 5 µL of ladder (Hyperladder 1kb) and electrophoresed for 60 minutes at 100V. Gels were then visualised under UV light and an image taken using BioDoc-It® 210 imaging system (UVP LLC, Upland, CA, US).

5.4.3 PCR product purification

5.4.3.1 PCR product purification using Qiaquick PCR purification kit

In order to purify DNA for downstream processes, a commercial kit was used supplied by Qiagen (Qiaquick PCR purification kit, Qiagen, Surrey, UK). Steps were followed as per the manufacturer's instructions. Briefly, the PCR product is salted at a pH ≤7.5 by the addition of 5 volumes of supplied buffer to one volume of product, the pH was then reduced by the addition of 10 µL of 3M sodium acetate prior to binding to a silica column through centrifugation at 10,000 rpm. The PCR product was then cleaned of associated primers, dNTPs and polymerases through the addition of an ethanol based buffer and further centrifugation steps. The cleaned product was then eluted by the addition of 30 µl of an elution buffer to the centre of the silica membrane followed by a final centrifugation step into a DNase/RNase free 2 mL collection tube.

5.4.3.2 PCR product purification by gel extraction method

The entire PCR reaction was loaded into a 1% agarose-TAE gel and electrophoresed for 90 minutes at 100V to endure complete separation of components. The bands of interest were then excised under UV light using a fresh scalpel blade and transferred to a sterile DNase/RNase free 1.5 mL tube. The product was then removed from the gel using a gel extraction kit (ISOLATE II PCR and Gel Kit, Bioline, London, UK) to the manufacturer's instructions. Briefly, a 450 µL of gel binding solubiliser was added to extracted band and incubated at 50 °C under the gel had completely melted. Following the addition of 50 µL of binding optimiser,

product was bound to a spin column by centrifugation at 10,000 rpm prior to being washed using a wash buffer followed by further centrifugation. Finally, 30 µL of an elution buffer was added to the membrane and PCR product eluted by centrifugation into a fresh 2 mL collection tube.

5.4.4 Vector Cloning

Vector cloning was carried out using a p-GEM®-T Easy Vector System (Promega, Madison, WI, US) according to the manufacturers' instructions with the under the following conditions. Firstly, the quantity of insert was optimised using equation **(5.1):**

$$\frac{\textbf{ng of vector x kb size of insert}}{\textbf{kb size of vector}} \textbf{ x insert: vector molar ratio = ng of insert} \quad \text{(eq 5.1)}$$

An insert:vector molar ratio of 1:1 was chosen for all reactions and 50 ng of the 3.0 kb p-GEM vector was used per reaction. Ligation reactions were prepared to according to Table 5.5, and the purified PCR product was diluted such that the ng of vector required (calculated from equation **(5.1)**) was present in 1-3µL of DNA free water.

Reagent	Volume added (µL)		
	Standard Reaction	Positive control	Background Control
2X Rapid ligation buffer, T4 DNA ligase	5	5	5
pGEM®-T Easy vector (50ng)	1	1	1
PCR product	X	-	-
Control insert DNA	-	2	-
T4 DNA ligase (3 Weiss units/µL)	1	1	1
De-ionised water to a final volume of	10	10	10

Table 5.4 Ligation reaction mixtures.

Ligation reactions were carried out overnight at 4 °C rather than 1 hour and 2 µL of ligation reaction added to 50 µL of competent cells and incubated on ice for 20 minutes. The cells were then heat shocked by placing cells at 42 °C for 45 seconds before being immediately returned to ice for 2 minutes. SOC medium was added to each reaction to bring the total volume to 1 mL prior to a further incubation step at 37 °C with shaking (150 rpm) for 90 minutes. At the end of the incubation period, the transformation culture was plated out onto Lysogeny Broth (LB) agar with ampicillin/IPTG/X-Gal (see 5.4.4.2) in 100 µl aliquots. Plates were left to dry before being incubated at 37 °C for 24 hours, before being transferred to 4 °C for 4 hours to

allow for any residual colour development. White colonies were then selected and further sub-cultured onto LB ampicillin/IPTG/X-Gal preceding downstream processes.

5.4.4.1 Preparation of SOC medium

2 g of tryptone (MC005) and 0.5 g of yeast extract powder (MC001) were added to 97.5 mL of de-ionised water and sterilised by autoclaving at 121 °C for 15 minutes. Upon sterilisation, the medium was allowed to cool before the addition of 1 mL of 2M glucose, 0.5 mL of 2M NaCl, 1 mL of 1M MgCl and 0.25 mL of 1M KCl (final concentrations of 20mM, 10mM, 10 mM and 2.5mM respectively). All the solutions were prepared in de-ionised water and filter sterilised using a 0.45 µm syringe filter unit, and the additions to the sterile SOC base prepared within a class II safety cabinet.

5.4.4.2 Preparation of LB ampicillin/IPTG/X-Gal plates

40 g of LB agar powder (LAB 168) was prepared in 1 L de-ionised water and autoclaved at 121 °C for 15 minutes, before being allowed to cool to 50 °C in a water bath prior to the addition of 1 mL of a filter sterilised 100 mg mL^{-1} ampicillin stock solution prepared in distilled water, giving a final concentration of 100 µg mL^{-1}. Following mixing, the molten agar was poured into 85 mm petri dishes (Sarstedt, Leicester, UK) and allowed to set, before being stored at 4°C prior to use. 100 µL of a 0.1 M stock solution of isopropyl β-D-1-thiogalactopyranoside (IPTG) and 20 µL of 50 mg mL^{-1} 5-bromo-4-chloro-3-indolyl-β-D-galactoside (X-Gal) were spread over the surface of the plate and allowed to absorb for 30 minutes at 37°C prior to the plating step described in 5.4.4. IPTG stock solution was prepared by adding 1.2 g to 50 mL distilled water before being filter sterilised under class II lamina flow and stored at 4°C. X-Gal stock solution was prepared by dissolving 100 mg in 2 mL N,N'-dimethyl-formamide, before storing at -20°C covered in foil to exclude light.

5.4.4.3 Plasmid extraction to verify insertion

Five clones were selected per insert for plasmid extraction and grown overnight in LB broth at 37 °C. Plasmid extraction was carried out using a commercial kit (ISOLATE II Plasmid mini kit (Bioline, London, UK)) following the manufacturers instruction. Briefly, the culture was pelleted by centrifugation at 10,000 rpm for 60 seconds and the supernatant completely removed. The cells were then re-suspended and lysed using the supplied buffers, following 5 minutes incubation at room temperature the reaction was neutralised using the appropriate buffer. The lysate was then centrifuged for 60 seconds at 10,000 rpm over a filter column to bind DNA, before further wash steps using the supplied buffers. Any residual ethanol was then removed by a final centrifugation step at 10,000 rpm for 2 minutes and the DNA eluted into a fresh collection tube using the supplied elution buffer. Plasmid concentration was measured and diluted to a concentration of 0.1-1 ng μL^{-1} in DNA grade water, PCR amplification of the

inserts was then carried out using standard primers M13 forward and M13 reverse under reaction conditions described previously 5.4.2.1. The resultant PCR products were then visualised using gel electrophoresis (see 5.4.2.5) in order to verify presence of the correct insert.

5.4.5 Sequencing

Following verification of successful insertion in section 5.4.5.3 for each insert, clones were sub-cultured into 96-well stab plates containing LB agar with 100 µg ml^{-1} ampicillin, whereby remaining downstream processes and sequencing were carried out by GATC Biotech (London, UK), employing dideoxy chain termination (Sanger) sequencing methods using the M13 forward primer only. Whole genome sequencing was carried out using next generation sequencing techniques and is discussed in further detail in Chapter 8.

5.4.6 Sequence analysis

Retrieved sequences were collated into a single .fasta file prior to analysis; with the each sequence separated by a '>', where a sequence name was imputed followed by a hard return (see Figure 5.1). The collated sequences were then checked for the presence of chimeras against a reference sequence using the UCHIME function contained within the MOTHUR project [209,210]. The obtained sequences were then trimmed using MEGA 5 for Windows [211], where primer artefacts and poor quality sequencing data were removed prior to submission to Genbank. For Eubacterial sequences the 16S rRNA sequence for *Escherichia coli* (Genbank accession number J01695), and for Archaeal sequences the 16S rRNA sequence for *Methanocaldococcus jannaschii* DSM 2661 (accession number L77117) were used as references for chimera checking. Both were retrieved from Genbank at the following URL http://www.ncbi.nlm.nih.gov/genbank [212].

Figure 5.1 Nomenclature of Fasta files containing collated sequence data.

Sequences were then analysed against the NCBI database using Basic Local Alignment Search Tool (MegaBLAST) utilising the 16S ribosomal RNA sequences for Bacteria and Archaea. Sequences were then placed into phylogenetic families based on the closest sequence from the

MegaBLAST output. Whole genome sequencing processing is discussed in further detail in Chapter 8.

5.4.7 Inference of phylogeny

Phylogenetic trees were constructed using the MEGA 5 software suite [211]. In order to estimate phylogenetic trees, sequences were first aligned. Obtained sequences were aligned with reference sequences obtained from either Genbank or the hierarchy browser component of the Ribosomal database project. Alignments were carried out using the MUSCLE (MUltiple Sequence Comparison by Log-Expectation) component of the MEGA suite under default clustering method (UPGMB)[213]. Phylogeny was then estimated using a neighbour joining method with reliability estimated using a 1000 replicate bootstrap analysis to produce a consensus tree.

5.4.8 Nucleotide accession numbers

The sequence data included within Chapter 7 was submitted to GenBank under accession numbers KM999232 to KM999360 and KM999361 to KM999498. The sequences presented in Chapter 9 were submitted to GenBank under accession numbers KP054397 to KP054455. The partial 16S rRNA gene sequence of the isolate discussed in Chapter 8 was submitted to Genbank under accession number KM411500 and subsequent whole genome sequence submitted under accession number JQGI00000000.

5.5 Microcosm studies

5.5.1 Batch feed cycles

Throughout experimental testing, microcosms were operated on a batch feed cycle. In each case the initial diluted inoculum was brought to a working volume through the addition of feed stock. Once at working volume (typically 500mL) the microcosm was then switched to the batch feed cycle. At the end of each batch a tenth of the working volume was removed and replaced with liquid feedstock. Unlike a single batch system this allows for the imposition of a growth rate upon the microcosm, such that micro-organisms within this system are not growing throughout the incubation period they are subsequently diluted out of microcosm or removed entirely. In each case, microcosms were batch fed in this manner such that the total working volume of microcosm fluid was replaced prior to the commencement of sampling for generation of chemical and ecological data.

5.5.2 Inoculum

5.5.2.1 Canal sediments

Samples of anaerobic sediment were collected from the bottom of the Leeds-Liverpool canal at the University of Huddersfield (SE 14890 16416) using a weighted bucket and collected in 500 mL sample tubs. Tubs were then topped to the rim with sediment to exclude atmosphere and were used within two weeks of collection to prevent spoilage

5.5.2.2 Reed bed sediments

Samples of anaerobic sediment were collected from the bottom of reed beds found at the national coal mining museum, Wakefield (SE 25076 16368) using a weighted bucket and collected in 500 mL sample tubs. Tubs were then topped to the rim with sediment to exclude atmosphere and were used within two weeks of collection to prevent spoilage. The sediments act as a source of iron reducing micro-organisms, since the reed beds are used to filter water effluent from the mine, whose rocks contain iron, which changes from ferrous to ferric iron in the presence of air. The permissions of the National Coal Mining Museum were acquired prior to sampling.

5.5.2.3 Hyperalkaline sediment

The anthropogenic site sits at Harpur Hill (SK 056 709). A hand cored sample was taken at sample point 6 (Figure 9.1) at a depth of ca. 5 cm diameter, and 5 cm depth and transferred to a sterile sample pot before being submerged with mineral media (5.2.1) adjusted to pH 10.0 to the rim.

5.5.3 Neutral pH Study

All microcosm were prepared in 500mL Schott bottles with a 3 port lid (GL45, Schott UK LTD, Stafford, UK) with inlet, outlet and septum ports. Methanogenic and sulphate reducing microcosms were prepared by the addition of 200 mL of canal sediment (5.6.1.1), 250 mL of mineral media (5.2.1) and 50 mL of CDP (5.2.2) to reaction vessel. To induce sulphate reducing conditions sodium sulphate was added to the vessel relative to moles of organic carbon in the CDP, methanogenic microcosms had nothing added to the original mix. To promote iron reducing conditions, reed bed sediment (5.6.1.2) was utilised in favour of the canal sediment (5.6.1.1) and calcined iron (III) oxide (identified as haematite within Chapter 6) was added to the microcosm relative to the moles of organic carbon in the CDP. The pH of the vessels was adjusted to pH 7.5 ± 0.1 using 2M hydrochloric acid. Vessels were then flushed for 20 minutes with nitrogen through the inlet port with the outlet open to remove any residual oxygen from the liquid phase and headspace gas before being sealed. Microcosms were incubated, unstirred in a 30°C water bath and underwent a weekly waste feed cycle in which at

the end of 7 days, the microcosms were swirled to produce a heterogeneous suspension, before 50 mL of the fluid was removed, 50mL of fresh CDP added and the pH readjusted to 7.5. This waste feed cycle was continued until the volume of fluid within the reactor had been completely replaced (10 cycles) prior to the commencement of sampling.

5.5.4 Methanogenic microcosms operating up to pH 11.0

All microcosms were prepared in 2 L shake flasks fitted a gas volume measurement outlet (Quick Scan 1.8c software and apparatus (Challenge Technology, Arkansas, US)) with gas sensors for methane (BCP-CH4), carbon dioxide (BCP-CO2) and hydrogen (BCP-H2) connected to BACCom12 multiplexer utilising BACVis software (BlueSens gas sensor GmbH, Herten, Germany). Microcosms initially contained 250 mL of canal sediment (5.6.1.1) alongside 200 mL of mineral media (5.2.1) and 50 mL of CDP (5.2.2) and pH adjusted to 7.5 using 2M hydrochloric acid, after which it was maintained at room temperature and stirred at 130 rpm. An initial pH 7.5 microcosm was batch fed 50 mL for 2 months and was continuously stirred using a 2" stirrer bar at 130 rpm. The inoculum in the pH 7.5 microcosm was then used as an inoculum for the subsequent pH 9.5 and 10.0 microcosms. Two 125 mL aliquots were taken and replaced with mineral media (5.2.1), the first was transferred to a fresh flask and 325 mL of mineral media and 50 mL CDP added. The pH was increased from 7.5 to 9.5 in 0.5 pH value increments over an 8 week period before being held at pH 9.5 for a further 6 weeks. The second aliquot was transferred to a fresh shake flask with 325 mL mineral media and 50 mL CDP and pH adjusted to 10.0 and maintained using a peristaltic pump (Bioconsole ADI1025 equipped with Biocontroller ADI1010, Applikon Biotechnology, Delft, Netherlands) delivering 4M sodium hydroxide. The microcosm was then maintained and fed for a further 6 weeks.

5.5.5 Methanogenic microcosms operating at pH 11.0 using hyperalkaline soil

All microcosms were prepared in 2 L shake flasks fitted a gas volume measurement outlet (Quick Scan 1.8c software and apparatus (Challenge Technology, Arkansas, US)) with gas sensors for methane (BCP-CH4), carbon dioxide (BCP-CO2) and hydrogen (BCP-H2) connected to BACCom12 multiplexer utilising BACVis software (BlueSens gas sensor GmbH, Herten, Germany). Microcosms initially contained 100 mL of Buxton sediment (5.6.1.3) alongside 200 mL of mineral media (5.2.1) and 50 mL of CDP (5.2.2) and pH adjusted to 11.0 using 4M sodium hydroxide and maintained at room temperature. Microcosms were fed 50 mL of CDP every two weeks with no waste to allow the volume to build to 500 mL. Microcosms were subsequently fed for 6 further feeds with a waste cycle to maintain the volume at 500 mL. Once the entire volume had been replaced through the waste feed regimen, sampling of the microcosms commenced.

5.5.6 Control microcosms

For the microcosms prepared in sections 5.6.2, 5.6.3 and 5.6.4; a set of control microcosms were prepared in the same proportions of components to a total volume of 50 mL in 100 mL Wheaton bottles in triplicate. Each microcosm was amended with chloramphenicol to a final concentration of 50 μg mL^{-1}, with samples removed on a daily basis over the course of the 7/14 day sample period, treated as per section 5.2.3.

5.6 Site study

Twelve hand cored samples (ca. 5 cm diameter, and 5 cm depth) were taken around the periphery of the site (Figure 9.1). Samples 1 to 6 were taken from regions where an established tufa deposit was present and in these cases the tufa was removed prior to sampling. Samples 7 to 12 were taken from regions where grassland had been recently inundated, as indicated by adjacent vegetation.

5.7 *Ex-situ* ISA generation experiments

Soils from the Buxton hyperalkaline site were taken from a region where the soil had not been exposed to the alkaline leachate. A 20 L sample of the alkaline leachate (pH 13.6) flowing from the brick culvert was collected and stored at 4ºC in the absence of air. A range of reaction vessels were established in 100 mL rubber butyl stoppered glass bottles, in which uncontaminated soil was mixed 5% w/v with filtered (0.22 μm filter unit, Millipore, US) alkaline leachate (pH 13.6) or leachate adjusted to pH 7.5 using conc HCl. In addition, both the alkaline and pH adjusted leachates were mixed with uncontaminated soil that had been double autoclaved prior to use. All reaction vessels were prepared within an anaerobic chamber (Bugbox, Don Whitely, UK). Reaction vessels were prepared in triplicate (9 per reaction condition) and incubated at 4, 10 or 20ºC. Samples (1 mL) were taken every 4 weeks.

5.8 Isolation of alkaliphilic micro-organisms

A sample (50 mL) of suspension was taken from the microcosm operating at pH 10.0. The sample was concentrated by centrifuging at 10,000 rpm for 20 minutes, 5 mL of supernatant was retained and the remaining 45 mL discarded. The retained 5 mL of supernatant was then used to reconstitute the pellet, before 10 μL was streaked out onto fastidious anaerobic agar (FAA) that had been pH adjusted to 10.0 using 4M NaOH prior to autoclaving. Streak plate was prepared under a constant stream of nitrogen, before being transferred to an anaerobic chamber (Bugbox, Don Whitley Ltd, UK) in an 80% nitrogen:10% carbon dioxide:10% hydrogen atmosphere at 25ºC. Plates were incubated for 48 hours prior to inspection for individual colonies. A single colony was picked from the plate and transferred to FAA (pH 10.0) and incubated for a further 48 hours. The resultant culture was then sub-cultured again

for further downstream processes described in Chapter 8 whilst the original culture was preserved through transfer to a cryovial (Pro-Lab Diagnostics, Germany) and stored at -80ºC.

5.9 Pure culture ISA degradation studies

A suspension of the isolate was prepared in maximum recovery diluent (MRD) amended with 0.05% cysteine (MRD-C) to an absorbance of 0.300 at a wavelength of 620 nm. The suspension was then diluted 4 fold by preparing serial dilutions in 9 ml MRD-C before 0.2 ml was transferred by injection into 4.8 ml of sterile, nitrogen purged medium containing 2 mM calcium isosaccharinic acid (Carbosynth, Ltd, Berkshire, UK) in a minimal media containing $NaHCO_3$ (30mM), NH_4Cl (4.7mM), $NaH_2PO_4.H_2O$ (4.4mM), KCl (1.4mM) and 2% v/v of a stock mineral solution containing (g L^{-1}): $MgSO_4.7H_2O$ (3.0), $MnSO_4.2H_2O$ (0.5), NaCl (1.0), $FeSO_4.7H_2O$ (0.1), $CoCl_2$ (0.1), $CaCl_2.2H_2O$ (0.1), $ZnSO_4$ (0.1), $CuSO_4.5H_2O$ (0.01), $Na_2MoO_4.2H_2O$ (0.01) adapted from [214] within 6 mL crimp top vials (Agilent, US) that had been autoclaved at 121ºC for 15 minutes prior to addition of inoculum. Vials were prepared in triplicate and incubated at 30ºC, where a 0.2 mL sample was recovered periodically and screened for ISA concentration using the HPAEC-PAD detection method described in 5.3.1. In addition, 0.2 mL of un-inoculated MRD-C was added to three separate vials containing the sterile nitrogen purged media to act as a sterile control. Again, samples were obtained and ISA concentration analysed by HPAEC-PAD. In order to determine cell biomass, a range of dilutions were prepared in MRD-C of both the starting inoculum and from each vial at the end of sampling. 50µL spiral plates were then prepared of each dilution using a Wasp2 Spiral Plater (Don Whitely Scienctific, UK) on FAA amended to pH 10.0 before incubation as described in 5.8.

5.10 Data Processing and statistical analysis

All general data processing and graph preparation was carried out employing Microsoft Excel.. Carbon closure calculations were carried out within Chapter 9. Liquid phase carbon mass balance closure was calculated as a percentage of output carbon mass divided by input carbon mass (eq 5.2):

$$\text{closure}(\%) = \frac{\text{carbon recovered}_{(aq)}\,[\sum C_{out}](mg)}{\text{initial carbon}_{(aq)}\,[\sum C_{in}]\,(mg)} \text{ x } 100 \qquad (eq\ 5.2)$$

Carbon recovered was calculated as the sum of the carbon present in the components analysed (eq 5.3), where other organic carbon was determined as the difference between the total organic carbon content and the identified carbon content (eq 5.4):

$$\text{Carbon recovered (mg)} = [\sum \text{α-ISA, β-ISA, acetic acid, other volatile fatty acids, inorganic carbon, other organic carbon}]\ \text{(mg)} \quad (eq\ 5.3)$$

$$\text{Other organic carbon(mg)} = \text{Total organic carbon} - [\sum \text{α-ISA, β-ISA, acetic acid, other volatile fatty acids}]\ \text{(mg)} \quad (eq\ 5.4)$$

Statistical analysis was carried out via SPSS V.20 (IBM Corporation, USA)

6.Biodegradation of ISAs from CDP at neutral pH

Biodegradation of ISA under neutral conditions.

6.1 Rationale

The aim of this first section of work was to determine the availability of cellulose degradation products and associated isosaccharinic acids as a potential carbon source for near surface microbial communities from anaerobic sediments under iron reducing, sulphate reducing and fermentative (methanogenic) conditions at pH 7.5 and 30 °C. Despite the absence of alkaline conditions, these terminal electron accepting processes were chosen as they reflect the most likely biogeochemical conditions to exist within micro-environments of a GDF concept. At the time the experiments were performed, 30ºC was chosen as the expected bulk temperature of a GDF in areas of ILW storage following maturation of the cementitious materials.

6.2 Results and discussion

6.1.1. Characterisation of cellulose degradation products

Forage fibre analysis indicated that the cellulose and hemicellulosic components constituted 161.8 g and 21.6 g of the original tissue respectively; post alkaline treatment, 59.3 g of cellulose and 1.75 g of the hemicellulose had been degraded. The resultant filtered liquor contained typically 3.54 ± 0.01 g L^{-1} total organic carbon of which 74% was contributed by the two stereoisomers of ISA in approximately equal quantities. Also present in the liquor were the α and β metasaccharinic acids and xylo-isosaccharinic acids resulting from the degradation of hemicellulose (6.6% of the total organic carbon)(Table 6.1). Finally, formic, acetic, propionic and iso-valeric acids were present, representing less than 1% of the total organic carbon combined (Table 6.1).

Biodegradation of ISA under neutral conditions.

Component	% of Total organic carbon
α-Isosaccharinic acid	40
β-Isosaccharinic acid	34.29
Xylo-isosaccharinic acid	3.37
α and β Metasaccharinic acids	3.23
Formic Acid	0.57
Acetic acid	0.29
Propionic acid	0.03
Isovaleric acid	0.06
Butyric acid	0.01
Hydroxybutyric acid	*
Octanedioic acid derivative	*
Total	81.84

*Detected by MS but not quantified

Table 6.1Composition of CDP feedstock. Individual components are expressed as a percetange of the total organic carbon.

6.1.2. Microcosm experiments

Across all microcosms, under iron reducing, sulphate reducing and methanogenic conditions, a significant proportion of organic carbon removal was associated with α and β ISA metabolism with no apparent difference between α and β ISA consumption profiles (Figures 6.1, 6.2 and 6.3).

Biodegradation of ISA under neutral conditions.

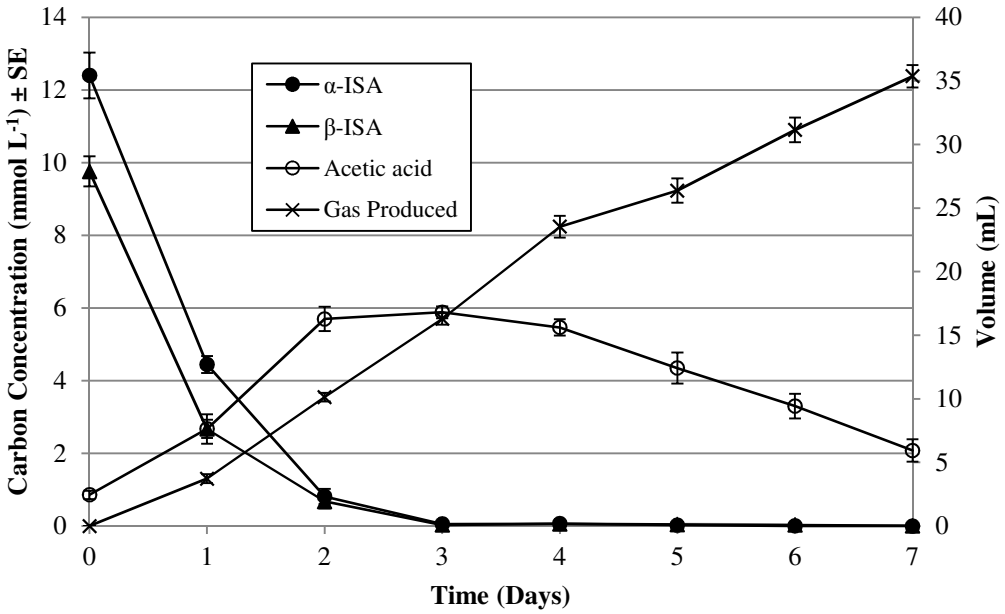

Figure 6.1 Chemical evolution of iron reducing reactors (n=6). Both stereoisomers of isosaccharinic acid were removed (α, closed circles. B, closed triangles) coinciding with the generation of gas (crosses) and generation and subsequent removal of acetic acid (open circles).

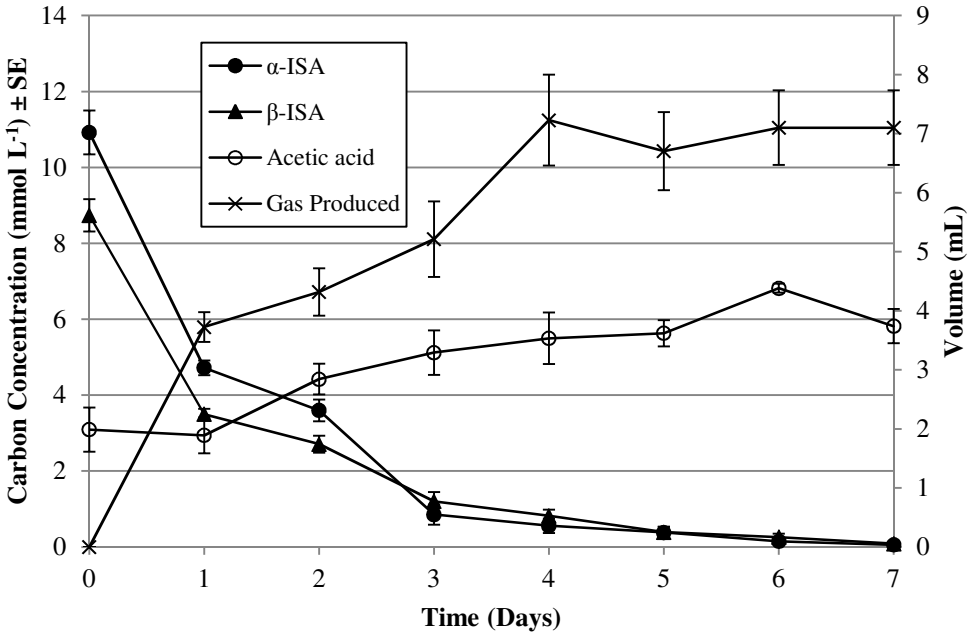

Figure 6.2 Chemical evolution of sulphate reducing reactors (n=6). Both stereoisomers of isosaccharinic acid were removed (α, closed circles. B, closed triangles) coinciding with the generation of gas (crosses) and generation and subsequent removal of acetic acid (open circles).

Biodegradation of ISA under neutral conditions.

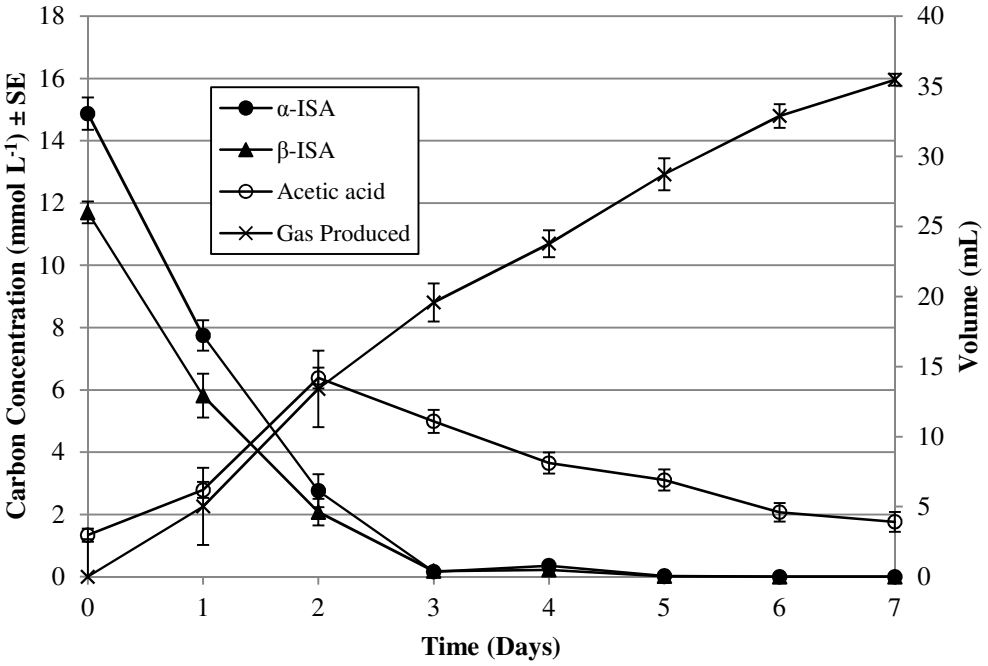

Figure 6.3 Chemical evolution of methanogenic reactors (n=6). Both stereoisomers of isosaccharinic acid were removed (α, closed circles. B, closed triangles) coinciding with the generation of gas (crosses) and generation and subsequent removal of acetic acid (open circles).

Degradation rates for ISA under anoxic conditions are not available in the literature, consequently first order degradation rates were calculated from the iron reducing, sulphate reducing and methanogenic α and β ISA removal data (Figure 6.4). The half-life first order degradation rates of both forms of ISA were calculated using equation 6.1.

$$t_{1/2} = \frac{ln2}{k} \qquad \text{(eq 6.1)}$$

Where $t_{1/2}$ is the timescale on which the initial concentration had reduced to half of its original value.

Biodegradation of ISA under neutral conditions.

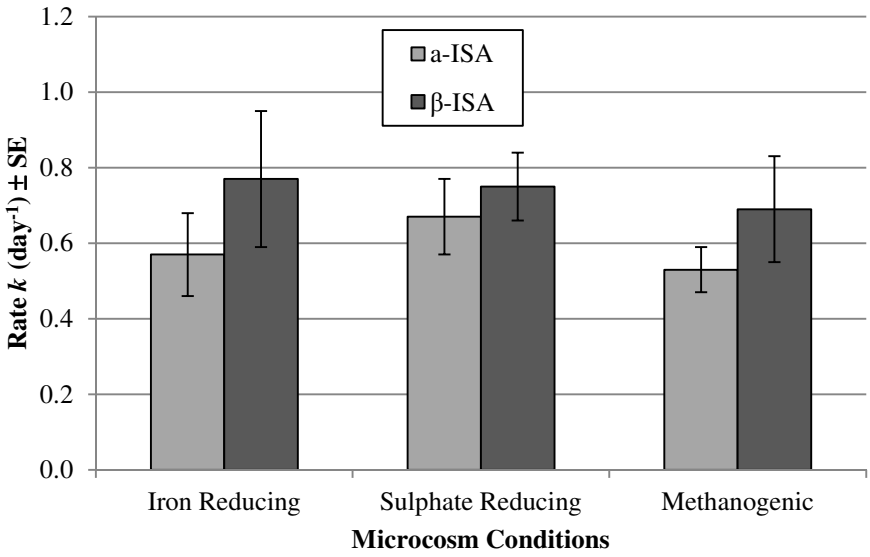

Figure 6.4 Mean first order degradation rates of individual stereoisomers of ISA under each microcosm condition. Values presented are the mean value ± SE (n=6).

No significant difference (ANOVA, n=6, p=>0.05) was found between the degradation rates of either α and β ISA under iron reduction, sulphate reduction or methanogenic conditions, giving an overall ISA degradation rate of 0.66 day^{-1} (n=36, SE±0.05). Fermentation processes were evident by the generation of acetic acid, which was the most prevalent volatile fatty acid formed, although other longer chain fatty acids including propionic, isobutyric, butyric and isovaleric acids were produced in sub mM concentrations (Figure 6.5 A-C). In general, these C3-5 VFAs were completely or partially degraded over the course of sampling. These data support a two stage degradation model for ISA with fermentation to short chain VFAs being the dominant, rate limiting step across all three consortia, followed by the iron reduction, sulphate reduction and methanogenesis of the fermentation end products.

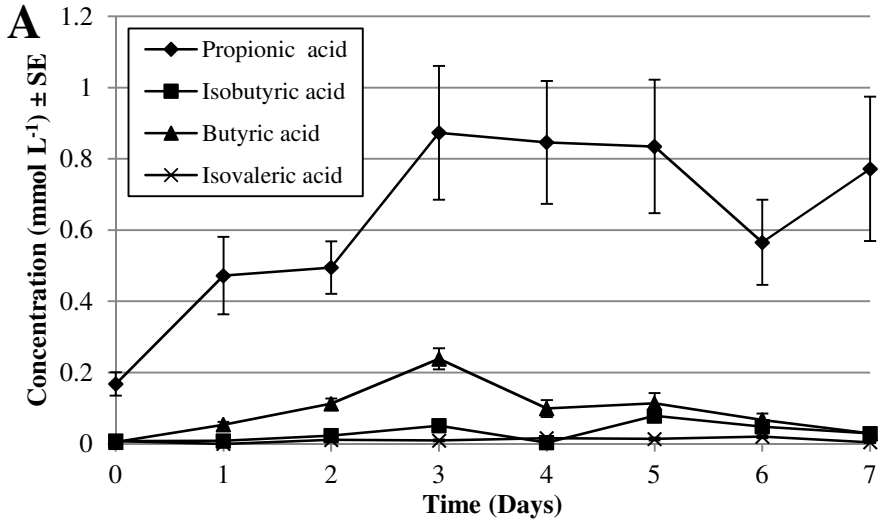

Biodegradation of ISA under neutral conditions.

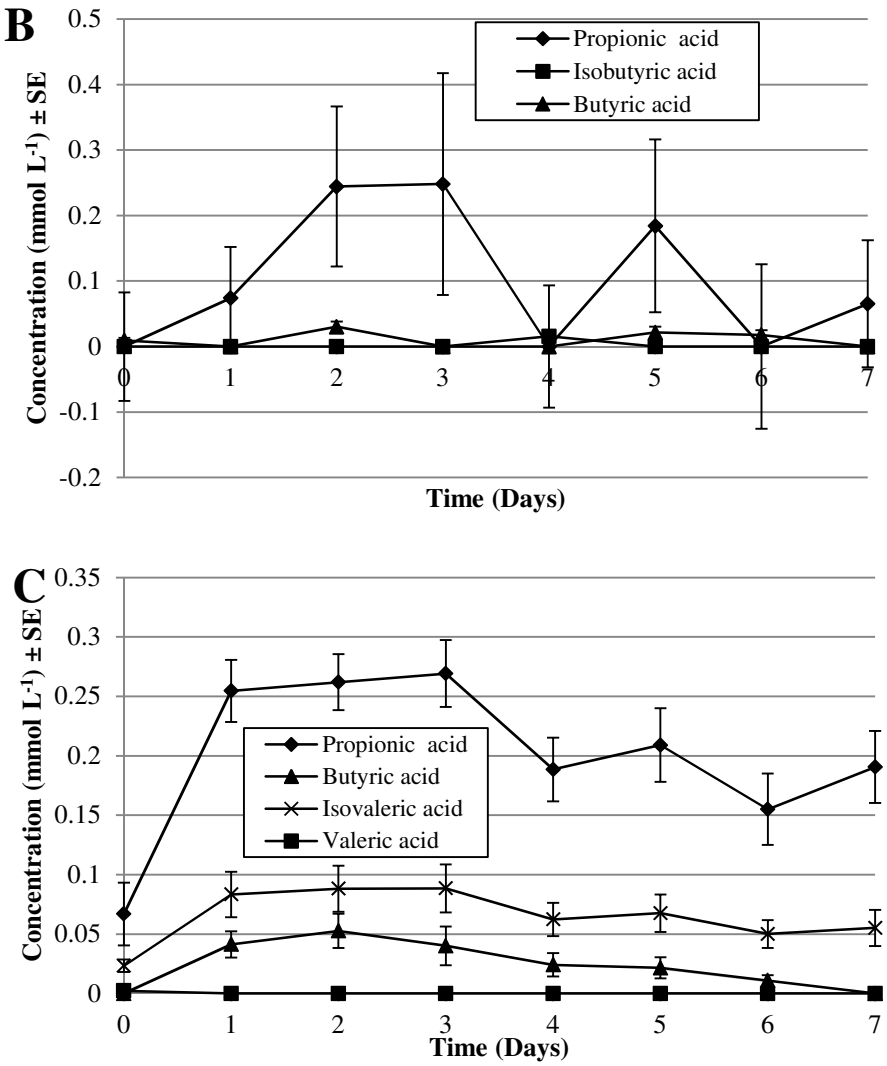

Figure 6.5 Non-acetic volatile fatty acid profiles within the iron reducing (A), sulphate reducing (B) and methanogenic (C) microcosms (n=6).

In microcosms amended with haematite, iron reduction was indicated by the generation of Fe (II) which coincided with the removal of both forms of ISA, reaching a peak concentration of 1.19 mmol L^{-1} at day 2. This contrasts with the associated control reactors where no Fe (II) generation or ISA removal was observed (Figure 6.6).

Biodegradation of ISA under neutral conditions.

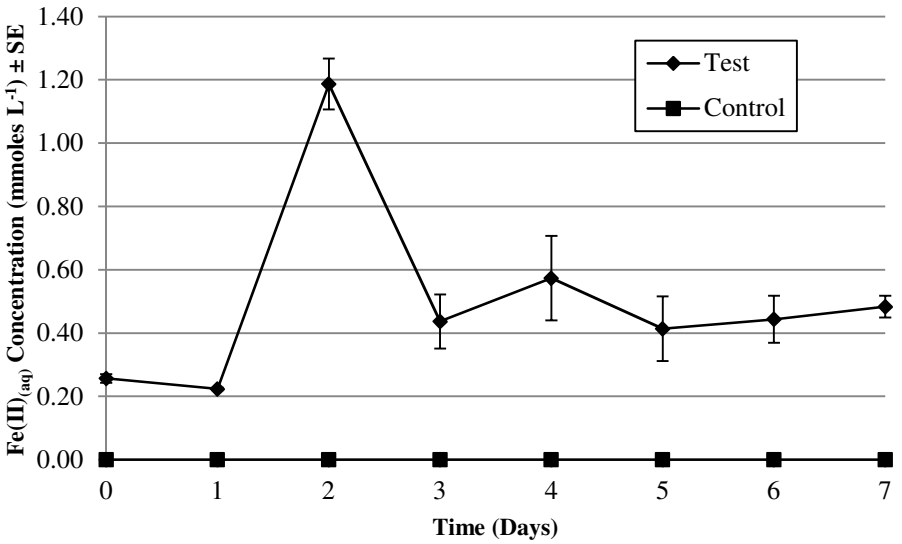

Figure 6.6 Iron (II) (aq) generation in biotic reactors (closed diamonds) amended with ferric iron.

In these iron reducing systems the fermentation of at least a portion of the ISA was illustrated by the initial generation of acetic acid. However, by the end of the incubation period, acetic acid levels had significantly reduced ($p<0.05$) indicating its subsequent degradation (Figure 6.1). The Fe (II) profiles indicate an initial generation followed by a reduction to a lower resting level. This profile is consistent with the precipitation of Fe (II) containing mineral phases, with the final solution phase concentrations determined by precipitation/dissolution reactions. This profile and the resting Fe (II) concentrations are also consistent with previously published data on haematite driven iron reduction systems [148]. XRD analysis confirmed the generation of Fe (II) mineral phases, in particular magnetite, that were absent from the original haematite (Figure 6.7). The presence of biogenic magnetite in bulk Fe (III) oxides has also been observed by previous authors employing XRD [215].

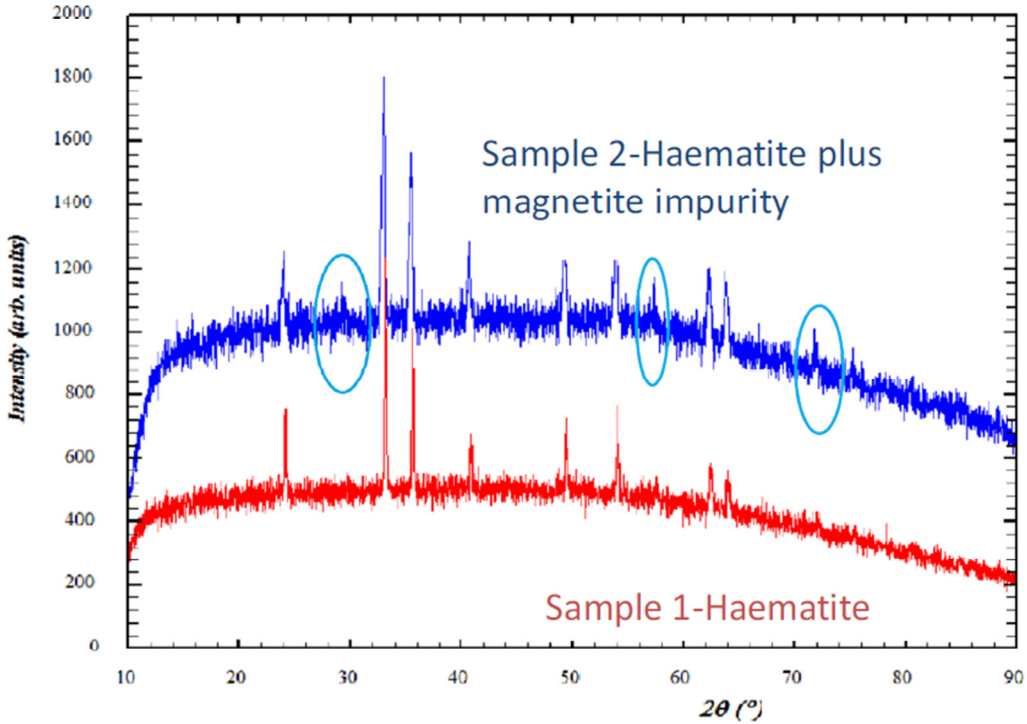

Figure 6.7 XRD patterns for the iron oxide used in microcosms (Sample 1), identified as haematite through comparison with diffraction database (peaks at 24, 33, 36, 41, 49 54, 62 and 64 2 Theta) and pattern at the end of the sampling period (Sample 2), where haematite contained an impurity, determined as magnetite through comparison with diffraction database (peaks at 30, 58 and 74 2 Theta, circled).

Biodegradation of ISA under neutral conditions.

The surface area (from 4.4 m^2 g^{-1} to 13.8 m^2 g^{-1}) and associated porosity (0.02 cm^3/g to 0.04 cm^3/g) of the haematite increased following iron reduction. This increased porosity was confirmed by SEM (Figure 6.8 A, B) which in conjunction with energy-dispersive x-ray spectroscopy (Figure 6.9) confirmed the formation of calcite on the haematite surface (Figure 6.8 C, D). This suggests that calcite formation is occurring due to biogenic CO_2 reacting with calcium present in the CDP. In contrast, both magnetite and calcite were absent from the sediment remaining in the control microcosms.

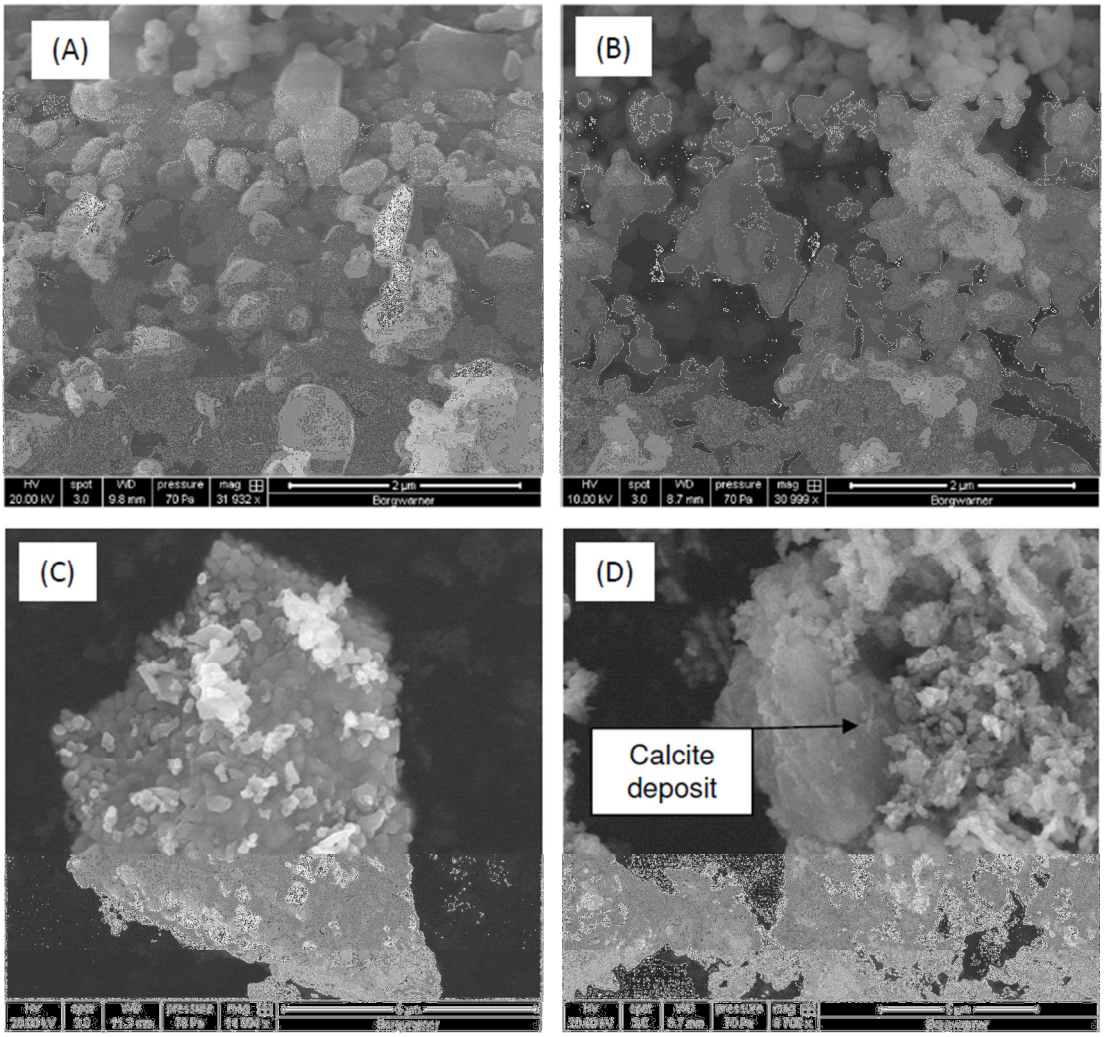

Figure 6.8 Scanning electron micrographs of calcined iron (III) oxide prior to microcosm insertion (A, C) and iron (III) oxide following incubation under iron reducing conditions (B, D).

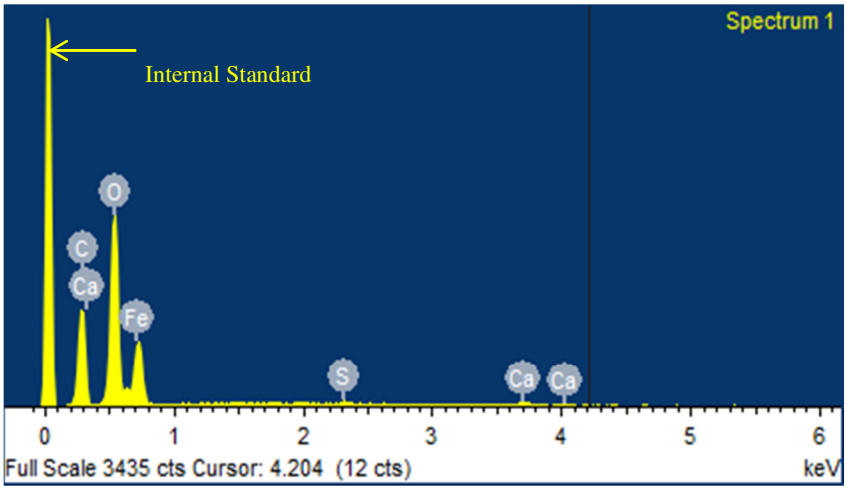

Figure 6.8 EDS output from analysis of calcite deposit in Figure 3, D. Carbon, calcium, oxygen and iron were the predominant elements detected, suggesting the potential presence of calcium carbonate amongst the bulk iron oxide.

The formation of methane (Figure 6.10) indicated that methanogens were also active alongside fermentative and iron reducing communities, suggesting that the crystalline nature of the Fe (III) source facilitates the presence of methanogenesis by limiting the rate of iron reduction. Haematite is known to support a lower rate of iron reduction than more amorphous Fe (III) phases or complexed Fe (III) [216]. Stoichiometric calculations [94] indicated that methanogenesis and accumulated acetic acid accounted for only 18% of the degraded ISA, confirming the role of iron reduction as the primary metabolic process within the system.

Of the Clostridia clusters investigated, direct and nested PCR approaches indicated that cluster IV was more abundant than clusters III and XIV, with cluster I being undetectable (Table 6.2). Iron reduction may be attributed to a mixture of *Geobacter* sp and organisms from sulphate reducing bacteria (SRB) groups 1, 3, 4, and 5. Previous authors have noted the ability of SRBs to enzymatically reduce Fe (III) from these groups [170]. Methanogenic bacteria capable of acetoclastic and hydrogenotrophic metabolism were also present within this community (Table 6.2).

Biodegradation of ISA under neutral conditions.

Target	Size	Terminal Electron Acceptor					
		Iron		Sulphate		Carbon Dioxide	
		D	N	D	N	D	N
Clostridium I	820	-	-	-	-	-	-
Clostridium III	720	-	+	+	+	+	+
Clostridium IV	580	+	+	+	+	-	-
Clostridium XIV	620	-	+	+	+	+	+
Methanococcales	340	-	+	-	-	-	+
Methanobacteriales	340	+	+	-	-	+	+
Methanomicrobiales	550	+	+	-	-	+	+
Methanosarcinales	350	+	+	-	-	+	+
Methanosaeta	250	+	+	-	-	+	+
SRB group 1	702	-	+	+	+	-	-
SRB group 2	1120	-	-	-	-	-	-
SRB group 3	840	+	+	+	+	-	-
SRB group 4	1150	-	-	+	+	-	-
SRB group 5	860	+	+	+	+	-	-
SRB group 6	620	+	+	+	+	-	-
Geobacter ssp	300	+	+	+	+	N	N
Shewanella ssp	1040	-	-	-	-	N	N

N-Not sampled

Table 6.2 DNA analysis by direct and nested PCR techniques.

Unlike iron reduction, the presence of sulphate allowed SRBs to dominate the terminal electron accepting processes as indicated by the absence of evolved methane within the headspace of these microcosms (Figure 6.10). Sulphide was generated in the aqueous phase as sulphate was removed (Figure 6.11); no free sulphide was detected in the associated control microcosms. The accumulation of acetic acid up to day 6 suggests that sulphate reduction of acetic acid is occurring at a slower rate than its generation. Through direct PCR the presence of groups 1, 3, 4, 5 and 6 sulphate reducing bacteria as described by [200] were observed alongside groups III, IV and XIV of the Clostridia.

Biodegradation of ISA under neutral conditions.

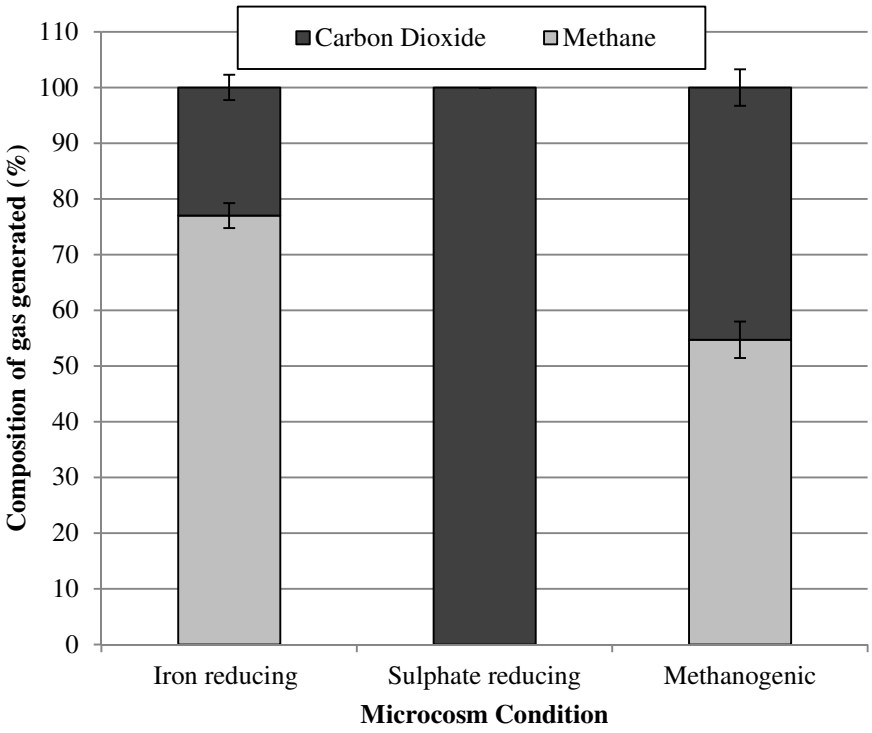

Figure 6.9 Composition of microcosm headspace gases (n=6). Methane and carbon dioxide were detected in both iron reducing and methanogenic microcosms, whereas carbon dioxide was detected exclusively within sulphate reducing microcoms

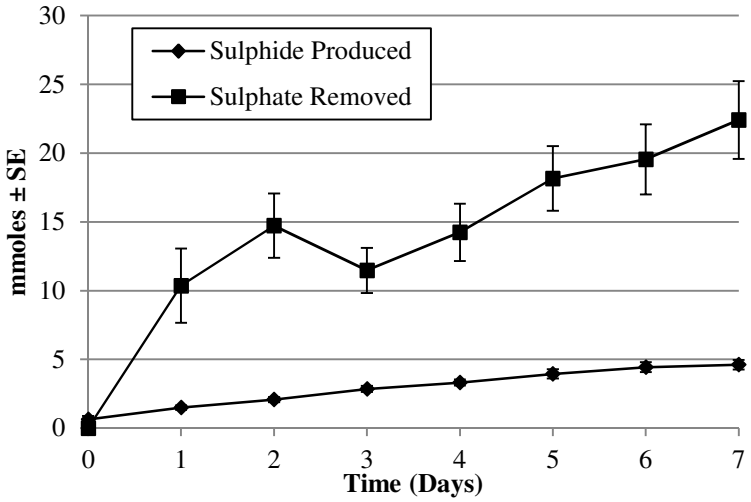

Figure 6.10 Generation of dissolved sulphides and removal of sulphates within the sulphate reducing microcosm.

In methanogenic microcosms (Figure 6.3) the removal of both forms of ISA was associated with the production and removal of acetic acid and the generation of methane which comprised 54.7% ± 3.3 of the gas generated. Direct and nested PCR confirmed the presence of Clostridia groups III and XIV and all five methanogen groups investigated.

Biodegradation of ISA under neutral conditions.

ISA is known to be subject to sorption and precipitation reactions [25,28], consequently a set of control microcosms treated with 50µg mL^{-1} chloramphenicol were sampled over the same period and analysed for ISA content. In this instance, ISA was not removed over the seven day sample period (Figure 6.12), suggesting that the removal previously seen was microbially mediated rather than through sorption or precipitation processes.

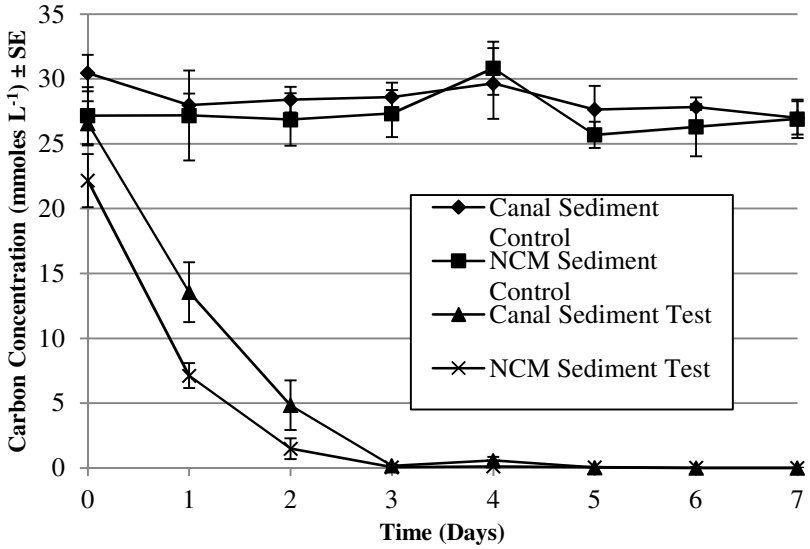

Figure 6.11 Removal of ISA is biotically mediated, where ISA remains in solution when microcosm is treated with chloramphenicol. Removal of ISA was seen with both biotic canal (closed triangles) and NCM sediments (crosses), with no distinct removal observed within chlormaphenicol treated canal (closed diamonds) and NCM (closed squares) sediments.

Other organic carbon sources were present within the CDP feed stock (<30% of total carbon) including the xylo-isosaccharinic acid and the α and β metasaccharinic acids (Table 6.1). These minor components are degraded in all three systems (data not shown), however the CDP did contain recalcitrant components that remained un-degraded throughout the incubation period (Figure 6.13).

Biodegradation of ISA under neutral conditions.

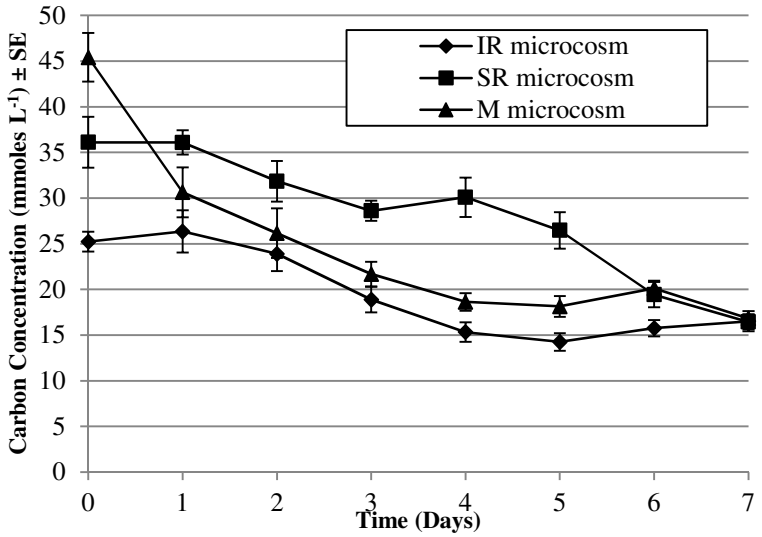

Figure 6.12 Removal and recalcitrance of other organic carbon components within the chemistry of iron reducing (closed diamonds), sulphate reducing (closed squares) and methanogenic (closed triangles) microcosms.

6.3 Conclusion

Although the α and β forms of ISA are not naturally observed in the wider environment, bacteria found in anoxic sediments are capable of degrading these compounds by utilising a range of terminal electron acceptors at circa neutral pH. Under iron reducing, sulphate reducing and methanogenic conditions the degradation of ISA followed the pathway seen in anoxic environments driven by the degradation of polymeric organic materials; i.e. the fermentation of polymer monomers followed by the degradation of fermentation end products by terminal electron accepting processes. In this case, however, hydrolysis is a chemical rather than a microbial process. The persistence of bacteria commonly associated with the anaerobic degradation of cellulose (the Clostridia) in these batch fed microcosms suggests that they may play an important role in the metabolism of ISA into common fermentation end products allowing electron and carbon flow within these systems. In summary, these findings indicate that the ability to degrade ISA (and more broadly, the organic carbon present within CDP) is common in near-surface microbial communities and consequently such communities represent a potential source of ISA degrading consortia for the colonisation of a GDF during the operational and pre-closure period.

The observed rates of ISA degradation suggest that at the interface between neutral and alkaline environments (e.g. within ungrouted wastes) ISA production will be the rate limiting step and that microbial activity will prevent the accumulation and transport of ISA and therefore prevent the enhanced migration of radionuclides. However, the activity of these communities within a GDF will be dependent on either the establishment of low pH environments within ungrouted wastes and/or their ability to adapt to the prevailing alkaline

conditions. Consequently, ISA may persist, migrate and complex in regions where the pH inhibits microbial activity.

6.4 Key Findings

- At pH 7.5, near surface microbial consortia are capable of degrading both the α and β stereoisomers of ISA under iron reducing, sulphate reducing and fermentative conditions, where they are fermented to volatile fatty acids, predominantly acetic acid.
- First reported first order degradation rates of ISA's under anaerobic conditions, statistically no significant difference in the rates across three microcosm types. This lack of significant difference suggested that a common group of microorganisms may be responsible for the fermentation, where Clostridium groups were detected in all three cases.
- Iron reduction with haematite in an unmixed system is hindered by the highly crystalline nature of the starting material, which allows for the formation of niches in which other microbial processes may occur.
- Since the initial inoculum contained a source of micro-organisms capable of the fermentation of ISAs, the culture was regarded as a candidate for testing the degradation capacity at higher pH values, discussed in Chapter 7**.**

The work presented here contributed to a subsequent publication:

Rout, S.P., Radford J., Laws A. P., Sweeney F., Elmekawy A., Gillie L. J., and Humphreys, P. N. (2014) *Biodegradation of the Alkaline Cellulose Degradation Products Generated During Radioactive Waste Disposal*. PLoS ONE 9.

Here I contributed to the experimental design, data acquisition/analysis and preparation of the manuscript. J. Radford provided assistance with monitoring and sampling of microcosms. F. Sweeney provided assistance with obtaining SEM images and EDS, A. Elmekawy and L.J. Gillie provided BET and XRD analysis respectively of iron samples. L.J. Gillie, A.P Laws and P.N Humphreys contributed to experimental design, data analysis and preparation of the manuscript.

7. Fermentation studies at elevated pH

Fermentation at elevated pH.

7.1 Rationale

As the previous chapter showed, isosaccharinic acids associated with the anaerobic, alkaline degradation of cellulose represent a source of organic carbon capable of supporting the metabolism of near surface micro-organisms at circum-neutral pH. The GDF concept for the long term storage of wastes will most likely experience pH values between 10.0 and 12.5 in the time following the closure of the facility. The aim of this section of work was to determine whether micro-organisms degrading ISA and other CDP's at pH 7.5 were capable of adapting to alkaline conditions at elevated pH values up to pH10.0. As such microcosms were gradually subjected to an increased pH as described in section 5.5.4.

7.2 Results and Discussion

Across all three microcosms, a removal of total organic carbon was observed, although more marked in the pH 7.5 system (Figure 7.1A). At pH 7.5, both forms of ISA were completely removed within 7 days. As the pH increased to 9.5 α-ISA was completely removed from the system within the sample period but as the pH increased to 10.0, 6.83 ± 1.82 mg of α-ISA remained. At both pH 9.5 and pH 10.0, β-ISA remained in the microcosm and appeared to be accumulating (Figure 7.1 B-D).

Fermentation at elevated pH.

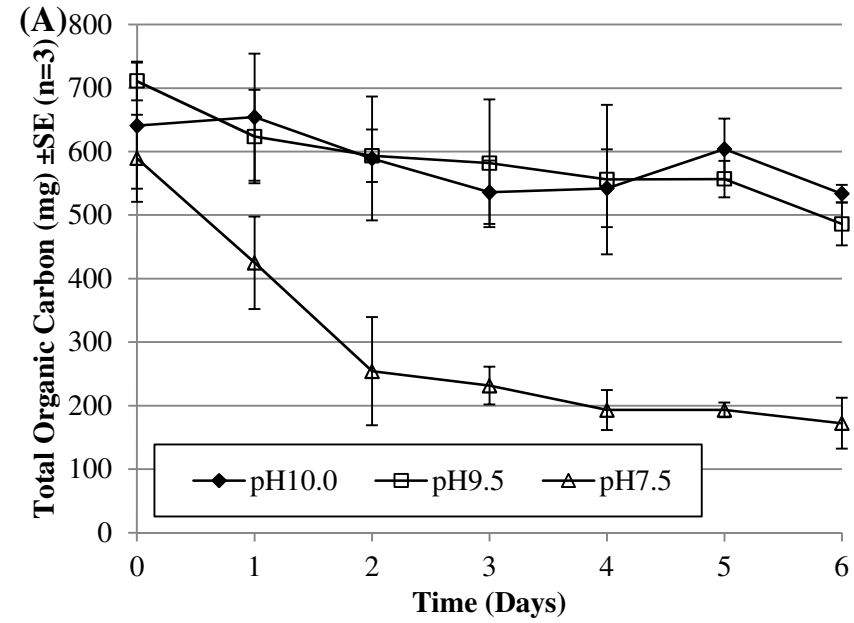

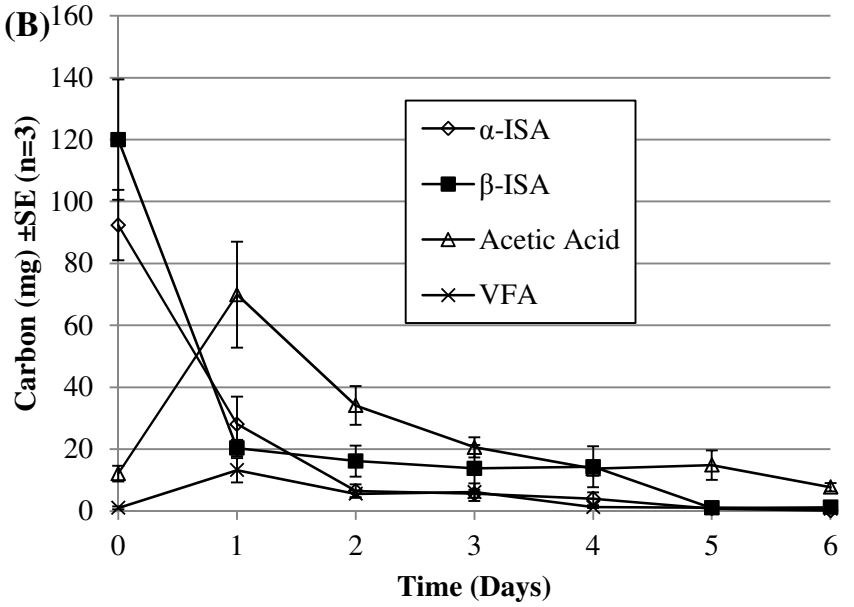

Fermentation at elevated pH.

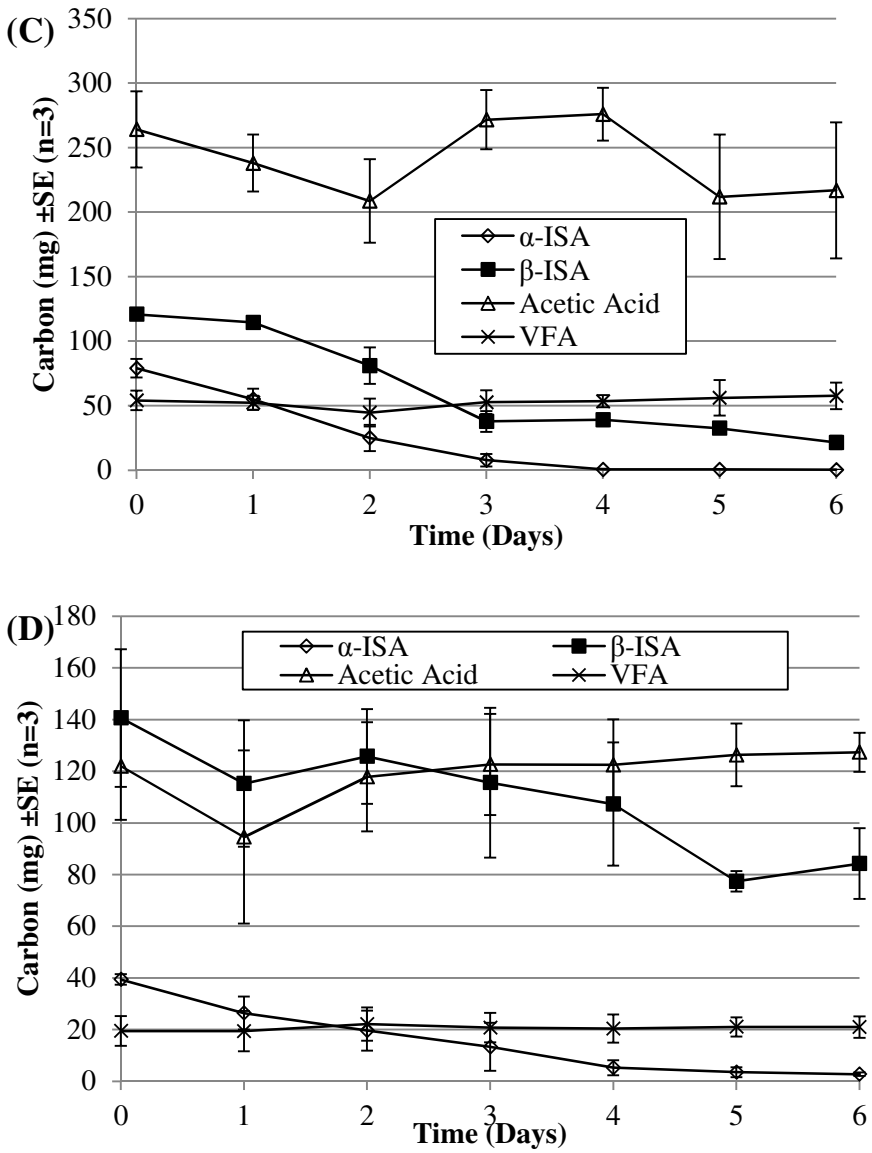

Figure 7.1 Removal of organic carbon from microcosms over 7 day sample period (A). pH 7.5 microcosm chemical evolution(B), pH 9.5 chemical evolution (C) and pH 10.0 chemical evolution (D). Mean values (n=3) are presented ± SE.

The half-life first order degradation rates of both forms of ISA are presented in Figure 7.2, using equation 6.1. The degradation rate of the α-ISA decreased from 8.40 x 10^{-1} day^{-1} to 4.41 x 10^{-1} day^{-1} between pH 7.5 and 9.5 and a further drop at pH 10.0 to 3.22 x 10^{-1} day^{-1}. The degradation rate of the β form had reduced from 1.13 day^{-1} at pH 7.5 to 2.13 x 10^{-1} day^{-1} at pH 9.5. A further reduction in degradation rate was seen for β-ISA between pH 9.5 and 10.0, falling to 8.97 x 10^{-2} day^{-1}. The rates of both α and β ISA degradation showed a strong linear relationship with pH (R^2 values > 0.99).

Fermentation at elevated pH.

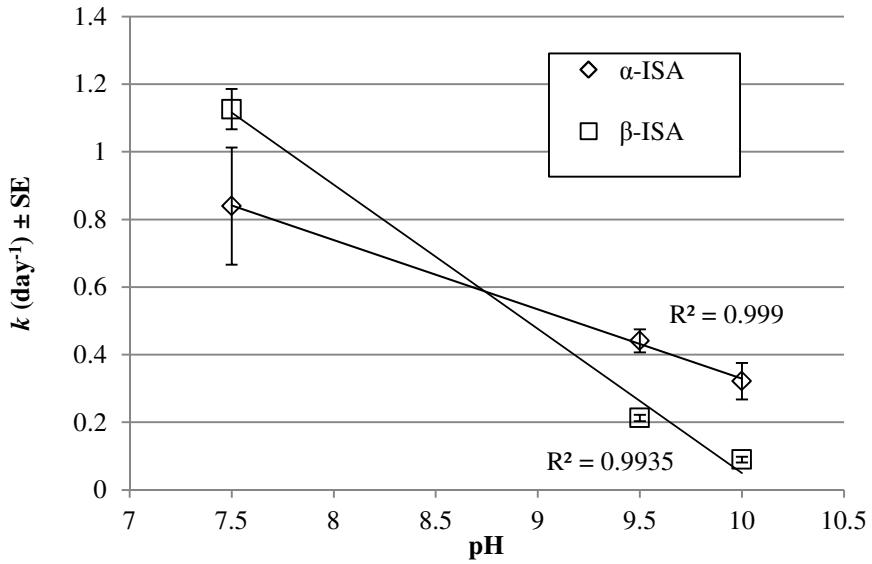

Figure 7.2 Rate of α and β ISA degradation at each pH system sampled. Mean values (n=3) are presented ± SE.

Fermentation processes were evident across all three microcosms through the generation of acetic acid as the most prevalent volatile fatty acid (VFA). In addition, propionic, isobutyric, butyric and isovaleric acids were generated across all three pH systems (Figure 7.3A-C). Acetic acid was generated at pH 7.5 by day 2 but was gradually removed by the end of sampling. At pH 9.5 and 10.0, acetic acid was generated but not completely removed from the system, and the carbon content was greater than that at pH 7.5 at the end of sampling.

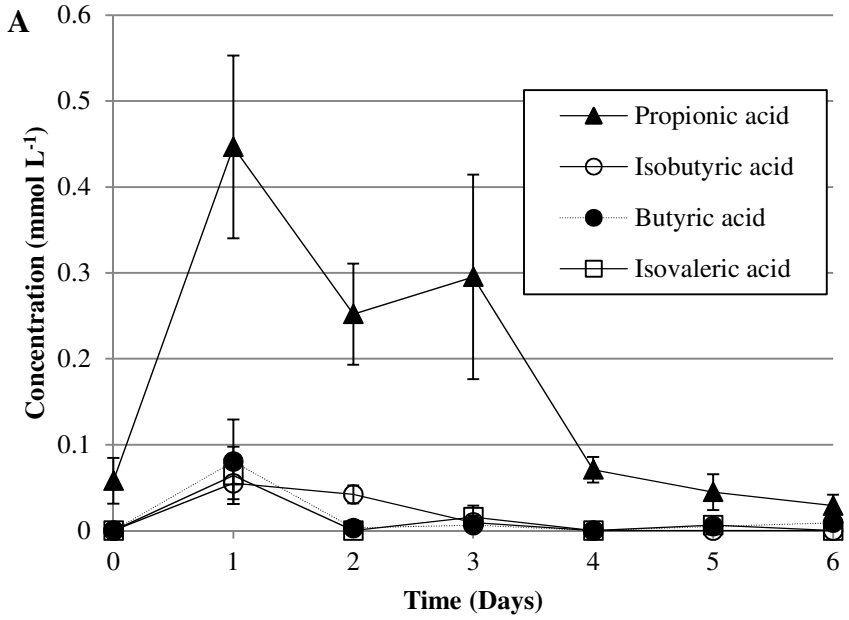

Fermentation at elevated pH.

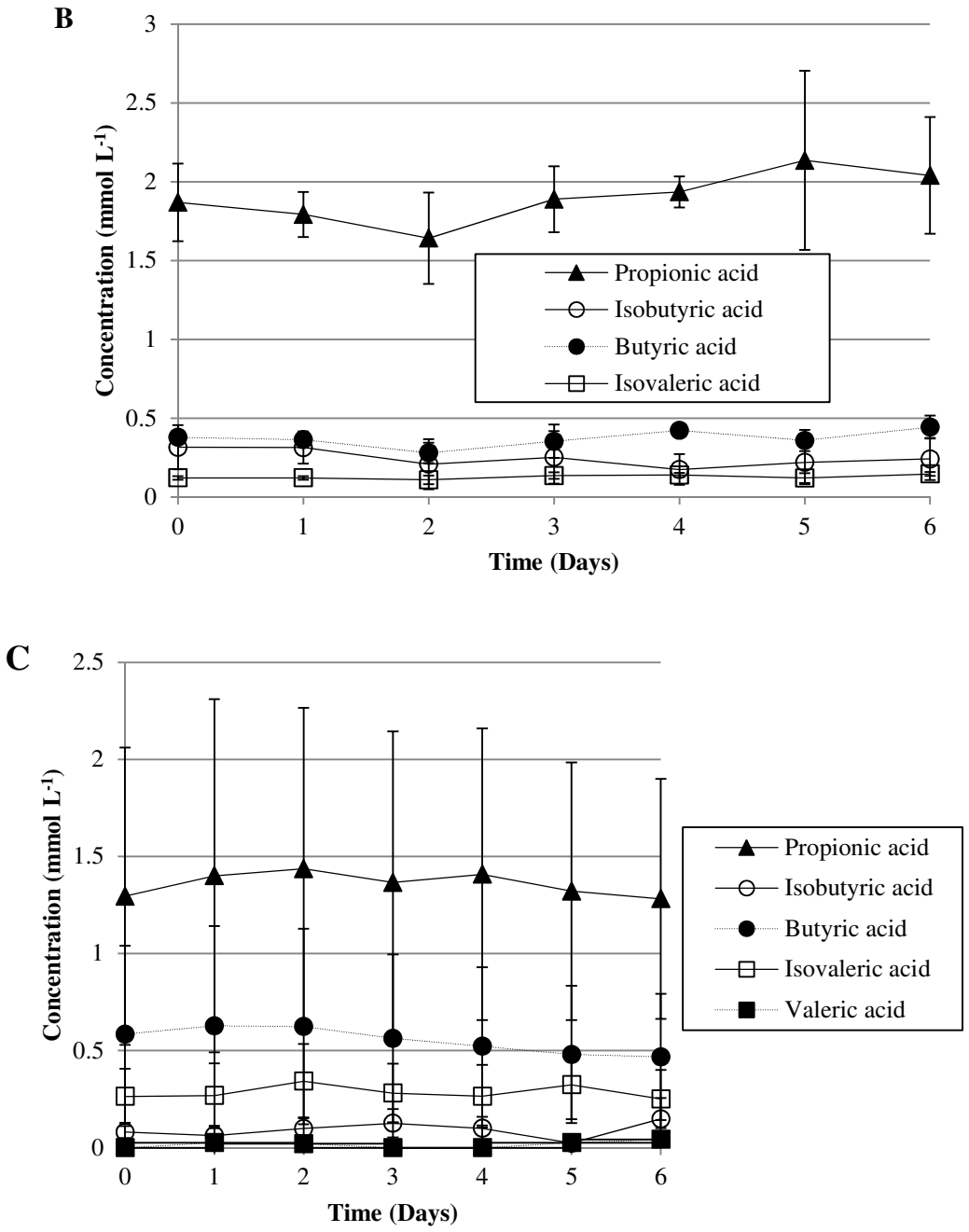

Figure 7.3 Non- acetic volatile fatty acid production at pH 7.5 (A), pH9.5 (B) and pH10.0 (C).

Fermentation at elevated pH.

Liquid phase carbon mass balance closure can be seen in Figure 7.4 (A-C). At pH 7.5, closure stood at 65.4%, increasing to 74.3% at pH 9.5 and 95.2% in the pH 10.0 system.

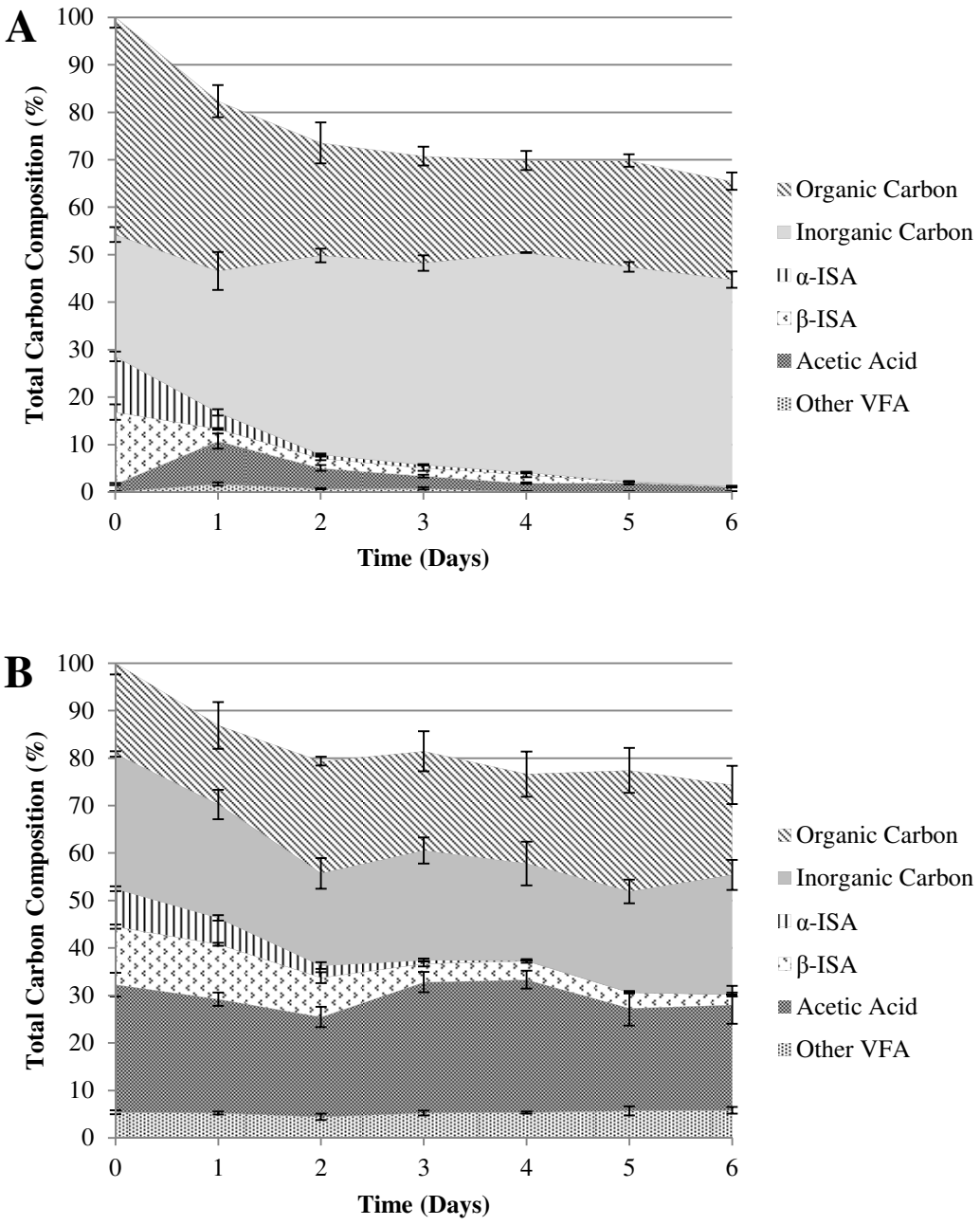

Fermentation at elevated pH.

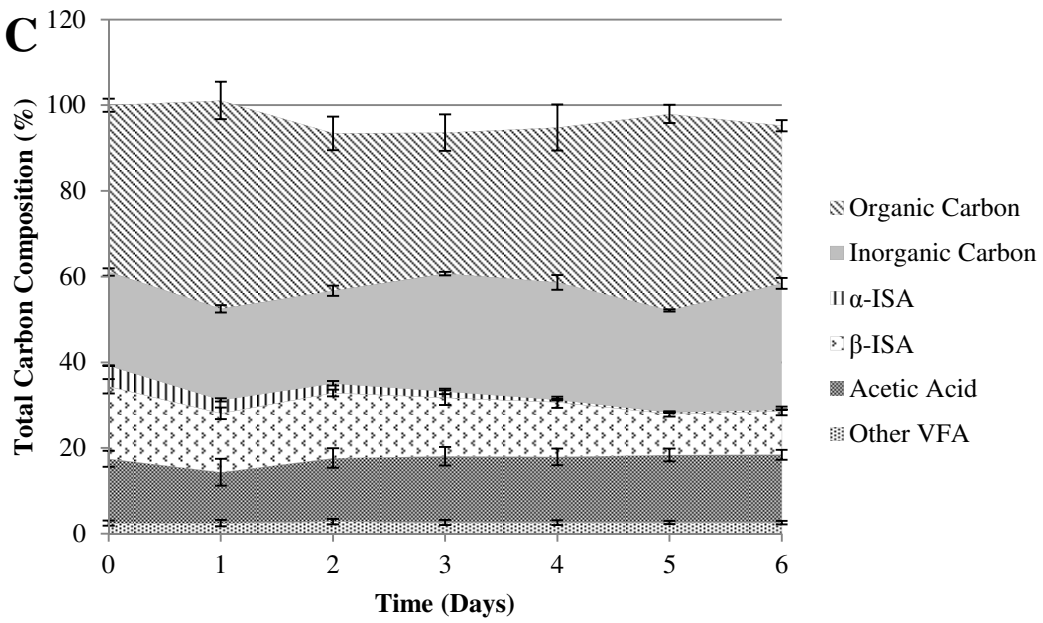

Figure 7.4 Liquid phase carbon mass balance profiles for pH7.5 (A), 9.5 (B) and 10.0 (C) microcosms. Mean values (n=3) are presented ± SE.

Protein and carbohydrate content (Figure 7.5 and 7.6) showed little variation throughout the 7 days of sampling. Methane gas evolved in each of the three microcosms (Figure 7.7), with methane as a greater percentage of the total gas generated in the pH 7.5 system; as pH increased, the volume of gas (Table 7.1) and percentage methane composition was also reduced. At the same time, the aqueous inorganic carbon increased at pH 7.5 but the increase was less marked at pH 9.5 and 10.0, potentially through the formation of carbonate precipitates.

Fermentation at elevated pH.

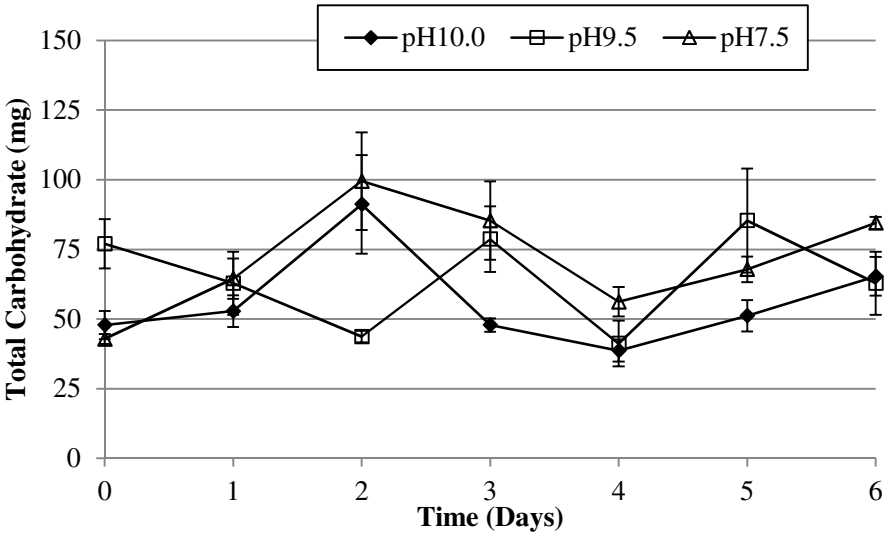

Figure 7.5 Bradford assayed protein levels across all pH7.5 (open triangles), pH9.5 (open squares) and pH 10.0 (closed diamonds) microcosms.

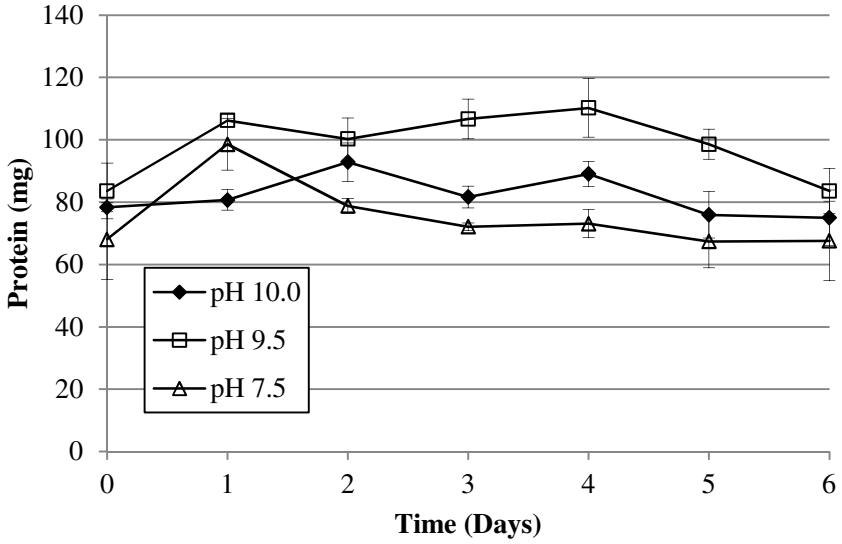

Figure 7.6 Total carbohydrate assay across pH7.5 (open triangles), pH9.5 (open squares) and pH 10.0 (closed diamonds) microcosms.

Fermentation at elevated pH.

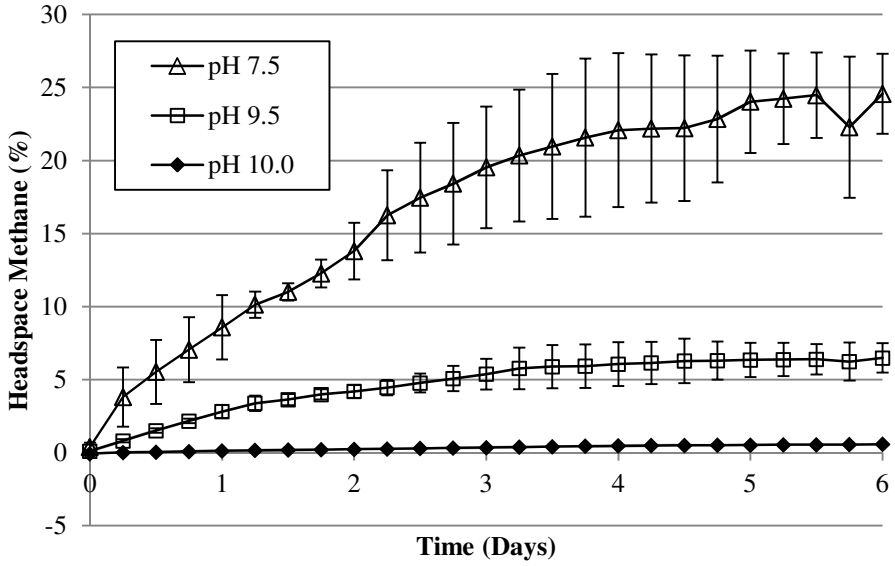

Figure 7.7 Methane gas evolution across pH7.5 (open triangles), pH9.5 (open squares) and pH 10.0 (closed diamonds) microcosms.

pH	Mean Gas Volume (mL)	St. err.
7.50	186.49	17.54
9.50	39.77	4.32
10.00	*	*

*Below detection range

Table 7.1 Gas generation volumes at each microcosm pH. Mean values are presented ± SEM (n=3).

In the control microcosms amended with chloramphenicol, removal of ISA was not observed across the three pH systems (Figure 7.8) indicating that removal of ISA in the test microcosms is microbially mediated and cannot be attributed to sorption or precipitation processes.

Fermentation at elevated pH.

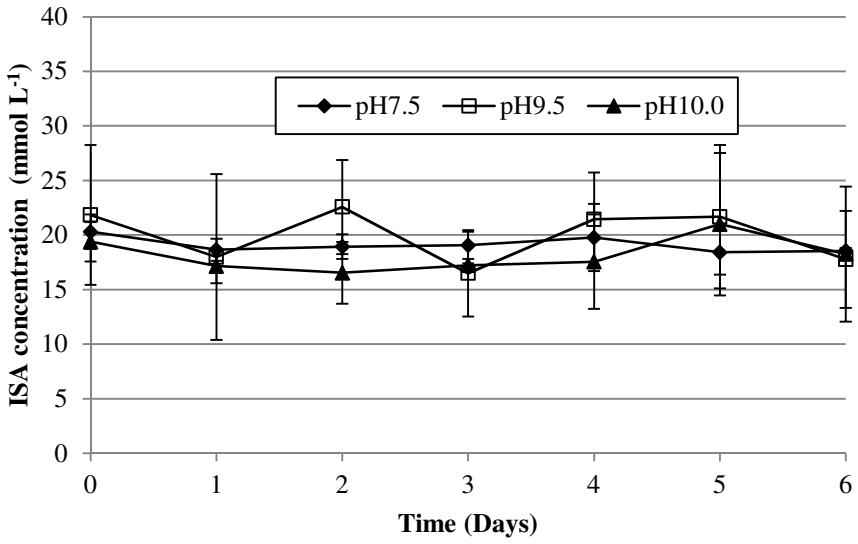

Figure 7.8 Total ISA is not degraded or subjected to sorption events when amended with chloramphenicol.

The taxonomic composition of the 16S rRNA gene clone libraries of the three microcosms are compared in Figure 7.9. 47 Eubacterial 16S rRNA gene sequences were obtained from the clone library from the pH 7.5 microcosm, of which 38 (79%) were associated with the phylogenetic class Clostridia (Figure 7.9). Within this class, 31 of the sequences belonged to the family Ruminococcaceae and 27 of these sequences were most closely related to Clostridium sporosphaeroides strain DSM 1294 (91-99% sequence similarity) when compared via the Blastn database. The pH 9.5 clone library was again dominated by Clostridia (67% of the 43 clones (Figure 7.9). Significantly, clones most closely matching Clostridium sporosphaeroides strain DSM 1294 were now completely absent from the clone library with only a total of four clones classified in the family Ruminococcaceae. At pH 9.5, within the Clostridia there was now a more even distribution of clones between the families Eubacteriaceae (8 sequences) Clostridium Insertae Sedis XII (7 sequences) and Clostridiaceae I (8 sequences). Clostridia sequences were further reduced in number in the pH 10.0 microcosm clone library but still represented 55% of the total, with the even distribution of clones observed at pH9.5 still evident (Figure 7.9). The most distinctive feature of the pH10.0 profile (Figure 7.9) appears within the non-Clostridia section of the clone library where Alcaligenes aquatilis strain LMG 22996 (98-99%, 12 sequences) from the family Burkholderiales was observed. These organisms had not previously been detected in the clone libraries from the pH7.5 and 9.5 microcosms.

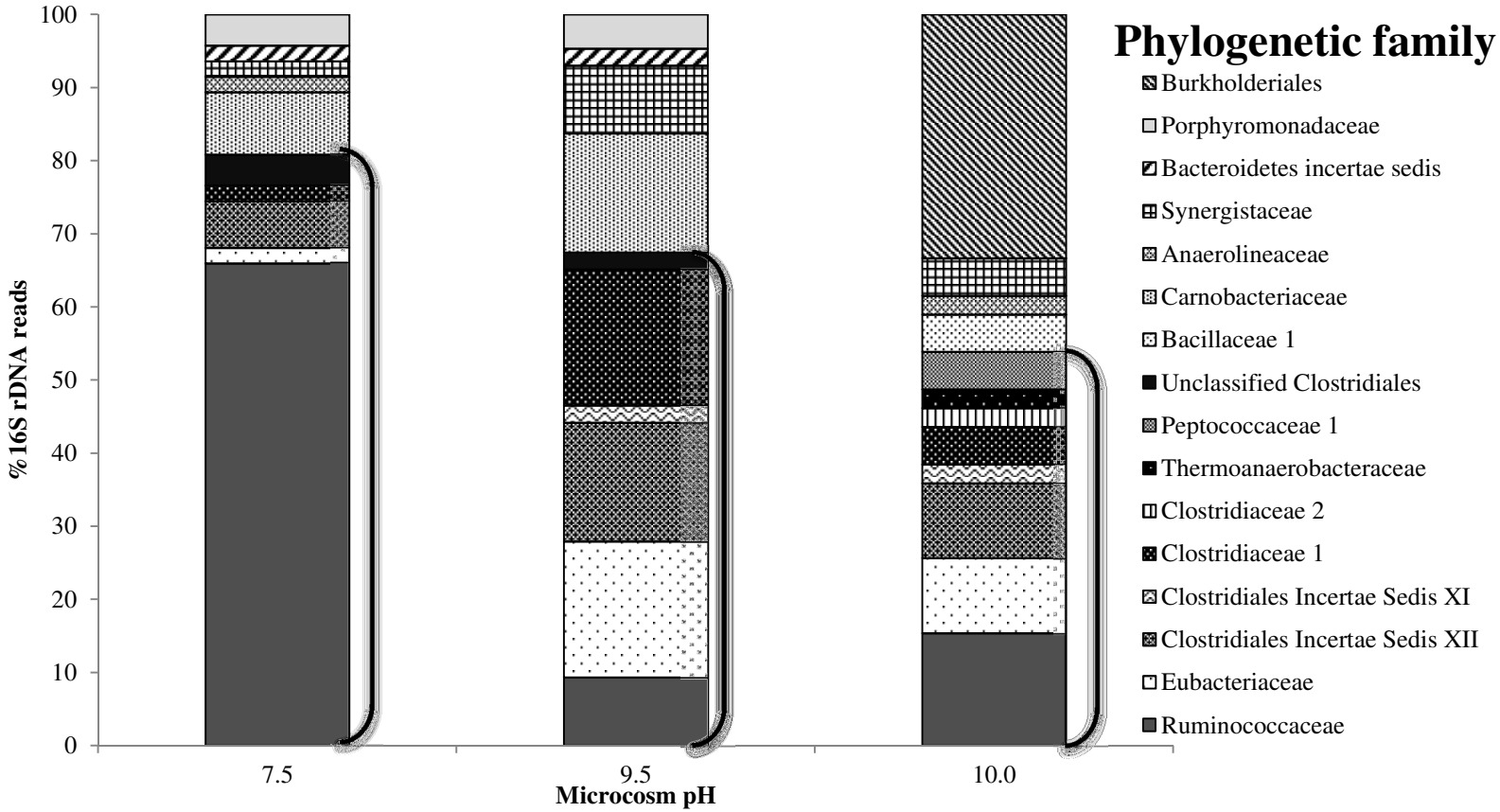

Figure 7.9 Eubacterial 16S rRNA gene clone libraries of CDP driven microcosms at pH7.5 (n=47), 9.5 (n=43) and 10.0 (n=39). Clones were assigned to a family based on the closest sequence match obtained through MegaBLAST database search. Families associated to the group Clostridia are indicated by the black parentheses.

Fermentation at elevated pH.

The Archaeal clone libraries were dominated by methanogenic taxa (Figure 7.10). At pH 7.5, 25 (n=45) of the sequences were found to match organisms from the family Methanocorpusculaceae, of which 23 sequences most closely matched *Methanocorpusculum aggregans* strain DSM 3027 (99% sequence similarity). The remaining sequences were spread across the families Methanosarcinaceae (7 sequences) and Methanomicrobiaceae (5 sequences), Thermoplasmatales insertae sedis (3 sequences), Thermofilaceae (4 sequences) and Methanosaetaceae (1 sequence). In the pH 9.5 microcosm, this profile had shifted significantly (Figure 7.10) with 46% (n=48) of the clones most closely matching organisms from the family Methanobacteriaceae, and 17 of those sequences most closely matching *Methanobacterium flexile* strain GH (99% sequence similarity). A further 46% of the clones most closely matched organisms from the family Thermoplasmatales insertae sedis, all of which were most closely related to *Methanomassiliicoccus luminyensis* strain B10 (88-89% sequence similarity). The remaining clones were present in Methanomicrobiaceae (3 sequences) and Methanocorpusculaceae (1 sequence) families (Figure 7.10). With pH increased to 10.0, the community structure again shifted such that sequences most closely associated with the family Methanocorpusculaceae predominated in the clone library (44% n=45), where sequences most closely matched *Methanocorpusculum aggregans* strain DSM 3027 (99% sequence similarity). The presence of sequences from the family Methanobacteriaceae had reduced to 27% of the total clones, and sequences most closely matched *Methanobacterium alcaliphilum* strain NBRC 105226 (99%), *Methanobacterium flexile* strain GH (99%) and *Methanobacterium subterraneum* strain A8p (99%). The remaining sequences were distributed amongst the families Methanomicrobiaceae (5 sequences), Methanosarcinaceae (5 sequences), Methanomicrobiales insertae sedis (2 sequences), and Thermofilaceae (1 sequence) (Figure 7.10).

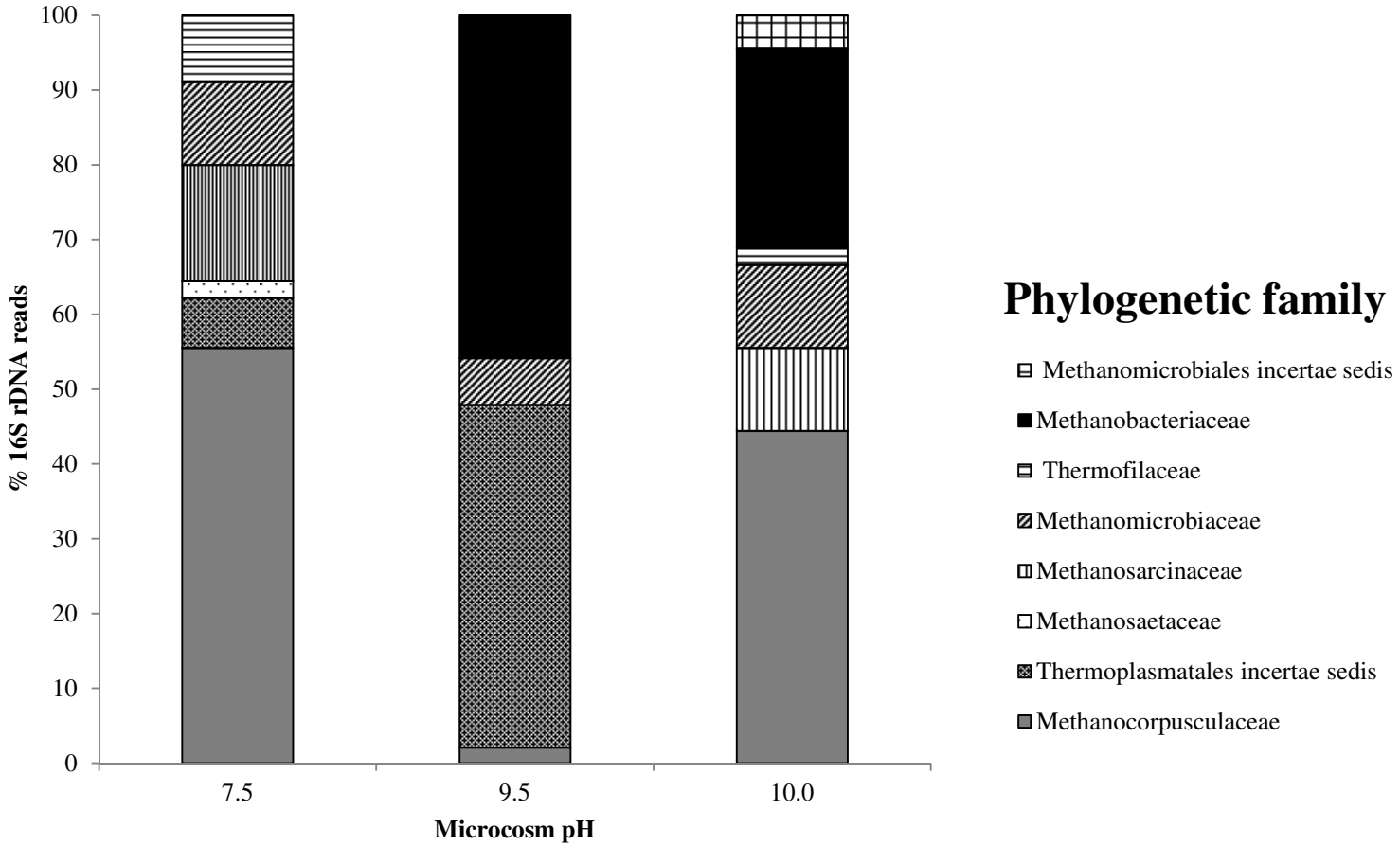

Figure 7.10 Archaeal 16S rRNA gene clone libraries of CDP driven microcosms at pH7.5 (column A n=45), 9.5 (column B n=48) and 10.0 (column C n=45). Clones were assigned to a family based on the closest sequence match obtained through MegaBLAST database search strategy.

Fermentation at elevated pH.

Although the α- and β- forms of isosaccharinic acid are not naturally encountered in the wider environment, bacteria that inhabit anoxic sediments are capable of degrading the products of alkaline cellulose hydrolysis through a fermentative, methanogenic pathway up to a pH of 10.0. Following an increase in pH to 11.0, further degradation of ISA failed to occur and it accumulated in the system to theoretical values following subsequent feeding cycles. pH appears to be an important rate limiting parameter, leading to the relative persistence of β-ISA in the system and accumulation of acetate at pH 9.5 and 10.0. Quantities of non-acetic volatile fatty acids were greater than those observed at pH 7.5, where accumulation was evident. In the microcosms operating at elevated pH (9.5 and 10.0), a greater portion of organic carbon remained in the microcosm and consequently, increased aqueous carbon closure at higher pH is most likely due to the reduced generation of biomass and biogas within the systems. Whilst a portion of the organic carbon present in all the reactors was recalcitrant, HPAEC-PAD data showed that one of the analytes present (peak 7, Figure 7.11) within the original CDP feedstock was accumulating and remaining un-degraded at elevated pH. Following fraction collection from the instrument and subsequent analysis via sequential MS/MS to determine m/z and fragmentation patterns for the relevant peaks, the analyte suggested the presence of a C-8 octanedioic acid derivative, potentially formed from the condensation of two smaller molecules, as observed in previous research [217]. The accumulation of a C-8 octanedioic acid derivative may be of interest should it exhibit any complexation, particularly if its recalcitrance is common at high pH, however there is no evidence within the literature to suggest if these compounds are complexants or not.

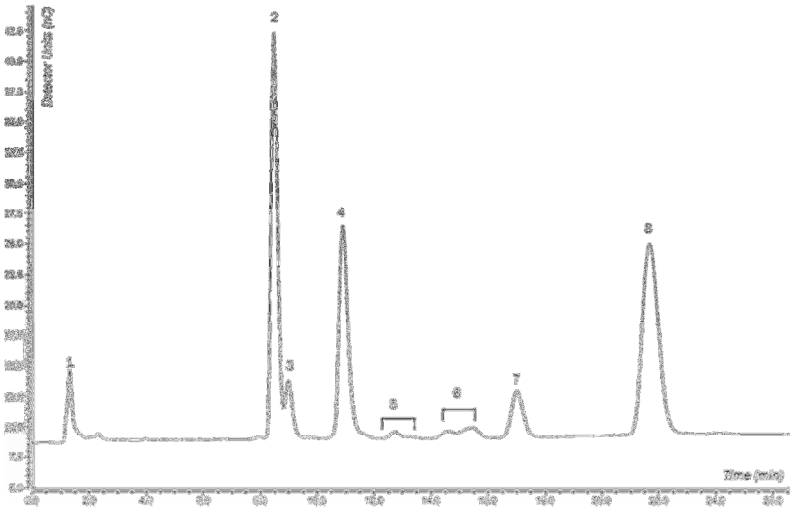

Figure 7.11 Typical HPAEC-PAD trace of CDP liquor system peak (1). α-ISA (2), X-ISA (3), β-ISA (4), α and β MSA (5), unknown (6) , octanedioic acid derivative (7) and D-ribonic acid(8), used as an internal standard for quantification.

Fermentation at elevated pH.

In the sediments studied, Clostridia appear to drive the metabolism of ISA to common fermentation end products allowing electron and carbon flow within these environments. At pH 7.5, organisms most closely related to *Clostridium sporosphaeroides* were most prevalent, where this organism and other organisms within its cluster are closely associated with anaerobic cellulose degradation resulting in fermentation to gas and volatile fatty acids [206,218]. Within the microcosms operating at pH 9.5 and 10.0, although Clostridia were the most prevalent class within the clone libraries, *Clostridium sporosphaeroides* was completely absent. The pH relationships of this species have not been previously reported, but members of this species cluster appear to be capable of degrading a range of organic substrates [219,220]. In the case of the pH 9.5 microcosm, organisms most closely matching: *Youngibacter multivorans*, *Acidaminobacter hydrogenoformans* and *Alkalibacter saccharofermentans* combined comprised 51% of the clone library (Figure7.8). Two of these species, *Y.multivorans* and *A.saccharofermentans*, have been reported to carry out fermentation processes on a range of organic substrates, resulting in the formation of formate and acetate alongside carbon dioxide and hydrogen [221,222]. In the case of *A.hydrogenoformans,* this organism is more commonly associated with the generation of volatile acids and gas through the fermentation of amino acids [223], suggesting that it may be responsible for the cycling of dead microbial biomass manifesting itself as increased proportions of other organic carbon (Figure 7.5), resulting from the increase in pH. Following through to the pH 10.0 microcosm, *Acidaminobacter hydrogenoformans* and *Alkalibacter saccharofermentans* were still the major constituents of the class Clostridia within the clone libraries. Both of these species have been reported to operate at alkaline pH [221,224], where the number of *Y. multivorans* had reduced, perhaps reflecting reported pH tolerances of 8.0 [222]. The number of species detected in the pH 10.0 microcosm increased to 17 from 14 at pH 7.5, with Clostridia still maintaining dominance. Among the species that were previously undetected was *Alcaligenes aquatilis*, which made up 31.6% of the clone library, where these strains have been reported to be capable of growth in anaerobic conditions and also involved again in the cycling of nitrogen [225], suggesting that they are responding to the increased levels of dead biomass at high pH.

Within the Archaeal clone libraries, hydrogenotrophic methanogens dominated across all three pH values. Acetoclastic methanogens were less abundant (24% at pH 7.5, 0% at pH 9.5 and 13.3% at pH 10.0) at least on the basis of sequence similarities; this is reflected in the chemical profiles of the microcosms where acetate was degraded completely at pH 7.5 (Figure 7.3B) yet appears to be accumulating due to reduced degradation at more alkaline pH values (9.5, 10, Figure 7.3C,D). This acetate accumulation coincided with a reduction in detection of *Methanosarcina* spp*,* which are capable of generating methane from acetate but reportedly exhibit sensitivity to high pH [226,227]. This accumulation of acetate was non-stoichiometric and previous authors have suggested that some methanogens, including *M. alcaliphilum* and

M. subterraneum, assimilate acetate as a growth factor, rather than as a carbon source for methanogenesis [189,228]. Reduced methane production at high pH from acetate was also observed by previous authors utilising soda lake consortia as starting inocula up to pH 10 [229]. Following an increase in pH to 9.5, increased detection of *Methanobacterium* strains was observed, all of which have been previously associated with hydrogenotrophic methanogenesis at elevated pH values [228,230].

7.3 Conclusion

This work is the first to have demonstrated that near surface microbial communities are capable of generating methane from the products of anaerobic alkaline cellulose degradation, i.e. ISAs, up to pH 10.0. Although, adaption to alkaline pH (≤10) was observed within a short timescale when compared to those expected for geological disposal, these results indicate that near surface microbial communities from circum neutral environments will be confined to niches where the pH is ≤10.0 unless further adaption occurs. In the absence of further adaption, the activity of these communities will be severely constrained by the ambient pH of a GDF which is expected to be >pH 11.0 for considerable periods of time [2]. A key constraint appears to be the presence of organisms from the genus *Alkaliphilus* within the consortia; their absence confines the fermentation of ISAs to a pH of ≤10.0. Members of this genus have been detected in anthropogenic hyper alkaline sites [135,163] where in-situ ISA formation has been observed [231] and in natural hyperalkaline systems[126]. As pH increases methane generation becomes confined to the hydrogenotrophic pathway due to the loss of acetoclastic methanogens, resulting in the accumulation of acetic acid. The degradation rates for α and β ISA reported here are the first to be described at pH 9.5 and 10.0 for mixed communities under methanogenic conditions. The slower rates of β-ISA degradation relative to the α-form may hold particular significance, indicating the potential for β-ISA to remain available for radionuclide complexation over longer timescales than α-ISA.

Fermentation at elevated pH.

7.4 Key Findings

- Biodegradation of CDP and associated ISA was observed at pH values up to 10.0 by near surface inoculum originating at pH7.5.
- ISA is fermented to acetic acid, hydrogen and carbon dioxide, as pH increases, methanogenesis appears to predominate through the hydrogenotrophic pathway.
- The rate of ISA degradation is impacted by pH, with the rate of β ISA being most impacted.
- The increase in pH also saw an increase in micro-organisms more closely associated with the cycling of dead biomass, suggesting the pH is reaching the limits of many of organisms present.

The work presented here contributed to a subsequent publication:

Rout, S.P., Charles, C.J., Doulgeris, C., McCarthy, A.J., Rooks, D.J., Loughnane, J.P. Laws, A.P and Humphreys P.N (2015) Anoxic biodegradation of isosaccharinic acids at alkaline pH by natural microbial communities. PLoS One 10 (9).

Here I contributed to the experimental design, data acquisition/analysis and preparation of the manuscript. C. J. Charles provided forage fibre analysis. C. Doulgeris provided assistance with carbon flow calculations. D.J. Rooks and J.P Loughnane provided assistance with the preparation and analysis of clone libraries. A.J. McCarthy, A.P Laws and P.N Humphreys contributed to experimental design, data analysis and preparation of the manuscript.

8. Isolation of ISA degrading micro-organisms

Isolation of ISA degrading micro-organisms.

8.1 Background

The isolation of micro-organisms from mixed cultures is always a challenge, where some organisms are almost impossible to culture using plate techniques as discussed in Chapter 2. The characterisation of the microcosms described thus far have used either PCR to detect the presence of organisms from particular a particular phylogenetic group, or clone libraries to describe the ecology. A single isolate capable of the degradation of CDPs and associated ISA would provide a model organism for further understanding of the biochemistry of ISA degradation. The pH 10 microcosm described in Chapter 7 was used as an inoculum for the isolation of a pure culture. The microcosm fluid was cultured using streak plating techniques under a stream of nitrogen, onto fastidious anaerobe agar that was adjusted to pH10. Single cultures were sub-cultured to purify. Sanger sequencing was used to determine the identity of the isolate via detection of the 16S rRNA gene. The isolate was identified as being a member of the Genus *Exiguobacterium.* The genus *Exiguobacterium* was first described by Collins *et al* in 1983 [232], where this genus falls within the phylum Firmicutes as part of the order Bacillales within the family Bacillales Insertae Sedis XII (Figure 8.1). *Exiguobacterium* spp have been isolated from a wide range of environments, where their presence is reflected in their ability to both survive and grow in extremes of temperature (-12 to 55°C), pH (5 to 11) and to tolerate stresses generated by UV radiation, antibiotics and exposure to heavy metals. Members of the genus are also noted for their ability to utilise a range of substrates as a source of organic carbon, with particular interest paid to their bioremediation potential.

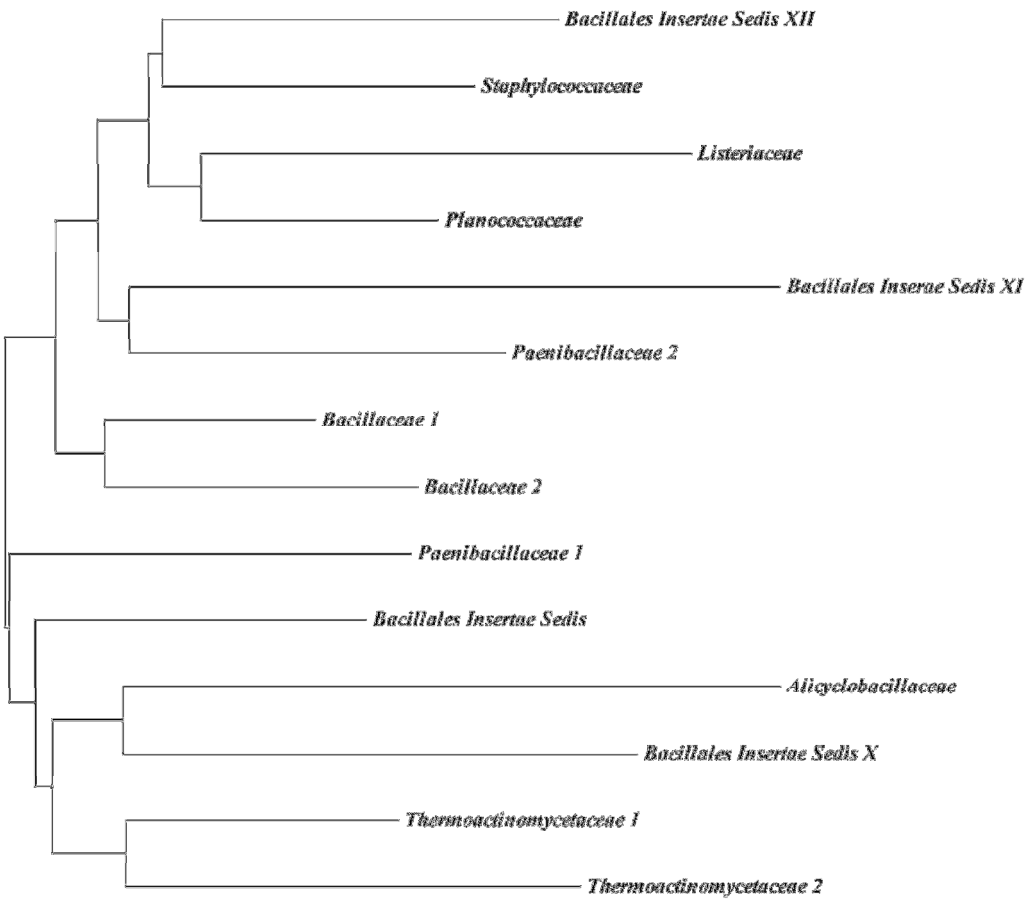

Figure 8.1 Phylogenetic representation of the order Bacillales, where members of the genus *Exiguobacterium* fall within the family Bacillales Insertae Sedis XII.

With regards to extremes of temperature, Rodrigues *et al* [233] isolated three isolates from the Siberian tundra, where temperatures are as low as -13.4°C, meaning that much of the habitat is frozen and availability of water and organic carbon in the soil is limited. The presence of the *Exiguobacterium* across a range of permafrosts was then confirmed using qPCR techniques to indicate the presence of three genes specific to the genus [234]. The same authors [235] used an *Exiguobacterium sibiricum* isolated from the Siberian permafrost to show that this isolate showed very little difference with its transcriptional behaviour across a large temperature range (4 to 28°C), but was capable of initiating the transcription of a range of stress response genes when subjected to temperatures of -2.5°C. Where some species of the *Exiguobacterium* have exhibited psychrophilic behaviour, others are known for being thermophilic in nature. A deep sea hydrothermal vent at a depth of 1600m was the isolation source of a novel *Exiguobacterium profundum* sp [236]. This isolate was capable of growth at a wide range of temperatures from 12 to 49°C, with an optimal growth temperature of 45°C. A range of other *Exiguobacterium* spp have also been identified within hot springs in the USA and India, where these isolates were capable of growth up to 50°C [237,238]. With regards to pH, Yumoto *et al*

[239] isolated a novel strain *Exiguobacterium oxidotolerans* from a drain of a fish processing plant routinely using H_2O_2 as a cleaning agent that was capable of growth up to a pH of 10.0. Activity of *Exiguobacterium aurantiacum* was also observed by Ueno *et al* above pH 10.0 [240]. Two further species of *Exiguobacterium* were isolated from industrial effluents in Gujarat that were capable of growth at pH 5.0 [241]. In the high altitude landscape of the Andean Altiplano, a sedimentary volcanic plateau approximately 4,000m above sea level, a range of lakes are present. These lakes present an extreme habitat where temperatures and heavy metal contents can vary, but are also exposed to high levels of UV-B radiation. Many studies into this region have found the presence of the *Exiguobacterium* inferring their resistance to radiation [242,243].

The ability of *Exiguobacterium* ssp to utilise a range of organic carbon sources and metals that would be otherwise toxic to many micro-organisms has generated significant interest in this genus in both research and industrial communities. Within the textile industry the presence of a number of suspected recalcitrant synthetic dyes have been reported that have subsequently been shown to be biodegradable by *Exiguobacterium* ssp. The works of Dhanve and colleagues [244,245] and Tan and colleagues [246] have all previously reported the abilities of *Exiguobacterium* ssp to utilise diazo dyes for decolourisation of textile wastewater effluent. The presence of the *Exiguobacterium* has also been observed in a petrochemical setting, again showing the practicality of the species in a bioremediation context [247,248]. In addition to the bioremediation of otherwise recalcitrant carbon sources, the species has also been shown to be capable of the reduction of chromate from a toxic hexavalent state (Cr (VI)) to the more stable trivalent form (Cr (III)) [249,250]. Reduction of arsenate and tolerance to mercury has also been noted [251-253]. Away from industrial processes, individual isolates have also shown the ability to utilise many organic carbon sources under both aerobic and anaerobic conditions, unsurprisingly a range of sugars are utilised alongside proteins and DNA [233,236,239,246]. As a result, the enzymes produced by *Exiguobacterium* ssp, particularly protease activity of alkaliphilic strains have received attention [254]. Away from environmental processes, *Exiguobacterium* ssp have not been particularly noted for their pathogenicity. More recently, the presence of these organisms within a clinical setting has been observed, where it appears to carry multidrug resistance genes within its gDNA [255,256]. As a novel isolate was obtained, a whole genome sequence was constructed within this body of work using next generation sequencing techniques. The genome obtained may provide an insight into the characteristics of this isolate, but also aid in the identification of genes required for ISA degradation.

Isolation of ISA degrading micro-organisms.

8.2 Results and discussion

8.2.1 Colony morphology

The isolate grew within 48 hours on fastidious anaerobe agar under anaerobic conditions (10% CO_2, 10% H_2, 80% N_2) at 30ºC and was also capable of growing in aerobic conditions indicating that the isolate was a facultative anaerobe. Colonies were approximately 1-2mm in diameter and opaque, with a viscous exudate. The isolate was shown to be a Gram positive short rod when subjected to staining (Figure 8.2).

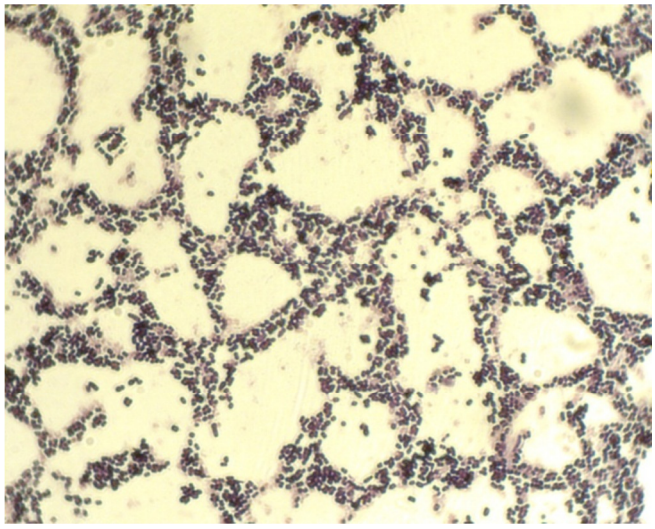

Figure 8.2 Gram stain of *Exiguobacterium* sp strain HUD. The strain exhibited morphology of short Gram positive rods.

8.2.2 ISA degradation potential of *Exiguobacterium* sp strain HUD

The *Exiguobacterium* isolate was sub-cultured into a $Ca(ISA)_2$ containing mineral media described in chapter 5 and incubated for 60 days. The results of the inoculated mineral media can be seen in Figures 8.3.

Isolation of ISA degrading micro-organisms.

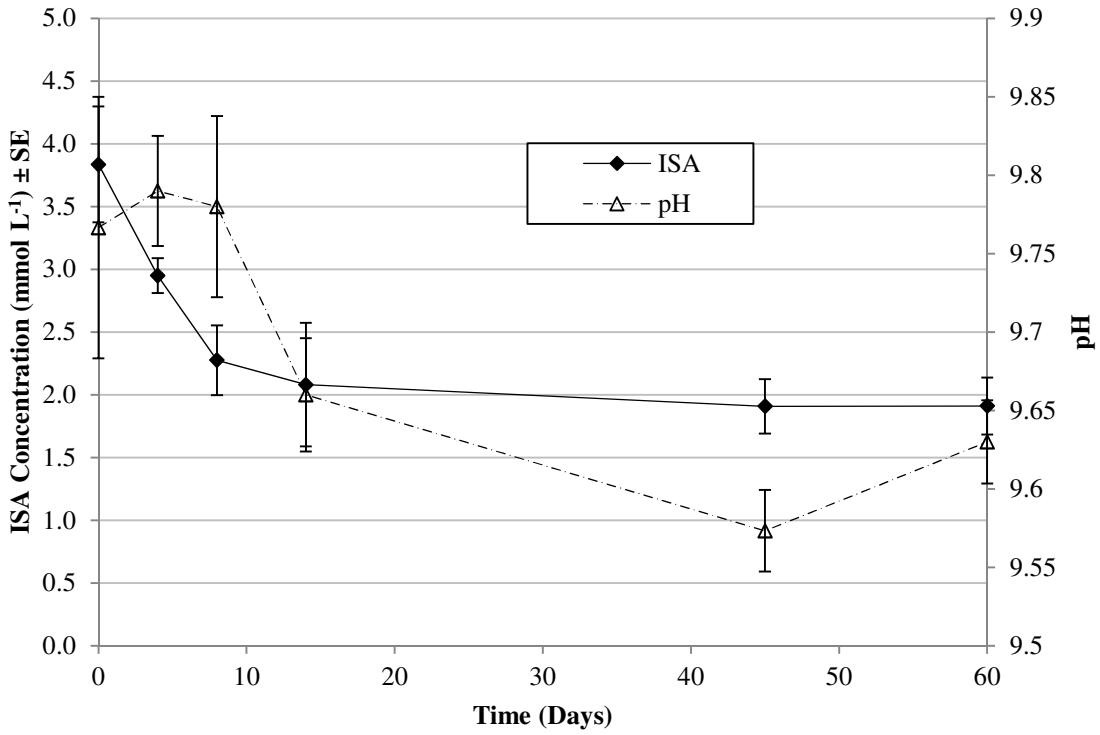

Figure 8.3 Degradation of ISA (closed diamonds) and pH evolution (open triangles) by Exiguobacterium sp strain HUD.

ISA removal (closed diamonds) was observed through the first 14 days of sampling to a concentration of 2.1 mmol L^{-1}. Sampling was continued to 45 and 60 days at which point ISA concentration appeared to remain constant at 1.9 mmol L^{-1}. In a similar fashion, pH dropped most sharply within the first 14 days of sampling, falling from 9.78 to 9.66. In the subsequent 45 day sample the pH had dropped to 9.57 before rising to 9.63 at day 60. The first order degradation rate across the 14 days of sampling was calculated to be 4.97×10^{-2} ($\pm 8.55 \times 10^{-3}$). The initial concentration of *Exiguobacterium* was determined to be 8.19×10^{2} CFU/mL, at the end of 60 days of sampling this had increased to $2.61 \times 10^{5} \pm 9.32 \times 10^{4}$ CFU/mL, representing a 2.5 $Log_{(10)}$ increase in biomass.

Isolation of ISA degrading micro-organisms.

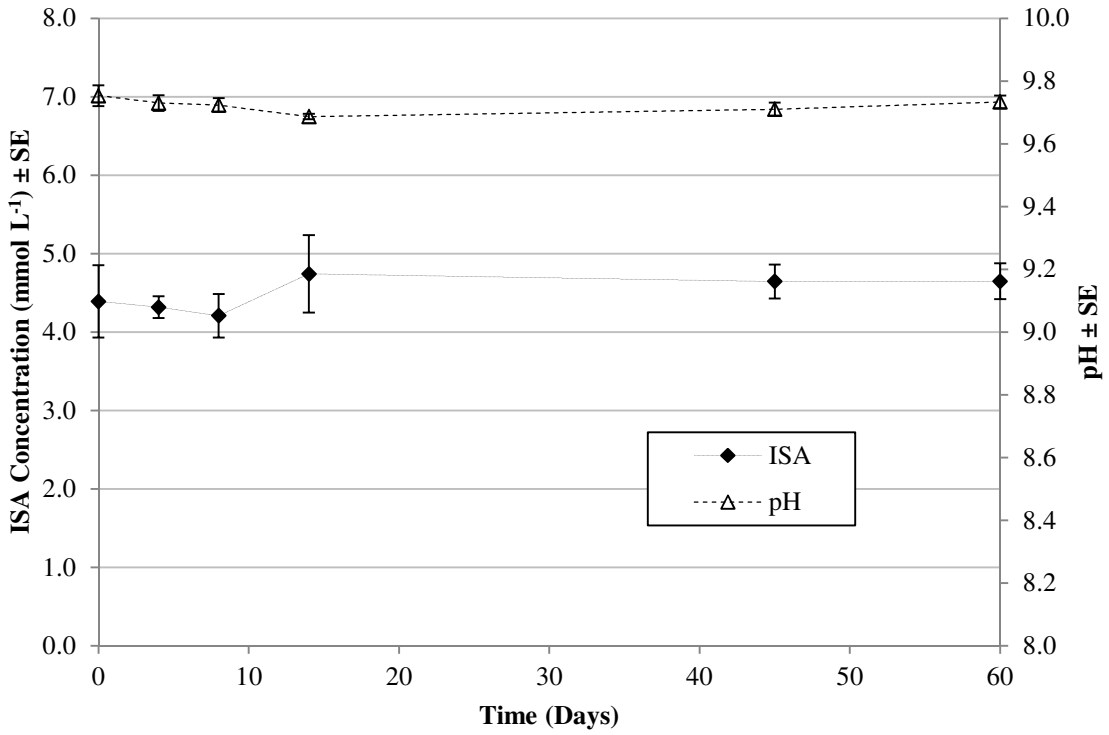

Figure 8.4 ISA degradation (closed diamonds) and pH evolution (open triangles) within uninoculated control reactions.

Within the media inoculated with sterile MRD-C (Figure 8.5), no discernable removal of ISA could be seen within the 60 day period. In fact, a slight increase in ISA concentration could be observed across the sampling period from 4.4 mmol L^{-1} to 4.6 mmol L^{-1}. Throughout the same time period pH also fell from 9.75 to 9.73, suggesting any influence on ISA concentration is likely to be abiotic and a result of equilibrium being established throughout the sample period. In a similar fashion, the increase in pH observed between days 45 and 60 may also be as a result of chemical equilibrium being established.

8.2.3 16S rDNA sequencing

Following DNA extraction, amplification of the 16S rRNA gene and subsequent Sanger sequencing following purification was carried out. The resultant sequence was chimera checked using the UCHIME 6.0 application within the Mothur suite [209]. The sequence was non chimeric, and subsequently compared against Genbank database using the MEGAblast search strategy [257] where the closest sequence was to *Exiguobacterium himgiriensis* strain K22-26 (99% sequence similarity). As a result of a high sequence match being obtained with the MEGAblast search strategy, a pairwise distance matrix was calculated to determine whether the sequence obtained was a duplicate of any of the sequence matches within the original search. In order to obtain a standard error estimate, a bootstrap analysis was carried out and the pairwise distances calculated using a kimura-2-parameter model [258], where the analysis was carried out using MEGA5 [211]. The distance matrix can be seen in table 8.1. A

distance of 0.000 would indicate that two sequences had no evolutionary divergence between them, where in this case the two *Exiguobacterium auranticum* strains (2 and 3 in Table 8.1) exhibited a lack of evolutionary divergence. This is understandable considering these two organisms are different strains of the same species, where differentiation between the two species would be likely to require comparison of alternative markers, such as phenotypic variation or through sequencing of the entire genome [259]. The small number of substitutions per site (0.001-0.012) are most likely a reflection of the small sample area (1313bp), where number of substitutions per site with members of the same genus are likely to be low. As a comparison, the same portion of rDNA from an *Alkalibacillus haloalkaliphilus* DSM 527 was also included in the analysis. This organism is within the same phylogenetic class, but is from a different genus, and this is reflected in the greater frequency of substitutions per site (up to 0.122) and hence divergence from the isolated strain.

A selection of these sequences was used to estimate the phylogenetic relationship between reference sequences of *Exiguobacterium* ssp and others representative of organisms within the order Bacillales and the resulting tree can be seen within Figure 8.5. The inferred phylogeny shows that the isolate, based on partial 16S rDNA sequence shows that the isolate clusters with the other members of the *Exiguobacterium* genus. Considering its apparent differentiation from other organisms within the genus, as well as its ability to degrade ISA; the isolate was sequenced further using next generation sequencing techniques to obtain a whole genome sequence described in section 8.2.4.

		1	2	3	4	5	6	7	8	9	10	11	12
1	Exiguobacterium_sp_strain_HUD-1 (This study)		0.001	0.002	0.002	0.002	0.002	0.003	0.003	0.003	0.002	0.003	0.010
2	Exiguobacterium_himgiriensis_strain_K22-26_NR118534.1	0.003		0.002	0.002	0.001	0.002	0.003	0.003	0.003	0.002	0.003	0.010
3	Exiguobacterium_aurantiacum_strain_NBRC_14763_NR113666.1	0.003	0.003		0.000	0.002	0.002	0.003	0.003	0.003	0.002	0.003	0.010
4	Exiguobacterium_aurantiacum_strain_DSM_6208_NR043478.1	0.003	0.003	0.000		0.002	0.002	0.003	0.003	0.003	0.002	0.003	0.010
5	Exiguobacterium_alkaliphilum_strain_12/1_NR116296.1	0.005	0.002	0.005	0.005		0.002	0.003	0.003	0.003	0.002	0.003	0.010
6	Exiguobacterium_aquaticum_strain_IMTB-3094_NR109413.1	0.005	0.004	0.005	0.005	0.004		0.003	0.003	0.003	0.002	0.003	0.010
7	Exiguobacterium_aestuarii_strain_TF-16_NR043005.1	0.008	0.011	0.011	0.011	0.012	0.013		0.001	0.001	0.003	0.002	0.010
8	Exiguobacterium_sp._AT1b_strain_AT1b_NR074970.1	0.009	0.012	0.012	0.012	0.012	0.015	0.002		0.001	0.003	0.002	0.010
9	Exiguobacterium_profundum_strain_10C_NR043204.1	0.009	0.012	0.012	0.012	0.012	0.012	0.002	0.002		0.003	0.002	0.010
10	Exiguobacterium_mexicanum_strain_8N_NR042424.1	0.003	0.003	0.003	0.003	0.005	0.005	0.011	0.012	0.012		0.003	0.010
11	Exiguobacterium_marinum_strain_TF-80_NR043006.1	0.011	0.012	0.012	0.012	0.014	0.013	0.005	0.006	0.004	0.012		0.010
12	Alkalibacillus_haloalkaliphilus_strain_DSM_5271_NR041985.1	0.121	0.121	0.119	0.119	0.118	0.122	0.119	0.119	0.119	0.121	0.116	

Table 8.1 Pairwise distance matrix to estimate the evolutionary distance between sequences. The numbers of base substitutions per site are shown (highlighted red). The standard error estimates can be seen above the diagonal (highlighted blue).

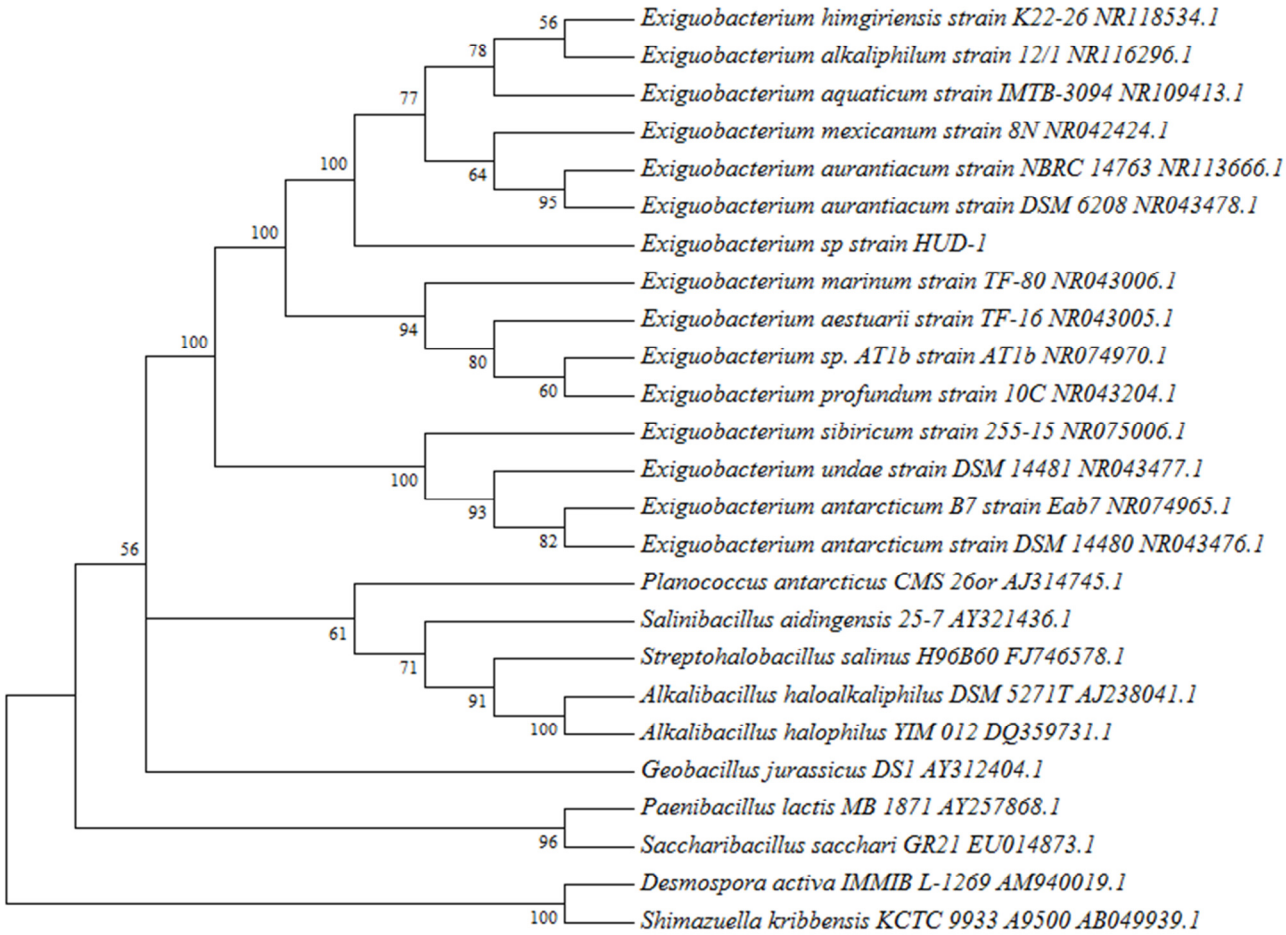

Figure 8.5 Bootstrap consensus tree inferred from 1000 replicates using neighbour joining method. Branches reproduced in >50% of the replicates are collapsed.

8.2.4 Whole genome sequencing and annotation

A draft whole genome sequence was obtained using a whole genome shotgun (WGS) sequence strategy. Paired-end 125 cycles sequence reads were generated using the Illumina HiSeq 2500 system (BaseClear, NL). FASTQ sequence files were generated using the Illumina Casava pipeline version 1.8.3 where quality was assessed using the Illumina Chastity filter. Reads containing adapter sequence or control signal were removed in-house. FASTQC quality control (tool v0.10.0) was used to carry out a second quality assessment. Low quality sequence from the FASTQ sequences were both trimmed and assembled using CLC Genomics Workbench version 7.0.4, optimal k-mer size was determined using KmerGenie [260]. The contigs were linked and placed into scaffolds or supercontigs. The orientation, order and distance between the contigs was estimated using the insert size between the paired-end and/or matepair reads using the SSPACE Premium scaffolder version 2.3 [261]. Whole genome sequencing generated 826 contigs with a draft genome 3,359,295 bp in length and G-C content of 51.1%. The draft genome contained a total of 3,484 coding sequences (CDS), where 19 pseudogenes, 9 genes coding for rRNA (5S, 16S, 23S), 69 genes coding for tRNAs and 1 ncRNA were present.

The whole genome sequence was then annotated using the RAST server [262], where the output from the subsystem annotation can be seen in Figure 8.6. Many of the proteins identified would be expected for normal cellular function and support, including those involved with cell wall, membrane transport, production of amino acids and proteins as well as DNA replication. A total of 98 proteins were annotated that were involved with DNA. repair As previously mentioned, members of the *Exiguobacterium* have been noted for their ability to tolerate and grow in a range of extremes. This is perhaps reflected in the detection of 61 genes related to DNA repair, with a further 75 genes related to stress response. The genes present here would suggest that the *Exiguobacterium* isolated may be capable of surviving stresses including osmotic shock, as well as heat and cold shocks. Genes were also present relating to responses to carbon starvation and oxidative stresses.

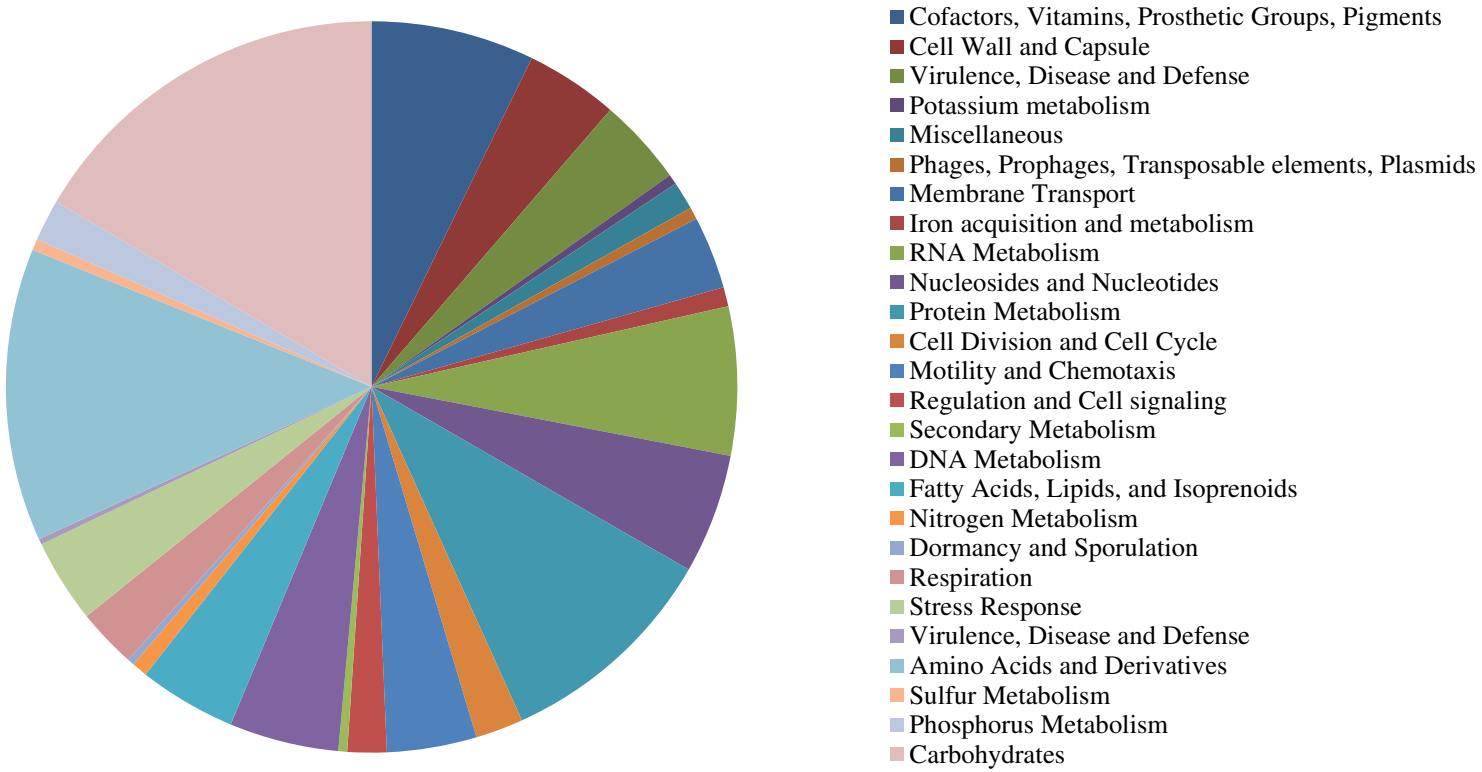

Figure 8.6 RAST subsystem output following annotation. The subsystem covered 48% of the genome where 1361 non-hypothetic proteins were coded alongside 81 hypothetical proteins.

Particular interest was shown in the subsystem categories involving metabolism, with the largest number of annotated proteins belonging to the carbohydrate subsystem (335). Within the genome *Exiguobacterium* sp Strain HUD contains genes encoding proteins involved in both aerobic and anaerobic processes with carbohydrates. Genes encoding the proteins involved in glycolysis and TCA cycle were evident, as well as those for gluconeogenesis. In terms of carbon sources, the genome suggests that the organisms can utilise a range of substrates including disaccharides, such as lactose, fructose and trehalose and single sugars such as galactose, xylose and mannose. Five genes were also present encoding proteins involved with the metabolism of aromatic compounds. Currently, no annotation exists for a protein used for ISA degradation, since none have been described within the literature. However, the wide range of carbon sources capable of being utilised within the literature for organisms of this genus suggest that the genes present may encode for multifunctional proteins. The isolate (*Exiguobacterium* sp. Strain HUD) contained a number of regions encoding for the degradation of proteins, suggesting that this organism may have played a role in the degradation of dead cell mass present within the microcosm in addition to playing a role in (at least) α-ISA degradation.

8.3 Conclusion

This chapter has presented a novel isolate of *Exiguobacterium* Strain HUD from the microcosm operating at pH 10.0 discussed in Chapter 7. The genome has shown that this isolate is capable of a number of both aerobic and anaerobic processes. With respect to the degradation of ISA, the isolated species was capable of partially degrading the calcium salt of α-isosaccharinic acid. The versatility of this genus that was observed within the literature was also hinted at within the genome of this novel strain, where the genes suggest that this isolate is also capable of degrading proteins, DNA and other components of cell matter. Outside the scope of this body of work, the genome also contains a range of genes encoding proteins involved in the resistance to a range of toxic elements and multidrug resistance with respect to a clinical setting.

8.4 Key Findings

- A portion of the micro-organisms present within microcosms are directly culturable using standard plate techniques.
- The novel *Exiguobacterium* species obtained was capable of ISA degradation.
- Whole genome sequencing revealed a number of genes suggesting this organism may display the ability to degrade a range of substrates. In addition, a number of genes associated with survival in extreme conditions were also present.

Isolation of ISA degrading micro-organisms.

The work presented here contributed to a subsequent publication:

Rout, S.P., Rai, A., and Humphreys, P.N. (2015) *Draft Genome Sequence of an Alkaliphilic Exiguobacterium sp Strain HUD, Isolated from a Polymicrobial Consortia*. Genome Announcements. 3 (1)

Here I contributed to the experimental design, data acquisition/analysis and preparation of the manuscript. A. Rai was responsible for the isolation of the *Exiguobacterium sp* under my supervision. P.N Humphreys contributed to experimental design and preparation of the manuscript.

9. Hyper-alkaline contaminated site field study

9.1 Rationale

As discussed in the chapter 7, when microcosms were challenged with a pH value of 11.0, the organisms present were not capable of surviving. As a result, a new sediment source was sought, where the local microbial community had been exposed to high alkalinity over a prolonged period of time. In addition, such a site may prove to be analogous to the conditions expected in a deep geological disposal concept. The site chosen for study was a hyper alkaline contaminated site at Brookbottom, Harpur Hill, Derbyshire. Up until 1944, a lime kiln was in operation adjacent to the site generating a range of CaO containing wastes which were deposited at the southern end of the site (Figure 9.1). A range of microbial studies have been carried out using the soil populations present at the site [96,106,114,163], however the presence of ISAs in the site had not been previously confirmed.

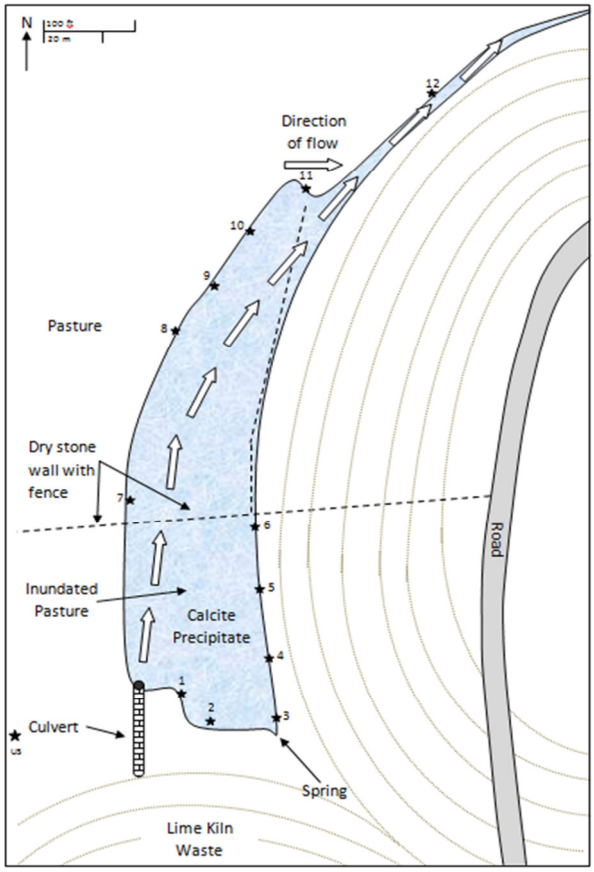

Figure 9.1 Overview of Brookbottom, Harpur Hill, Derbyshire. Sampling points are numbered and indicated by black stars. (Image reproduced from Google Maps.)

9.2 Results and Discussion

Rainwater percolation through the waste generates an alkaline leachate (pH 12.0-13.0) which emerges both from a culvert in the SW corner and a spring in the SE corner of the site (Figure 9.1), the leachate then flows in a N/NW direction following the path of the original brook. On emergence the alkaline waters absorb atmospheric $CO_2(g)$ generating a tufa deposit which has

infilled the valley floor and is encroaching on the adjacent farmland. Since operation began in 1872, the site has had ca. 140 years to allow for the evolution of a chemical and microbial environment analogous to those within a GDF. The site has been subject to a number of microbiological and geochemical investigations [114,163], however the presence of the stereoisomers of ISA have not yet been determined. The site was investigated for the presence of ISA's, but also of volatile fatty acids as markers of fermentation of organic compounds (not limited to ISA). In addition the presence of terminal electron acceptors within the site was investigated to determine the range of microbial processes that could potentially take place.

ISA was detected in the porewater and sediments from sample sites where an alkaline pH predominated (Table 9.1). pH values within the sediments ranged from 7.70 to 11.70, whereas within the porewaters, pH values were as high as 12.70. ISA extracted from the sediments was solely in the α conformation, reflecting the limited solubility of the Ca^{2+} salt of α-ISA at high pH [32,263]. The greater solubility of β-ISA under high pH, calcium rich conditions is reflected in its absence from sediment samples; although some β-ISA and X-ISA were detectable in soil porewaters. This absence is likely to be due to a combination of enhanced mobility and availability as a carbonaceous substrate. The α-ISA was most abundant in samples which had been subjected to longer term tufa contamination (S1-6; Figure 9.1) rather than those most recently inundated (S7-12). The uncontaminated soil sample showed no evidence of ISA generation following acid extraction. The surrounding porewaters also contained volatile fatty acids throughout sites 1-12 in varying concentrations. Acetic acid was found in site 1, 2, 7 and 9, where concentrations exceeded 800 μmol L^{-1} in the latter two. Of the other volatile fatty acids, propionic, butyric, isobutryic, valeric and isocaproic acids were observed. A range of terminal electron acceptors were also observed, reflecting results obtained in other studies [114,163]. The presence of both nitrate and sulphate suggested that microbial nitrate and sulphate reduction could occur in-situ. The detection of ferric and ferrous iron suggested that microbially mediated iron reduction may also be occurring in situ.

Site	Porewater Analyses										Soil analysis		
	pH	µmol L^{-1}									pH	Eh	µmol g^{-1}
		Fe(II)	Fe(III)	α-ISA	β-ISA	X-ISA	Acetic Acid	Other VFA	Sulphate	Nitrate			α-ISA
1	12.14	2.99	2.29	16.70	27.70	151.71	190.36	58.07	279.27	31.13	11.70	-62.00	15.78
2	7.80	0.03	14.19	0.00	6.88	37.67	248.24	248.52	8.96	8.55	7.70	-66.00	28.78
3	12.50	0.80	3.98	5.06	3.28	18.21	0.00	148.70	626.88	1267.10	11.20	-49.00	344.72
4	12.40	0.00	0.98	0.00	0.00	45.70	0.00	95.34	121.88	258.87	11.07	-43.00	111.72
5	12.70	0.00	1.43	5.26	8.35	0.00	0.00	240.65	555.94	1809.19	11.35	-47.00	0.07
6	12.10	1.10	2.34	16.43	39.67	96.96	0.00	122.78	103.85	110.32	10.80	-34.00	0.13
7	12.40	4.84	7.59	0.00	21.90	0.00	1102.21	214.32	162.92	5.16	10.17	-74.00	0.79
8	12.10	0.00	5.17	0.00	0.00	0.00	0.00	134.08	186.98	2.90	10.30	-89.00	0.21
9	8.00	0.07	5.55	10.72	45.82	250.73	815.26	568.25	77.19	4.68	8.00	-42.00	0.22
10	11.20	1.83	9.03	0.00	0.00	0.00	0.00	152.29	58.96	4.68	9.00	-26.00	4.44
11	8.10	0.00	6.06	0.00	0.00	0.00	0.00	176.10	169.27	0.00	7.85	-25.00	0.21
12	11.50	0.00	5.90	0.00	0.00	0.00	0.00	178.17	36.98	98.39	10.30	43.00	0.22

Table 9.1 Pore water and soil analysis from twelve sample sites around the Brookfoot site, Harpur Hill, Buxton, UK

The results of combining alkaline leachate with uncontaminated soil from the area surrounding the site can be seen in Figure 9.2. In abiotic experiments, where soil was double autoclaved prior to the addition of the alkaline leachate, ISA was generated at all three temperatures across the 16 weeks of sampling. In contrast, in the presence of neutralised alkaline leachate no ISA was generated within the 16 weeks of sampling (data not shown).

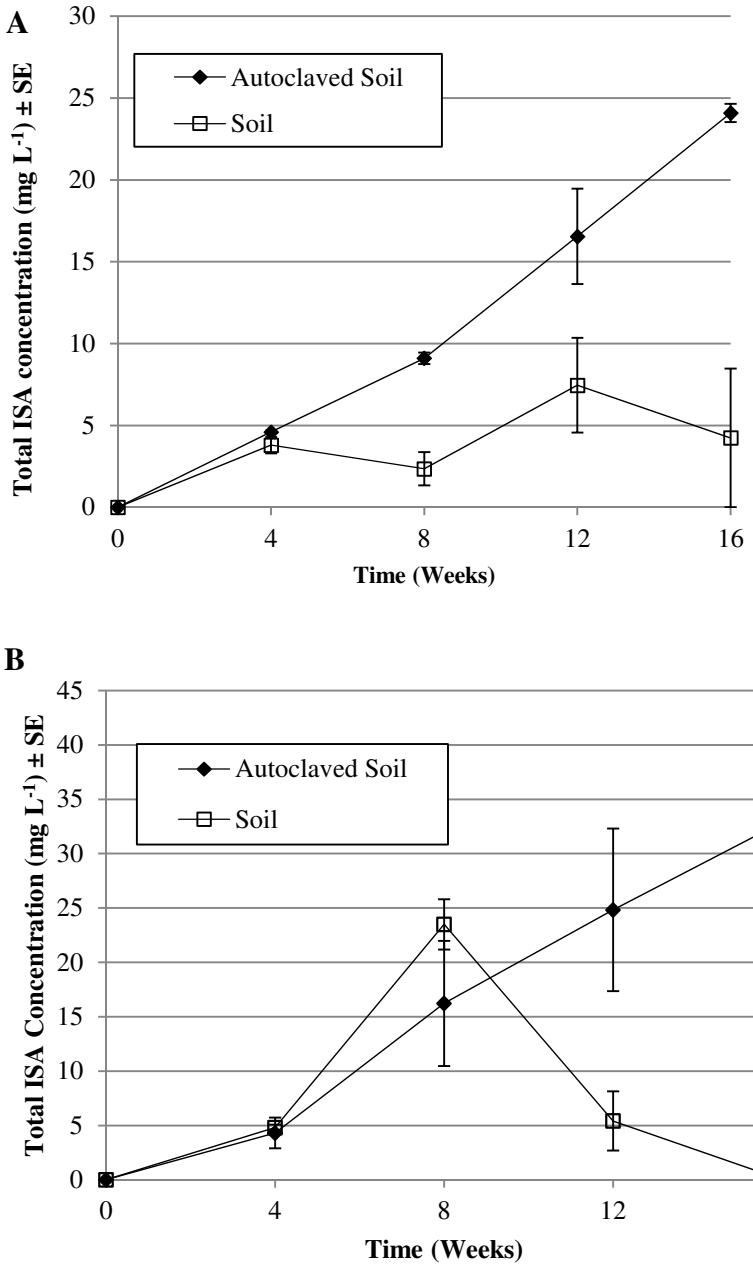

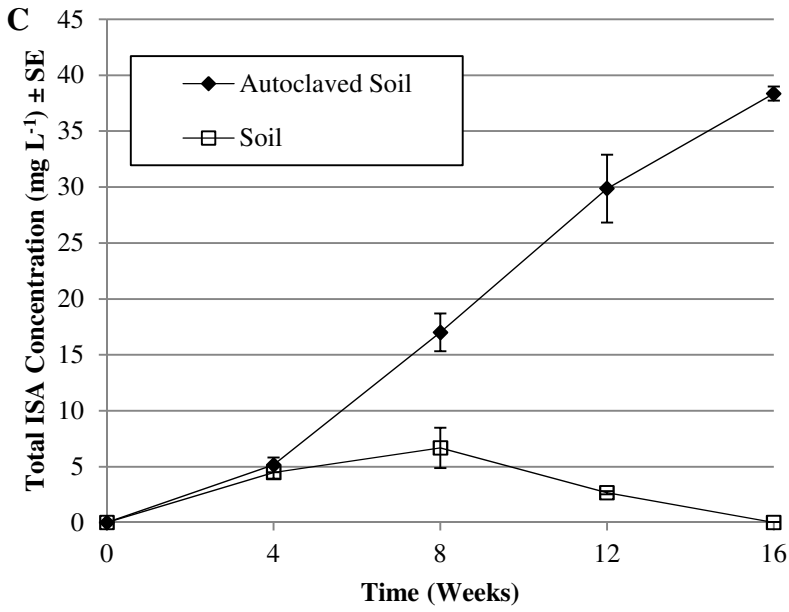

Figure 9.2 Generation of ISA's in abiotic (closed diamonds) and biotic (open squares) uncontaminated soils mixed with hyperalkaline leachate at 4ºC (A), 10ºC (B) and 20ºC (C).

The rate of ISA generation increased with temperature, as observed by other authors employing pure cellulose and sodium hydroxide [264]. An Arrhenius plot of the calculated rates (Figure 9.3, $R^2 = 0.95$) allowed the activation energy (21.4 J mol^{-1}) of ISA generation to be calculated. This value is lower than reported values [264] for the propagation of the peeling reaction with cellulose and 1.25M NaOH, which may reflect the degree of amorphism of the cellulosic materials present within the soils. In the biotic experiments where soil had not been autoclaved, generated ISA was either partially (4ºC) or completely removed (10 and 20ºC) by the end of 16 weeks of sampling. Indicating that temperature influenced both the rate of ISA generation and its subsequent microbial degradation.

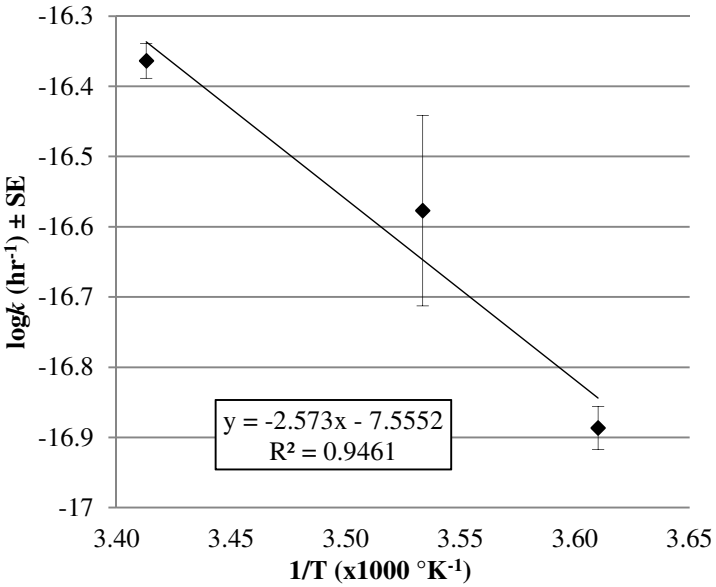

Figure 9.3 Arrhenius plot of rates of ISA generation.

The batch fed microcosm established using soil collected from the site (Figure 9.4) demonstrated significant ISA degradation at pH 11.0. The microcosm demonstrated mean first order degradation rate for the individual stereoisomers of ISA of 1.69 x 10^{-1} day^{-1} (SE 3.28 x 10^{-2}) for α-ISA and 1.13 x 10^{-1} day^{-1} (SE 1.07 x 10^{-2}) for β-ISA. These rates are greater than those observed with consortia obtained from neutral sediments operating at pH 10.0 [265], indicating the greater degree of alkaline adaption seen at the Harpur Hill site. The microcosm consortia fermented ISA to hydrogen and acetic acid of which the latter was subsequently removed (Figure 9.4). Methane accumulated within the headspace at a consistent rate after day 2 and its production did not correlate directly with the generation and removal of acetic acid (Figure 9.4). Similarly, no clear trend could be observed with regards to the generation and removal of hydrogen within the system linked to the formation of methane. Carbon dioxide from fermentation processes is likely to precipitate as a carbonate within the alkaline conditions of the microcosm. Previous authors have noted the ability of methanogens to utilise calcite as a carbon source, suggesting that the rate of hydrogenotrophic methanogenesis is impacted by the availability of carbon dioxide [266].

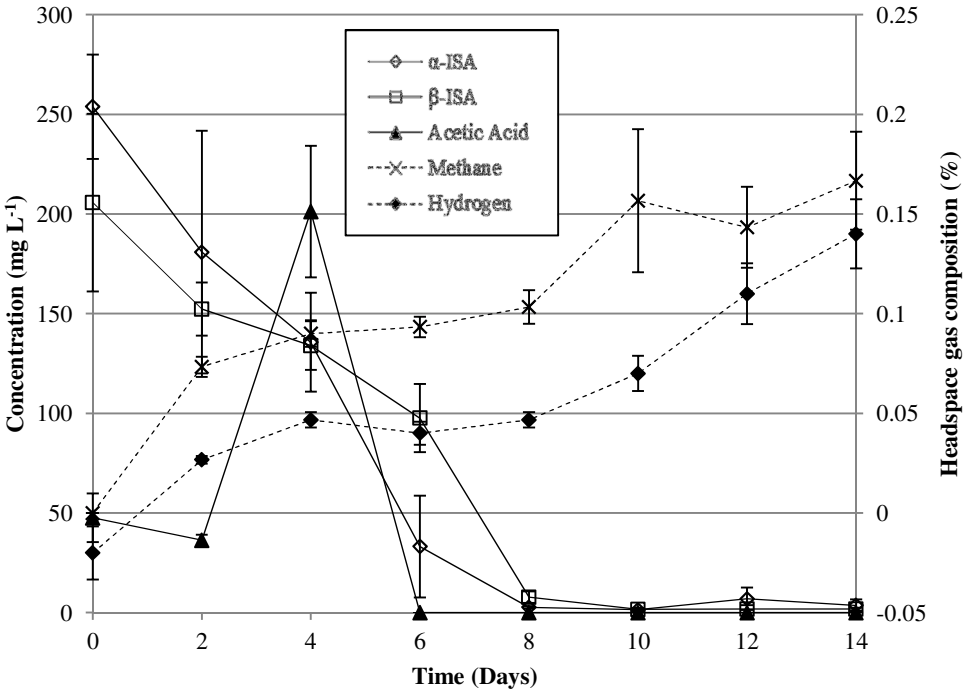

Figure 9.4 pH 11.0 microcosm chemistry. Both stereoisomers of ISA (open diamonds, open squares) were removed over the course of sampling. Acetic acid (closed triangles) was generated and subsequently removed alongside the generaton of methane (crosses) and hydrogen (closed diamonds).

In samples amended with chloramphenicol, removal of ISAs from solution was not evident, the presence of VFAs was limited to those present within the CDP liquor and methane was not detected in the headspace gas (Figure 9.5). This indicates that the ISA removal observed is microbially mediated rather than being the result of sorption or chemical degradation processes (Figure 9.6).

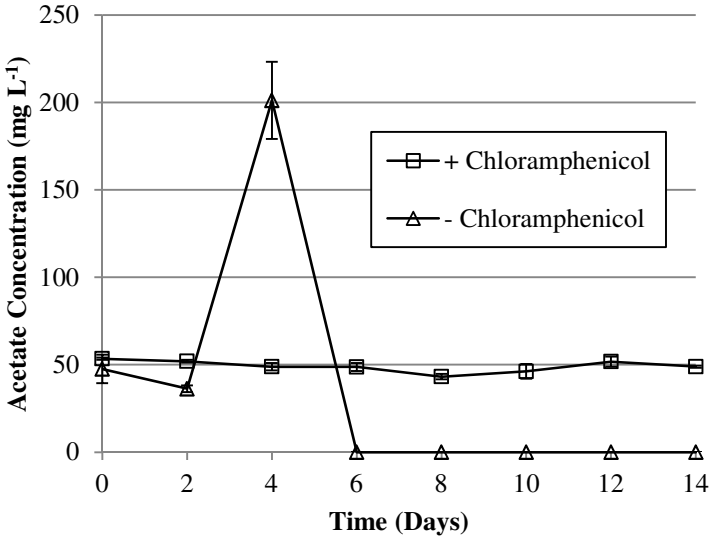

Figure 9.5 Fate of acetic acid in biotic (open triangles) and abiotic (open squares) reactions.

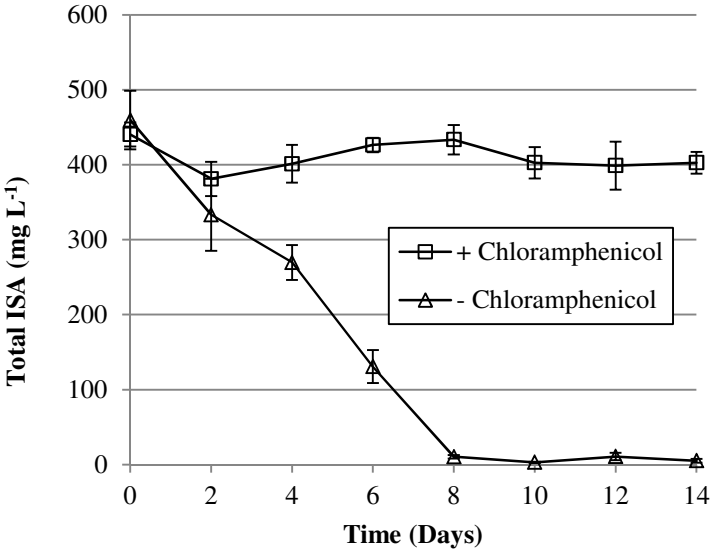

Figure 9.6 Fate of total ISA in biotic (open triangles) and abiotic (open squares) reactions. The bacterial library was dominated by members of Clostridiaceae 2 where methanobacteriaceae dominated the archaeal library.

The taxonomic composition of the 16S rRNA gene clone library is presented in Figure 9.7A. 33 Eubacterial 16S rRNA gene sequences were obtained, of which 53% were most closely associated with the Family Clostridiaceae 2. Within this family, all the sequences were most closely related to sequences from the genera *Alkaliphilus*, with 8 sequences most closely matching *Alkaliphilus crotonatoxidans* strain B11-2, 7 sequences most closely matching *Alkaliphilus metalliredigens* strain QYMF and 2 most closely matching *Alkaliphilus transvaalensis* strain SAGM1. The isolation of this genera from hyperalkaline sites is well

documented, as is their ability to metabolise a range of carbon sources [158,267-270], and as a wider class, Clostridia are well documented in their ability for carry out fermentation processes [271,272]. Of the remaining clones, 25% most closely matched organisms from the family Bacillaceae 1, where sequences most closely matched *Anaerobacillus alkalilacustris* strain Z-0521 (3 sequences), *Bacillus alcalophilus* strain NBRC 15653 (2 sequences), and *Bacillus okhensis* strain Kh10-101 (3 sequences). Much like the Clostridiaceae 2, the organisms observed here are also capable of metabolising carbohydrates and sugars as a carbon source under anaerobic conditions [273,274]. The remaining sequences most closely matched organisms belonging to the class α-Proteobacteria, which are associated with a range of processes [275,276].

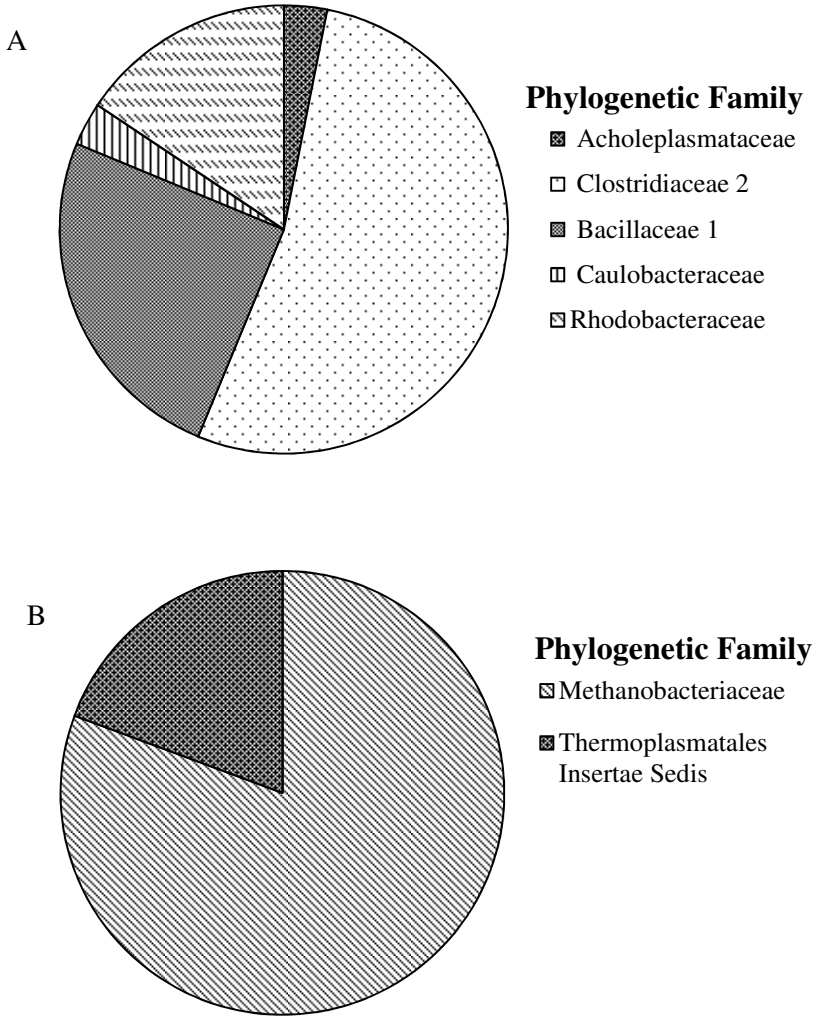

Figure 9.7 Taxonomic composition of Eubacterial (A) and Archaeal (B) clone libraries.

The taxonomic composition is represented in Figure 9.7B. In this case 81% of the clone library (n=31), was represented by organisms from the family Methanobacteriaceae where 12 sequences most closely matched *Methanobacterium alcaliphilum* strain NBRC 105226 with the remaining sequences from this family (13 sequences) most closely matching *Methanobacterium flexile* strain GH. Both of these strains are hydrogenotrophic Archaea and have been shown to be phylogenetically related to one another [230], *M. alcaliphilum* has been isolated from alkaline sediments in Egypt with optimal growth conditions of pH9.9 under laboratory conditions [193]. At the time of writing, *M. flexile* has only been isolated from mesophilic, neutral pH lake sediments, where no further testing of pH tolerances was carried out [230]. The 6 remaining sequences from the clone library most closely matched hydrogenotrophic methanogen *Methanomassiliicoccus luminyensis* strain B10 from the family Thermoplasmatales insertae sedis. Again, this hydrogenotrophic methanogen has been more

commonly associated with the digestive tract of other organisms [277], and information regarding its tolerance of alkaline conditions are not available in the wider literature. The obligate hydrogenotrophic nature of the Archaeal clone library contradicts the removal of acetic acid seen within the system. This acetic acid metabolism may be linked to assimilation/anabolism by *Methanobacterium* sp [189,228,278], or degradation by Eubacteria within the consortia, where *Alkaliphilus* sp and α –Proteobacteria are capable of acetate utilisation [279,280]. The latter would require an as yet unidentified terminal electron acceptor to be present within the system.

9.3 Conclusion

This survey of the hyper-alkaline site at Harpur Hill, represents the first demonstration of the *in-situ* generation of both the α and β forms of ISA in terrestrial environments through the hydrolysis of soil organic material by anthropogenic alkaline leachates. Sediments at the site contain active microbial consortia able to ferment both forms of ISA with the subsequent generation of acetic acid, hydrogen and methane at a pH of 11.0. Molecular analysis of these consortia indicates that they are dominated by alkaliphilic Clostridia and hydrogenotrophic Methanobacteriaceae. These observations suggest that ISA may act as a key electron donor supporting the diverse subsurface microbial population previously observed at this site [106,114,281].

Regarding ILW disposal, this survey suggests that microbial populations able to degrade ISA may evolve within decades of site closure provided that the ambient pH is in the region of pH 11.0. Current estimates for near-field pH of a cementitious GDF suggest that the ambient pH will remain above pH 12.0 for hundreds to thousands of years [2], suggesting that ISA degrading consortia will be confined to lower pH regions within the waste or in the alkaline disturbed zone surrounding the GDF. Provided microbial activity is not inhibited by the ambient pH these results suggest that a microbial population similar to that which has evolved at Harpur Hill will be able to metabolise both the α and β forms of ISA generated within the site and in so doing mitigate the impact that these complexing will have on the transport of radionuclides.

9.4 Key Findings

- The presence of ISA's was detected in both the pore waters and soils present at the site.
- These ISA's are generated through the contact of the alkaline leachate with organic matter present within the soil.
- The microbial consortia present in the hyperalkaline contaminated soil were capable of ISA degradation and methanogenesis at pH 11.0, where alkaliphilic Clostridia and

hydrogenotrophic Methanobacteriaceae were the dominant Eubacterial and Archaeal phylogenetic groups.

The work presented here contributed to a subsequent publication:

Rout, S.P., Charles, C.J., Garratt, E.J., Laws, A.P., Gunn, J. and Humphreys, P.N. (2015) *Evidence of the generation of isosaccharinic acids and their subsequent degradation by local microbial consortia within hyper-alkaline contaminated soils, with relevance to intermediate level radioactive waste disposal*. PLoS One 10.

Here I contributed to the experimental design, sample acquisition, data acquisition/analysis and preparation of the manuscript. C. J. Charles contributed to the preparation and acquisition of data within ISA generation from soil experiments. E.J Garratt was responsible for the sampling and maintenance of ISA generation from soil experiments. J. Gunn provided site access and assisted in the preparation of the manuscript. A.P. Laws and P.N Humphreys contributed to experimental design, data analysis and preparation of the manuscript.

10. Concluding remarks

The long term disposal of the United Kingdom's nuclear waste legacy presents a major challenge, requiring significant research input from a range of disciplines [2]. The current strategy for this long term storage is that of a deep cementitious facility, expected to be up to 500 m below ground level [2]. This geological disposal facility (GDF) will be expected to contain a number of different types of waste which are broadly categorised into low-, intermediate- and high level based upon their heat and radioactive outputs [1]. One of the most important attributes of any such facility is the retention of the radionuclide contaminated wastes within the facility for very long periods of time. Retention of radionuclides within the cementitious GDF concept is associated with the maintenance of high pH values through the dissolution of the cementitious backfill by intruding groundwater. In this high pH system, radionuclides are retained by sorption onto the cementitious materials or precipitation/co-precipitation events [282].

Cellulosic materials constitute a significant (2,000 t) proportion of the intermediate level waste inventory [1]. Under the anaerobic, alkaline conditions placed upon a GDF through cement backfill, these cellulosic materials are expected to degrade. Amorphous regions of the cellulose are subjected to the 'peeling' reaction where anhydroglucose units are stripped back along the cellulose chain, until an eventual stopping reaction takes place, usually associated with the source of hydroxide reaching a highly crystalline region [9,11,20]. The main products (70%+) of this degradation are the α- and β- forms of isosaccharinic acid (ISA), alongside a range of other small (C1-C6) organic molecules [12,23]. ISA has received considerable attention when assessing the safety of a GDF, as it is capable of influencing radionuclide retention through the formation of soluble complexes which may then leave the GDF, potentially entering the alkaline disturbed zone surrounding the GDF and eventually biosphere [26-28,31].

As an organic carbon source, ISA represents a potential substrate for microbial action where gas generation from these substrates may also impact on the performance of a GDF [283]. Microbes are expected to colonise a GDF through contamination of the disposed wastes, and during the construction and operational phases of the facility where micro-organisms may enter through ground water flow [147]. The high pH nature of the GDF may act as a barrier to growth for mesophilic micro-organisms, however microbial activity within other high pH sites such as alkaline soda lakes and land contaminated with hydroxide forming wastes suggest that alkaliphilic and alkali tolerant consortia are likely to develop given time [114,178]. ISA itself is not naturally found within any environment, although its presence has been observed as a bi-product of the Kraft paper pulping process [284]. Previous research has suggested that ISA may be utilised by micro-organisms under methanogenic and denitrifying conditions [93,284], however in both of these studies measurement of ISA concentrations have been lacking or limited to the calcium salt.

Conclusion 1: near surface microbial consortia are capable of the anaerobic degradation of CDP including ISA's without prior exposure.

The initial investigations discussed in Chapter 3 sought to determine whether anaerobic, near surface microbial consortia were capable of the degradation of cellulose degradation products and associated ISA, where ferric iron, sulphate and carbon dioxide were available as the sole electron acceptor across three mesophilic microcosms. These conditions were selected as they provide an insight into the potential behaviour of microbial consortia when interacting with an alkaline, CDP (and ISA) containing plume at the interface with a neutral niche. pH conditions close to neutrality are likely to be experienced within a GDF in ungrouted waste packages, however neutral conditions are also representative of those outside the alkaline disturbed zone in the far field of a GDF. It is important to consider the far field in this case should pH be a barrier to colonisation of the local microbial consortia present within the environment of a potential GDF. Under these conditions, both forms of ISA were readily utilised as a substrate for growth, no significant difference (n=6, p=0.118) was observed when comparing the degradation rate across each of the geochemical conditions giving a mean degradation rate of 4.7×10^{-2} hr^{-1} (n=36, SE±2.9×10^{-3}). These rates represent the first reported for combined α/β ISA degradation within the literature. Subsequent PCR analysis of the DNA within each microcosm showed the presence of Clostridia across all three microcosms. Although the PCR techniques used mean that the fermentation processes cannot be directly attributed to these organisms, they are synonymous in the literature with the production of volatile fatty acids, carbon dioxide and hydrogen from a range of organic substrates [206,219,285-288]. This suggested the presence of a two stage pathway, where the initial fermentation (with acetogenesis of longer chain fatty acids) preceded iron reduction, sulphate reduction or methanogenesis of these fermentation products (Figure 10.1).

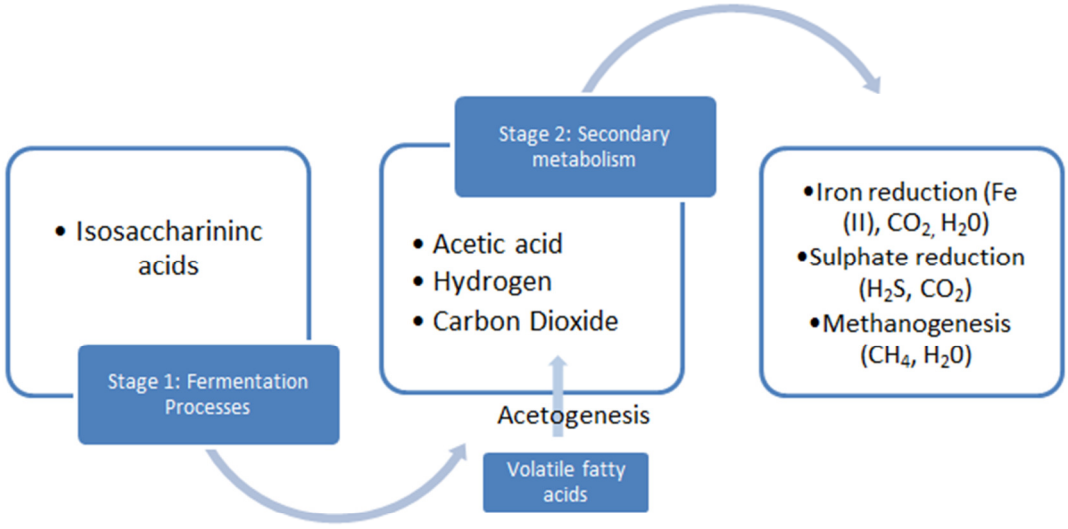

Figure 10.1 Two stage pathway of complete ISA biodegradation at neutral pH values. Initial fermentation to volatile fatty acids, hydrogen and carbon dioxide is followed by iron reduction, sulphate reduction and methanogenesis dependent on the presence/absence of required terminal electron acceptors.

Iron reducing bacteria *Geobacter* sp were detected using PCR, which is well known for its ability to reduce ferric iron to oxidise a range of organic substrates as well as hydrogen [289,290]. Interestingly, sulphate reducing bacteria were also detected by PCR, which reflects the work of other authors showing that many of the SRB are capable of not only the reduction of sulphate, but also the reduction of a range of other elements, as well as carrying out some fermentation processes [170,291]. In addition to iron reduction, methanogenesis was also observed in the iron reducing reactor. This reflected the high crystallinity of the haematite used as a source of ferric iron, this coupled with the unstirred nature of the microcosm allowed for niches where methanogenesis could occur, where previously low crystallinity ferric iron has been seen to inhibit methanogenesis [292]. Both acetoclastic methanogens and hydrogenotrophic methanogens were detected using PCR in both the iron reducing and methanogenic microcosms. This first body of work has significant implications should pH inhibit microbial activity within a GDF, where microbial activity would be limited to the interfaces between alkaline and neutral regions such as those found in ungrouted wastes and around the far field of a repository should significant ISA migration occur. As a result, the ability of near surface micro-organisms to adapt to an increase in pH was the focus of the second stage of the investigation. The results of this stage of the research are reported in [293]

Conclusion 2a: near surface anaerobic microbial consortia are capable of adapting to increasing pH utilising CDP as an organic carbon source.

Given that the presence of ferric iron and sulphate are likely to be limited to niches within the facility, carbon dioxide is likely to be the predominant terminal electron acceptor, particularly as a result of the fermentation processes. With this in mind, the second study discussed in Chapter 7 focussed on the abilities of near surface microbial consortia to adapt and thrive under fermentative, methanogenic conditions when the stress of increasing pH was introduced. The microcosm operating at pH 7.5 was retained as a means of comparison with the microcosms operating close to (9.5), and at the minimum pH (10.0) expected to evolve within the timescale of storage in a GDF. The results presented in Chapter 7 showed that the microbial consortia present within the canal sediment at pH 7.5 was capable of generating methane from ISA up to a pH of 10.0. Although Clostridia were the most dominant class within all three microcosms, variation was observed with regards to the genera within this class. *Clostridium sporosphaeroides* clones made up a significant proportion of the clone library at pH 7.5, yet were completely absent within the pH 9.5 and 10.0 clone libraries. Both clone libraries at the elevated pH values exhibited a wider variety of genera in comparison to that at pH 7.5 within the Clostridia class, with increased detection of alkaliphilic strains such as *Alkalibacter* and *Acidaminobacter* ssp.

Conclusion 2b: Alkaliphilic and alkalitolerant phyla are present within mesophilic soils and begin to thrive as pH increases.

These findings suggested that near-surface microbial consortia are likely to contain alkaliphilic or alkalitolerant micro-organisms that become prominent as pH increases, as had previously been observed by Grant *et al* [93]. The inability to detect *C. sporosphaeroides* in the microcosms operating at elevated pH also suggests that the increase in pH is also imposing an increased death rate upon the system [93]. This was also reflected in the increased detection of micro-organisms more commonly associated with the degradation of proteins and other cell matter such as *Cloacibacillus* and *Acidaminobacter* ssp [294,295]. The most prominent non-Clostria within the pH 10.0 microcosm was *Alcaligenes faecalis*, which, contrasting with *C. sporosphaeroides* was only detected in this microcosm, reinforcing the potentially increased death rate at high pH through its ability to cycle amino acids and other cell associated matter [225].

Conclusion 2c: with increasing pH, rates of ISA degradation and methanogenesis are impacted.

The chemistry of the microcosms followed the same two stage pathway format observed with the microcosms in Chapter 6, where ISA was subjected to fermentation to acetic acid as a predominant volatile fatty acid alongside carbon dioxide and hydrogen. The predominance of

the Clostridia within the clone libraries again suggest that this class is playing a major role in fermentation processes. Within the chemistry of the microcosms, the overall rate of ISA degradation decreased with increasing pH, with rates falling to 3.6×10^{-3} (n=3, SE=2.6×10^{-4}) from 3.0×10^{-2} (n=3, SE=4.7×10^{-3}) at pH7.5. The work of Grant *et al* [296] also observed variation in total ISA degradation rates with pH, using an alkaliphilic biofilm consortia. The alkaliphilic nature of the biofilm meant that degradation rates were retarded at pH 7, but a decrease in rate was also observed with a pH transition of 10.0 to 11.0. The degradation rates of the individual stereoisomers showed that the rate of β-ISA degradation was most impacted by the increase in pH, resulting in persistence within microcosms. This study represents the first case of a differential in microbial behaviour towards the individual stereoisomers with varying pH, where previous studies within the literature have focussed solely on the α- form [106] or have quantified total ISA, rather than the individual forms [296].

A persistence of acetic acid was also observed in the microcosms operating at the more elevated pH. At pH 9.5, the accumulated acetic acid was at a greater concentration than at pH 10.0, where the reduced rate of fermentation was almost certainly accountable. At pH 7.5, acetic acid was completely consumed at the end of the sampling, which coincided with the detection of acetoclastic methanogens within the clone library. At a genus level, *Methanosarcina* and *Methanosaeta* ssp were observed, where under mesophilic conditions these organisms are well documented for their utilisation of acetic acid to generated methane [226,227,297,298]. The detection of these species was reduced following the increase in pH to both 9.5 and 10.0, explaining the increased levels of acetic acid remaining at the end of each feed cycle. A small amount of acetate was also removed from the system, this may be as a result of small levels of acetoclastic methanogens being present within the reactor. Since methane was still detected in both higher pH microcosms, the primary routes for methanogenesis at higher pH values appear to be that of hydrogenotrophy. This was reflected in the dominance of hydrogenotrophic methanogens within the clone libraries, where *Methanocorpusculum, Methanomassiliicoccus* and *Methanobacterium* ssp were most commonly matched within the sequence database. No previous reports of an alkaliphilic *Methanomassiliicoccus* could be found within the literature, although organisms within both the genus *Methanocorpusculum* and *Methanobacterium* have both been observed within alkaline soda lakes [229]. Interestingly, organisms from the genus *Methanobacterium* also require the assimilation of acetic acid as a growth factor [193,228], this may account for the removal of at least a portion of acetic acid within the pH 9.5 and 10 systems. The reduction in methane generation may also be as a result of a reducing population size. Across all three microcosms, a portion of organic carbon was remained un-degraded at the end of sampling. Subsequent inspection of the sugars present within the sample using HPAEC-PAD, an octanedioic acid derivative was identified as a component of this recalcitrant organic carbon.

This compound was most likely a result of the merging of two smaller molecules as previously observed [217], however data with regards to the complexation potential and microbial utilisation are absent from the literature. Further investigation into this compound was beyond the remit of the body of work presented here, and is discussed merely as an observation. The findings associated with conclusion 2 are presented within [265].

Conclusion 3: the use of microcosms presents a concentrated source of alkaliphilic ISA-degrading micro-organisms for further study.

Attempts to culture organisms present within the microcosm operating at pH 10 resulted in the isolation of a novel isolate. The *Exiguobacterium* sp described in Chapter 8 was isolated using standard culturing techniques via a streak plate method. This Clostridia was not detected within the clone libraries, previous authors have noted that organisms cultured using plate based methods do not always represent the dominant species within a particular system as discussed in Chapter 2 [299,300]. Culturing of the isolated *Exiguobacterium* sp with a minimal media where $Ca(\alpha\text{-ISA})_2$ was the sole carbon source showed that it was capable of degrading α-ISA under anaerobic conditions. Interestingly, subsequent whole genome sequencing of this organism suggested the presence of a range of genes encoding proteins for the utilisation of a range of carbohydrates, an observation consistent with the ability of the organism to degrade ISA. Further analysis of the genome showed genes encoding proteins that could be involved with the cycling of dead biomass, including protein, lipid and DNA were present. These findings are presented within [301]

Conclusion 4: anthropogenic and natural analogues to hyperalkaline conditions present a source of micro-organisms capable of CDP utilisation at elevated pH.

The canal sediment microcosms operating at pH 10.0 were also sub-cultured and amended to a pH of 11.0. The batch feeding process was again carried out and the concentration of ISA measured at regular intervals. Calculation of total ISA concentration within the feedstock allows for a theoretical curve to be generated indicating the concentration of ISA present within the reactor if no microbial activity takes place (Figure 10.2). In this case, the concentration of ISA reaches a plateau, where at this point the amount of ISA removed from the abiotic system is equal to that added into the system. When the ISA concentration was measured within the pH 11.0 reactor at regular intervals throughout the feed cycle, that the theoretical plateau had been reached and this, alongside a measurement of ATP suggested that no microbial activity was taking place.

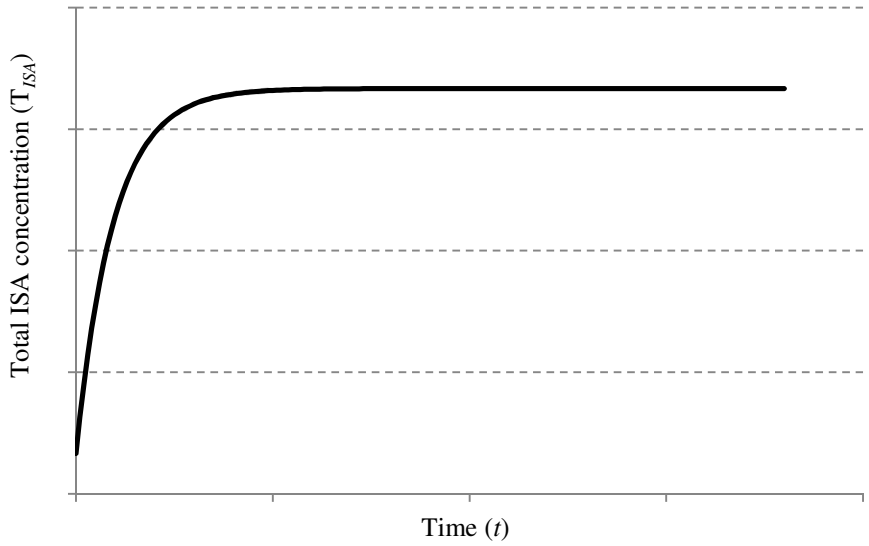

Figure 10.2 Theoretical curve of total ISA concentration in an abiotic system employing the batch waste feed cycle. Continued batch feeding of the abiotic system results in ISA concentration approaching the concentration of the feedstock before microcosm inoculum is completely replaced by feedstock where the concentration plateaus.

The inability of the mesophilic near surface consortia to develop tolerance to alkaline conditions (> pH10.0) within a short time scale suggested that a different consortium would need to be sought out. A hyper alkaline contaminated site at Buxton, UK presented a potential microbial consortium that had been subjected to pH values of 10.0-13.0 for up to 140 years. An initial investigation of the contaminated soil showed that ISAs were present, where the α- form was more prominent, most likely as a result of its poor solubility as a calcium salt [32]. Within the pore waters both the α- and β- forms of ISA were detected suggesting that the cellulose degradation had occurred *in-situ* during the lifetime of the site. The presence of terminal electron acceptors within the pore waters suggested that a range of microbial processes could occur, where the detection of volatile fatty acids within the soil suggested that fermentation processes were taking place at high pH. In the south-west corner of the site is a region that remains uncontaminated by the inflowing leachate where soil pH was ~7.8. When this soil was autoclaved and mixed with the alkaline leachate evidence of ISA generation was clear. Assuming that the soil was heterogeneous, the rate of ISA generation was linked to temperature, such that faster generation was observed at higher temperatures. Following on from this, extrapolation of the data into an Arrhenius plot showed that the activation energy (21.4 J mol^{-1}) was far lower than those reported in the literature [264]. This finding was not unexpected, considering the work carried out by Van Loon and Glaus in [264] involved the use of pure cellulose in laboratory conditions, whereas the cellulose sources present in the soil are likely to be diverse where the volume of amorphous region open to alkaline attack cannot be defined. In biotic experiments where the soil was not sterilised prior to contact with the

alkaline leachate, a clear removal of ISA from the solution was observed following an initial period of ISA generation. This suggests that a range of alkaliphilic ISA degrading micro-organisms were present within the soils in the site, even in regions of soil that have not been exposed to the alkaline leachate. As such, contaminated soil was collected for subculture into further CDP driven microcosms.

In addition to the increased pH, a longer growth rate was imposed by using a waste feed cycle of 14 days. This was done in order to reduce the probability of active organisms being 'washed' out of the system where an organism, particularly with respect to facultative alkaliphiles, that may be growing at a slower rate due to the stress imposed by increased pH [302]. The consortium obtained from the hyperalkaline site was capable of the degradation of both forms of ISA, where pH in this case did not appear to retard the rate of β-ISA degradation as it had at with the canal consortia. The total rate of ISA degradation was also greater than that observed with the canal sediments at pH 9.5 and 10.0 (Figure 10.3).

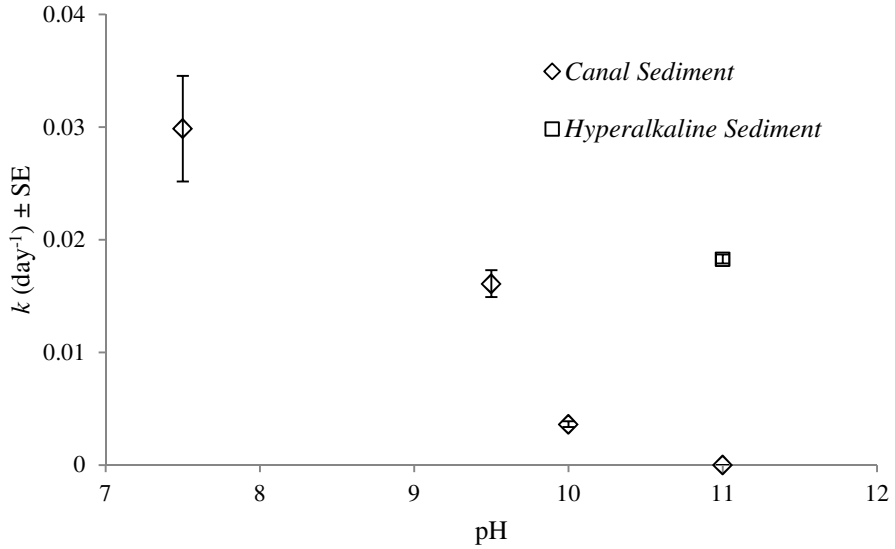

Figure 10.3 Rates of total ISA degradation across all microcosm studies using both canal (open diamonds) and hyperalkaline sediments (open squares).

Within the clone libraries generated from the microcosm, Clostridia were again the dominant organisms. Over 50% of the sequenced clones most closely matched organisms from the genus *Alkaliphilus,* a range of organisms which have been isolated from a range of alkaline environments [267-269,280,303]. In addition, the range of substrates utilised by these organisms is diverse, where the use heavy metal terminal electron acceptors have also been observed, although the chemistry of the system in this case limited these organisms to fermentation processes. Within the remainder of the clone libraries, the presence of Bacilli was detected, comprising 25% of the clone libraries. In particular, sequence matches were observed that were most closely related to *Anaerobacillus alkalilacustris,* which has been co-cultured with *Geoalkalibacter ferrihydriticus* within the literature. In these cases, *A. alkalilacustris*

provides a source of acetic acid through fermentation processes which then acts as an electron donor for *G. ferrihydriticus* which reduces ferric iron in the presence of the acetic acid [304]. Members of the genus *Anaerobacillus* were also observed almost exclusively in a single batch iron reducing reactor operating at pH 10 using Harpur hill soils as a starting inoculum [106]. The remaining *Bacillus* ssp detected were commonly isolated from alkaline environments within the literature [305,306]. These findings are presented within [231]

Within the canal sediment microcosms operating at pH 10, the accumulation of acetic acid was observed as a result of a reduced detection of acetoclastic methanogens. Within the pH 11 microcosm using the Harpur hill soil as an inoculum, again, a generation of acetic acid was observed through fermentation processes but was subsequently degraded by the end of the 14 day sample period. This initially suggested that the imposition of a 14 day growth cycle may have improved the ability of acetoclastic methanogens to grow at higher pH. Subsequent analysis of the clone libraries indicated that the Archaea present within the microcosm were exclusively hydrogenotrophic, as had been observed within the pH 10.0 microcosm in Chapter 7. Organisms from the genera *Methanobacterium* and *Methanomassiliicoccus* were observed, as they had done with the canal sediment reactors. Again, a degree of acetic acid removal is likely to be as a result of assimilation by the Archaea present, however the remaining portion may be subjected to degradation by members of the α- proteobacteria observed within the Eubacterial clone library. Acetate degraders were present within the library, however it was unclear as to the electron acceptor utilised in order to oxidise the acetic acid [276,279]. This was an interesting observation, since it would have been expected that within alkaline microcosms, acetoclastic methanogenesis would dominate since the carbon dioxide required for hydrogenotrophic methanogenesis would be unavailable via precipitation as a carbonate. In both alkaline microcosms (mesophilic inoculum; pH10.0 and alkaline inoculum; pH11.0) the dominance of hydrogenotrophic methanogens suggests that the carbonates present are bioavailable. Hydrogenotrophic methanogenesis from carbonate has been recently observed in *Methanocalculus natroniphilus* [307], these taxa were absent from the clone libraries suggesting that the ability to utilise carbonates for methanogenesis is not limited to this species.

Overall, the work presented throughout this thesis suggests that microbial activity utilising organic carbon generated from the anaerobic alkaline hydrolysis is likely to take place within a GDF concept within the lifetime of its operation. Here microbial activity utilising ISA as a substrate has been demonstrated up to a pH of 11 within batch fed microcosms. Current information on the evolution of the near field within a potential site suggest that pH is likely to be 13.5 post closure (stage I, Figure 10.4), with a fall in pH to 12.5>pH>10 during stage III of the evolution (Figure 10.4).

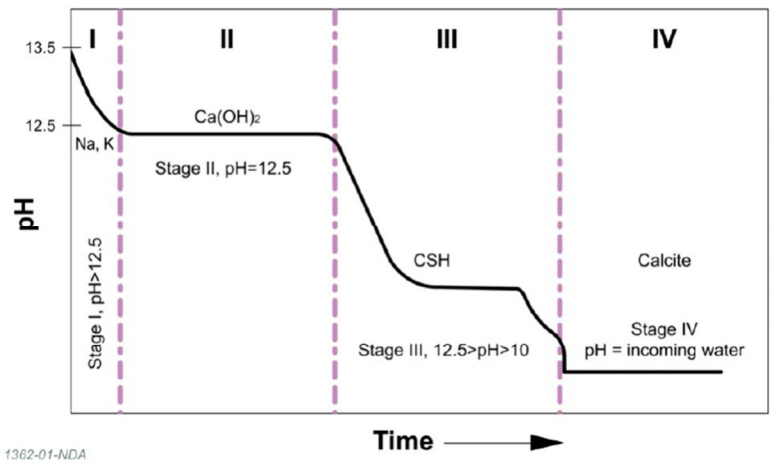

Figure 10.4 pH evolution of the near-field post closure of an ILW-GDF.

It would therefore appear that once in the presence of ISA, microbes capable of tolerating the prevailing pH will degrade both stereoisomers within a relatively short timescale in comparison to the long timescales in which the GDF is expected to be operational. Those with the greatest adaptation rates are likely to influence the performance of the GDF within the alkaline disturbed zone, where microbial activity is likely to occur during the early part of stage III of the pH evolution (Figure 10.3), where growth at pH>12.5 is unlikely [147]. Despite microbial metabolism being highly unlikely at these high pH values, the presence of micro-organisms may still be possible through the presence of bacterial spores introduced in the construction phase of a GDF. When certain micro-organisms are subjected to extreme conditions and stresses, they are capable of changing their gene expression profiles in order to sporulate [308]. Sporulation allows the organism to enter a dormant state where it is capable of persisting until conditions become more favourable [309]. In the case of the Harpur Hill inoculum, members of the genus *Alkaliphilus* are capable forming endospores [268,269], which may be of benefit when entering a GDF in the constructional phases where they are likely to experience the most extreme of pH values in the opening stages of chemical evolution.

Although the work presented here shows that microbial ISA degradation was possible up to a pH of 11.0, the micro-organisms present in the soil at Harpur Hill were experiencing pH values up to 11.7, where the pore waters were as 12.8. This suggests that the consortium present may be capable of biodegradation at pH values >11.0. In the case of Harpur hill sediments, the microbial consortium has developed a tolerance to the *in-situ* pH within 140 years. In addition to the presence of spore forming micro-organisms, those consortia that are capable of biofilm formation at high pH are also likely to play a role in GDF colonisation. Research by Grant *et al* [296] has already shown the advantages in terms of survival at high pH for micro-organisms to reside within these complex biofilms within the low carbon and mineral content present within

a GDF. Mesophilic micro-organisms capable of biofilm formation have also been shown to tolerate pH values above 10.0 under sulphate reducing conditions.

The presence of alkaliphilic micro-organisms within the canal sediments showed that tolerance to a pH of 10.0 could be observed within a matter of months and as such these findings suggest that microbial activity outside the GDF may be limited to ISA leaving the facility via localised environments where microbial intrusion was unable to take place, for instance through rock pores that may have previously been blocked via carbonate formation at elevated pH. Access for microbes to CDP is likely to also be an important factor. Current best estimations suggest that all the degradable proportion of cellulose within the ILW will have been degraded within 100,000 years [11]. Within the initial post closure phase of a GDF, where metal hydroxide phases are likely to dominate and buffer pH values to 12.5-13.5, previous studies suggest the concentration of α-ISA in the presence of cementitious materials is likely to be limited to 50 mmol L^{-1}, where the rest is likely to precipitate as a calcium salt [264,310]. This value is likely to fall to 20 mmol L^{-1} once pH values drop below 12.5, however the solubility of the β-ISA is not impacted in the same manner, where both the sodium and calcium salts formed are likely to illicit an effect on radionuclide complexation [11].

The slow rates of ISA generation and implication of ISA precipitation may have an impact on the microbial activity occurring within a GDF, based upon the concentration of ISA (particularly the α stereoisomer) available within solution. The work of Bassil *et al* [106] suggests that under nitrate reducing and iron reducing conditions, the degradation of α-ISA does not occur below a concentration of 3 mmol L^{-1} using a consortium from the Harpur Hill site. In the experiments conducted here using the Harpur Hill consortium, complete degradation of ISA's was observed. Within isolation experiments, the calcium salt of ISA was used to assess the ISA degrading potential of *Exiguobacterium* sp. Strain HUD and again there appeared to be a concentration at which no more degradation could occur (~2 mmol L^{-1}).These conflicting findings suggest that selection of ISA source should be considered when conducting experiments intended for assessment purposes. The use of ISA's as part of CDP for microcosm experiments would appear to be a more representative approach to predicting the degradation potential of total ISA within the system. Since ~25% of the total organic carbon within the CDP prepared in these experiments was in forms other than ISA, it is clear that the use of a pure form of ISA such as the sodium/calcium salt or free acid are more appropriate for pure culture work.

In addition to potentially degrading ISA as it is generated within the alkaline conditions, micro-organisms capable of tolerating the extreme pH values may be able to utilise the cellulose present within the wastes directly as a source of organic carbon. Undegraded or partially degraded cellulose fibres within the repository also present a platform and carbon

source for the formation of microbial biofilms, which, as previously stated may provide a source of protection against the oxidative stress associated with hyperalkaline conditions. Recently, the work by Charles *et al* [311] found that the microbes present within the Buxton analogue used in the experiments in Chapter 9 were capable of forming biofilms on the surface of cellulose *in situ* at the site through the emplacement of cotton cellulose into boreholes. The emplacement of the cotton revealed a microbial community containing Clostridia and methanogenic Archaea present upon the cotton within a biofilm matrix where ISA was also detected.

As a result of microbial activity, radionuclide migration is likely to be impacted. Studies on the effects of ISA (in particular the α stereoisomer, on account of its easier preparation) suggest that radionuclide solubility of plutonium, thorium, nickel and caesium are increased [22,27-29,31]. In an ISA free system, the high pH conditions of a GDF causes insoluble complexes to form and sorption to cementitious materials facilitates the retention of radionuclides [282]. The presence of ISA is likely to be reduced or removed entirely by colonising microbial consortia, and as such radionuclide mobility through the formation of soluble ISA complexes is also likely to be reduced. Although the degradation of ISAs is likely to be the initial effect within a GDF, acidogenesis and gas production may also play a role in radionuclide migration. The work of Bots *et al* [312] suggests that decreases in local pH are likely to affect the solubility of uranium, where pH reduction caused the formation soluble uranium species. The production of gas was observed throughout all the microcosm experiments, potentially affecting the pressurisation of a GDF as well as influencing ^{14}C transport. Recent findings suggest that $^{14}CO_2$ is released from irradiated graphite, where it is likely to be retained as a carbonate [313]. Within the work reported here, methanogenesis appeared to be almost exclusively through the hydrogenotrophic pathway at alkaline pH, indicating precipitation of CO_2 as carbonate is not a barrier to methanogenesis and therefore suggests that the formation of mobile ^{14}C as $^{14}CH_4$ is a likely consideration. The predicted rates of ISA degradation and subsequent gas generation presented within this work are likely to aid in repository performance calculations and the release of Carbon-14 bearing gas has been modelled within the C14-BIG project integrating the rates obtained in Chapter 7 [314]. In conclusion, the findings presented within this thesis show the ability of near surface micro-organisms to degrade CDP's and associated ISA from neutral conditions approaching the geochemical conditions expected within a GDF concept. The use of the Harpur Hill inoculum showed that micro-organisms are capable adapting to alkaline pH conditions within short timescales in comparison to those expected for long term storage of radioactive wastes. The degradation of ISA and associated gas generation is likely to contribute to assessments into GDF performance.

11.References

References

1. NDA (2011) The 2010 UK Radioactive Waste Inventory. NDA/ST/STY(11)0004 Nuclear Decommissioning Authority (Radioactive Waste Management Directorate), Harwell, Didcot, Oxfordshire, UK.

2. NDA (2010) Near-field Evolution Status Report. NDA/RWMD/033 Nuclear Decommissioning Authority (Radioactive Waste Management Directorate), Harwell, Didcot, Oxfordshire, UK.

3. Anon (2009) UK Government and Devolved Administration Response to the Committee on Radioactive Waste Management (CoRWM) Report on '*Interim Storage of Higher Activity Wastes and the Management of Spent Fuels, Plutonium and Uranium*' (PB 12303) Department of Energy and Climate Change, Whitehall, London

4. Anon (2010) http://llwrsite.com/. LLWR repository limited.

5. Beadle IR, Humphreys PN, Pettit C, Small J (2001) Integrating microbiology into the Drigg Post-closure radiological safety assessment. Materials Research Society Proceedings 655.

6. NDA (2010) Geological disposal: generic disposal system and functional specification NDA/RWMD/043 Nuclear Decommissioning Authority (Radioactive Waste Management Directorate), Harwell, Didcot, Oxfordshire, UK.

7. Chambers AV, Gould LJ, Harris AW, Pilkington NJ, Williams SJ (2003) Evolution of the Near Field of the Nirex Disposal Concept AEAT/R/ENV/0236 AEA Technology plc, Harwell, Didcot, Oxfordshire, UK

8. Anon (2008) The longevity of intermediate-level radioactive waste packages for geological disposal: A review NWAT/Nirex/06/003 Environment agency

9. Askarieh MM, Chambers AV, Daniel FBD, FitzGerald PL, Holtom GJ, et al. (2000) The chemical and microbial degradation of cellulose in the near field of a repository for radioactive wastes. Waste Management 20 1: 93-106.

10. Libert M, Bildstein O, Esnault L, Jullien M, Sellier R (2011) Molecular hydrogen: An abundant energy source for bacterial activity in nuclear waste repositories. Physics and Chemistry of the Earth 36 2011: 1616-1623.

11. Humphreys P, Laws A, Dawson J (2010) A Review of Cellulose Degradation and the Fate of Degradation Products under Repository Conditions SERCO/TAS/002274/001 Serco Contractors Report for the Nuclear Decommissioning Authority, UK.

12. Knill CJ, Kennedy JF (2003) Degradation of cellulose under alkaline conditions. Carbohydrate Polymers 51 3: 281-300.

13. Kidby DW (2000) A Review of Lignin Biodegradation, and its Relevance to the Disposal of Low and Intermediate Level Radioactive Waste in Underground Repositories AEAT/R/ENV/O163 AEA Technology plc, Harwell, Didcot, Oxfordshire

14. Bugg TD, Ahmad M, Hardiman EM, Rahmanpour R (2011) Pathways for degradation of lignin in bacteria and fungi. Natural Product Reports 28 12: 1883-1896.

15. Astbury W, Davies M (1944) Structure of cellulose. Nature 154: 84.

16. Ebringerova A, Hromadkova Z, Heinze T (2005) Hemicellulose. Polysaccharides I: Springer. pp. 1-67.

17. Glaus MA, van Loon LR, Achatz S, Chodura A, Fischer K (1999) Degradation of cellulosic materials under the alkaline conditions of a cementitious repository for low and intermediate level radioactive waste: Part I: Identification of degradation products. Analytica Chimica Acta 398 1: 111-122.

18. Leschine SB (1995) Cellulose Degradation in Anaerobic Environments. Annual Review of Microbiology 49 1: 399-426.

19. Pavasars I, Hagberg J, Boran H, Allard B (2003) Alkaline Degradation of Cellulose: Mechanisms and Kinetics. Journal of Polymers and the Environment 11 2: 39-47.

20. Van Loon LR, Glaus MA, Laube A, Stallone S (1999) Degradation of Cellulosic Materials Under the Alkaline Conditions of a Cementitious Repository for Low- and Intermediate-Level Radioactive Waste. II. Degradation Kinetics. Journal of Polymers and the Environment 7 1: 41-51.

21. Almond M, Shaw PB, Humphreys PN, Chadha MJ, Niemelä K, et al. (2012) Behaviour of xyloisosaccharinic acid and xyloisosaccharino-1, 4-lactone in aqueous solutions at varying pHs. Carbohydrate Research 363: 51-57.

22. Randall M, Rigby B, Thomson O, Trivedi D (2013) Assessment of the effects of cellulose degradation products on the behaviour of europium and thorium 12239 Part A Issue 4 National Nuclear Laboratory, Chadwick House, Warington, UK.

23. Motellier S, Richet C, Merel P (1998) Analysis of cellulose degradation products by capillary electrophoresis. Journal of Chromatography A 804 1: 363-370.

24. Shaw PB, Robinson GF, Rice CR, Humphreys PN, Laws AP (2012) A robust method for the synthesis and isolation of β-gluco-isosaccharinic acid ((2R,4S)-2,4,5-trihydroxy-2-(hydroxymethyl)pentanoic acid) from cellulose and measurement of its aqueous pKa. Carbohydrate Research 349 0: 6-11.

25. Greenfield B, Hurdus M, Spindler M, Thomason H (1997) The effects of the products from the anaerobic degradation of cellulose on the solubility and sorption of radioelements in the near field NSS/R375 AEA Technology plc, Harwell, Didcot, Oxfordshire, UK.

26. Allard S, Ekberg C (2006) Complexing Properties of α-Isosaccharinate: Stability Constants, Enthalpies and Entropies of Th-complexation with Uncertainty Analysis. Journal of Solution Chemistry 35 8: 1173-1186.

27. Vercammen K, Glaus M, Van Loon LR (2001) Complexation of Th (IV) and Eu (III) by α-isosaccharinic acid under alkaline conditions. Radiochimica Acta 89 6/2001: 393.

28. Warwick P, Evans N, Hall T, Vines S (2003) Complexation of Ni(II) by α-isosaccharinic acid and gluconic acid from pH 7 to pH 13. Radiochimica Acta 91 4-2003: 233-240.

29. Warwick P, Evans N, Hall T, Vines S (2004) Stability constants of uranium (IV)-α-isosaccharinic acid and gluconic acid complexes. Radiochimica Acta/International journal for chemical aspects of nuclear science and technology 92 12/2004: 897-902.

30. Wieland E, Tits J, Dobler J, Spieler P (2002) The effect of α-isosaccharinic acid on the stability of and Th (IV) uptake by hardened cement paste. Radiochimica Acta 90 9-11/2002: 683-688.

31. Tits J, Wieland E, Bradbury M (2005) The effect of isosaccharinic acid and gluconic acid on the retention of Eu (III), Am (III) and Th (IV) by calcite. Applied Geochemistry 20 11: 2082-2096.

32. Rai D, Rao L, Xia Y (1998) Solubility of crystalline calcium isosaccharinate. Journal of Solution Chemistry 27 12: 1109-1122.

33. Rydholm SA (1965) Pulping processes: Krieger Publishing Company, Florida, US.

34. Kringstad KP, Lindström K (1984) Spent liquors from pulp bleaching. Environmental Science & Technology 18 8: 236A-248A.

35. Vreeland RH, Piselli Jr AF, McDonnough S, Meyers SS (1998) Distribution and diversity of halophilic bacteria in a subsurface salt formation. Extremophiles 2 3: 321-331.

36. Eaton AD, Clesceri LS, Rice EW, Greenberg AE, editors (2005) Standard Methods for the Examination of Water and Wastewater 21st Edition. 21 ed. Washington, US: APHA/AWWA/WEF.

37. Fukunaga S, Jintoku T, Iwata Y, Nakayama M, Tsuji T, et al. (2005) Investigation of microorganisms in bentonite deposits. Geomicrobiology Journal 22 7-8: 361-370.

38. Horn JM, Masterson BA, Rivera A, Miranda A, Davis MA, et al. (2004) Bacterial growth dynamics, limiting factors, and community diversity in a proposed geological nuclear waste repository environment. Geomicrobiology Journal 21 4: 273-286.

39. Hallbeck L, Pedersen K (2008) Characterization of microbial processes in deep aquifers of the Fennoscandian Shield. Applied Geochemistry 23 7: 1796-1819.

40. Tanner RS, Hurst CJ, Crawford RL, Garland JL, Lipson DA, et al. (2007) Cultivation of bacteria and fungi. Manual of Environmental Microbiology Ed. 3: 69-78.

41. Rappé MS, Giovannoni SJ (2003) The uncultured microbial majority. Annual Reviews in Microbiology 57 1: 369-394.

42. Fields MW, Yan T, Rhee S-K, Carroll SL, Jardine PM, et al. (2005) Impacts on microbial communities and cultivable isolates from groundwater contaminated with high levels of nitric acid–uranium waste. FEMS Microbiology Ecology 53 3: 417-428.

43. Nedelkova M, Merroun ML, Rossberg A, Hennig C, Selenska-Pobell S (2007) Microbacterium isolates from the vicinity of a radioactive waste depository and their interactions with uranium. FEMS Microbiology Ecology 59 3: 694-705.

44. Gillow JB, Dunn M, Francis AJ, Lucero DA, Papenguth HW (2000) The potential of subterranean microbes in facilitating actinide migration at the Grimsel Test Site and Waste Isolation Pilot Plant. Radiochimica Acta International Journal for Chemical Aspects of Nuclear Science and Technology 88 9-11/2000: 769.

45. Icopini GA, Boukhalfa H, Neu MP (2007) Biological reduction of Np (V) and Np (V) citrate by metal-reducing bacteria. Environmental Science & Technology 41 8: 2764-2769.

46. Horn J, Martin S, Carrillo C, Lian T (2005) Microbial Effects on Nuclear Waste Packaging Materials UCRL-TR--213915 Lawrence Livermore National Laboratory (LLNL), Livermore, CA

47. Kelly EJ, Bell DI, Johnstone TL (1998) Lysimeter studies to investigate the leaching of ^{241}Am from low level radioactive waste. Journal of Alloys and Compounds 271: 227-230.

48. Fox JR, Mortimer RJG, Lear G, Lloyd JR, Beadle I, et al. (2006) The biogeochemical behaviour of U (VI) in the simulated near-field of a low-level radioactive waste repository. Applied Geochemistry 21 9: 1539-1550.

49. Francis AJ, Gillow JB, Dodge CJ, Dunn M, Mantione K, et al. (1998) Role of bacteria as biocolloids in the transport of actinides from a deep underground radioactive waste repository. Radiochimica Acta 82: 347-354.

50. Christofi N, West JM, Robbins JE, McKinley IG (1983) The geomicrobiology of the Harwell and Altnabreac boreholes FLPU--83-4 Fluid Processes Unit, Institute of Geological Sciences, Harwell (UK).

51. Chicote E, García AM, Moreno DA, Sarró MI, Lorenzo PI, et al. (2005) Isolation and identification of bacteria from spent nuclear fuel pools. Journal of Industrial Microbiology and Biotechnology 32 4: 155-162.

52. Moter A, Göbel UB (2000) Fluorescence *in situ* hybridization (FISH) for direct visualization of microorganisms. Journal of Microbiological Methods 41 2: 85-112.

53. Pernthaler A, Amann R (2004) Simultaneous fluorescence in situ hybridization of mRNA and rRNA in environmental bacteria. Applied and Environmental Microbiology 70 9: 5426-5433.

54. Knowles JR (1980) Enzyme-catalyzed phosphoryl transfer reactions. Annual Review of Biochemistry 49 1: 877-919.

55. Eydal HSC, Pedersen K (2007) Use of an ATP assay to determine viable microbial biomass in Fennoscandian Shield groundwater from depths of 3-1000 m. Journal of Microbiological Methods 70 2: 363-373.

56. Hedrick DB, Peacock AD, White DC, Hurst CJ, Crawford RL, et al. (2007) Lipid analyses for viable microbial biomass, community composition, metabolic status, and in situ metabolism. Manual of Environmental Microbiology Ed. 3: 112-125.

57. Stroes-Gascoyne S, Hamon CJ, Vilks P, Gierszewski P (2002) Microbial, redox and organic characteristics of compacted clay-based buffer after 6.5 years of burial at AECL's Underground Research Laboratory. Applied Geochemistry 17 10: 1287-1303.

58. Stroes-Gascoyne S, Schippers A, Schwyn B, Poulain S, Sergeant C, et al. (2007) Microbial community analysis of Opalinus clay drill core samples from the Mont Terri underground research laboratory, Switzerland. Geomicrobiology Journal 24 1: 1-17.

59. Griffiths RI, Whiteley AS, O'Donnell AG, Bailey MJ (2000) Rapid Method for Coextraction of DNA and RNA from Natural Environments for Analysis of Ribosomal DNA- and rRNA-Based Microbial Community Composition. Applied and Environmental Microbiology 66 12: 5488-5491.

60. Miller D, Bryant J, Madsen E, Ghiorse W (1999) Evaluation and optimization of DNA extraction and purification procedures for soil and sediment samples. Applied and Environmental Microbiology 65 11: 4715-4724.

61. Saiki RK, Gelfand DH, Stoffel S, Scharf SJ, Higuchi R, et al. (1988) Primer-directed enzymatic amplification of DNA with a thermostable DNA polymerase. Science 239 4839: 487-491.

62. McDonald JE, Lockhart RJ, Cox MJ, Allison HE, McCarthy AJ (2008) Detection of novel Fibrobacter populations in landfill sites and determination of their relative abundance via quantitative PCR. Environmental Microbiology 10 5: 1310-1319.

63. Lockhart RJ, Van Dyke MI, Beadle IR, Humphreys P, McCarthy AJ (2006) Molecular Biological Detection of Anaerobic Gut Fungi (*Neocallimastigales*) from Landfill Sites. Applied and Environmental Microbiology 72 8: 5659-5661.

64. Acinas SG, Sarma-Rupavtarm R, Klepac-Ceraj V, Polz MF (2005) PCR-induced sequence artifacts and bias: insights from comparison of two 16S rRNA clone libraries constructed from the same sample. Applied and Environmental Microbiology 71 12: 8966-8969.

65. Kanagawa T (2003) Bias and artifacts in multitemplate polymerase chain reactions (PCR). Journal of Bioscience and Bioengineering 96 4: 317-323.

66. Lueders T, Friedrich MW (2003) Evaluation of PCR Amplification Bias by Terminal Restriction Fragment Length Polymorphism Analysis of Small-Subunit rRNA and mcrA Genes by Using Defined Template Mixtures of Methanogenic Pure Cultures and Soil DNA Extracts. Applied and Environmental Microbiology 69 1: 320-326.

67. Green SJ, Prakash O, Jasrotia P, Overholt WA, Cardenas E, et al. (2012) Denitrifying Bacteria from the Genus *Rhodanobacter* Dominate Bacterial Communities in the Highly Contaminated Subsurface of a Nuclear Legacy Waste Site. Applied and Environmental Microbiology 78 4: 1039-1047.

68. Lear G, McBeth JM, Boothman C, Gunning DJ, Ellis BL, et al. (2009) Probing the biogeochemical behavior of technetium using a novel nuclear imaging approach. Environmental Science & Technology 44 1: 156-162.

69. Muyzer G, Smalla K (1998) Application of denaturing gradient gel electrophoresis (DGGE) and temperature gradient gel electrophoresis (TGGE) in microbial ecology. Antonie van Leeuwenhoek 73 1: 127-141.

70. Muyzer G (1999) DGGE/TGGE a method for identifying genes from natural ecosystems. Current Opinion in Microbiology 2 3: 317-322.

71. Torsvik V, Øvreås L (2002) Microbial diversity and function in soil: from genes to ecosystems. Current Opinion in Microbiology 5 3: 240-245.

72. Islam E, Paul D, Sar P (2014) Microbial Diversity in Uranium Deposits from Jaduguda and Bagjata Uranium Mines, India as revealed by clone library and Denaturing Gradient Gel Electrophoresis analyses. Geomicrobiology Journal 31 10.

73. Head IM, Saunders JR, Pickup RW (1998) Microbial Evolution, Diversity, and Ecology: A Decade of Ribosomal Analysis of Uncultivated Microorganisms. Microbial Ecology 35 1998: 1-21.

74. Wilkins MJ, Livens FR, Vaughan DJ, Beadle I, Lloyd JR (2007) The influence of microbial redox cycling on radionuclide mobility in the subsurface at a low-level radioactive waste storage site. Geobiology 5 3: 293-301.

75. Pedersen K (1996) Investigations of subterranean bacteria in deep crystalline bedrock and their importance for the disposal of nuclear waste. Canadian Journal of Microbiology 42 4: 382-391.

76. Dunbar J, Takala S, Barns SM, Davis JA, Kuske CR (1999) Levels of bacterial community diversity in four arid soils compared by cultivation and 16S rRNA gene cloning. Applied and Environmental Microbiology 65 4: 1662-1669.

77. Lukow T, Dunfield PF, Liesack W (2000) Use of the T-RFLP technique to assess spatial and temporal changes in the bacterial community structure within an agricultural soil planted with transgenic and non-transgenic potato plants. FEMS Microbiology Ecology 32 3: 241-247.

78. Benson DA, Cavanaugh M, Clark K, Karsch-Mizrachi I, Lipman DJ, et al. (2013) GenBank. Nucleic Acids Research: gks1195.

79. Wheeler DL, Church DM, Federhen S, Lash AE, Madden TL, et al. (2003) Database resources of the National Center for Biotechnology. Nucleic Acids Research 31 1: 28-33.

80. Venter JC, Remington K, Heidelberg JF, Halpern AL, Rusch D, et al. (2004) Environmental genome shotgun sequencing of the Sargasso Sea. Science 304 5667: 66-74.

81. Rondon MR, August PR, Bettermann AD, Brady SF, Grossman TH, et al. (2000) Cloning the soil metagenome: a strategy for accessing the genetic and functional diversity of uncultured microorganisms. Applied and Environmental Microbiology 66 6: 2541-2547.

82. Edwards JL, Smith DL, Connolly J, McDonald JE, Cox MJ, et al. (2010) Identification of carbohydrate metabolism genes in the metagenome of a marine biofilm community shown to be dominated by Gammaproteobacteria and Bacteroidetes. Genes 1 3: 371-384.

83. Fierer N, Leff JW, Adams BJ, Nielsen UN, Bates ST, et al. (2012) Cross-biome metagenomic analyses of soil microbial communities and their functional attributes. Proceedings of the National Academy of Sciences 109 52: 21390-21395.

84. Qin J, Li Y, Cai Z, Li S, Zhu J, et al. (2012) A metagenome-wide association study of gut microbiota in type 2 diabetes. Nature 490 7418: 55-60.

85. Logares R, Sunagawa S, Salazar G, Cornejo-Castillo FM, Ferrera I, et al. (2014) Metagenomic 16S rDNA Illumina tags are a powerful alternative to amplicon sequencing to explore diversity and structure of microbial communities. Environmental Microbiology 16 9.

86. Shah N, Tang H, Doak TG, Ye Y (2012) Comparing bacterial communities inferred from 16S rRNA gene sequencing and shotgun metagenomics. Pacific Symposium on Biocomputing 16: 165-176.

87. Zakrzewski M, Goesmann A, Jaenicke S, Jünemann S, Eikmeyer F, et al. (2012) Profiling of the metabolically active community from a production-scale biogas plant by means of high-throughput metatranscriptome sequencing. Journal of Biotechnology 158 4: 248-258.

88. Lesniewski RA, Jain S, Anantharaman K, Schloss PD, Dick GJ (2012) The metatranscriptome of a deep-sea hydrothermal plume is dominated by water column methanotrophs and lithotrophs. The ISME journal 6 12: 2257-2268.

89. Limam I, Mezni M, Guenne A, Madigou C, Driss M, et al. (2013) Evaluation of biodegradability of phenol and bisphenol A during mesophilic and thermophilic municipal solid waste anaerobic digestion using ^{13}C-labeled contaminants. Chemosphere 90 2: 512-520.

90. Eichorst SA, Kuske CR (2012) Identification of cellulose-responsive bacterial and fungal communities in geographically and edaphically different soils by using stable isotope probing. Applied and Environmental Microbiology 78 7: 2316-2327.

91. Dumont MG, Pommerenke B, Casper P, Conrad R (2011) DNA, rRNA and mRNA based stable isotope probing of aerobic methanotrophs in lake sediment. Environmental Microbiology 13 5: 1153-1167.

92. Jones MD, Singleton DR, Sun W, Aitken MD (2011) Multiple DNA extractions coupled with stable-isotope probing of anthracene-degrading bacteria in contaminated soil. Applied and Environmental Microbiology 77 9: 2984-2991.

93. Grant WG, Greedy R, G.J. H, O'Kelly N, Rosevear A, et al. (2001) The Survival of Micro-Organisms in a Deep Cementitious Repository under Alkaline, High Temperature Conditions AEAT/R/ENV/0227 AEA Technology plc, Harwell, Didcot, Oxfordshire, UK

94. Rittmann BE, McCarty PL (2001) Environmental Biotechnology: McGraw Hill, New York, US.

95. Madigan MT, Martinko JM, Parker J, Brock TD (1997) Biology of microorganisms: Prentice Hall Upper Saddle River, New Jersey, US.

96. Rizoulis A, Steele H, Morris K, Lloyd J (2012) The potential impact of anaerobic microbial metabolism during the geological disposal of intermediate-level waste. Mineralogical Magazine 76 8: 3261-3270.

97. Nirex (1997) Sellafield Geological and Hydrogeological Investigations: the Hydrochemistry of Sellafield UK NIREX Ltd, Harwell, Oxfordshire, UK

98. Williams A, Morrison I (1982) Studies on the Production of Saccharinic Acids by the Alkialine Treatment of Young Grass and Their Effectiveness as Substrates for Mixed Rumen Microorganisms *In Vitro*. Journal of the Science of Food and Agriculture 33 1982: 21-29.

99. Horiko K, Kita Y, Koide K (1985) Method for cultivation of microorganism. US 4514501 A.

100. Strand SE, Dykes J, Chiang V (1984) Aerobic Microbial Degradation of Glucoisosaccharinic Acid. Applied and Environmental Microbiology 47 2: 268-271.

101. Bailey MJ (1986) Utilization of glucoisosaccharinic acid by a bacterial isolate unable to metabolize glucose. Applied Microbiology and Biotechnology 24 6: 493-498.

102. Pekarovičová A, Mikulášová M (1991) Biodegradation of black liquor hydroxyacids by *Micrococcus lylae.* Journal of Chemical Technology and Biotechnology 52 4: 539-543.

103. Wang S, McCarthy, J. & Ferguson, J. (1993) Utilization of Glucoisosaccharinic Acid and Components of Kraft Black Liquor as Energy Sources for Growth of Anaerobic Bacteria. Holzforschung 47 1993: 141-148.

104. Francis AJ, Dodge CJ (2006) Microbial Transformations of TRU and Mixed Wastes: Actinide Speciation and Waste Volume Reduction BNL-77300-2006 Project Report to Department of Energy, Environmental Sciences Department, Brookhaven National Laboratory, Upton, New York, US

105. Maset ER, Sidhu SH, Fisher A, Heydon A, Worsfold PJ, et al. (2006) Effect of organic co-contaminants on technetium and rhenium speciation solubility under reducing conditions. Environmental Science & Technology 40: 5472-5477.

106. Bassil NM, Bryan N, Lloyd JR (2014) Microbial degradation of isosaccharinic acid at high pH. The ISME journal 9: 310-320.

107. Padan E, Bibi E, Ito M, Krulwich TA (2005) Alkaline pH homeostasis in bacteria: new insights. Biochimica et Biophysica Acta (BBA)-Biomembranes 1717 2: 67-88.

108. Speelmans G, Poolman B, Abee T, Konings WN (1993) Energy transduction in the thermophilic anaerobic bacterium Clostridium fervidus is exclusively coupled to sodium ions. Proceedings of the National Academy of Sciences 90 17: 7975-7979.

109. Krulwich TA, Ito M, Gilmour R, Guffanti AA (1997) Mechanisms of cytoplasmic pH regulation in alkaliphilic strains of *Bacillus*. Extremophiles 1 4: 163-170.

110. Horikoshi K (1999) Alkaliphiles: some applications of their products for biotechnology. Microbiology and Molecular Biology Reviews 63 4: 735-750.

111. Aono R, Horikoshi K (1983) Chemical composition of cell walls of alkalophilic strains of *Bacillus*. Journal of General Microbiology 129 4: 1083-1087.

112. Jones BE, Grant WD, Duckworth AW, Owenson GG (1998) Microbial diversity of soda lakes. Extremophiles 2 3: 191-200.

113. Simmons AM, Stuckless JS (2010) Analogues to Features and Processes of a High-Level Radioactive Waste Repository Proposed for Yucca Mountain, Nevada. U.S. Geological Survey Professional Paper 1779 Los Alamos National Laboratory, Los Alamos, New Mexico, US

114. Burke I, Mortimer R, Palani S, Whittleston R, Lockwood C, et al. (2012) Biogeochemical reduction processes in a hyper-alkaline affected leachate soil profile. Geomicrobiology Journal 29 9: 769-779.

115. Humayoun SB, Bano N, Hollibaugh JT (2003) Depth distribution of microbial diversity in Mono Lake, a meromictic soda lake in California. Applied and Environmental Microbiology 69 2: 1030-1042.

116. Rees HC, Grant WD, Jones BE, Heaphy S (2004) Diversity of Kenyan soda lake alkaliphiles assessed by molecular methods. Extremophiles 8 1: 63-71.

117. Khoury H, Salameh E, Clark I, Fritz P, Bajjali W, et al. (1992) A natural analogue of high pH cement pore waters from the Maqarin area of northern Jordan. I: introduction to the site. Journal of Geochemical Exploration 46 1: 117-132.

118. Blum JS, Bindi AB, Buzzelli J, Stolz JF, Oremland RS (1998) *Bacillus arsenicoselenatis*, sp. nov., and *Bacillus selenitireducens*, sp. nov.: two haloalkaliphiles from Mono Lake, California that respire oxyanions of selenium and arsenic. Archives of Microbiology 171 1: 19-30.

119. Hoover RB, Pikuta EV, Bej AK, Marsic D, Whitman WB, et al. (2003) *Spirochaeta americana* sp. nov., a new haloalkaliphilic, obligately anaerobic spirochaete isolated from soda Mono Lake in California. International Journal of Systematic and Evolutionary Microbiology 53 3: 815-821.

120. Gorlenko V, Tsapin A, Namsaraev Z, Teal T, Tourova T, et al. (2004) *Anaerobranca californiensis* sp. nov., an anaerobic, alkalithermophilic, fermentative bacterium isolated from a hot spring on Mono Lake. International Journal of Systematic and Evolutionary Microbiology 54 3: 739-743.

121. Oremland RS, Dowdle PR, Hoeft S, Sharp JO, Schaefer JK, et al. (2000) Bacterial dissimilatory reduction of arsenate and sulfate in meromictic Mono Lake, California. Geochimica and Cosmochimica Acta 64 18: 3073-3084.

122. Scholten J, Joye S, Hollibaugh J, Murrell J (2005) Molecular Analysis of the Sulfate Reducing and ArchaealCommunity in a Meromictic Soda Lake (Mono Lake, California) by Targeting 16S rRNA, *mcrA, apsA*, and *dsrAB* Genes. Microbial Ecology 50 1: 29-39.

123. Sorokin DY, Gorlenko VM, Tsapin AI, Nealson KH, Kuenen GJ (2002) *Thioalkalimicrobium cyclicum* sp. nov. and *Thioalkalivibrio jannaschii* sp. nov., novel species of haloalkaliphilic, obligately chemolithoautotrophic sulfur-oxidizing bacteria from hypersaline alkaline Mono Lake (California). International Journal of Systematic and Evolutionary Microbiology 52 3: 913-920.

124. Vargas VA, Delgado OD, Hatti-Kaul R, Mattiasson B (2005) *Bacillus bogoriensis* sp. nov., a novel alkaliphilic, halotolerant bacterium isolated from a Kenyan soda lake. International Journal of Systematic and Evolutionary Microbiology 55 2: 899-902.

125. Alexander WR, Milodowski AE (2011) Cyprus Natural Analogue Project (CNAP): Phase II Final Report. POSIVA, Olkiluoto, Finland

126. Rizoulis A, Milodowski AE, Morris K, Lloyd JR (2014) Bacterial diversity in the hyperalkaline Allas Springs (Cyprus), a natural analogue for cementitious radioactive waste repository. Geomicrobiology Journal Accepted online 24th September 2014.

127. Bath A, Christofi N, Neal C, Philp J, Cave M, et al. (1987) Trace Element and Microbiological Studies of Alkaline Groundwaters in Oman, Arabian Gulf: A Natural Analogue for Cement Pore-Waters Technical Report 87-16 British Geological Survey, Keyworth, Nottinghamshire, UK

128. Pedersen K, Nilsson E, Arlinger J, Hallbeck L, O'Neill A (2004) Distribution, diversity and activity of microorganisms in the hyper-alkaline spring waters of Maqarin in Jordan. Extremophiles 8 2: 151-164.

129. Turpeinen R, Kairesalo T, Häggblom MM (2004) Microbial community structure and activity in arsenic-, chromium-and copper-contaminated soils. FEMS Microbiology Ecology 47 1: 39-50.

130. Viti C, Pace A, Giovannetti L (2003) Characterization of Cr (VI)-resistant bacteria isolated from chromium-contaminated soil by tannery activity. Current Microbiology 46 1: 0001-0005.

131. Stewart DI, Burke IT, Hughes-Berry DV, Whittleston RA (2010) Microbially mediated chromate reduction in soil contaminated by highly alkaline leachate from chromium containing waste. Ecological Engineering 36 2: 211-221.

132. Megharaj M, Kantachote D, Singleton I, Naidu R (2000) Effects of long-term contamination of DDT on soil microflora with special reference to soil algae and algal transformation of DDT. Environmental Pollution 109 1: 35-42.

133. Abramowicz DA (1990) Aerobic and anaerobic biodegradation of PCBs: a review. Critical Reviews in Biotechnology 10 3: 241-251.

134. Wilson SC, Jones KC (1993) Bioremediation of soil contaminated with polynuclear aromatic hydrocarbons (PAHs): a review. Environmental pollution 81 3: 229-249.

135. Milodowski AE, Shaw RP, Stewart DI (2013) The Harpur Hill Site: its geology, evolutionary history and a catalogue of materials present British Geological Survey Commissioned Report CR/13/104 43pp British Geological Survey, Keyworth, Nottinghamshire, UK

136. Deakin D, West L, Stewart D, Yardley B (2000) Leaching behaviour of a chromium smelter waste heap. Waste Management Series 1: 392-401.

137. Whittleston RA, Stewart DI, Mortimer RJ, Burke IT (2013) Enhancing microbial iron reduction in hyperalkaline, chromium contaminated sediments by pH amendment. Applied Geochemistry 28: 135-144.

138. Yuan H, Chen Y, Zhang H, Jiang S, Zhou Q, et al. (2006) Improved bioproduction of short-chain fatty acids (SCFAs) from excess sludge under alkaline conditions. Environmental Science & Technology 40 6: 2025-2029.

139. Liu Q, Zhang XL, Jun Z, Zhao AH, Chen SP, et al. (2012) Effect of carbonate on anaerobic acidogenesis and fermentative hydrogen production from glucose using leachate as supplementary culture under alkaline conditions. Bioresource Technology 113: 37-43.

140. Lovley D, & Phillips, E. (1987) Rapid assay for microbially reducible ferric iron in aquatic sediments. Applied and Environmental Microbiology 53 7: 1536-1540.

141. Reguera G, McCarthy KD, Mehta T, Nicoll JS, Tuominen MT, et al. (2005) Extracellular electron transfer via microbial nanowires. Nature 435 7045: 1098-1101.

142. Von Canstein H, Ogawa J, Shimizu S, Lloyd JR (2008) Secretion of flavins by *Shewanella* species and their role in extracellular electron transfer. Applied and Environmental Microbiology 74 3: 615-623.

143. Lovley DR (1997) Microbial Fe (III) reduction in subsurface environments. FEMS Microbiology Reviews 20 3□4: 305-313.

144. Lovley DR, Coates JD, Blunt-Harris EL, Phillips EJ, Woodward JC (1996) Humic substances as electron acceptors for microbial respiration. Nature 382 6590: 445-448.

145. Taillefert M, Beckler JS, Carey E, Burns JL, Fennessey CM, et al. (2007) *Shewanella putrefaciens* produces an Fe(III)-solubilizing organic ligand during anaerobic respiration on insoluble Fe(III) oxides. Journal of Inorganic Biochemistry 101 11–12: 1760-1767.

146. Weber KA, Achenbach LA, Coates JD (2006) Microorganisms pumping iron: anaerobic microbial iron oxidation and reduction. Nature Reviews Microbiology 4 10: 752-764.

147. Humphreys PN, West JM, Metcalfe R (2010) Microbial Effects on Repository Performance QRS-1378Q-1, Version 3.0 Quintessa Contractors Report for the Nuclear Decommissioning Authority, UK

148. Lovley DR, Phillips EJ (1988) Novel mode of microbial energy metabolism: organic carbon oxidation coupled to dissimilatory reduction of iron or manganese. Applied and Environmental Microbiology 54 6: 1472-1480.

149. Lovley D, Phillips E (1986) Organic Matter Mineralisation with Reduction of Ferric Iron in Anaerobic Sediments. Applied and Environmental Microbiology 51 4: 683-689.

150. Lovley DR, Phillips EJ (1986) Availability of ferric iron for microbial reduction in bottom sediments of the freshwater tidal Potomac River. Applied and Environmental Microbiology 52 4: 751-757.

151. Islam FS, Gault AG, Boothman C, Polya DA, Charnock JM, et al. (2004) Role of metal-reducing bacteria in arsenic release from Bengal delta sediments. Nature 430 6995: 68-71.

152. Cummings DE, Caccavo F, Fendorf S, Rosenzweig RF (1999) Arsenic mobilization by the dissimilatory Fe (III)-reducing bacterium *Shewanella alga* BrY. Environmental Science & Technology 33 5: 723-729.

153. Wielinga B, Mizuba MM, Hansel CM, Fendorf S (2001) Iron promoted reduction of chromate by dissimilatory iron-reducing bacteria. Environmental Science & Technology 35 3: 522-527.

154. Lovley DR (1993) Dissimilatory metal reduction. Annual Reviews in Microbiology 47 1: 263-290.

155. Greene AC, Patel BK, Sheehy AJ (1997) *Deferribacter thermophilus* gen. nov., sp. nov., a novel thermophilic manganese-and iron-reducing bacterium isolated from a petroleum reservoir. International Journal of Systematic Bacteriology 47 2: 505-509.

156. Semple K, Westlake D (1987) Characterization of iron-reducing *Alteromonas putrefaciens* strains from oil field fluids. Canadian Journal of Microbiology 33 5: 366-371.

157. Head IM, Swannell RP (1999) Bioremediation of petroleum hydrocarbon contaminants in marine habitats. Current Opinion in Biotechnology 10 3: 234-239.

158. Ye Q, Roh Y, Carroll SL, Blair B, Zhou J, et al. (2004) Alkaline anaerobic respiration: isolation and characterization of a novel alkaliphilic and metal-reducing bacterium. Applied and Environmental Microbiology 70 9: 5595-5602.

159. Zavarzina D, Kolganova T, Boulygina E, Kostrikina N, Tourova T, et al. (2006) *Geoalkalibacter ferrihydriticus* gen. nov. sp. nov., the first alkaliphilic representative of the family Geobacteraceae, isolated from a soda lake. Microbiology 75 6: 673-682.

160. Zhilina T, Zavarzina D, Osipov G, Kostrikina N, Tourova T (2009) *Natronincola ferrireducens* sp. nov., and *Natronincola peptidovorans* sp. nov., new anaerobic alkaliphilic peptolytic iron-reducing bacteria isolated from soda lakes. Microbiology 78 4: 455-467.

161. Pollock J, Weber KA, Lack J, Achenbach LA, Mormile MR, et al. (2007) Alkaline iron (III) reduction by a novel alkaliphilic, halotolerant, *Bacillus* sp. isolated from salt flat sediments of Soap Lake. Applied Microbiology and Biotechnology 77 4: 927-934.

162. Thorpe CL, Morris K, Boothman C, Lloyd JR (2012) Alkaline Fe(III) reduction by a novel alkali-tolerant *Serratia* sp. isolated from surface sediments close to Sellafield nuclear facility, UK. FEMS Microbiology Letters 327 2: 87-92.

163. Williamson AJ, Morris K, Shaw S, Byrne JM, Boothman C, et al. (2013) Microbial Reduction of Fe(III) under Alkaline Conditions Relevant to Geological Disposal. Applied Environmental Microbiology 79 11: 3320-3326.

164. Postgate JR (1979) The sulphate reducing bacteria: Cambridge University Press, Cambridge, UK.

165. Carbonero F, Benefiel AC, Alizadeh-Ghamsari AH, Gaskins HR (2012) Microbial pathways in colonic sulfur metabolism and links with health and disease. Frontiers in Physiology 3.

166. Bradley A, Leavitt W, Johnston D (2011) Revisiting the dissimilatory sulfate reduction pathway. Geobiology 9 5: 446-457.

167. Chang IS, Shin PK, Kim BH (2000) Biological treatment of acid mine drainage under sulphate-reducing conditions with solid waste materials as substrate. Water Research 34 4: 1269-1277.

168. Elliott P, Ragusa S, Catcheside D (1998) Growth of sulfate-reducing bacteria under acidic conditions in an upflow anaerobic bioreactor as a treatment system for acid mine drainage. Water Research 32 12: 3724-3730.

169. Beech IB, Gaylarde CC (1999) Recent advances in the study of biocorrosion: an overview. Revista de Microbiologia 30 3: 117-190.

170. Lovley DR, Roden EE, Phillips EJP, Woodward JC (1993) Enzymatic iron and uranium reduction by sulfate-reducing bacteria. Marine Geology 113 1: 41-53.

171. Sorokin DY, Tourova TP, Henstra AM, Stams AJ, Galinski EA, et al. (2008) Sulfidogenesis under extremely haloalkaline conditions by *Desulfonatronospira thiodismutans* gen. nov., sp. nov., and *Desulfonatronospira delicata* sp. nov.–a novel lineage of Deltaproteobacteria from hypersaline soda lakes. Microbiology 154 5: 1444-1453.

172. Foti M, Sorokin DY, Lomans B, Mussman M, Zacharova EE, et al. (2007) Diversity, activity, and abundance of sulfate-reducing bacteria in saline and hypersaline soda lakes. Applied and Environmental Microbiology 73 7: 2093-2100.

173. Sorokin DY, Rusanov II, Pimenov NV, Tourova TP, Abbas B, et al. (2010) Sulfidogenesis under extremely haloalkaline conditions in soda lakes of Kulunda Steppe (Altai, Russia). FEMS Microbiology Ecology 73 2: 278-290.

174. Oremland RS, Stolz JF, Hollibaugh JT (2004) The microbial arsenic cycle in Mono Lake, California. FEMS Microbiology Ecology 48 1: 15-27.

175. Kulp T, Hoeft S, Miller L, Saltikov C, Murphy J, et al. (2006) Dissimilatory arsenate and sulfate reduction in sediments of two hypersaline, arsenic-rich soda lakes: Mono and Searles Lakes, California. Applied and Environmental Microbiology 72 10: 6514-6526.

176. Pikuta EV, Hoover RB, Bej AK, Marsic D, Whitman WB, et al. (2003) *Desulfonatronum thiodismutans* sp. nov., a novel alkaliphilic, sulfate-reducing bacterium capable of

lithoautotrophic growth. International Journal of Systematic and Evolutionary Microbiology 53 5: 1327-1332.

177. Abd-el-Malek Y, Rizk S (1963) Bacterial sulphate reduction and the development of alkalinity. III. Experiments under natural conditions in the Wadi Natrun. Journal of Applied Bacteriology 26 1: 20-26.

178. Jones BE, Grant WD, Collins NC, Mwatha WE (1994) Alkaliphiles: diversity and identification. Bacterial Diversity and Systematics: 195-230.

179. Duckworth A, Grant W, Jones B, Steenbergen Rv (1996) Phylogenetic diversity of soda lake alkaliphiles. FEMS Microbiology Ecology 19 3: 181-191.

180. Zhilina T, Zavarzin G, Rainey F, Pikuta E, Osipov G, et al. (1997) *Desulfonatronovibrio hydrogenovorans* gen. nov., sp. nov., an alkaliphilic, sulfate-reducing bacterium. International Journal of Systematic Bacteriology 47 1: 144-149.

181. Goeres D, Nielsen PH, Smidt H, Frølund B (1998) The effect of alkaline pH conditions on a sulphate reducing consortium from a Danish district heating plant. Biofouling 12 4: 273-286.

182. Woese CR (1981) Archaebacteria. Scientific American 244: 98-122.

183. Fox G, Stackebrandt E, Hespell R, Gibson J, Maniloff J, et al. (1980) The phylogeny of prokaryotes. Science 209 4455: 457.

184. Rouviere PE, Wolfe RS (1988) Novel biochemistry of methanogenesis. The Journal of Biological Chemistry 263 17: 7913-7916.

185. Thauer RK, Kaster A, Seedorf H, Buckel W, Hedderich R (2008) Methanogenic archaea: ecologically relevant differences in energy conservation. Nature Reviews Microbiology 6 8: 579-591.

186. Ferry JG (2011) Fundamentals of methanogenic pathways that are key to the biomethanation of complex biomass. Current Opinion in Biotechnology 22 3: 351-357.

187. Balch W, Fox G, Magrum L, Woese C, Wolfe R (1979) Methanogens: reevaluation of a unique biological group. Microbiological Reviews 43 2: 260.

188. Demirel B, Scherer P (2008) The roles of acetotrophic and hydrogenotrophic methanogens during anaerobic conversion of biomass to methane: a review. Reviews in Environmental Science and Biotechnology 7 2008: 173-190.

189. Wu W-M, Jain MK, De Macario EC, Thiele JH, Zeikus JG (1992) Microbial composition and characterization of prevalent methanogens and acetogens isolated from syntrophic methanogenic granules. Applied Microbiology and Biotechnology 38 2: 282-290.

190. Oremland RS, Marsh L, DesMarais DJ (1982) Methanogenesis in Big Soda Lake, Nevada: an alkaline, moderately hypersaline desert lake. Applied and Environmental Microbiology 43 2: 462-468.

191. Mathrani IM, Boone DR, Mah RA, Fox GE, Lau PP (1988) Methanohalophilus zhilinae sp. nov., an Alkaliphilic, Halophilic, Methylotrophic Methanogen. International Journal of Systematic Bacteriology 38 2: 139-142.

192. Oremland R, Miller L (1993) Biogeochemistry of natural gases in three alkaline, permanently stratified (meromictic) lakes. In: The Future of Energy Gases Ed. D.Howell, US Geological Survey, Reston, Virginia, US

193. Worakit S, Boone DR, Mah RA, Abdel-Samie ME, El-Halwagi MM (1986) *Methanobacterium alcaliphilum* sp. nov., an H_2-utilizing methanogen that grows at high pH values. International Journal of Systematic Bacteriology 36 3: 380-382.

194. Boone DR, Worakit S, Mathrani IM, Mah RA (1986) Alkaliphilic methanogens from high-pH lake sediments. Systematic and Applied Microbiology 7 2: 230-234.

195. B.S.I (2005) BS ISO 14853:2005 Plastics-Determination of the ultimate anaerobic biodegradation of plastic materials in an aqueous system- Method by measurement of biogas production British Standards Institute, London, UK

196. Cowper M, Marshall T, Swanton S (2011) Sorption detriments in the geosphere: the effect of cellulose degradation products. Phase 1 Experimental study. NR3169/026 Serco Contracters Report for UK Nirex Ltd, Harwell, Didcot, Oxfordshire, UK

197. Viollier E, Inglett P, Hunter K, Roychoudhury A, Van Cappellen P (2000) The ferrozine method revisited: Fe (II)/Fe (III) determination in natural waters. Applied Geochemistry 15 6: 785-790.

198. Bradford MM (1976) A rapid and sensitive method for the quantitation of microgram quantities of protein utilizing the principle of protein-dye binding. Analytical Biochemistry 72 1: 248-254.

199. Masuko T, Minami A, Iwasaki N, Majima T, Nishimura S-I, et al. (2005) Carbohydrate analysis by a phenol–sulfuric acid method in microplate format. Analytical Biochemistry 339 1: 69-72.

200. Daly K, Sharp RJ, McCarthy AJ (2000) Development of oligonucleotide probes and PCR primers for detecting phylogenetic subgroups of sulfate-reducing bacteria. Microbiology 146 7: 1693-1705.

201. Edwards U, Rogall T, Blöcker H, Emde M, Böttger EC (1989) Isolation and direct complete nucleotide determination of entire genes. Characterization of a gene coding for 16S ribosomal RNA. Nucleic Acids Research 17 19: 7843-7853.

202. Gantner S, Andersson AF, Alonso-Sáez L, Bertilsson S (2011) Novel primers for 16S rRNA-based archaeal community analyses in environmental samples. Journal of Microbiological Methods 84 1: 12-18.

203. Kuntze K, Shinoda Y, Moutakki H, McInerney MJ, Vogt C, et al. (2008) 6-Oxocyclohex-1-ene-1-carbonyl-coenzyme A hydrolases from obligately anaerobic bacteria: characterization and identification of its gene as a functional marker for aromatic compounds degrading anaerobes. Environmental Microbiology 10 6: 1547-1556.

204. Shigematsu T, Tang Y, Kawaguchi H, Ninomiya K, Kijima J, et al. (2003) Effect of dilution rate on structure of a mesophilic acetate-degrading methanogenic community during continuous cultivation. Journal of Bioscience and Bioengineering 96 6: 547-558.

205. Todorova SG, Costello AM (2006) Design of *Shewanella*-specific 16S rRNA primers and application to analysis of *Shewanella* in a minerotrophic wetland. Environmental Microbiology 8 3: 426-432.

206. Van Dyke M, McCarthy A (2002) Molecular biological detection and characterization of *Clostridium* populations in municipal landfill sites. Applied and Environmental Microbiology 68 4: 2049-2053.

207. Yanisch-Perron C, Vieira J, Messing J (1985) Improved M13 phage cloning vectors and host strains: nucleotide sequences of the M13mpl8 and pUC19 vectors. Gene 33 1: 103-119.

208. Yu Y, Lee C, Kim J, Hwang S (2005) Group-specific primer and probe sets to detect methanogenic communities using quantitative real-time polymerase chain reaction. Biotechnology and Bioengineering 89 6: 670-679.

209. Schloss PD, Westcott SL, Ryabin T, Hall JR, Hartmann M, et al. (2009) Introducing mothur: open-source, platform-independent, community-supported software for describing and comparing microbial communities. Applied and Environmental Microbiology 75 23: 7537-7541.

210. Edgar RC, Haas BJ, Clemente JC, Quince C, Knight R (2011) UCHIME improves sensitivity and speed of chimera detection. Bioinformatics 27 16: 2194-2200.

211. Tamura K, Peterson D, Peterson N, Stecher G, Nei M, et al. (2011) MEGA5: molecular evolutionary genetics analysis using maximum likelihood, evolutionary distance, and maximum parsimony methods. Molecular Biology and Evolution 28 10: 2731-2739.

212. Wheeler DL, Barrett T, Benson DA, Bryant SH, Canese K, et al. (2007) Database resources of the national center for biotechnology information. Nucleic Acids Research 35 suppl 1: D5-D12.

213. Edgar RC (2004) MUSCLE: multiple sequence alignment with high accuracy and high throughput. Nucleic Acids Research 32 5: 1792-1797.

214. Balch WE, Fox G, Magrum L, Woese C, Wolfe R (1979) Methanogens: reevaluation of a unique biological group. Microbiological reviews 43 2: 260.

215. Chaudhuri SK, Lack JG, Coates JD (2001) Biogenic magnetite formation through anaerobic biooxidation of Fe (II). Applied and Environmental Microbiology 67 6: 2844-2848.

216. Lovley DR (1991) Dissimilatory Fe(III) and Mn(IV) reduction. Microbiological Reviews 55 2: 259-287.

217. Niemelä K (1990) The formation of hydroxy monocarboxylic acids and dicarboxylic acids by alkaline thermochemical degradation of cellulose. Journal of Chemical Technology and Biotechnology 48 1: 17-28.

218. Xing D, Ren N, Li Q, Lin M, Wang A, et al. (2006) *Ethanoligenens harbinense* gen. nov., sp. nov., isolated from molasses wastewater. International Journal of Systematic and Evolutionary Microbiology 56 4: 755-760.

219. Hsiao C-L, Chang J-J, Wu J-H, Chin W-C, Wen F-S, et al. (2009) *Clostridium* strain co-cultures for biohydrogen production enhancement from condensed molasses fermentation solubles. International Journal of Hydrogen Energy 34 17: 7173-7181.

220. Jeon BS, Kim B-C, Um Y, Sang B-I (2010) Production of hexanoic acid from D-galactitol by a newly isolated *Clostridium* sp. BS-1. Applied Microbiology and Biotechnology 88 5: 1161-1167.

221. Garnova E, Zhilina T, Tourova T, Kostrikina N, Zavarzin G (2004) Anaerobic, alkaliphilic, saccharolytic bacterium *Alkalibacter saccharofermentans* gen. nov., sp. nov. from a soda lake in the Transbaikal region of Russia. Extremophiles 8 4: 309-316.

222. Lawson PA, Wawrik B, Allen TD, Johnson CN, Marks CR, et al. (2014) *Youngiibacter fragilis* gen. nov., sp. nov., isolated from natural gas production-water and reclassification of *Acetivibrio multivorans* as *Youngiibacter multivorans* comb. nov. International Journal of Systematic and Evolutionary Microbiology 64 Pt 1: 198-205.

223. Stams AJM, Hansen TA (1984) Fermentation of glutamate and other compounds by *Acidaminobacter hydrogenoformans* gen. nov. sp. nov., an obligate anaerobe isolated from black mud. Studies with pure cultures and mixed cultures with sulfate-reducing and methanogenic bacteria. Archives of Microbiology 137 4: 329-337.

224. Huang L, Chen B, Pistolozzi M, Wu Z, Wang J (2014) Inoculation and alkali coeffect in volatile fatty acids production and microbial community shift in the anaerobic fermentation of waste activated sludge. Bioresource Technology 153: 87-94.

225. Van Trappen S, Tan T-L, Samyn E, Vandamme P (2005) *Alcaligenes aquatilis* sp. nov., a novel bacterium from sediments of the Weser Estuary, Germany, and a salt marsh on Shem Creek in Charleston Harbor, USA. International Journal of Systematic and Evolutionary Microbiology 55 6: 2571-2575.

226. Elberson M, Sowers K (1997) Isolation of an aceticlastic strain of *Methanosarcina siciliae* from marine canyon sediments and emendation of the species description for *Methanosarcina siciliae*. International Journal of Systematic Bacteriology 47 4: 1258-1261.

227. Maestrojuan GM, Boone DR (1991) Characterization of *Methanosarcina barkeri* MST and 227, *Methanosarcina mazei* S-6T, and *Methanosarcina vacuolata* Z-761T. International Journal of Systematic Bacteriology 41 2: 267-274.

228. Kotelnikova S, Macario AJ, Pedersen K (1998) *Methanobacterium subterraneum* sp. nov., a new alkaliphilic, eurythermic and halotolerant methanogen isolated from deep granitic groundwater. International Journal of Systematic Bacteriology 48 2: 357-367.

229. Nolla-Ardèvol V, Strous M, Sorokin DY, Merkel AY, Tegetmeyer HE (2012) Activity and diversity of haloalkaliphilic methanogens in Central Asian soda lakes. Journal of Biotechnology 161 2: 167-173.

230. Zhu J, Liu X, Dong X (2011) *Methanobacterium movens* sp. nov. and *Methanobacterium flexile* sp. nov., isolated from lake sediment. International Journal of Systematic and Evolutionary Microbiology 61 12: 2974-2978.

231. Rout SP, Charles CJ, Garratt EJ, Laws AP, Gunn J, et al. (2015) Evidence of the generation of isosaccharinic acids and their subsequent degradation by local microbial consortia within hyper-alkaline contaminated soils, with relevance to intermediate level radioactive waste disposal. PLoS One 10 3.

232. Collins M, Lund B, Farrow J, Schleifer K (1983) Chemotaxonomic Study of an Alkalophilic Bacterium, *Exiguobacterium aurantiacum* gen. nov., sp. nov. Journal of General Microbiology 129 7: 2037-2042.

233. Rodrigues DF, Goris J, Vishnivetskaya T, Gilichinsky D, Thomashow MF, et al. (2006) Characterization of Exiguobacterium isolates from the Siberian permafrost. Description of Exiguobacterium sibiricum sp. nov. Extremophiles 10 4: 285-294.

234. Rodrigues DF, Tiedje JM (2007) Multi-locus real-time PCR for quantitation of bacteria in the environment reveals *Exiguobacterium* to be prevalent in permafrost. FEMS Microbiology Ecology 59 2: 489-499.

235. Rodrigues DF, Ivanova N, He Z, Huebner M, Zhou J, et al. (2008) Architecture of thermal adaptation in an *Exiguobacterium sibiricum* strain isolated from 3 million year old permafrost: a genome and transcriptome approach. BMC Genomics 9 1: 547.

236. Crapart S, Fardeau M-L, Cayol J-L, Thomas P, Sery C, et al. (2007) *Exiguobacterium profundum* sp. nov., a moderately thermophilic, lactic acid-producing bacterium isolated from a deep-sea hydrothermal vent. International Journal of Systematic and Evolutionary Microbiology 57 2: 287-292.

237. Vishnivetskaya TA, Kathariou S (2005) Putative transposases conserved in *Exiguobacterium* isolates from ancient Siberian permafrost and from contemporary surface habitats. Applied and Environmental Microbiology 71 11: 6954-6962.

238. Knudston KE, Haas EJ, Iwen PC, Ramaley WC, Ramaley RF (2001) Characterization of a gram-positive, non-spore-forming *Exiguobacterium*-like organism isolated from a Western Colorado (USA) hot spring. Abstracts Of The General Meeting Of The American Society For Microbiology 101: 30.

239. Yumoto I, Hishinuma-Narisawa M, Hirota K, Shingyo T, Takebe F, et al. (2004) *Exiguobacterium oxidotolerans* sp. nov., a novel alkaliphile exhibiting high catalase activity. International Journal of Systematic and Evolutionary Microbiology 54 6: 2013-2017.

240. Ueno S, Kaieda N, Koyama N (2000) Characterization of a P-type Na+-ATPase of a Facultatively Anaerobic Alkaliphile, *Exiguobacterium aurantiacum*. Journal of Biological Chemistry 275 19: 14537-14540.

241. Pandit RJ, Patel B, Kunjadia PD, Nagee A (2013) Isolation, characterization and molecular identification of heavy metal resistant bacteria from industrial effluents, Amala-khadi-Ankleshwar, Gujarat. International Journal of Environmental Sciences 3 5: 1689-1699.

242. Ordoñez OF, Flores MR, Dib JR, Paz A, Farías ME (2009) Extremophile culture collection from Andean lakes: extreme pristine environments that host a wide diversity of microorganisms with tolerance to UV radiation. Microbial Ecology 58 3: 461-473.

243. Flores MR, Ordoñez OF, Maldonado MJ, Farías ME (2009) Isolation of UV-B resistant bacteria from two high altitude Andean lakes (4,400 m) with saline and non saline conditions. The Journal of General and Applied Microbiology 55 6: 447-458.

244. Dhanve RS, Shedbalkar UU, Jadhav JP (2008) Biodegradation of diazo reactive dye Navy Blue HE2R (Reactive Blue 172) by an isolated *Exiguobacterium* sp. RD3. Biotechnology and Bioprocess Engineering 13 1: 53-60.

245. Dhanve RS, Kalyani DC, Phugare SS, Jadhav JP (2009) Coordinate action of Exiguobacterial oxidoreductive enzymes in biodegradation of reactive yellow 84A dye. Biodegradation 20 2: 245-255.

246. Tan L, Qu Y-y, Zhou J-t, Li A, Gou M (2009) Identification and characteristics of a novel salt-tolerant *Exiguobacterium* sp. for azo dyes decolorization. Applied Biochemistry and Biotechnology 159 3: 728-738.

247. Mohanty G, Mukherji S (2008) Biodegradation rate of diesel range n-alkanes by bacterial cultures *Exiguobacterium aurantiacum* and *Burkholderia cepacia*. International Biodeterioration & Biodegradation 61 3: 240-250.

248. Nazina TN, Pavlova NK, Ni F, Shestakova NM, Ivoilov VS, et al. (2008) Regulation of geochemical activity of microorganisms in a petroleum reservoir by injection of H_2O_2 or water-air mixture. Microbiology 77 3: 324-333.

249. Alam MZ, Malik A (2008) Chromate resistance, transport and bioreduction by *Exiguobacterium* sp. ZM-2 isolated from agricultural soil irrigated with tannery effluent. Journal of Basic Microbiology 48 5: 416-420.

250. Sarangi A, Krishnan C (2008) Comparison of in vitro Cr (VI) reduction by CFEs of chromate resistant bacteria isolated from chromate contaminated soil. Bioresource Technology 99 10: 4130-4137.

251. Karami K, Zolgharnein H, Assadi MM, Savari A, Dadollahi S (2011) New report on the occurrence of *Exiguobacterium* sp. AT1b in the persian gulf and its resistance to mercury pollution. Current Research in Bacteriology 4 1.

252. Petrova MA, Mindlin SZ, Gorlenko ZM, Kalyaeva ES, Soina VS, et al. (2002) Mercury-resistant bacteria from permafrost sediments and prospects for their use in comparative studies of mercury resistance determinants. Russian Journal of Genetics 38 11: 1330-1334.

253. Anderson CR, Cook GM (2004) Isolation and characterization of arsenate-reducing bacteria from arsenic-contaminated sites in New Zealand. Current Microbiology 48 5: 341-347.

254. Kasana RC, Yadav SK (2007) Isolation of a psychrotrophic *Exiguobacterium* sp. SKPB5 (MTCC 7803) and characterization of its alkaline protease. Current Microbiology 54 3: 224-229.

255. Pitt TL, Malnick H, Shah J, Chattaway MA, Keys CJ, et al. (2007) Characterisation of *Exiguobacterium aurantiacum* isolates from blood cultures of six patients. Clinical Microbiology and Infection 13 9: 946-948.

256. Keynan Y, Weber G, Sprecher H (2007) Molecular identification of *Exiguobacterium acetylicum* as the aetiological agent of bacteraemia. Journal of Medical Microbiology 56 4: 563-564.

257. Altschul SF, Madden TL, Schäffer AA, Zhang J, Zhang Z, et al. (1997) Gapped BLAST and PSI-BLAST: a new generation of protein database search programs. Nucleic Acids Research 25 17: 3389-3402.

258. Kimura M (1980) A simple method for estimating evolutionary rates of base substitutions through comparative studies of nucleotide sequences. Journal of Molecular Evolution 16 2: 111-120.

259. Ludwig W (2010) Molecular Phylogeny of Microorganisms: Is rRNA Still a Useful Marker? Molecular Phylogeny of Microorganisms: 65.

260. Chikhi R, Medvedev P (2013) Informed and automated k-mer size selection for genome assembly. Bioinformatics: btt310.

261. Boetzer M, Henkel CV, Jansen HJ, Butler D, Pirovano W (2011) Scaffolding pre-assembled contigs using SSPACE. Bioinformatics 27 4: 578-579.

262. Aziz RK, Bartels D, Best AA, DeJongh M, Disz T, et al. (2008) The RAST Server: rapid annotations using subsystems technology. BMC Genomics 9 1: 75.

263. Van Loon L, Glaus M, Stallone S, Laube A (1997) Sorption of isosaccharinic acid, a cellulose degradation product, on cement. Environmental Science & Technology 31 4: 1243-1245.

264. Van Loon L, Glaus M (1997) Review of the kinetics of alkaline degradation of cellulose in view of its relevance for safety assessment of radioactive waste repositories. Journal of Polymers and the Environment 5 2: 97-109.

265. Rout SP, Charles CJ, Doulgeris C, McCarthy AJ, Rooks DJ, et al. (2015) Anoxic biodegradation of isosaccharinic acids at alkaline pH by natural microbial communities. PLos One Accepted, in Press.

266. Virden BT, Kral TA (2010) Methanogen use of insoluble carbonates and the implications for life on Mars. Astrobiology Science Conference 2010: Evolution and Life: Surviving Catastrophes and Extremes on Earth and Beyond 1538: 5152.

267. Wu X-Y, Shi K-L, Xu X-W, Wu M, Oren A, et al. (2010) *Alkaliphilus halophilus* sp. nov., a strictly anaerobic and halophilic bacterium isolated from a saline lake, and emended description of the genus *Alkaliphilus*. International Journal of Systematic and Evolutionary Microbiology 60 12: 2898-2902.

268. Zhilina T, Zavarzina D, Kolganova T, Lysenko A, Tourova T (2009) *Alkaliphilus peptidofermentans* sp. nov., a new alkaliphilic bacterial soda lake isolate capable of peptide fermentation and Fe (III) reduction. Microbiology 78 4: 445-454.

269. Cao X, Liu X, Dong X (2003) *Alkaliphilus crotonatoxidans* sp. nov., a strictly anaerobic, crotonate-dismutating bacterium isolated from a methanogenic environment. International Journal of Systematic and Evolutionary Microbiology 53 4: 971-975.

270. Takai K, Moser DP, Onstott TC, Spoelstra N, Pfiffner SM, et al. (2001) Alkaliphilus transvaalensis gen. nov., sp. nov., an extremely alkaliphilic bacterium isolated from a deep South African gold mine. International Journal of Systematic and Evolutionary Microbiology 51 4: 1245-1256.

271. Van Dyke M, McCarthy A (2002) Molecular biological detection and characterization of Clostridium populations in municipal landfill sites. Applied and Environmental Microbiology 68 4: 2049-2053.

272. Rout SP, Radford J, Laws AP, Sweeney F, Elmekawy A, et al. (2014) Biodegradation of the Alkaline Cellulose Degradation Products Generated During Radioactive Waste Disposal. PLoS ONE 9 9.

273. Zavarzina D, Tourova T, Kolganova T, Boulygina E, Zhilina T (2009) Description of *Anaerobacillus alkalilacustre* gen. nov., sp. nov.—Strictly anaerobic diazotrophic bacillus isolated from soda lake and transfer of *Bacillus arseniciselenatis*, *Bacillus macyae*, and *Bacillus alkalidiazotrophicus* to *Anaerobacillus* as the new combinations *A. arseniciselenatis* comb. nov., *A. macyae* comb. nov., and *A. alkalidiazotrophicus* comb. nov. Microbiology 78 6: 723-731.

274. Boyer E, Ingle M, Mercer G (1973) *Bacillus alcalophilus* subsp. *halodurans* subsp. nov.: An alkaline-amylase-producing, alkalophilic organism. International Journal of Systematic Bacteriology 23 3: 238-242.

275. Oehmen A, Zeng RJ, Saunders AM, Blackall LL, Keller J, et al. (2006) Anaerobic and aerobic metabolism of glycogen-accumulating organisms selected with propionate as the sole carbon source. Microbiology 152 9: 2767-2778.

276. Wong M-T, Tan FM, Ng WJ, Liu W-T (2004) Identification and occurrence of tetrad-forming Alphaproteobacteria in anaerobic–aerobic activated sludge processes. Microbiology 150 11: 3741-3748.

277. Dridi B, Fardeau M-L, Ollivier B, Raoult D, Drancourt M (2012) *Methanomassiliicoccus luminyensis* gen. nov., sp. nov., a methanogenic archaeon isolated from human faeces. International Journal of Systematic and Evolutionary Microbiology 62 Pt 8: 1902-1907.

278. Montero B, García-Morales J, Sales D, Solera R (2009) Analysis of methanogenic activity in a thermophilic-dry anaerobic reactor: Use of fluorescence *in situ* hybridization. Waste management 29 3: 1144-1151.

279. Oehmen A, Yuan Z, Blackall LL, Keller J (2005) Comparison of acetate and propionate uptake by polyphosphate accumulating organisms and glycogen accumulating organisms. Biotechnology and Bioengineering 91 2: 162-168.

280. Roh Y, Chon C-M, Moon J-W (2007) Metal reduction and biomineralization by an alkaliphilic metal-reducing bacterium, *Alkaliphilus metalliredigens* (QYMF). Geosciences Journal 11 4: 415-423.

281. Williamson AJ, Morris K, Shaw S, Byrne JM, Boothman C, et al. (2013) Microbial Reduction of Fe(III) under Alkaline Conditions Relevant to Geological Disposal. Applied and Environmental Microbiology 79 11: 3320-3326.

282. Evans N (2008) Binding mechanisms of radionuclides to cement. Cement and concrete research 38 4: 543-553.

283. NDA (2010) Gas Status Report NDA/RWMD/037 Nuclear Decommissioning Authority (Radoactive Waste Management Directorate), Currie Av, Harwell, Didcot, Oxfordshire, UK

284. Wang S, McCarthy J, Ferguson J (1993) Utilization of Glucoisosaccharinic Acid and Components of Kraft Black Liquor as Energy Sources for Growth of Anaerobic Bacteria. Holzforschung 47 1993: 141-148.

285. Andreesen JR, Schaupp A, Neurauter C, Brown A, Ljungdahl LG (1973) Fermentation of Glucose, Fructose, and Xylose by *Clostridium thermoaceticum*: Effect of Metals on Growth Yield, Enzymes, and the Synthesis of Acetate from CO_2. Journal of Bacteriology 114 2: 743-751.

286. Biebl H (2001) Fermentation of glycerol by *Clostridium pasteurianum*—batch and continuous culture studies. Journal of Industrial Microbiology and Biotechnology 27 1: 18-26.

287. Chen W-M, Tseng Z-J, Lee K-S, Chang J-S (2005) Fermentative hydrogen production with *Clostridium butyricum* CGS5 isolated from anaerobic sewage sludge. International Journal of Hydrogen Energy 30 10: 1063-1070.

288. Han S-K, Shin H-S (2004) Biohydrogen production by anaerobic fermentation of food waste. International Journal of Hydrogen Energy 29 6: 569-577.

289. Caccavo F, Lonergan DJ, Lovley DR, Davis M, Stolz JF, et al. (1994) *Geobacter sulfurreducens* sp. nov., a hydrogen-and acetate-oxidizing dissimilatory metal-reducing microorganism. Applied and Environmental Microbiology 60 10: 3752-3759.

290. Lovley DR, Giovannoni SJ, White DC, Champine JE, Phillips E, et al. (1993) *Geobacter metallireducens* gen. nov. sp. nov., a microorganism capable of coupling the complete oxidation of organic compounds to the reduction of iron and other metals. Archives of Microbiology 159 4: 336-344.

291. Tebo BM, Obraztsova AY (1998) Sulfate-reducing bacterium grows with Cr (VI), U (VI), Mn (IV), and Fe (III) as electron acceptors. FEMS Microbiology Letters 162 1: 193-198.

292. Qu D, Ratering S, Schnell S (2004) Microbial reduction of weakly crystalline iron (III) oxides and suppression of methanogenesis in paddy soil. Bulletin of Environmental Contamination and Toxicology 72 6: 1172-1181.

293. Rout SP, Radford J, Laws AP, Sweeney F, Elmekawy A, et al. (2014) Biodegradation of the Alkaline Cellulose Degradation Products Generated during Radioactive Waste Disposal. PloS one 9 9: e107433.

294. Stams A, Hansen T (1984) Fermentation of glutamate and other compounds by *Acidaminobacter hydrogenoformans* gen. nov. sp. nov., an obligate anaerobe isolated from black mud. Studies with pure cultures and mixed cultures with sulfate-reducing and methanogenic bacteria. Archives of Microbiology 137 4: 329-337.

295. Ganesan A, Chaussonnerie S, Tarrade A, Dauga C, Bouchez T, et al. (2008) *Cloacibacillus evryensis* gen. nov., sp. nov., a novel asaccharolytic, mesophilic, amino-acid-degrading bacterium within the phylum 'Synergistetes', isolated from an anaerobic sludge digester. International Journal of Systematic and Evolutionary Microbiology 58 9: 2003-2012.

296. Grant WD, Holtom GJ, O'Kelly N, Malpass J, Rosevear A, et al. (2002) Microbial Degradation of Cellulose-derived Complexants Under Repository Conditions AEAT/ERRA-0301 AEA Technology and University of Leicester for UK Nirex Ltd. Harwell, Didcot, Oxfordshire, UK

297. Beckmann S, Lueders T, Krüger M, von Netzer F, Engelen B, et al. (2011) Acetogens and Acetoclastic Methanosarcinales Govern Methane Formation in Abandoned Coal Mines. Applied and Environmental Microbiology 77 11: 3749-3756.

298. Penning H, Claus P, Casper P, Conrad R (2006) Carbon isotope fractionation during acetoclastic methanogenesis by *Methanosaeta concilii* in culture and a lake sediment. Applied and Environmental Microbiology 72 8: 5648-5652.

299. Hugenholtz P (2002) Exploring prokaryotic diversity in the genomic era. Genome Biology 3 2.

300. Staley JT, Konopka A (1985) Measurement of in situ activities of nonphotosynthetic microorganisms in aquatic and terrestrial habitats. Annual Reviews in Microbiology 39 1: 321-346.

301. Rout SP, Rai A, Humphreys PN (2015) Draft genome sequence of alkaliphilic *Exiguobacterium* sp. strain HUD, isolated from a polymicrobial consortia. Genome Announcements 3 1.

302. Kumar CG, Takagi H (1999) Microbial alkaline proteases: from a bioindustrial viewpoint. Biotechnology Advances 17 7: 561-594.

303. Takai K, Moser DP, Onstott TC, Spoelstra N, Pfiffner SM, et al. (2001) *Alkaliphilus transvaalensis* gen. nov., sp. nov., an extremely alkaliphilic bacterium isolated from a deep South African gold mine. International Journal of Systematic and Evolutionary Microbiology 51 4: 1245-1256.

304. Zavarzina D, Kevbrin V, Zhilina T, Chistyakova N, Shapkin A, et al. (2011) Reduction of synthetic ferrihydrite by a binary anaerobic culture of *Anaerobacillus alkalilacustris* and *Geoalkalibacter ferrihydriticus* grown on mannitol at pH 9.5. Microbiology 80 6: 743-757.

305. Nowlan B, Dodia MS, Singh SP, Patel B (2006) *Bacillus okhensis* sp. nov., a halotolerant and alkalitolerant bacterium from an Indian saltpan. International Journal of Systematic and Evolutionary Microbiology 56 5: 1073-1077.

306. Boyer E, Ingle M, Mercer G (1973) *Bacillus alcalophilus* subsp. halodurans subsp. nov.: An alkaline-amylase-producing, alkalophilic organism. International Journal of Systematic Bacteriology 23 3: 238-242.

307. Zhilina T, Zavarzina D, Kevbrin V, Kolganova T (2013) *Methanocalculus natronophilus* sp. nov., a new alkaliphilic hydrogenotrophic methanogenic archaeon from a soda lake, and proposal of the new family Methanocalculaceae. Microbiology 82 6: 698-706.

308. Hilbert DW, Piggot PJ (2004) Compartmentalization of gene expression during *Bacillus subtilis* spore formation. Microbiology and Molecular Biology Reviews 68 2: 234-262.

309. Setlow P (2007) I will survive: DNA protection in bacterial spores. Trends in Microbiology 15 4: 172-180.

310. Hurdus M, Pilkington NJ (2000) The Solubility and Sorption of 2-C-(Hydroxymethyl)-3-deoxy-D-pentanoic Acid in the Presence of Nirex Reference Vault Backfill and its Degradation under Alkaline Conditions AEAT/ERRA-0153 AEA Technology plc, Harwell, Didcot, Oxfordshire, UK

311. Charles CJ, Rout SP, Garratt EJ, Patel K, Laws AP, et al. (2015) The enrichment of an alkaliphilic biofilm consortia capable of the anaerobic degradation of isosaccharinic acid from cellulosic materials incubated within an anthropogenic, hyperalkaline environment. FEMS Microbial Ecology Published Online 20th July 2015.

312. Bots P, Morris K, Hibberd R, Law GT, Mosselmans JFW, et al. (2014) Formation of Stable Uranium (VI) Colloidal Nanoparticles in Conditions Relevant to Radioactive Waste Disposal. Langmuir 30 48.

313. Baston G, Preston S, Otlett R, Walker J, Clacher A, et al. (2014) Carbon-14 release from Oldbury graphite AMEC/5352/002 Issue 3 Report prepared for Nuclear Decommissioning Authority/Radioactive Waste Management, Harwell, Didcot, Oxfordshire, UK

314. Doulgeris C, Humphreys PN, Rout S (2015) An approach to modelling the impact of ^{14}C release from reactor graphite in a geological disposal facility. Mineralogical Magazine Accepted: In Press.

Data

Chapter 6

Microcosm studies		Carbon Concentration (mM)												Volume (mL)		Concentration (mM)			
		TOC		Alpha ISA		Beta ISA		Acetic acid		Other VFA		Other organic carbon		Gas		Iron/Sulphide		Sulphate removed	
Type	Day	Mean	SE	Mean	SE	Mean	SE	Mean	SE	Mean	SE	Mean	SE	Mean	SE	Mean	SE	Mean	SE
Iron Reducing conditions	0	48.31	1.04	12.40	0.63	9.76	0.41	0.86	0.11	0.08	0.02	25.22	1.09	0.00	0.00	0.26	0.01		
	1	36.36	2.12	4.45	0.23	2.67	0.25	2.67	0.41	0.21	0.04	26.35	2.33	3.72	0.35	0.22	0.00		
	2	31.33	1.85	0.81	0.21	0.68	0.20	5.70	0.33	0.26	0.03	23.88	1.87	10.13	0.34	1.19	0.08		
	3	25.10	1.37	0.06	0.01	0.03	0.00	5.88	0.16	0.27	0.03	18.89	1.40	16.29	0.45	0.44	0.09		
	4	21.06	0.93	0.06	0.02	0.06	0.01	5.47	0.23	0.21	0.02	15.32	1.08	23.54	0.86	0.57	0.13		
	5	18.89	0.76	0.03	0.01	0.04	0.01	4.35	0.43	0.23	0.02	14.25	0.98	26.38	0.96	0.41	0.10		
	6	19.37	0.63	0.00	0.00	0.03	0.01	3.30	0.34	0.28	0.05	15.75	0.89	31.14	0.97	0.44	0.07		
	7	18.94	1.01	0.00	0.00	0.01	0.00	2.08	0.31	0.33	0.08	16.52	1.09	35.36	0.89	0.48	0.03		
Sulphate Reducing conditions	0	58.90	2.37	10.92	0.58	8.74	0.43	3.10	0.58	0.04	0.01	36.11	2.79	0.00	0.00	1.28	0.49	0.00	0.00
	1	47.29	1.63	4.72	0.20	3.50	0.14	2.94	0.47	0.03	0.01	36.10	1.33	3.73	0.25	3.00	0.33	20.72	5.40
	2	42.64	1.91	3.60	0.28	2.71	0.23	4.42	0.40	0.06	0.01	31.85	2.22	4.32	0.40	4.16	0.37	29.45	4.69
	3	33.46	1.36	0.85	0.27	1.20	0.24	5.12	0.59	0.07	0.01	28.60	1.10	5.22	0.64	5.70	0.44	22.96	3.29
	4	37.31	1.58	0.56	0.19	0.82	0.16	5.50	0.68	0.04	0.01	30.10	2.16	7.23	0.77	6.63	0.44	28.50	4.17
	5	32.93	1.94	0.38	0.15	0.39	0.14	5.63	0.34	0.06	0.01	26.46	2.01	6.71	0.66	7.89	0.66	36.31	4.70
	6	26.72	1.38	0.15	0.06	0.26	0.09	6.82	0.12	0.06	0.01	19.43	1.38	7.10	0.63	8.87	0.72	39.10	5.11
	7	22.45	0.96	0.06	0.02	0.09	0.04	5.82	0.45	0.04	0.01	16.45	0.82	7.10	0.63	9.24	0.69	44.84	5.66
Methanogenic	0	73.35	2.58	14.87	0.52	11.70	0.35	1.33	0.22	0.03	0.01	45.41	2.67	0.00	0.00				
	1	47.10	3.08	7.75	0.49	5.81	0.71	2.79	0.26	0.12	0.01	30.63	2.75	5.02	0.12				
	2	37.54	3.40	2.76	0.53	2.08	0.43	6.38	0.33	0.15	0.02	26.16	2.73	13.41	0.53				
	3	26.97	1.56	0.16	0.01	0.18	0.01	4.99	0.37	0.13	0.02	21.68	1.35	19.57	0.64				
	4	23.10	1.38	0.36	0.08	0.22	0.05	3.65	0.34	0.09	0.01	18.64	0.97	23.77	0.73				
	5	21.39	1.41	0.03	0.01	0.02	0.01	3.10	0.34	0.09	0.01	18.15	1.14	28.71	0.70				
	6	22.26	1.10	0.00	0.00	0.00	0.00	2.07	0.30	0.07	0.01	20.12	0.84	32.88	0.74				
	7	18.66	0.56	0.00	0.00	0.00	0.00	1.76	0.32	0.08	0.01	16.82	0.43	35.47	0.72				

Other VFA data		Concentration (mM)									
Type	Day	Propionic acid		Isobutyric acid		Butyric acid		Isovaleric acid		Valeric acid	
		Mean	SE	Mean	SE	Mean	SE	Mean	SE	Mean	SE
Iron Reducing conditions	0	0.17	0.03	0.01	0.00	0.00	0.00	0.01	0.00	ND	ND
	1	0.47	0.11	0.01	0.00	0.05	0.01	0.00	0.00	ND	ND
	2	0.49	0.07	0.02	0.01	0.11	0.01	0.01	0.00	ND	ND
	3	0.87	0.19	0.05	0.01	0.24	0.03	0.01	0.00	ND	ND
	4	0.85	0.17	0.00	0.00	0.10	0.02	0.02	0.00	ND	ND
	5	0.83	0.19	0.08	0.01	0.11	0.03	0.01	0.00	ND	ND
	6	0.57	0.12	0.05	0.01	0.07	0.02	0.02	0.00	ND	ND
	7	0.77	0.20	0.03	0.01	0.03	0.01	0.00	0.00	ND	ND
Sulphate Reducing conditions	0	0.00	0.08	0.00	0.00	0.01	0.00	ND	ND	ND	ND
	1	0.07	0.08	0.00	0.00	0.00	0.00	ND	ND	ND	ND
	2	0.24	0.12	0.00	0.00	0.03	0.01	ND	ND	ND	ND
	3	0.25	0.17	0.00	0.00	0.00	0.00	ND	ND	ND	ND
	4	0.00	0.09	0.02	0.01	0.00	0.00	ND	ND	ND	ND
	5	0.18	0.13	0.00	0.00	0.02	0.01	ND	ND	ND	ND
	6	0.00	0.13	0.00	0.00	0.02	0.01	ND	ND	ND	ND
	7	0.07	0.10	0.00	0.00	0.00	0.00	ND	ND	ND	ND
Methanogenic Conditions	0	0.07	0.03	ND	ND	0.00	0.00	0.02	0.01	0.00	0.00
	1	0.25	0.03	ND	ND	0.04	0.01	0.08	0.02	0.00	0.00
	2	0.26	0.02	ND	ND	0.05	0.01	0.09	0.02	0.00	0.00
	3	0.27	0.03	ND	ND	0.04	0.02	0.09	0.02	0.00	0.00
	4	0.19	0.03	ND	ND	0.02	0.01	0.06	0.01	0.00	0.00
	5	0.21	0.03	ND	ND	0.02	0.01	0.07	0.02	0.00	0.00
	6	0.16	0.03	ND	ND	0.01	0.00	0.05	0.01	0.00	0.00
	7	0.19	0.03	ND	ND	0.00	0.00	0.06	0.02	0.00	0.00

Headspace Gas	Headspace gas (%)			
Reactor type	Methane		Carbon Dioxide	
	Mean	SE	Mean	SE
Iron Reducing Conditions	76.99	2.26	23.01	2.26
Sulphate Reducing Conditions	0.00	0.00	100.00	0.00
Methanogenic Conditions	54.70	3.28	45.30	3.28

Control data		Concentration (mM)					
Type	Day	Alpha-ISA		Beta-ISA		Total ISA	
		Mean	SE	Mean	SE	Mean	SE
Canal sediment	0	18.41	2.50	12.05	0.37	30.45	1.40
	1	15.16	2.63	12.82	1.51	27.98	0.89
	2	15.56	1.61	12.84	1.34	28.40	0.99
	3	15.71	0.52	12.89	1.37	28.60	1.10
	4	15.72	1.24	13.93	3.83	29.65	2.72
	5	15.65	0.49	11.99	3.07	27.64	1.82
	6	15.50	1.57	12.34	1.94	27.83	0.22
	7	15.10	1.37	11.90	2.56	27.00	1.29
NCM sediment	0	15.38	3.06	11.79	2.21	27.17	2.19
	1	12.72	2.49	14.47	3.46	27.19	3.47
	2	14.31	2.28	12.55	1.37	26.86	2.02
	3	13.96	1.82	13.37	1.48	27.33	1.82
	4	14.65	1.00	16.17	2.58	30.82	2.05
	5	12.66	1.20	13.03	1.00	25.69	1.01
	6	13.22	2.29	13.09	1.56	26.31	2.26
	7	13.58	1.22	13.34	1.30	26.92	1.48

Rate Data	Rate (day^{-1})					
Microcosm	α-ISA		β-ISA		Total-ISA	
	Mean	SEM	Mean	SEM	Mean	SEM
Iron reducing conditions	0.57	0.11	0.77	0.18	0.82	0.16
Sulphate reducing conditions	0.67	0.10	0.75	0.09	0.76	0.10
Methanogenic conditions	0.53	0.06	0.69	0.14	0.55	0.05
Total	0.59	0.05	0.74	0.08	0.66	0.05

Chapter 7

Microcosm Chemistry		Carbon Concentration (mM)											
	Day	TOC		Alpha ISA		Beta ISA		Acetic acid		Other VFA		Other organic carbon	
pH		Mean	SE	Mean	SE	Mean	SE	Mean	SE	Mean	SE	Mean	SE
7.5	0	94.33	10.95	14.78	3.64	19.20	6.23	1.94	0.81	0.17	0.15	58.24	11.99
	1	67.99	11.65	4.49	2.85	3.26	0.85	11.19	5.47	2.11	1.25	46.95	11.57
	2	40.69	13.59	1.04	0.70	2.59	1.61	5.46	2.00	0.90	0.35	30.70	15.88
	3	37.06	4.74	0.90	0.42	2.21	2.43	3.30	1.04	0.98	0.91	29.67	7.09
	4	30.90	5.07	0.65	0.66	2.30	2.10	2.20	0.73	0.20	0.09	25.56	7.79
	5	30.93	1.84	0.13	0.18	0.16	0.21	2.38	1.52	0.18	0.16	28.13	3.33
	6	27.57	6.42	0.03	0.05	0.20	0.35	1.24	0.43	0.12	0.12	25.98	6.05
9.5	0	113.77	4.89	12.64	2.28	19.32	1.08	42.26	9.42	8.65	2.41	30.90	13.27
	1	99.79	11.79	8.80	2.60	18.31	0.50	38.08	7.05	8.36	1.76	26.24	23.13
	2	94.94	6.60	3.99	3.25	12.96	4.54	33.36	10.36	7.14	3.44	37.48	3.87
	3	93.08	16.09	1.23	1.54	6.04	2.56	43.45	7.33	8.43	2.92	33.92	21.07
	4	88.97	18.81	0.10	0.14	6.25	1.54	44.15	6.55	8.55	1.49	29.93	23.10
	5	89.08	4.58	0.10	0.11	5.18	0.71	33.89	15.44	8.96	4.40	40.94	23.31
	6	77.75	5.41	0.05	0.03	3.43	1.69	34.70	16.85	9.22	3.29	30.35	19.70
10.0	0	102.52	15.89	6.31	0.63	22.50	8.52	19.52	6.65	3.11	1.85	51.08	9.68
	1	104.67	16.00	4.22	2.04	18.43	7.83	15.13	10.71	3.10	2.51	63.79	18.62
	2	94.26	15.61	3.14	2.48	20.12	5.87	18.85	6.77	3.54	2.07	48.70	17.72
	3	85.76	8.01	2.13	2.96	18.49	9.28	19.63	6.27	3.32	1.83	42.19	14.30
	4	86.77	9.81	0.84	0.94	17.17	7.62	19.60	5.63	3.26	1.73	45.90	17.95
	5	96.61	7.65	0.56	0.61	12.38	1.26	20.21	3.89	3.37	1.19	60.10	11.45
	6	85.38	2.20	0.44	0.23	13.48	4.37	20.37	2.43	3.35	1.33	47.74	0.93

Rates	k (day^{-1})			
pH	Alpha ISA		Beta ISA	
	Mean	SE	Mean	SE
7.5	0.84	0.17	1.12	0.05
9.5	0.44	0.03	0.21	0.01
10.0	0.32	0.05	0.09	0.01

VFA		Concentration (mM)									
pH	Day	Propionic acid		Isobutyric acid		Butyric acid		Isovaleric acid		Valeric acid	
		Mean	SE	Mean	SE	Mean	SE	Mean	SE	Mean	SE
7.5	0	0.06	0.03	0.00	0.00	0.00	0.00	0.00	0.00	ND	ND
	1	0.45	0.11	0.06	0.02	0.08	0.05	0.06	0.03	ND	ND
	2	0.25	0.06	0.04	0.01	0.00	0.00	0.00	0.00	ND	ND
	3	0.30	0.12	0.01	0.01	0.01	0.01	0.02	0.01	ND	ND
	4	0.07	0.01	0.00	0.00	0.00	0.00	0.00	0.00	ND	ND
	5	0.04	0.02	0.00	0.00	0.00	0.00	0.01	0.01	ND	ND
	6	0.03	0.01	0.00	0.00	0.01	0.01	0.00	0.00	ND	ND
9.5	0	1.87	0.25	0.38	0.14	0.32	0.02	0.38	0.02	0.12	0.01
	1	1.79	0.14	0.36	0.10	0.31	0.05	0.36	0.05	0.12	0.01
	2	1.64	0.29	0.28	0.16	0.21	0.06	0.28	0.06	0.11	0.03
	3	1.89	0.21	0.35	0.17	0.25	0.11	0.35	0.11	0.14	0.02
	4	1.94	0.10	0.42	0.10	0.18	0.01	0.42	0.01	0.14	0.01
	5	2.14	0.57	0.36	0.14	0.22	0.07	0.36	0.07	0.12	0.03
	6	2.04	0.37	0.44	0.13	0.24	0.07	0.44	0.07	0.15	0.01
10.0	0	1.30	0.77	0.08	0.03	0.58	0.46	0.26	0.14	0.00	0.00
	1	1.40	0.91	0.06	0.04	0.63	0.51	0.27	0.17	0.03	0.00
	2	1.44	0.83	0.10	0.06	0.62	0.50	0.34	0.19	0.02	0.01
	3	1.37	0.78	0.13	0.07	0.56	0.43	0.28	0.15	0.00	0.00
	4	1.41	0.75	0.10	0.06	0.52	0.41	0.27	0.16	0.00	0.00
	5	1.32	0.66	0.02	0.01	0.48	0.35	0.32	0.18	0.03	0.02
	6	1.28	0.62	0.15	0.11	0.47	0.33	0.25	0.15	0.04	0.00

Gas	Volume (mL)	
pH	Mean	SE
7.50	186.49	17.54
9.50	39.77	4.32
10.00	*	*

*Below detection range

Headspace Gas						
pH7.5	CO2		CH4		H2	
Time (Days)	Mean	SE	Mean	SE	Mean	SE
0.00	0.26	0.45	0.39	0.28	-0.14	0.08
0.25	2.16	0.67	3.81	2.03	0.23	0.21
0.50	2.65	0.42	5.53	2.20	0.37	0.24
0.75	3.05	0.54	7.05	2.22	0.54	0.25
1.00	3.39	0.61	8.58	2.20	0.70	0.23
1.25	3.76	0.26	10.13	0.89	0.88	0.08
1.50	4.04	0.17	11.01	0.59	0.97	0.05
1.75	4.38	0.57	12.27	0.96	1.11	0.11
2.00	4.64	0.50	13.80	1.94	1.34	0.27
2.25	5.27	1.34	16.25	3.08	1.63	0.35
2.50	5.29	1.31	17.46	3.76	1.79	0.44
2.75	5.29	1.19	18.41	4.17	1.92	0.50
3.00	5.42	1.18	19.53	4.17	2.07	0.51
3.25	5.48	1.24	20.34	4.51	2.19	0.56
3.50	5.47	1.24	20.96	4.96	2.28	0.62
3.75	5.41	1.18	21.57	5.42	2.37	0.68
4.00	5.46	1.15	22.08	5.28	2.43	0.68
4.25	5.48	1.16	22.19	5.07	2.45	0.66
4.50	5.47	1.14	22.22	4.99	2.46	0.65
4.75	5.65	0.94	22.84	4.35	2.55	0.58
5.00	5.89	0.90	24.03	3.50	2.68	0.49
5.25	5.82	1.00	24.23	3.11	2.73	0.46
5.50	5.85	0.89	24.47	2.92	2.76	0.45
5.75	5.47	1.11	22.28	4.83	2.48	0.64
6.00	5.97	0.64	24.57	2.75	2.78	0.44

pH9.5	CO2		CH4		H2	
Time (Days)	Mean	SE	Mean	SE	Mean	SE
0.00	0.07	0.01	0.11	0.07	-0.05	0.02
0.25	0.00	0.03	0.81	0.12	0.07	0.01
0.50	0.00	0.02	1.51	0.15	0.15	0.01
0.75	0.01	0.02	2.17	0.16	0.25	0.03
1.00	0.03	0.03	2.81	0.45	0.34	0.06
1.25	0.05	0.04	3.39	0.53	0.42	0.05
1.50	0.05	0.04	3.64	0.39	0.44	0.04
1.75	0.07	0.04	3.98	0.35	0.48	0.06
2.00	0.10	0.06	4.20	0.44	0.53	0.06
2.25	0.12	0.07	4.46	0.52	0.57	0.07
2.50	0.12	0.06	4.77	0.65	0.60	0.08
2.75	0.13	0.07	5.07	0.87	0.64	0.11
3.00	0.14	0.05	5.37	1.05	0.69	0.14
3.25	0.16	0.04	5.77	1.43	0.74	0.20
3.50	0.16	0.04	5.89	1.48	0.75	0.20
3.75	0.15	0.04	5.92	1.49	0.76	0.20
4.00	0.17	0.03	6.07	1.50	0.77	0.19
4.25	0.18	0.04	6.15	1.45	0.79	0.19
4.50	0.17	0.04	6.28	1.53	0.79	0.18
4.75	0.19	0.06	6.30	1.30	0.81	0.18
5.00	0.19	0.06	6.35	1.17	0.81	0.17
5.25	0.18	0.06	6.37	1.14	0.81	0.17
5.50	0.18	0.07	6.39	1.05	0.82	0.16
5.75	0.17	0.05	6.23	1.31	0.80	0.18
6.00	0.20	0.09	6.49	1.00	0.83	0.15

pH10.0	CO2		CH4		H2	
Time (Days)	Mean	SE	Mean	SE	Mean	SE
0.00	0.10	0.02	-0.06	0.03	0.01	0.01
0.25	0.54	0.09	0.02	0.02	0.17	0.10
0.50	0.88	0.23	0.04	0.03	0.30	0.21
0.75	1.28	0.19	0.08	0.03	0.45	0.32
1.00	1.51	0.16	0.12	0.03	0.59	0.46
1.25	1.78	0.17	0.16	0.03	0.77	0.61
1.50	1.96	0.21	0.18	0.02	0.93	0.73
1.75	2.17	0.21	0.21	0.03	1.03	0.84
2.00	2.35	0.25	0.23	0.02	1.15	0.92
2.25	2.62	0.27	0.26	0.02	1.27	1.01
2.50	2.88	0.32	0.29	0.03	1.34	1.03
2.75	3.13	0.33	0.32	0.03	1.41	1.08
3.00	3.35	0.39	0.35	0.03	1.48	1.13
3.25	3.57	0.46	0.38	0.04	1.56	1.17
3.50	3.88	0.58	0.41	0.06	1.61	1.26
3.75	4.07	0.68	0.44	0.07	1.65	1.28
4.00	4.25	0.58	0.47	0.05	1.71	1.33
4.25	4.39	0.48	0.49	0.04	1.83	1.33
4.50	4.48	0.48	0.50	0.04	1.94	1.41
4.75	4.56	0.44	0.51	0.04	2.02	1.47
5.00	4.64	0.34	0.53	0.04	2.14	1.53
5.25	4.79	0.47	0.54	0.03	2.21	1.55
5.50	4.83	0.41	0.55	0.04	2.28	1.60
5.75	4.87	0.42	0.55	0.04	2.33	1.63
6.00	5.01	0.48	0.57	0.05	2.42	1.67

Bradford assay	Protein (mg)					
Day	pH7.5		pH9.5		pH10.0	
	Mean	SE	Mean	SE	Mean	SE
0	68.08	12.95	83.56	8.93	78.32	1.44
1	98.56	8.34	106.18	1.98	80.70	3.31
2	78.80	2.40	100.23	6.77	92.84	6.19
3	72.13	1.24	106.65	6.37	81.65	3.51
4	73.08	4.53	110.23	9.37	89.03	3.97
5	67.37	8.45	98.56	4.82	75.94	7.49
6	67.61	12.74	83.56	7.23	74.99	8.93

Total Carbohydrate assay	Carbohydrate (mg)					
Day	pH7.5		pH9.5		pH10.0	
	Mean	SE	Mean	SE	Mean	SE
0	42.83	1.73	77.00	8.82	47.83	5.02
1	64.50	7.22	62.83	11.31	52.83	5.67
2	99.50	17.50	43.67	2.10	91.17	17.68
3	85.33	14.10	78.67	11.79	47.83	2.41
4	56.17	5.29	41.17	8.22	38.67	3.94
5	67.83	4.59	85.33	18.64	51.17	5.67
6	84.50	2.20	62.83	11.31	65.33	6.99

Control Data	ISA concentration (mM)					
Day	pH7.5		pH9.5		pH10.0	
	Mean	SE	Mean	SE	Mean	SE
0	20.30	1.59	21.84	6.41	19.39	1.80
1	18.65	1.01	17.98	7.59	17.16	1.59
2	18.93	1.12	22.57	4.31	16.54	2.83
3	19.07	1.25	16.49	3.95	17.23	0.17
4	19.77	3.08	21.44	4.28	17.56	4.33
5	18.43	2.07	21.68	6.58	21.00	6.52
6	18.56	0.25	17.77	4.44	18.25	6.20

Chapter 8

ISA consumption +pH	Test				Control			
	ISA Concentration(mM)		pH		ISA Concentration(mM)		pH	
Day	Mean	SEM	Mean	SEM	Mean	SEM	Mean	SEM
0	3.84	0.46	9.77	0.08	4.39	0.73	9.75	0.03
4	2.95	0.14	9.79	0.04	4.32	0.35	9.73	0.03
8	2.28	0.28	9.78	0.06	4.21	0.49	9.72	0.02
14	2.08	0.49	9.66	0.04	4.74	0.67	9.69	0.01
45	1.91	0.22	9.57	0.03	4.65	0.35	9.71	0.02
60	1.91	0.23	9.63	0.03	4.65	0.41	9.73	0.02

RAST analysis Subsytem	Number of associated proteins
Cofactors, Vitamins, Prosthetic Groups, Pigments	146
Cell Wall and Capsule	83
Virulence, Disease and Defense	78
Potassium metabolism	9
Miscellaneous	25
Phages, Prophages, Transposable elements, Plasmids	11
Membrane Transport	65
Iron acquisition and metabolism	17
RNA Metabolism	133
Nucleosides and Nucleotides	107
Protein Metabolism	201
Cell Division and Cell Cycle	43
Motility and Chemotaxis	80
Regulation and Cell signaling	35
Secondary Metabolism	8
DNA Metabolism	98
Fatty Acids, Lipids, and Isoprenoids	87
Nitrogen Metabolism	14
Dormancy and Sporulation	6
Respiration	53
Stress Response	75
Virulence, Disease and Defense	5
Amino Acids and Derivatives	262
Sulfur Metabolism	10
Phosphorus Metabolism	37
Carbohydrates	335

Chapter 9

Microcosm chemistry	Concentration (mg L^{-1})						Headspace Gas %			
	Alpha ISA		Beta ISA		Acetic Acid		Methane		Hydrogen	
Time (Days)	Mean	SE	Mean	SE	Mean	SE	Mean	SE	Mean	SE
0	253.84	26.22	205.72	44.55	47.59	12.21	0.00	0.00	0.00	0.00
2	180.89	60.85	152.29	13.29	36.29	2.85	0.07	0.01	0.03	0.00
4	135.68	24.76	134.00	12.21	201.27	33.01	0.09	0.01	0.05	0.00
6	33.16	25.48	97.61	17.13	0.00	0.00	0.09	0.01	0.04	0.01
8	2.70	0.62	7.76	2.82	0.00	0.00	0.10	0.01	0.05	0.01
10	1.42	0.82	1.60	0.67	0.00	0.00	0.16	0.04	0.07	0.01
12	6.95	5.67	3.81	1.94	0.00	0.00	0.14	0.02	0.11	0.02
14	3.64	2.95	1.45	0.74	0.00	0.00	0.17	0.02	0.14	0.02

Control data	Total ISA (mgL^{-1})	
Time (Day	Mean	SE
0.00	440.29	15.98
2.00	381.14	22.79
4.00	401.26	25.01
6.00	426.26	9.60
8.00	433.31	19.52
10.00	402.58	20.93
12.00	398.71	31.97
14.00	402.63	14.64

First order rate	*k* (day^{-1})	
	Mean	SE
Alpha ISA	0.325	0.009
Beta ISA	0.407	0.002
Total ISA	0.349	0.008

Autoclaved Soil +leachate	ISA Concentration (mg L^{-1})					
	4°C		10°C		20°C	
Time (Weeks)	Mean	SE	Mean	SE	Mean	SE
0	0.00	0.00	0.00	0.00	0.00	0.00
4	4.60	0.08	4.30	1.42	5.15	0.66
8	9.10	0.35	16.22	5.76	17.01	1.69
12	16.54	2.91	24.82	7.48	29.87	3.04
16	24.08	0.56	32.90	7.30	25.15	8.20

Soil +leachate	ISA Concentration (mg L^{-1})					
	4°C		10°C		20°C	
Time (Weeks)	Mean	SE	Mean	SE	Mean	SE
0	0.00	0.00	0.00	0.00	0.00	0.00
4	3.79	0.49	4.81	0.28	4.47	0.55
8	2.35	1.02	23.50	2.31	6.68	1.80
12	7.45	2.89	5.40	2.72	2.67	0.15
16	4.24	4.24	0.00	0.00	0.00	0.00

Clone Libraries

Chapter 7 bacteria

pH7.5

Clone ID	Closest Sequence Match	Similarity (%)
7.5EUB8	Acidaminobacter hydrogenoformans strain glu 65 16S ribosomal RNA gene, partial sequence	99
7.5EUB19	Acidaminobacter hydrogenoformans strain glu 65 16S ribosomal RNA gene, partial sequence	99
7.5EUB37	Acidaminobacter hydrogenoformans strain glu 65 16S ribosomal RNA gene, partial sequence	99
7.5EUB23	Alkalibacter saccharofermentans strain Z-79820 16S ribosomal RNA gene, partial sequence	97
7.5EUB27	Anaerolinea thermophila strain UNI-1 16S ribosomal RNA gene, complete sequence	89
7.5EUB17	Christensenella minuta strain YIT 12065 16S ribosomal RNA gene, partial sequence	88
7.5EUB18	Christensenella minuta strain YIT 12065 16S ribosomal RNA gene, partial sequence	88
7.5EUB26	Cloacibacillus porcorum strain CL-84 16S ribosomal RNA gene, partial sequence	91
7.5EUB48	Clostridium alkalicellulosi strain Z-7026	96
7.5EUB3	Clostridium sporosphaeroides strain DSM 1294 16S ribosomal RNA gene, complete sequence	96
7.5EUB4	Clostridium sporosphaeroides strain DSM 1294 16S ribosomal RNA gene, complete sequence	98
7.5EUB5	Clostridium sporosphaeroides strain DSM 1294 16S ribosomal RNA gene, complete sequence	95
7.5EUB6	Clostridium sporosphaeroides strain DSM 1294 16S ribosomal RNA gene, complete sequence	99
7.5EUB7	Clostridium sporosphaeroides strain DSM 1294 16S ribosomal RNA gene, complete sequence	96
7.5EUB9	Clostridium sporosphaeroides strain DSM 1294 16S ribosomal RNA gene, complete sequence	97
7.5EUB11	Clostridium sporosphaeroides strain DSM 1294 16S ribosomal RNA gene, complete sequence	98
7.5EUB13	Clostridium sporosphaeroides strain DSM 1294 16S ribosomal RNA gene, complete sequence	97
7.5EUB14	Clostridium sporosphaeroides strain DSM 1294 16S ribosomal RNA gene, complete sequence	97
7.5EUB15	Clostridium sporosphaeroides strain DSM 1294 16S ribosomal RNA gene, complete sequence	95
7.5EUB16	Clostridium sporosphaeroides strain DSM 1294 16S ribosomal RNA gene, complete sequence	91
7.5EUB20	Clostridium sporosphaeroides strain DSM 1294 16S ribosomal RNA gene, complete sequence	97
7.5EUB21	Clostridium sporosphaeroides strain DSM 1294 16S ribosomal RNA gene, complete sequence	98
7.5EUB22	Clostridium sporosphaeroides strain DSM 1294 16S ribosomal RNA gene, complete sequence	97
7.5EUB24	Clostridium sporosphaeroides strain DSM 1294 16S ribosomal RNA gene, complete sequence	100
7.5EUB25	Clostridium sporosphaeroides strain DSM 1294 16S ribosomal RNA gene, complete sequence	97
7.5EUB29	Clostridium sporosphaeroides strain DSM 1294 16S ribosomal RNA gene, complete sequence	100
7.5EUB30	Clostridium sporosphaeroides strain DSM 1294 16S ribosomal RNA gene, complete sequence	97
7.5EUB31	Clostridium sporosphaeroides strain DSM 1294 16S ribosomal RNA gene, complete sequence	94
7.5EUB35	Clostridium sporosphaeroides strain DSM 1294 16S ribosomal RNA gene, complete sequence	95
7.5EUB39	Clostridium sporosphaeroides strain DSM 1294 16S ribosomal RNA gene, complete sequence	99
7.5EUB40	Clostridium sporosphaeroides strain DSM 1294 16S ribosomal RNA gene, complete sequence	96
7.5EUB41	Clostridium sporosphaeroides strain DSM 1294 16S ribosomal RNA gene, complete sequence	98
7.5EUB42	Clostridium sporosphaeroides strain DSM 1294 16S ribosomal RNA gene, complete sequence	98
7.5EUB44	Clostridium sporosphaeroides strain DSM 1294 16S ribosomal RNA gene, complete sequence	98
7.5EUB45	Clostridium sporosphaeroides strain DSM 1294 16S ribosomal RNA gene, complete sequence	98
7.5EUB46	Clostridium sporosphaeroides strain DSM 1294 16S ribosomal RNA gene, complete sequence	97
7.5EUB47	Draconibacterium orientale 16S ribosomal RNA, complete sequence	90
7.5EUB43	Parabacteroides chartae strain NS31-3 16S ribosomal RNA gene, partial sequence	88
7.5EUB28	Proteiniphilum acetatigenes strain TB107 16S ribosomal RNA gene, complete sequence	96
7.5EUB10	Ruminococcus albus strain 7 16S ribosomal RNA gene, complete sequence	93
7.5EUB34	Saccharofermentans acetigenes strain P6 16S ribosomal RNA gene, complete sequence	91
7.5EUB38	Saccharofermentans acetigenes strain P6 16S ribosomal RNA gene, complete sequence	93
7.5EUB12	Trichococcus pasteurii strain KoTa2 16S ribosomal RNA gene, complete sequence	99
7.5EUB32	Trichococcus pasteurii strain KoTa2 16S ribosomal RNA gene, complete sequence	99
7.5EUB33	Trichococcus pasteurii strain KoTa2 16S ribosomal RNA gene, complete sequence	98
7.5EUB36	Trichococcus pasteurii strain KoTa2 16S ribosomal RNA gene, complete sequence	99
7.5EUB1	Youngiibacter multivorans strain DSM 6139 16S ribosomal RNA gene, partial sequence	99

pH9.5

9.5EUB42	Acetobacterium woodii strain DSM 1030 16S ribosomal RNA gene, complete sequence	99
9.5EUB5	Acidaminobacter hydrogenoformans strain glu 65 16S ribosomal RNA gene, partial sequence	96
9.5EUB8	Acidaminobacter hydrogenoformans strain glu 65 16S ribosomal RNA gene, partial sequence	97
9.5EUB11	Acidaminobacter hydrogenoformans strain glu 65 16S ribosomal RNA gene, partial sequence	96
9.5EUB14	Acidaminobacter hydrogenoformans strain glu 65 16S ribosomal RNA gene, partial sequence	98
9.5EUB25	Acidaminobacter hydrogenoformans strain glu 65 16S ribosomal RNA gene, partial sequence	96
9.5EUB45	Acidaminobacter hydrogenoformans strain glu 65 16S ribosomal RNA gene, partial sequence	95
9.5EUB46	Acidaminobacter hydrogenoformans strain glu 65 16S ribosomal RNA gene, partial sequence	96
9.5EUB2	Alkalibacter saccharofermentans strain Z-79820 16S ribosomal RNA gene, partial sequence	96
9.5EUB6	Alkalibacter saccharofermentans strain Z-79820 16S ribosomal RNA gene, partial sequence	96
9.5EUB22	Alkalibacter saccharofermentans strain Z-79820 16S ribosomal RNA gene, partial sequence	96
9.5EUB27	Alkalibacter saccharofermentans strain Z-79820 16S ribosomal RNA gene, partial sequence	97
9.5EUB28	Alkalibacter saccharofermentans strain Z-79820 16S ribosomal RNA gene, partial sequence	95
9.5EUB37	Alkalibacter saccharofermentans strain Z-79820 16S ribosomal RNA gene, partial sequence	95
9.5EUB40	Alkalibacter saccharofermentans strain Z-79820 16S ribosomal RNA gene, partial sequence	96
9.5EUB21	Aminivibrio pyruvatiphilus strain 4F6E 16S ribosomal RNA gene, partial sequence	98
9.5EUB32	Aminivibrio pyruvatiphilus strain 4F6E 16S ribosomal RNA gene, partial sequence	97
9.5EUB17	Christensenella minuta strain YIT 12065 16S ribosomal RNA gene, partial sequence	86
9.5EUB19	Cloacibacillus porcorum strain CL-84 16S ribosomal RNA gene, partial sequence	93
9.5EUB35	Cloacibacillus porcorum strain CL-84 16S ribosomal RNA gene, partial sequence	89
9.5EUB36	Clostridium thermocellum DSM 1313 16S ribosomal RNA, complete sequence	90
9.5EUB29	Draconibacterium orientale 16S ribosomal RNA, complete sequence	90
9.5EUB1	Paludibacter propionicigenes strain WB4 16S ribosomal RNA gene, complete sequence	98
9.5EUB44	Paludibacter propionicigenes strain WB4 16S ribosomal RNA gene, complete sequence	89
9.5EUB31	Saccharofermentans acetigenes strain P6 16S ribosomal RNA gene, complete sequence	91
9.5EUB33	Saccharofermentans acetigenes strain P6 16S ribosomal RNA gene, complete sequence	95
9.5EUB34	Saccharofermentans acetigenes strain P6 16S ribosomal RNA gene, complete sequence	95
9.5EUB13	Tissierella creatinini strain BN11 16S ribosomal RNA gene, partial sequence	93
9.5EUB9	Trichococcus pasteurii strain KoTa2 16S ribosomal RNA gene, complete sequence	99
9.5EUB12	Trichococcus pasteurii strain KoTa2 16S ribosomal RNA gene, complete sequence	98
9.5EUB15	Trichococcus pasteurii strain KoTa2 16S ribosomal RNA gene, complete sequence	98
9.5EUB16	Trichococcus pasteurii strain KoTa2 16S ribosomal RNA gene, complete sequence	98
9.5EUB23	Trichococcus pasteurii strain KoTa2 16S ribosomal RNA gene, complete sequence	98
9.5EUB41	Trichococcus pasteurii strain KoTa2 16S ribosomal RNA gene, complete sequence	99
9.5EUB43	Trichococcus pasteurii strain KoTa2 16S ribosomal RNA gene, complete sequence	98
9.5EUB39	Youngiibacter fragilis strain 232.1	99
9.5EUB3	Youngiibacter multivorans strain DSM 6139 16S ribosomal RNA gene, partial sequence	99
9.5EUB7	Youngiibacter multivorans strain DSM 6139 16S ribosomal RNA gene, partial sequence	98
9.5EUB10	Youngiibacter multivorans strain DSM 6139 16S ribosomal RNA gene, partial sequence	99
9.5EUB20	Youngiibacter multivorans strain DSM 6139 16S ribosomal RNA gene, partial sequence	99
9.5EUB24	Youngiibacter multivorans strain DSM 6139 16S ribosomal RNA gene, partial sequence	87
9.5EUB30	Youngiibacter multivorans strain DSM 6139 16S ribosomal RNA gene, partial sequence	99
9.5EUB38	Youngiibacter multivorans strain DSM 6139 16S ribosomal RNA gene, partial sequence	99

pH10.0

10EUB1	Acidaminobacter hydrogenoformans strain glu 65 16S ribosomal RNA gene, partial sequence	98
10EUB2	Acidaminobacter hydrogenoformans strain glu 65 16S ribosomal RNA gene, partial sequence	97
10EUB32	Acidaminobacter hydrogenoformans strain glu 65 16S ribosomal RNA gene, partial sequence	96
10EUB33	Acidaminobacter hydrogenoformans strain glu 65 16S ribosomal RNA gene, partial sequence	94
10EUB3	Alcaligenes aquatilis strain LMG 22996 16S ribosomal RNA gene, partial sequence	99
10EUB5	Alcaligenes aquatilis strain LMG 22996 16S ribosomal RNA gene, partial sequence	99
10EUB9	Alcaligenes aquatilis strain LMG 22996 16S ribosomal RNA gene, partial sequence	99
10EUB11	Alcaligenes aquatilis strain LMG 22996 16S ribosomal RNA gene, partial sequence	98
10EUB18	Alcaligenes aquatilis strain LMG 22996 16S ribosomal RNA gene, partial sequence	99
10EUB21	Alcaligenes aquatilis strain LMG 22996 16S ribosomal RNA gene, partial sequence	99
10EUB22	Alcaligenes aquatilis strain LMG 22996 16S ribosomal RNA gene, partial sequence	99
10EUB29	Alcaligenes aquatilis strain LMG 22996 16S ribosomal RNA gene, partial sequence	99
10EUB38	Alcaligenes aquatilis strain LMG 22996 16S ribosomal RNA gene, partial sequence	99
10EUB40	Alcaligenes aquatilis strain LMG 22996 16S ribosomal RNA gene, partial sequence	99
10EUB43	Alcaligenes aquatilis strain LMG 22996 16S ribosomal RNA gene, partial sequence	99
10EUB44	Alcaligenes aquatilis strain LMG 22996 16S ribosomal RNA gene, partial sequence	98
10EUB45	Alcaligenes aquatilis strain LMG 22996 16S ribosomal RNA gene, partial sequence	99
10EUB7	Alkalibacter saccharofermentans strain Z-79820 16S ribosomal RNA gene, partial sequence	95
10EUB28	Alkalibacter saccharofermentans strain Z-79820 16S ribosomal RNA gene, partial sequence	96
10EUB30	Alkalibacter saccharofermentans strain Z-79820 16S ribosomal RNA gene, partial sequence	97
10EUB39	Alkalibacter saccharofermentans strain Z-79820 16S ribosomal RNA gene, partial sequence	97
10EUB26	Aminivibrio pyruvatiphilus strain 4F6E 16S ribosomal RNA gene, partial sequence	95
10EUB8	Bacillus pseudofirmus OF4 strain OF4 16S ribosomal RNA, complete sequence	99
10EUB20	Cloacibacillus porcorum strain CL-84 16S ribosomal RNA gene, partial sequence	93
10EUB37	Clostridium formicaceticum strain DSM 92 16S ribosomal RNA gene, partial sequence	96
10EUB23	Clostridium thermocellum strain ATCC 27405 16S ribosomal RNA gene, complete sequence	91
10EUB24	Clostridium thermocellum strain ATCC 27405 16S ribosomal RNA gene, complete sequence	87
10EUB27	Clostridium thermocellum strain ATCC 27405 16S ribosomal RNA gene, complete sequence	88
10EUB42	Dehalobacter sp. CF strain CF 16S ribosomal RNA, complete sequence	94
10EUB41	Dehalobacter sp. CF strain CF 16S ribosomal RNA, complete sequence	93
10EUB15	Levilinea saccharolytica strain KIBI-1 16S ribosomal RNA gene, partial sequence	87
10EUB31	Moorella humiferrea strain 64_FGQ	89
10EUB34	Paenibacillus polymyxa strain DSM 36 16S ribosomal RNA gene, partial sequence	88
10EUB10	Saccharofermentans acetigenes strain P6 16S ribosomal RNA gene, complete sequence	94
10EUB14	Saccharofermentans acetigenes strain P6 16S ribosomal RNA gene, complete sequence	91
10EUB6	Sporobacter termitidis strain SYR 16S ribosomal RNA gene, complete sequence	94
10EUB12	Tissierella creatinini strain DSM 9508 16S ribosomal RNA gene, partial sequence	99
10EUB4	Youngiibacter fragilis strain 232.1 16S ribosomal RNA gene, partial sequence	98
10EUB36	Youngiibacter multivorans strain DSM 6139 16S ribosomal RNA gene, partial sequence	99

Chapter 7 Archaea

pH7.5

Clone ID	Closest Sequence Match	Similarity (%)
7.5ARC3	Methanocorpusculum aggregans strain DSM 3027 16S ribosomal RNA gene, partial sequence	99
7.5ARC4	Methanocorpusculum aggregans strain DSM 3027 16S ribosomal RNA gene, partial sequence	99
7.5ARC5	Methanocorpusculum aggregans strain DSM 3027 16S ribosomal RNA gene, partial sequence	99
7.5ARC6	Methanocorpusculum aggregans strain DSM 3027 16S ribosomal RNA gene, partial sequence	99
7.5ARC15	Methanocorpusculum aggregans strain DSM 3027 16S ribosomal RNA gene, partial sequence	99
7.5ARC17	Methanocorpusculum aggregans strain DSM 3027 16S ribosomal RNA gene, partial sequence	99
7.5ARC18	Methanocorpusculum aggregans strain DSM 3027 16S ribosomal RNA gene, partial sequence	99
7.5ARC20	Methanocorpusculum aggregans strain DSM 3027 16S ribosomal RNA gene, partial sequence	99
7.5ARC21	Methanocorpusculum aggregans strain DSM 3027 16S ribosomal RNA gene, partial sequence	99
7.5ARC22	Methanocorpusculum aggregans strain DSM 3027 16S ribosomal RNA gene, partial sequence	98
7.5ARC24	Methanocorpusculum aggregans strain DSM 3027 16S ribosomal RNA gene, partial sequence	99
7.5ARC26	Methanocorpusculum aggregans strain DSM 3027 16S ribosomal RNA gene, partial sequence	99
7.5ARC28	Methanocorpusculum aggregans strain DSM 3027 16S ribosomal RNA gene, partial sequence	99
7.5ARC31	Methanocorpusculum aggregans strain DSM 3027 16S ribosomal RNA gene, partial sequence	99
7.5ARC33	Methanocorpusculum aggregans strain DSM 3027 16S ribosomal RNA gene, partial sequence	99
7.5ARC34	Methanocorpusculum aggregans strain DSM 3027 16S ribosomal RNA gene, partial sequence	99
7.5ARC36	Methanocorpusculum aggregans strain DSM 3027 16S ribosomal RNA gene, partial sequence	99
7.5ARC37	Methanocorpusculum aggregans strain DSM 3027 16S ribosomal RNA gene, partial sequence	99
7.5ARC38	Methanocorpusculum aggregans strain DSM 3027 16S ribosomal RNA gene, partial sequence	99
7.5ARC39	Methanocorpusculum aggregans strain DSM 3027 16S ribosomal RNA gene, partial sequence	99
7.5ARC43	Methanocorpusculum aggregans strain DSM 3027 16S ribosomal RNA gene, partial sequence	99
7.5ARC44	Methanocorpusculum aggregans strain DSM 3027 16S ribosomal RNA gene, partial sequence	99
7.5ARC47	Methanocorpusculum aggregans strain DSM 3027 16S ribosomal RNA gene, partial sequence	99
7.5ARC16	Methanocorpusculum aggregans strain DSM 3027 16S ribosomal RNA gene, partial sequence	98
7.5ARC8	Methanocorpusculum labreanum strain Z 16S ribosomal RNA gene, complete sequence	99
7.5ARC9	Methanomassiliicoccus luminyensis strain B10 16S ribosomal RNA gene, partial sequence	99
7.5ARC11	Methanomassiliicoccus luminyensis strain B10 16S ribosomal RNA gene, partial sequence	94
7.5ARC13	Methanomassiliicoccus luminyensis strain B10 16S ribosomal RNA gene, partial sequence	94
7.5ARC30	Methanosaeta concilii strain GP6 16S ribosomal RNA gene, complete sequence	95
7.5ARC27	Methanosarcina lacustris strain ZS 16S ribosomal RNA gene, partial sequence	99
7.5ARC2	Methanosarcina siciliae strain T4/M 16S ribosomal RNA gene, partial sequence	99
7.5ARC10	Methanosarcina siciliae strain T4/M 16S ribosomal RNA gene, partial sequence	99
7.5ARC32	Methanosarcina siciliae strain T4/M 16S ribosomal RNA gene, partial sequence	99
7.5ARC35	Methanosarcina siciliae strain T4/M 16S ribosomal RNA gene, partial sequence	99
7.5ARC46	Methanosarcina siciliae strain T4/M 16S ribosomal RNA gene, partial sequence	99
7.5ARC25	Methanosarcina vacuolata strain Z-761 16S ribosomal RNA gene, partial sequence	99
7.5ARC7	Methanosphaerula palustris strain E1-9c 16S ribosomal RNA gene, complete sequence	91
7.5ARC14	Methanosphaerula palustris strain E1-9c 16S ribosomal RNA gene, complete sequence	96
7.5ARC19	Methanosphaerula palustris strain E1-9c 16S ribosomal RNA gene, complete sequence	95
7.5ARC23	Methanosphaerula palustris strain E1-9c 16S ribosomal RNA gene, complete sequence	94
7.5ARC29	Methanosphaerula palustris strain E1-9c 16S ribosomal RNA gene, complete sequence	94
7.5ARC1	Thermofilum pendens Hrk 5 16S ribosomal RNA, complete sequence	84
7.5ARC12	Thermofilum pendens Hrk 5 16S ribosomal RNA, complete sequence	83
7.5ARC40	Thermofilum pendens Hrk 5 16S ribosomal RNA, complete sequence	84
7.5ARC41	Thermofilum pendens Hrk 5 16S ribosomal RNA, complete sequence	84

pH9.5

9.5ARC4	Methanobacterium alcaliphilum strain NBRC 105226 16S ribosomal RNA gene, partial sequence	99
9.5ARC2	Methanobacterium flexile strain GH 16S ribosomal RNA gene, partial sequence	99
9.5ARC12	Methanobacterium flexile strain GH 16S ribosomal RNA gene, partial sequence	99
9.5ARC13	Methanobacterium flexile strain GH 16S ribosomal RNA gene, partial sequence	99
9.5ARC15	Methanobacterium flexile strain GH 16S ribosomal RNA gene, partial sequence	99
9.5ARC16	Methanobacterium flexile strain GH 16S ribosomal RNA gene, partial sequence	99
9.5ARC17	Methanobacterium flexile strain GH 16S ribosomal RNA gene, partial sequence	99
9.5ARC18	Methanobacterium flexile strain GH 16S ribosomal RNA gene, partial sequence	99
9.5ARC19	Methanobacterium flexile strain GH 16S ribosomal RNA gene, partial sequence	99
9.5ARC20	Methanobacterium flexile strain GH 16S ribosomal RNA gene, partial sequence	99
9.5ARC28	Methanobacterium flexile strain GH 16S ribosomal RNA gene, partial sequence	99
9.5ARC29	Methanobacterium flexile strain GH 16S ribosomal RNA gene, partial sequence	99
9.5ARC30	Methanobacterium flexile strain GH 16S ribosomal RNA gene, partial sequence	99
9.5ARC32	Methanobacterium flexile strain GH 16S ribosomal RNA gene, partial sequence	99
9.5ARC34	Methanobacterium flexile strain GH 16S ribosomal RNA gene, partial sequence	99
9.5ARC37	Methanobacterium flexile strain GH 16S ribosomal RNA gene, partial sequence	99
9.5ARC40	Methanobacterium flexile strain GH 16S ribosomal RNA gene, partial sequence	99
9.5ARC47	Methanobacterium flexile strain GH 16S ribosomal RNA gene, partial sequence	99
9.5ARC42	Methanobacterium palustre strain F 16S ribosomal RNA gene, partial sequence	99
9.5ARC7	Methanobacterium subterraneum strain A8p 16S ribosomal RNA gene, partial sequence	99
9.5ARC27	Methanobacterium subterraneum strain A8p 16S ribosomal RNA gene, partial sequence	99
9.5ARC38	Methanobacterium subterraneum strain A8p 16S ribosomal RNA gene, partial sequence	99
9.5ARC5	Methanocorpusculum aggregans strain DSM 3027 16S ribosomal RNA gene, partial sequence	99
9.5ARC39	Methanomassiliicoccus luminyensis strain B10 16S ribosomal RNA gene, partial sequence	89
9.5ARC1	Methanomassiliicoccus luminyensis strain B10 16S ribosomal RNA gene, partial sequence	89
9.5ARC3	Methanomassiliicoccus luminyensis strain B10 16S ribosomal RNA gene, partial sequence	88
9.5ARC6	Methanomassiliicoccus luminyensis strain B10 16S ribosomal RNA gene, partial sequence	89
9.5ARC8	Methanomassiliicoccus luminyensis strain B10 16S ribosomal RNA gene, partial sequence	89
9.5ARC9	Methanomassiliicoccus luminyensis strain B10 16S ribosomal RNA gene, partial sequence	89
9.5ARC10	Methanomassiliicoccus luminyensis strain B10 16S ribosomal RNA gene, partial sequence	88
9.5ARC14	Methanomassiliicoccus luminyensis strain B10 16S ribosomal RNA gene, partial sequence	89
9.5ARC23	Methanomassiliicoccus luminyensis strain B10 16S ribosomal RNA gene, partial sequence	88
9.5ARC24	Methanomassiliicoccus luminyensis strain B10 16S ribosomal RNA gene, partial sequence	89
9.5ARC25	Methanomassiliicoccus luminyensis strain B10 16S ribosomal RNA gene, partial sequence	88
9.5ARC26	Methanomassiliicoccus luminyensis strain B10 16S ribosomal RNA gene, partial sequence	88
9.5ARC31	Methanomassiliicoccus luminyensis strain B10 16S ribosomal RNA gene, partial sequence	88
9.5ARC33	Methanomassiliicoccus luminyensis strain B10 16S ribosomal RNA gene, partial sequence	88
9.5ARC35	Methanomassiliicoccus luminyensis strain B10 16S ribosomal RNA gene, partial sequence	89
9.5ARC36	Methanomassiliicoccus luminyensis strain B10 16S ribosomal RNA gene, partial sequence	89
9.5ARC41	Methanomassiliicoccus luminyensis strain B10 16S ribosomal RNA gene, partial sequence	89
9.5ARC43	Methanomassiliicoccus luminyensis strain B10 16S ribosomal RNA gene, partial sequence	89
9.5ARC44	Methanomassiliicoccus luminyensis strain B10 16S ribosomal RNA gene, partial sequence	89
9.5ARC45	Methanomassiliicoccus luminyensis strain B10 16S ribosomal RNA gene, partial sequence	88
9.5ARC46	Methanomassiliicoccus luminyensis strain B10 16S ribosomal RNA gene, partial sequence	89
9.5ARC48	Methanomassiliicoccus luminyensis strain B10 16S ribosomal RNA gene, partial sequence	89
9.5ARC11	Methanosphaerula palustris strain E1-9c 16S ribosomal RNA gene, complete sequence	94
9.5ARC21	Methanosphaerula palustris strain E1-9c 16S ribosomal RNA gene, complete sequence	95
9.5ARC22	Methanosphaerula palustris strain E1-9c 16S ribosomal RNA gene, complete sequence	96

pH10.0

10ARC23	Methanobacterium alcaliphilum strain NBRC 105226 16S ribosomal RNA gene, partial sequence	99
10ARC24	Methanobacterium alcaliphilum strain NBRC 105226 16S ribosomal RNA gene, partial sequence	99
10ARC35	Methanobacterium alcaliphilum strain NBRC 105226 16S ribosomal RNA gene, partial sequence	99
10ARC7	Methanobacterium flexile strain GH 16S ribosomal RNA gene, partial sequence	99
10ARC18	Methanobacterium flexile strain GH 16S ribosomal RNA gene, partial sequence	99
10ARC21	Methanobacterium flexile strain GH 16S ribosomal RNA gene, partial sequence	99
10ARC38	Methanobacterium flexile strain GH 16S ribosomal RNA gene, partial sequence	99
10ARC40	Methanobacterium flexile strain GH 16S ribosomal RNA gene, partial sequence	99
10ARC5	Methanobacterium subterraneum strain A8p 16S ribosomal RNA gene, partial sequence	99
10ARC32	Methanobacterium subterraneum strain A8p 16S ribosomal RNA gene, partial sequence	99
10ARC45	Methanobacterium subterraneum strain A8p 16S ribosomal RNA gene, partial sequence	99
10ARC47	Methanobacterium subterraneum strain A8p 16S ribosomal RNA gene, partial sequence	99
10ARC11	Methanocalculus taiwanensis strain P2F9704a 16S ribosomal RNA gene, partial sequence	99
10ARC25	Methanocalculus taiwanensis strain P2F9704a 16S ribosomal RNA gene, partial sequence	99
10ARC1	Methanocorpusculum aggregans strain DSM 3027 16S ribosomal RNA gene, partial sequence	99
10ARC3	Methanocorpusculum aggregans strain DSM 3027 16S ribosomal RNA gene, partial sequence	99
10ARC4	Methanocorpusculum aggregans strain DSM 3027 16S ribosomal RNA gene, partial sequence	99
10ARC6	Methanocorpusculum aggregans strain DSM 3027 16S ribosomal RNA gene, partial sequence	99
10ARC8	Methanocorpusculum aggregans strain DSM 3027 16S ribosomal RNA gene, partial sequence	99
10ARC10	Methanocorpusculum aggregans strain DSM 3027 16S ribosomal RNA gene, partial sequence	99
10ARC12	Methanocorpusculum aggregans strain DSM 3027 16S ribosomal RNA gene, partial sequence	99
10ARC13	Methanocorpusculum aggregans strain DSM 3027 16S ribosomal RNA gene, partial sequence	99
10ARC14	Methanocorpusculum aggregans strain DSM 3027 16S ribosomal RNA gene, partial sequence	99
10ARC15	Methanocorpusculum aggregans strain DSM 3027 16S ribosomal RNA gene, partial sequence	99
10ARC16	Methanocorpusculum aggregans strain DSM 3027 16S ribosomal RNA gene, partial sequence	99
10ARC17	Methanocorpusculum aggregans strain DSM 3027 16S ribosomal RNA gene, partial sequence	99
10ARC26	Methanocorpusculum aggregans strain DSM 3027 16S ribosomal RNA gene, partial sequence	99
10ARC27	Methanocorpusculum aggregans strain DSM 3027 16S ribosomal RNA gene, partial sequence	99
10ARC29	Methanocorpusculum aggregans strain DSM 3027 16S ribosomal RNA gene, partial sequence	99
10ARC30	Methanocorpusculum aggregans strain DSM 3027 16S ribosomal RNA gene, partial sequence	99
10ARC33	Methanocorpusculum aggregans strain DSM 3027 16S ribosomal RNA gene, partial sequence	99
10ARC41	Methanocorpusculum aggregans strain DSM 3027 16S ribosomal RNA gene, partial sequence	99
10ARC43	Methanocorpusculum aggregans strain DSM 3027 16S ribosomal RNA gene, partial sequence	99
10ARC46	Methanocorpusculum aggregans strain DSM 3027 16S ribosomal RNA gene, partial sequence	99
10ARC9	Methanosarcina mazei Go1 16S ribosomal RNA, complete sequence	99
10ARC20	Methanosarcina siciliae strain T4/M 16S ribosomal RNA gene, partial sequence	99
10ARC34	Methanosarcina siciliae strain T4/M 16S ribosomal RNA gene, partial sequence	99
10ARC36	Methanosarcina siciliae strain T4/M 16S ribosomal RNA gene, partial sequence	99
10ARC19	Methanosarcina vacuolata strain Z-761 16S ribosomal RNA gene, partial sequence	99
10ARC2	Methanosphaerula palustris strain E1-9c 16S ribosomal RNA gene, complete sequence	95
10ARC28	Methanosphaerula palustris strain E1-9c 16S ribosomal RNA gene, complete sequence	95
10ARC31	Methanosphaerula palustris strain E1-9c 16S ribosomal RNA gene, complete sequence	95
10ARC37	Methanosphaerula palustris strain E1-9c 16S ribosomal RNA gene, complete sequence	95
10ARC44	Methanosphaerula palustris strain E1-9c 16S ribosomal RNA gene, complete sequence	95
10ARC22	Thermofilum pendens Hrk 5 16S ribosomal RNA, complete sequence	84

Chapter 9

Bacteria

Clone ID	Closest Sequence Match	Similarity (%)
METHEUB1	Bacillus alcalophilus strain NBRC 15653 16S ribosomal RNA gene, partial sequence	94
METHEUB2	Bacillus alcalophilus strain NBRC 15653 16S ribosomal RNA gene, partial sequence	94
METHEUB3	Bacillus okhensis strain Kh10-101 16S ribosomal RNA gene, partial sequence	96
METHEUB4	Alkaliphilus transvaalensis strain SAGM1 16S ribosomal RNA gene, partial sequence	90
METHEUB5	Bacillus okhensis strain Kh10-101 16S ribosomal RNA gene, partial sequence	96
METHEUB6	Anaerobacillus alkalilacustris strain Z-0521 16S ribosomal RNA gene, partial sequence	96
METHEUB7	Alkaliphilus crotonatoxidans strain B11-2 16S ribosomal RNA gene, partial sequence	97
METHEUB8	Alkaliphilus crotonatoxidans strain B11-2 16S ribosomal RNA gene, partial sequence	97
METHEUB9	Roseicitreum antarcticum strain ZS2-28 16S ribosomal RNA gene, partial sequence	90
METHEUB10	Octadecabacter arcticus strain 238 16S ribosomal RNA gene, complete sequence	83
METHEUB11	Roseicitreum antarcticum strain ZS2-28 16S ribosomal RNA gene, partial sequence	91
METHEUB12	Alkaliphilus metalliredigens strain QYMF 16S ribosomal RNA gene, complete sequence	97
METHEUB13	Alkaliphilus crotonatoxidans strain B11-2 16S ribosomal RNA gene, partial sequence	97
METHEUB14	Roseicitreum antarcticum strain ZS2-28 16S ribosomal RNA gene, partial sequence	90
METHEUB15	Alkaliphilus metalliredigens strain QYMF 16S ribosomal RNA gene, complete sequence	94
METHEUB16	Alkaliphilus metalliredigens strain QYMF 16S ribosomal RNA gene, complete sequence	97
METHEUB17	Alkaliphilus metalliredigens strain QYMF 16S ribosomal RNA gene, complete sequence	94
METHEUB18	Alkaliphilus transvaalensis strain SAGM1 16S ribosomal RNA gene, partial sequence	90
METHEUB19	Bacillus okhensis strain Kh10-101 16S ribosomal RNA gene, partial sequence	95
METHEUB20	Alkaliphilus metalliredigens strain QYMF 16S ribosomal RNA gene, complete sequence	94
METHEUB21	Alkaliphilus metalliredigens strain QYMF 16S ribosomal RNA gene, complete sequence	97
METHEUB22	Alkaliphilus metalliredigens strain QYMF 16S ribosomal RNA gene, complete sequence	94
METHEUB23	Alkaliphilus crotonatoxidans strain B11-2 16S ribosomal RNA gene, partial sequence	97
METHEUB24	Roseicitreum antarcticum strain ZS2-28 16S ribosomal RNA gene, partial sequence	90
METHEUB25	Anaerobacillus alkalilacustris strain Z-0521 16S ribosomal RNA gene, partial sequence	96
METHEUB26	Alkaliphilus crotonatoxidans strain B11-2 16S ribosomal RNA gene, partial sequence	97
METHEUB27	Acholeplasma parvum strain H23M 16S ribosomal RNA gene, partial sequence	90
METHEUB28	Alkaliphilus crotonatoxidans strain B11-2 16S ribosomal RNA gene, partial sequence	97
METHEUB29	Brevundimonas diminuta strain ATCC 11568 16S ribosomal RNA gene, complete sequence	99
METHEUB30	Alkaliphilus crotonatoxidans strain B11-2 16S ribosomal RNA gene, partial sequence	97
METHEUB31	Alkaliphilus crotonatoxidans strain B11-2 16S ribosomal RNA gene, partial sequence	97
METHEUB32	Anaerobacillus alkalilacustris strain Z-0521 16S ribosomal RNA gene, partial sequence	96

Archaea

Clone ID	Closest Sequence Match	Similarity (%)
METHARC2	Methanobacterium alcaliphilum strain NBRC 105226 16S ribosomal RNA gene, partial sequence	99
METHARC3	Methanobacterium alcaliphilum strain NBRC 105226 16S ribosomal RNA gene, partial sequence	99
METHARC4	Methanobacterium alcaliphilum strain NBRC 105226 16S ribosomal RNA gene, partial sequence	99
METHARC5	Methanomassiliicoccus luminyensis strain B10 16S ribosomal RNA gene, partial sequence	92
METHARC7	Methanobacterium flexile strain GH 16S ribosomal RNA gene, partial sequence	99
METHARC9	Methanobacterium flexile strain GH 16S ribosomal RNA gene, partial sequence	99
METHARC10	Methanobacterium flexile strain GH 16S ribosomal RNA gene, partial sequence	99
METHARC11	Methanobacterium alcaliphilum strain NBRC 105226 16S ribosomal RNA gene, partial sequence	99
METHARC12	Methanobacterium alcaliphilum strain NBRC 105226 16S ribosomal RNA gene, partial sequence	99
METHARC13	Methanobacterium flexile strain GH 16S ribosomal RNA gene, partial sequence	99
METHARC14	Methanobacterium flexile strain GH 16S ribosomal RNA gene, partial sequence	99
METHARC15	Methanobacterium flexile strain GH 16S ribosomal RNA gene, partial sequence	100
METHARC16	Methanobacterium flexile strain GH 16S ribosomal RNA gene, partial sequence	99
METHARC17	Methanobacterium flexile strain GH 16S ribosomal RNA gene, partial sequence	99
METHARC20	Methanobacterium flexile strain GH 16S ribosomal RNA gene, partial sequence	99
METHAR25	Methanomassiliicoccus luminyensis strain B10 16S ribosomal RNA gene, partial sequence	89
METHARC28	Methanomassiliicoccus luminyensis strain B10 16S ribosomal RNA gene, partial sequence	89
METHARC29	Methanomassiliicoccus luminyensis strain B10 16S ribosomal RNA gene, partial sequence	89
METHARC31	Methanobacterium alcaliphilum strain NBRC 105226 16S ribosomal RNA gene, partial sequence	99
METHARC34	Methanobacterium alcaliphilum strain NBRC 105226 16S ribosomal RNA gene, partial sequence	99
METHARC35	Methanomassiliicoccus luminyensis strain B10 16S ribosomal RNA gene, partial sequence	89
METHARC36	Methanobacterium alcaliphilum strain NBRC 105226 16S ribosomal RNA gene, partial sequence	99
METHARC37	Methanobacterium flexile strain GH 16S ribosomal RNA gene, partial sequence	99
METHARC38	Methanobacterium alcaliphilum strain NBRC 105226 16S ribosomal RNA gene, partial sequence	99
METHARC40	Methanobacterium alcaliphilum strain NBRC 105226 16S ribosomal RNA gene, partial sequence	99
METHARC41	Methanobacterium alcaliphilum strain NBRC 105226 16S ribosomal RNA gene, partial sequence	99
METHARC42	Methanobacterium alcaliphilum strain NBRC 105226 16S ribosomal RNA gene, partial sequence	99
METHARC43	Methanomassiliicoccus luminyensis strain B10 16S ribosomal RNA gene, partial sequence	89
METHARC44	Methanomassiliicoccus luminyensis strain B10 16S ribosomal RNA gene, partial sequence	99

Statistical Analyses

Chapter 6 comparisons

Comparison between geochemical conditions

ANOVA

		Sum of Squares	df	Mean Square	F	Sig.
AISACONC	Between Groups	.064	2	.032	.585	.569
	Within Groups	.824	15	.055		
	Total	.889	17			
BISACONC	Between Groups	.017	2	.009	.069	.933
	Within Groups	1.883	15	.126		
	Total	1.901	17			

Comparison between stereoisomers

Independent Samples Test

		Levene's Test for Equality of Variances		t-test for Equality of Means						
									95% Confidence Interval of the Difference	
		F	Sig.	t	df	Sig. (2-tailed)	Mean Difference	Std. Error Difference	Lower	Upper
Conc	Equal variances assumed	.803	.376	-1.508	34	.141	-.14399	.09547	-.33801	.05004
	Equal variances not assumed			-1.508	30.046	.142	-.14398	.09547	-.33895	.05099

Data and Statistical analyses

Acetic acid within IRB reactor

ANOVA

ACETIC

	Sum of Squares	df	Mean Square	F	Sig.
Between Groups	112.022	6	18.670	5.430	.001
Within Groups	113.473	33	3.439		
Total	225.495	39			

Post Hoc

Multiple Comparisons

Dependent Variable: ACETIC

Tukey HSD

(I) Day	(J) Day	Mean Difference (I-J)	Std. Error	Sig.	95% Confidence Interval	
					Lower Bound	Upper Bound
1.00	2.00	-1.81833	1.07060	.622	-5.1769	1.5402
	3.00	-5.02833*	1.07060	.001	-8.3869	-1.6698
	4.00	-4.61000*	1.19697	.008	-8.3650	-.8550
	5.00	-3.49167*	1.07060	.037	-6.8502	-.1331
	6.00	-2.44500	1.07060	.282	-5.8036	.9136
	7.00	-1.22167	1.07060	.910	-4.5802	2.1369
2.00	1.00	1.81833	1.07060	.622	-1.5402	5.1769
	3.00	-3.21000	1.07060	.069	-6.5686	.1486
	4.00	-2.79167	1.19697	.259	-6.5466	.9633
	5.00	-1.67333	1.07060	.706	-5.0319	1.6852
	6.00	-.62667	1.07060	.997	-3.9852	2.7319
	7.00	.59667	1.07060	.998	-2.7619	3.9552
3.00	1.00	5.02833*	1.07060	.001	1.6698	8.3869
	2.00	3.21000	1.07060	.069	-.1486	6.5686
	4.00	.41833	1.19697	1.000	-3.3366	4.1733
	5.00	1.53667	1.07060	.779	-1.8219	4.8952
	6.00	2.58333	1.07060	.225	-.7752	5.9419
	7.00	3.80667*	1.07060	.018	.4481	7.1652
4.00	1.00	4.61000*	1.19697	.008	.8550	8.3650
	2.00	2.79167	1.19697	.259	-.9633	6.5466
	3.00	-.41833	1.19697	1.000	-4.1733	3.3366
	5.00	1.11833	1.19697	.964	-2.6366	4.8733
	6.00	2.16500	1.19697	.552	-1.5900	5.9200
	7.00	3.38833	1.19697	.099	-.3666	7.1433

5.00	1.00	3.49167*	1.07060	.037	.1331	6.8502
	2.00	1.67333	1.07060	.706	-1.6852	5.0319
	3.00	-1.53667	1.07060	.779	-4.8952	1.8219
	4.00	-1.11833	1.19697	.964	-4.8733	2.6366
	6.00	1.04667	1.07060	.955	-2.3119	4.4052
	7.00	2.27000	1.07060	.365	-1.0886	5.6286
6.00	1.00	2.44500	1.07060	.282	-.9136	5.8036
	2.00	.62667	1.07060	.997	-2.7319	3.9852
	3.00	-2.58333	1.07060	.225	-5.9419	.7752
	4.00	-2.16500	1.19697	.552	-5.9200	1.5900
	5.00	-1.04667	1.07060	.955	-4.4052	2.3119
	7.00	1.22333	1.07060	.910	-2.1352	4.5819
7.00	1.00	1.22167	1.07060	.910	-2.1369	4.5802
	2.00	-.59667	1.07060	.998	-3.9552	2.7619
	3.00	-3.80667*	1.07060	.018	-7.1652	-.4481
	4.00	-3.38833	1.19697	.099	-7.1433	.3666
	5.00	-2.27000	1.07060	.365	-5.6286	1.0886
	6.00	-1.22333	1.07060	.910	-4.5819	2.1352

*. The mean difference is significant at the 0.05 level.